封二位置

中国科学院上海应用物理研究所

年 报

2007–2008

（第 23 卷）

《中国科学院上海应用物理研究所年报》
编辑委员会

内 容 简 介

本书为 2007–2008 年度中国科学院上海应用物理研究所年报，主要由全所各科研机构负责人以中英文介绍该部门或研究组于 2007–2008 年在相关研究领域中的工作进展，内容包括上海光源工程、核物理、核分析技术与交叉学科研究、高分子材料辐射改性与环境治理、放射性药物、核电子学、辐射加工用电子束辐照装置等。附录记载了 2007–2008 年度本所的学术活动、国际交流、人才培养等情况。

本年报供本所上级主管中国科学院和上海市各有关部门的领导与各类管理人员阅读，供各科研院所相关领域的科研人员、高等院校师生，以及本所科研人员和研究生阅读参考。

前　言

全面建设上海光源，奠定新时期发展框架

2007–2008 年，我所认真实施中国科学院知识创新工程三期，按照“两个一盘棋”的要求，在确保上海光源工程计划进度、工程质量和经费控制的同时，加强学科发展战略研究，围绕同步辐射进行实质性的学科调整，确定了建设“世界级”研究所的发展目标，奠定了我所新时期发展框架。围绕新的学科布局，调整队伍和结构，明确研究方向，落实科研任务，加速形成我所的学科优势，呈现出良好的发展势头。

一、上海光源出光，工程建设势如破竹

两年来，上海光源建安工程完成竣工验收备案工作；公用设施各系统调试基本完成，试运行情况良好；加速器和光束线工程全面进入加工、安装、调试阶段，建设现场捷报频传，工程任务胜利在望。2007 年，工艺设备研制、安装工作取得了突破性进展，直线加速器安装完成，全部达到性能指标；增强器安装完成，成功实现电子束升能；储存环总体安装完成，以国际上少有的速度获得束流储存和积累，在上海光源工程破土开工三周年时——比原计划提前 4 个月——实现了出光目标；光束线站全面进入设备加工、制造阶段，并完成了前端区的隧道内安装。2008 年，经过三个阶段的总体调试，储存环电子能量、流强、束流寿命、发射度、轨道稳定性等主要性能都达到设计指标；首批七条光束线站全部完成安装与离线测试，并完成五条线站的同步光调试，其中小角散射线站、衍射线站和成像线站已基本达到验收指标，并进行了初步实验。

同时，积极开展用户与首批实验工作。按照上海光源工程领导小组的决定，落实筹建“上海光源科学中心（筹）”，并制定相应规章制度，筹备上海光源运行和用户工作体系。遴选首批实验课题，向全国 102 所“211”大学、104 家科研机构、约 300 名专家发函，征集上海光源首批实验申请，截止年底已收到约百份用户课题申请、累计一千多个机时。

二、开展发展战略研究，调整研究所学科布局

经过两年的学科发展战略研究，我所围绕同步辐射进行学科布局调整。确定了建设“世界级”研究所的发展目标，学科布局调整为加速器物理与技术、光子科学、核物理与核技术、前沿交叉学科四大学科。这一轮的学科调整突出和树立“学科”观念，统筹兼顾基础研究和应用研究，强调发展，研究所的学科方向将根据科学发展、国家需求以及研究所的实际情况不断进行调整。2007–2008 年度，共争取到各类科研任务 88 项、总经费 5154 万元，其中国家重大科学研究计划(973)项目 1 项、国家杰出青年基金 2 项。

两年来，研究所工作取得了重要成果和重大进展。上海软 X 射线自由电子激光装置大科学工程的项目建议书已报国家发展改革委审批，上海深紫外自由电子激光平台建设目标调整为用户装置并启动部件加工和安装，系列化烟气脱硫用加速器研制成功。积极争取上海光源线站能力升级大科学工程项目，参与的国家蛋白质科学设施（上海）大科学工程已获得国家发展改革委批准立项，上海激光电子伽玛源预研样机实现了纳秒量级的激光束与电子束碰撞实验；成功测定了人源

μ 晶状体蛋白三维结构。核物理与核科学技术学科方面，发现纳米水通道的电学开关特性并设计出纳米尺度水泵，MicroSPECT 实验室样机达到 0.8 毫米空间分辨率，RHIC-STAR 相对论重离子碰撞国际合作研究取得一系列成果，壳聚糖作为鱼药添加剂已报农业部审批。前沿交叉学科方面，研制出新型电化学 DNA 传感器和 ATP 传感器，设计出一种快速简便的可视化的可卡因检测方法，设计出一套增大碳基材料中铁磁性的可控性方法，纳米（生物）水通道的系列研究取得新成果。

2007–2008 年，在国内外学术期刊上共发表论文 460 篇，其中影响因子 3 以上的高水平论文 98 篇；申请专利 44 项、授权专利 22 项。“中能重离子碰撞中的核液气相变和同位旋相关的物理”获 2008 年度上海市自然科学二等奖，“基于 DNA 分子设计与调控的生物传感检测方法及应用”获得中国分析测试协会科学技术奖(CAIA 奖)一等奖。中科院创新重大项目“核技术应用的关键技术”的系列加速器研制成功；国家“973”项目“人工纳米生物机器构筑与生物医学应用的基础研究”通过中期评审。

三、在稳定的基础上寻求科技产业化的新发展

加强科技成果转化，在稳定所投资企业的基础上寻求科技产业化的新发展。科研成果“膜生物反应器”成功转让，与上海过滤器有限公司共同投资组建了“上海斯纳普膜分离科技有限公司”；与浙江省嘉善县人民政府共建了“浙江中科辐射高分子材料研发中心”；经中科院批准，上海日环科技投资有限公司将变更为我所独资的经营性国有资产管理和运作企业；完成世龙公司和辐照基地的社会化改革。国家发展改革委“民用非动力核技术”高技术产业化专项的“辐射改性功能型高分子新材料高技术产业化示范工程”，启动一期工程——世龙公司新基地的建设，至 2008 年底已完成土建结构工程。2007–2008 年，全所签订科技成果转化“四技”合同 95 项，所投资企业完成销售收入约 12000 万元。

四、借助上海光源平台，推动各学科的合作交流

借助上海光源这一世界级的科研交流平台，实质性地推动了我所各学科领域与院内兄弟所、国内主要高校以及其他国家创新单元之间的合作交流。2007–2008 年，我所与美国阿贡国家实验室(ANL)和劳伦斯伯克利国家实验室(LBNL)、日本同步辐射研究机构、澳大利亚光源，以及中科院高能物理所、清华大学工程物理系、上海交通大学、中科院生物物理所、上海超级计算中心签订了全面合作协议或战略合作协议；与日本原子能研究机构就同步辐射研究领域、辐射化学与材料、环境科学等领域签订院级合作协议子协议；与意大利国家核物理研究机构(INFN)签订了参与中微子国际合作项目的合作协议。承办了“同步辐射和前沿交叉研究系列研讨会”、EPICS collaboration meeting 2008 and EPICS Seminar、ICFA Mini-Workshop on Deflecting/Crabbing Cavity Applications in Accelerators 等国际会议以及六期东方科技论坛，并与浙江中科辐射高分子材料研发中心合作承办了亚洲核合作论坛(FNCA)。

中科院国际合作重点项目“上海光源工程”，成功开发高频低电平控制系统，研制数字化电源和高性能深低温传输管线；与韩国光源合作完成同步辐射光束线镜面压弯机构的设计与研制；完成 RHIC-STAR 国际合作项目 STAR-TOF 探测系统的升级计划。

五、规划实验室建设，加强特色技术支撑

2007–2008 年，我所对四大学科领域的实验室和平台建设进行了研讨规划，加强特色科技平程建设中的技术创新、管理创新、队伍建设和文化建设，在凝练中弘扬上海光源精神。随着上海光源工程建设取得重大进展和我所综合实力的提升，我所的社会影响日益扩大，温家宝总理、刘延东国务委员、全国政协阿不来提·阿不都热西提副主席等党和国家领导人视察上海光源，据不完全统计，我所两年内共接待了约 235 次、8600

多名各级领导、中外专家和各界人士的视察访问和科普参观；上海光源团队荣获“2004–2006 年度上海市劳模集体”称号。此外，我所积极开展社区共建与结对帮扶，与嘉定区徐行镇政府签订社区共建协议，与崇明县庙镇鸽龙村签订结对帮扶协议；组织“一日捐”活动，全所 682 人捐款 48475 元；为汶川大地震捐款 114020 元，交纳特殊党费 61506 元；召开职工运动会，组织我所职工参加广播操、乒乓球、羽毛球、跳绳等比赛，丰富所内生活。

2007–2008 年，我所在上海光源工程建设、基础研究、科技产业化、国内外合作、人才队伍建设、体制机制改革、管理创新与文化建设等各方面都取得了可喜的成绩。展望未来，上海光源工程建设即将完成并转入运行与应用阶段，蛋白质科学研究设施的线站建设、上海软 X 射线自由电子激光装置、上海光源线站能力升级工程等项目的立项工作已启动。机遇和挑战并存，在多项目、多类工作、两园区管理的情况下，我所面临着思想认识、人才队伍、组织管理和学术作风等多方面的考验。全所同志应发扬“上海光源精神”，再接再厉，立足国家战略需求，抓住重大历史机遇，为把我所建设成为“世界级研究所”而奋斗。

空白页

目录

上海光源 Shanghai Synchrotron Radiation Facility

核物理与核技术 Nuclear Physics and Nuclear Technology

附录

上海光源

Shanghai Synchrotron Radiation Facility

电子直线加速器与相关研究进展

电子直线加速器部　赵明华

本组设计研制直线型电子加速器。为在加速过程中保持电子束的品质，须研究其束流动力学，特别是电子与自场、外部电磁场的相互作用。我们的研究内容还包括各种类型的电子枪和射频结构。这些工作可应于第三代同步辐射光源的预注入器，也是第四代光源高性能电子直线加速器的技术积累。

我们设计研制的上海同步辐射装置(SSRF)的150 MeV 电子直线加速器，已在规的时间和经费下，成功完成调束，达到设计值，并通过了长期运行的考验。此外，由中国国家自然科学基金委支持的光阴极微波电子枪测试平台，也已调试完成，并通过了基金委组织的验收。

150 MeV 电子直线加速器

图 1　150 MeV 电子直线加速器

SSRF 的初期方案是 100 MeV 电子直线加速器，包括 1 个热阴极注入器、4 根 SLAC 型加速管组成和 1 套 45 MW 的微波功率源。因储存环将以恒流模式运行，为简化定时系统设计并减小束流损失，直线加速器的工作频率设计为储存环工作频率的整数倍。在优化设计中，为提高增强器在低能时的稳定性，直线加速器的能量提高到 150 MeV，增加 1 套 45 MW 微波功率源，束流线布局保持不变。

直线加速器的安装从 2006 年 11 月开始，2007 年 1 月，直线加速器的隧道安装工作结束(图 1)。同时，两套 45 MW 微波功率源通过测试验收，主要指标达到设计要求。2007 年 4 月，所有设备完成安装调试，电子枪和微波系统分别开始高压和高功率老炼，1 个月后完成。至 5 月中旬，电子直线加速器所有子系统完成调试。

电子直线加速器的束流调试从 5 月 14 日开始，当天就将电子束流传输到加速器出口，能量 130 MeV。这表明直线加速器束流元件的准直安装误差很小，完全达到设计要求。经 3 个月的调试，直线加速器的各项束流参数达到设计指标(表 1)。

2007 年 10 月 1 日，直线加速器的电子束流成功注入增强器，传输效率达 80%。直线加速器的初期运行(7000 小时)情况，故障时间约 70 小时。

表 1　150 MeV 电子直线加速器的束流参数

参数	单脉冲模式	多脉冲模式
能量 / MeV	157.57	156.88
束流宽度 / ns	0.092*	189.77
脉冲电荷量 / nC	1.07	3.53
能量稳定度 / %	0.093	0.11
能散 / %(RMS)	0.31	0.34
归一化发射度 /mm·mrad	H: 40.5/V: 47.1	H: 46.2/V: 48.8

光阴极微波电子枪测试平台

光阴极微波电子枪测试平台是国家自然科学基金委“深紫外自由电子激光关键技术研究”项目的子项目，其目标是集成和调试一套光阴极微波电子枪系统，获得其产生的电子束团的束流参数，并开展可用于高增益自由电子激光的高亮度注入器的实验研究。该项目 2004 年中期评审后，转由我所承担。

该测试平台由一个光阴极微波电子枪、一套光阴极驱动激光系统、一套 30 MW 微波功率源、一套束流测量系统，以及辅助系统和设备组成(图 2)。光阴极微波电子枪采用 BNL 第四代 1.6 腔的枪型设计，由清华大学研制。阴极材料为铜，实验中需用数十微焦脉冲能量的真空紫外激光，才能获得足够的电子束团的电荷量。考虑到真空紫外激光的传输和横向整形，以及激光器运行的稳定性和可靠性，选择了激光脉冲能量大于 200 微焦的 YLF 激光器产品。

该平台的关键工作之一，是验证光阴极微波电子枪产生的电子束流的品质，因此平台上安装了很多束流测量元件。除常规的能量、电荷量和束流截面的测量，我们采用胡椒孔屏方法和偏转结构来测量空间电荷力占优的束流发射度和皮秒量级的束流长度。此外，为了同步测试平台中所有的设备，同

步系统包含了一套纳秒级的慢同步系统和一套皮秒级的快同步系统，以满足不同设备和实验的需要。

图 2　光阴极微波电子枪测试平台的束流元件

2007 年 8–10 月，光阴极微波电子枪测试平台在 100 MeV 电子直线加速器隧道内安装。12 月，完成高功率微波系统和电子枪的老炼。第一阶段调试在 2008 年 2–3 月进行，测试了束流能量、暗电流和光电子束流流强。测量表明，国产铜的量子效率比国外报道高 2 倍左右，也使暗电流有很大增长。在 5 月开始的第二轮调试中，测量了除束团长度的其它束流参数。11 月，安装了高能物理研究所研制的偏转结构后，所有的束流参数都可测量。最终测量到的束流参数如下：

电荷量	30°	0.6 nC
	90°	1.1 nC
能量		4.2 MeV
归一化发射度		4.1 mm·mrad
束团长度(RMS)		5.1 ps

其他相关研究

腔式束流位置探测器(CBPM, cavity beam position monitor)，其灵敏度和精度高于传统的束流位置探测器，且可应用在基于直线加速器的光源和对撞机的高精度束流准直上，我们研制的 CBPM 样机已在光阴极微波电子枪测试平台上完成测试，并设定了下一步研究目标。

高梯度加速结构，有利于加速器的小型化并降低造价，我们正在开展一个 C 波段高梯度加速结构的研究项目。

高功率高亮度电子源，是未来高功率自由电子激光的关键部件之一，我们正在设计一台 350 kV 的高压型电子枪及其测试平台。

筹建中的电子枪实验室将构建一个电子枪关键技术的测试平台，可在其上进行诸如高压、阴极制备与测量、以及高功率电子束流的参数测量等实验。

微波测量实验室将建立一个射频结构的测量平台，将设计和加工有机的结合在一起，为加速结构和测量结构的研制提供必要的测试手段。

上海深紫外自由电子激光装置，是我国首台基于电子直线加速器的高增益自由电子激光实验装置。该装置将于明年进行安装调试，并获得初步的实验结果。这将是我们迈向软 X 射线和硬 X 射线自由电子激光装置的关键的第一步。

Progresses in Developing the SSRF Linac and Related Researches

ZHAO Minghua, Division of Linear Accelerators

The Division is mainly to develop the SSRF linac and ensure the specified beam parameters of the accelerator. For beam dynamics of the linac, especially interactions among the electron bunches, and the self fields and the external fields, are considered carefully to minimize the beam quality degradation. In addition, techniques of various types of the electron gun and radiofrequency structures are developed to meet the requirements on the electron beam for existing and future facilities. The research programs are not only for the pre-injector of the third generation light source, but also for the high performance linac of the next generation light source.

In 2007–2008, the 150 MeV linac of SSRF was installed and commissioned to its design specifications within the time schedule and the project budget. The photocathode RF gun test bench, a project supported by the Nature Science Foundation of China (NSFC), was completed. And R&D efforts were made on key techniques related to linac developments.

1 The SSRF linac

Fig.1 The linac of SSRF.

Initially, the linac was designed as a 100 MeV linac, with a thermionic injector and 4 accelerating tubes of modified SLAC type, supplied by a 45 MW klystron. It has two operation modes: the single pulse mode and multi-pulse mode, and this meets the requirements of different filling patterns of the storage ring. Considering the top-up operation of SSRF, one should make the working frequency of the linac accelerating structures to exact multiple of the main RF frequency of the storage ring, so as to simplify the timing system and minimize the beam loss and radiation dose. In order to improve stability of the booster during the ramping process, especially in the injection period, the linac energy was increased to 150 MeV in the revised design, which is the initial design plus basically one more 45 MW klystron.

Installation of the linac was started in November 2006. The four accelerating tubes were installed in January 2007, and in March installations in the linac tunnel were completed. Figure 1 shows the linac in the tunnel, with the electron gun on the right. The microwave system based on two 45 MW klystrons were installed and accepted in January 2007, and the waveguide system connecting the accelerating structures and klystrons was completed. In April and May, we did the high voltage conditioning of the electron gun, and high power conditioning of the waveguide system and accelerating structures. By the end of May, all the joint sub-system commissioning had been successfully finished.

On May 14, 2007 commissioning of the linac started and electron beams at 130 MeV were transported to the end of the linac, indicating a good alignment of the tunnel installation, and good performance of the components. In three months of commissioning, beam parameters of the linac in two operation modes achieved the design specifications, as shown in Table 1.

On October 1, 2007, the beam was injected into the booster successfully and a high efficient of over 80% was achieved. As of the end of 2008, the linac was in operation for over 7000 h, with a down time of less than 70 h.

Table 1 The measured beam parameters

Parameters	Single bunch mode	Multi bunch mode
Energy / MeV	157.57	156.88
Beam length / ns	0.092*	189.77
Beam charge / nC	1.07	3.53
Energy stability / %	0.093	0.11%
Energy spread / %(RMS)	0.31	0.34
Normalized emittance / mm·mrad	H: 40.5/V: 47.1	H: 46.2/V: 48.8

The photocathode RF gun test bench

The photocathode RF gun test bench is a sub-project of the NSFC project of Research on Key Technology of the Deep Ultraviolet Free Electron Laser, for integrating and commissioning the DUFEL system, measuring the electron beam parameters, and starting experiments on high brightness electron sources for the high gain FEL. In 2004, after the mid-term review, this project was moved to SINAP for the system integration and commissioning.

The test bench consists of a photocathode RF gun, a driver laser system, and a 30 MW RF power system based on a pulsed klystron, plus the beam diagnostics and other accessories (Fig. 2). The photocathode RF gun is based on the design of BNL IV type 1.6 cell gun made by Tsinghua University. The gun is equipped with a copper cathode, which requires an ultraviolet laser of tens of micro-joules in pulse energy, so as to produce enough charge for the experiments. Considering the transportation loss, the shaping and the correction in the transverse space, and the stability and reliability operation, a commercial YLF laser of 200 μJ in pulse energy was chosen. Because of the importance of validating the electron beam parameters,

various beam instrumentations were adopted to measure the parameters. In addition to devices for measuring the energy, charge and profile of the beams, the pepper-port and the RF deflecting structure were used to measure emittance of the space-charge dominated beams and the bunch length in pico-seconds. To synchronize these devices, a timing system with an ns slow synchronizer and ps fast synchronizer was established.

Fig.2 The beam line of the photocathode RF gun test bench.

The test bench was installed in August and September 2007 in the existing 100 MeV linac tunnel, followed by two months of conditioning the high power transfer line and the RF gun. In February and March of 2008, the first phase commissioning of the photocathode RF gun was conducted, and the dark current, beam current and beam energy were measured. The result showed that quantum efficiency of the Chinese-made copper was about 2 times higher than that in international literatures, but this was also the main reason of the higher dark current. After the tunnel was available again in May, all the beam parameters except the bunch length were measured. In November, the RF deflecting structure from Institute of High Energy Physics, Chinese Academy of Sciences was installed and conditioned to its working field. With this powerful tool, the bunch length was measured. The entire parameters of electron beam of the photocathode RF gun are as follows.

Bunch charge	30°	0.6 nC
	90°	1.1 nC
Beam energy		4.2 MeV
Normalized emittance		4.1 mm·mrad
Bunch length (RMS)		5.1 ps

Other research activities

The cavity beam position monitor (CBPM) has much higher sensitivity and accuracy than traditional BPMs, and is the most powerful instrument for aligning a linac-based light source. A prototype CBPM was developed and tested on the photocathode RF gun test bench. The first results are encouraging and further researches on the CBPM are under way.

With high gradient accelerating structures, a linac can be more compact, hence less cost. A proposal for R&D of a high gradient C-band accelerating structure has been approved, and the design of a constant gradient structure with low field coupler has been started.

A high power high brightness gun based on high voltage DC and photocathode technology is the key component for future high power FELs and ERLs. A conceptual design of a 350 kV DC gun and its test bench has been started, aimed at its application on the future FIR-ERL project in Shanghai.

In the electron gun laboratory, a platform will be established to test key technologies and components, such as ultra high voltage/field, surface processing, cathode preparation and measurement, and high power beam generation, transportation and measurement.

In the microwave measurement laboratory, a platform will be established to measure radiofrequency structure for accelerating and diagnosing the beams.

Efforts have been made towards constructing the linac-based high gain free electron laser test facility — Shanghai Deep Ultraviolet Free Electron Laser (SDEUVFEL). This will be the first step towards the soft and hard X-ray free electron laser projects.

SSRF 磁铁电源系统

电源技术部

沈天健　李 瑞　郭春龙　朱世明

磁铁电源组在上海光源的工程建设阶段，承担磁铁电源的设计、研制、安装和测试，同时建设了电源的稳定性测试和 DDCT 性能测试系统，并建立了大功率磁铁电源和动态电源的测试实验室。近几年来研制的数字化电源控制器，成功地运用在上海光源的部分设施中。我组还开展了电流传感器的数字化研究和其他特种电源的研究工作。在上海光源的运行阶段，我们不断地提高电源的可靠性，改进电源性能，制定电源系统的安全运行制度，努力提升电源系统的平均故障间隔时间(MTBF)指标。

上海光源主要由三个部分组成：150 MeV 直线加速器，增强器和储存环。每部分使用大批电磁铁，以确保电子束的高品质。该直线加速器有磁铁 55 块，增强器(包括高低能输运线)磁铁有 56 块，储存环磁铁则多达 520 块。所有磁铁都采用开关电源驱动。单极性电源采用斩波器与桥式(或半桥式)电路结构，双极性电源采用 H 桥双向变换的电路结构。1 kW 以上电源采用单体电源结构，电源采用 19"标准机箱，功率较小电源用插件式电源、公共直流源结构，公共直流源用标准 AC/DC48V 模块电源。

储存环磁铁电源是静态电源，要求高精度、高稳定性、高重复性，如储存环的二级磁铁电源指标为 850 A/800V，长期(24 h)稳定性 15 ppm。增强器磁铁电源系统，是在将电子束从 150 MeV 加速到 3.5 GeV 的过程中，动态地为增强器磁铁提供所需励磁电流。根据物理设计，输运线磁铁和增强器校正磁铁采用静态电源方式，而增强器二、四、六极磁铁电源是动态电源工作方式，电源的输出电流须同步地随束流能量变化。增强器二极磁铁、四极磁铁和六极磁铁电源输出 2 Hz 的动态电流，脉冲波形为偏置的升正弦曲线。

SSRF 磁铁电源采用数字调节电源方式，用瑞士光源(SLS)的全数字化调节控制方案。一块控制卡和一块 ADC 卡组成数字化电源控制器，并将通讯接口与电源控制调节合二为一。数字化电源控制器内置于各个电源机箱中，作为电源的有机组成部分。电源控制器通过光纤连接 IOC，实现与控制系统的连结和通讯。全数字化电源控制器的主要优点，是高稳定性和高重复性、以及数字控制的高灵活性。

我们设计的数字化电源控制器，经过严格的评审，成功地运用在 SSRF 直线加速器与增强器的一百多台中小电源中。通过指标测试、系统联调、调束实验，SSRF 磁铁电源的各项性能指标达到或超过了设计指标。一年多的调束运行证明，我们的磁铁电源系统有较好稳定性和可靠性，它们的 MTBF 不差于进口产品。

在研制第一代国产数字化电源控制器的基础上，我们开始了快校正电源的数字化电源控制器研制，希望将来能应用于储存环轨道快校正系统中。

The Magnet Power Supply System of SSRF

SHEN Tianjian LI Rui GUO Chunlong ZHU Shiming

Division of Power Supply

The Shanghai Synchrotron Radiation Facility (SSRF) has hundreds of magnet power supplies, namely 510 on the storage ring, 54 on the booster, and 65 on the linac. All the power supplies are in pulse width-modulated (PWM) mode with insulated gate bipolar transistors (IGBT). High precision DC power supplies for the 40 dipole magnets of the storage ring are rated at 840 A/800 V with a stability of $\pm 2\times10^{-5}$/8 h. The main windings of quadrupoles are excited by chopper type power supplies, which are of a total of 200 sets. In the booster ring, two sets of dynamic power supply for the dipoles, and two sets for quadrupoles, run at the biased 2 Hz quasi sinusoidal wave. All the power supplies work with digital power supply controllers designed by PSI or SINAP. And the power supplies were made in China by qualified manufacturers.

The construction of the SSRF power supply system for the magnet was finished in 2007. From tests of the power supplies, and from the SSRF commissioning, the results show that the entire magnet power supply system satisfies the design specifications. During the SSRF operation of over one year, the power supplies worked with high stability and reliability.

Digital Power Supplies and Their Controller of the Storage Ring

上海光源注入引出系统

电源技术部

谷 鸣　陈志豪　欧阳联华　刘 波　袁启兵　王锐萍 吴勇华

上海光源(SSRF)由150 MeV直线加速器、同步增强器和3.5 GeV 储存环组成。三台加速器的连接系统就是注入引出系统，包括增强器注入、增强器引出和储存环注入等三个设备系统。注入引出系统由总共15台脉冲磁铁、励磁电源和控制器组成。

增强器注入由1台冲击磁铁和1台切割磁铁实现单圈同轴注入；增强器引出由1台冲击磁铁、3台切割磁铁和3台凸轨磁铁联合实施3.5 GeV的电子束引出。

储存环注入系统对脉冲磁铁的要求，比增强器的注入引出系统还要高。4台冲击磁铁和2台切割磁铁在一个12 m长的直线节内组成注入系统。要求4台冲击磁铁的性能特性完全相同，这样才能确保注入系统的凸轨不会对储存束流产生影响。

同时，切割磁铁的漏场也要尽可能地小而不影响储存束流。

切割磁铁

SSRF注入引出切割磁铁采用涡流板类型的切割磁铁。所有六块切割磁铁设计为相同的结构，只是长度和弧度不同，所有磁铁均运行在真空环境中。磁铁磁芯采用0.1 mm厚的特种硅钢片。

切割板的作用是脉冲磁场在切割板内产生涡流，从而产生磁场，以抵抗主磁场的泄露。为尽量增加切割板的厚度，将磁铁设计成随从束流转弯的弧形磁铁。这样不仅增加了切割板的平均厚度，也使切割磁铁的束流孔径最大化。

切割磁铁的励磁波形是60 μs 的半正弦电流脉冲。为降低切割磁铁对储存束流的阻抗突变效应，储存环注入切割磁铁真空箱内设计了储存束流过渡连接管道，保证束流阻抗的平滑连接。

为进一步降低漏场对储存束流的影响，在束流管道外还专门设计包围了磁屏蔽层。测试结果表明，储存环注入切割磁铁的漏场小于50 μT·m，达到同类磁铁的国际先进指标水平。

冲击磁铁和凸轨磁铁

增强器注入引出冲击磁铁也是运行在真空条件中的快速脉冲磁铁，由铁氧体磁芯和单圈线圈构成。为尽量减小梯形励磁电流脉冲的前后沿时间，磁铁励磁脉冲电源紧贴着磁铁安装。采用同轴电缆线作为脉冲成形线。

储存环注入冲击磁铁是带镀膜陶瓷真空室的真空外脉冲磁铁，励磁电流波形为3.8 μs的半正弦波。储存环注入要求4台冲击磁铁要有完全相同的性能参数。除了磁铁和电源的一致性要求外，陶瓷真空室的镀膜厚度和均匀性也是严格要求的指标之一。钛膜既要让脉冲磁场穿透，又要保证储存环的束流阻抗平滑。

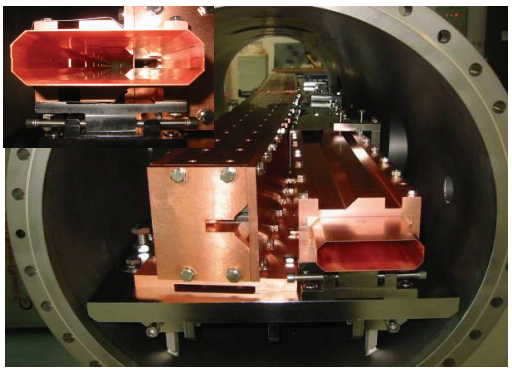

储存环注入切割磁铁

增强器引出设计采用了3块凸轨磁铁，凸轨磁铁相对来说是常规的磁铁，励磁脉冲为200 ms的半正弦电流波形。

上海光源的性能指标达到和超过了设计要求。物理调束和光源试运行验证了注入引出脉冲磁铁系统的优良的性能指标和稳定可靠性。注入引出脉冲磁铁系统的研制，吸收采纳了国内外先进的设计、技术和材料。研制的漏场小于 0.01%的切割磁铁，注入冲击磁铁波形的精确调整和定时的一致性，使储存环注入对储存束的扰动降至很低水平，也为恒流运行模式提供了前提条件。

Pulsed Magnet Systems for SSRF Injection and Extraction

GU M CHEN Z H OUYANG L H LIU B YUAN Q B WANG R P WU Y H

Division of Power Supply

The injector and storage ring of the Shanghai Synchrotron Radiation Facility (SSRF) were built and commissioned satisfactorily. For the booster injection and extraction, in-vacuum ferrite kicker magnets, eddy current septa and 200 ms bump magnets are used, while injecting the storage ring needs four identical kickers having ceramic vacuum chamber and two septa coated with a sheet of magnetic screening material to protect the stored beam bunches from the magnetic fields. While the septa are stressed on minimizing the field leakage, the four identical kickers for storage ring injection are emphasized on achieving the best possible tracking in time and amplitude of the magnetic field waveforms, so as to minimize the residual closed-orbit disturbance for top-up injection. The test and commissioning results show that the injection and extraction systems are highly reliable. The magnets, power supplies and controllers work perfectly and excellent injection efficiency is achieved.

Booster Kicker

The booster kickers are in-vacuum ferrite kicker magnets with window-frame core. The kicker pulser is located near the kicker magnet in the tunnel. The thyratron and PFL cable are main components of the pulser that provides trapezoidal current pulses to excite the kicker magnet.

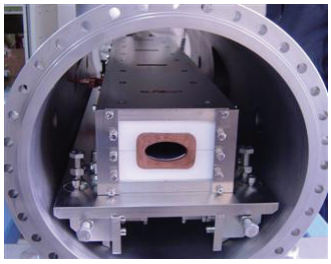

Septa

The type of septum is eddy current shielded magnet. Lengthways axis of the core is designed to follow the beam trace so as to maximize the beam aperture and increase the thickness of shielding sheet. The magnet is excited with a 60-μs pulse of half sine wave. A magnetic screen is placed around the stored beam to minimize the septum leakage field. At the maximum bumped beam position the leakage field was measured at less than 50 μT·m.

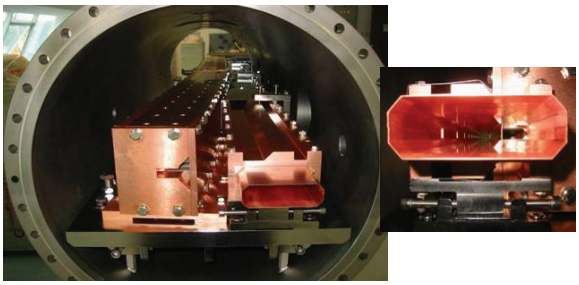

Storage Ring Kicker

Four identical kickers with ceramic vacuum chamber are installed at a long straight section of the SSRF storage ring for symmetric bump up of the stored beam.

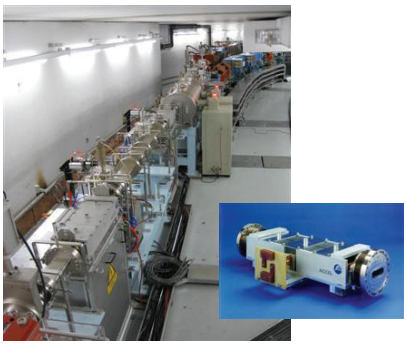

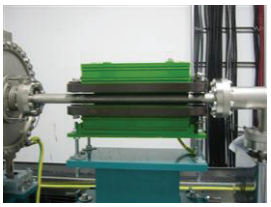

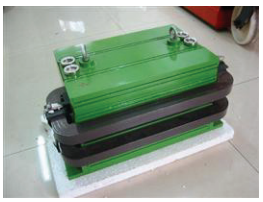

Booster Bumper

Three bump magnets are equipped at extraction section of the booster. C-shaped frame core enables easy installation outside the beam chamber. The magnets are excited by half sine waves of 200-ms width to avoid field attenuation when it passes through the metal vacuum chamber. Each bumper is driven by a programmed DC power supply.

Commissioning

The top-up injection is a prospective operation mode for SSRF. High reliability and careful setting-up of the injection are required. The residual orbit disturbance in horizontal plane is reduced to about 100 μm by tuning the kicker amplitude and trigger delay. By correcting the kicker's setting the vertical disturbance decreased to around 50 μm. This can be further lowered through fine tuning of the whole system.

上海光源电气安装工艺

电源技术部

金　江　张惠民　顾彩英　顾惠国　曹丹平
缪国灿　金　林　周学厚　沈志清　李德明

在SSRF的建设过程中，加速器的电气安装工艺一直是我们十分重视的问题。好多电气安装工艺不仅使安装设备整洁、漂亮，还是保证加速器性能、效率、可靠性、安全性的一个重要方面。

工艺设计和安装要求

(1) 要满足加速器各设备系统的技术设计要求，避免相互干扰。

(2) 要满足加速器各设备系统安装，维修和检查的方便性和使用上的可操作性。

(3) 要便于加速器运行和维修人员出入加速器的各个区域。

(4) 力求使得整个加速器各个区域整洁，外观漂亮。

加速器工艺工作主要任务

(1) 对SSRF各条隧道、技术走廊、各技术厅（包括电源厅、高频厅等）和技术夹层等区域的各类电缆桥架、电缆沟支架，进行布局设计和精心安装，各类设备主电缆线并测试（包括地线系统）。

(2) 技术走廊及各技术厅内各类电气设备机柜的就位和安装。

(3) 各加速器上须水冷却设备的冷却水管路系统的设计、安装（包括安装前对管路和相关器件进行清洗、安装后的冷却水质检测等）；冷却水管路系统上测量元件和控制元件的安装、调试和检测。

(4) 各加速器上用气设备的压缩空气管路系统的设计、安装。

(5) 对各加速器上大功率装置(如大功率磁铁、真空室、大功率串联电缆等)须安装温度控制装置，进行检测和安全连锁(包括温控器件性能的检测，温控信号电缆的布局和安装等)。

2007–2008年是加速器工艺安装最为紧张的两年。在三个加速器安装过程中 共完成下述工作：

各类型号的主电缆 /根	>100000
敷设电缆用的桥架 /m	>3000
设备机柜 /台	500
各类阀门和水流分配器 /只	>4000
水流量控制开关 /只	>600
温度测量探头 /只	>700
有机玻璃屏蔽罩 /个	432

机器运行过程中发现的工艺故障

上海光源加速器运行以来，也发现了一些辅助设备问题，如冷水系统的软管因长时间运行而出现破裂，各类流量开关在调试和运行过程中也有误报或不动作现象。电气系统机柜风扇和柜内照明也发生多次故障。储存环地沟中电缆桥架上电缆由于功率大、布局密，加上辐射防护安全封堵对散热的影响，沟中电缆的温度偏高。这些问题，有的已解决，有的正在解决。

进一步优化水电系统工艺 确保它们稳定可靠

从工艺方面优化细化，防患于未然，以确保机器正常运行、减少故障率、延长机器连续运行时间。

(1) 值班勤巡检、记录要细化，仔细分析已出现的问题和故障，避免同类事件重复发生。

(2) 完善备品、备件。

(3) 充分利用检修或参观等停机机会，进行维护保养、更换有问题器件，把故障解决在未发状态。

The Electric Equipment Installation of SSRF

JIN J ZHANG H M GU C Y GU H G CAO D P MIAO G C
JIN L ZHOU X H SHEN Z Q LI D M

Division of Power Supply

In constructing the linac, booster and storage ring of SSRF, it is very important to take special cares, and to adopt correct technologies, in installing the electric equipment. These would not only bring visual pleasantness of the accelerators, but also contribute to ensuring performance, efficiency, reliability and safety of the entire facility.

In 2007–2008, during installations of the three accelerators, we completed the following tasks of electric equipment installation:

Main cables* / pcs	>100 000
Cable trays / m	>3000
Equipment cabinets /set	~500
Valves and flow splitters /set	>4000
Water flow control switches /set	>600
Temperature-monitoring probes /set	>700
Plexiglass covers / set	432

* not including cables in cabinets

Basically, the electric equipment installations have been proved good during the accelerator operations. However, problems were found. Most of the problems were solved, and solutions are being worked out to tackle the other problems.

In order to ensure stable and reliable operation of SSRF, and to reduce the failure rate for extended hours of continuous operation, we shall make even more efforts to optimize technological design of the equipment installation, and to improve ourselves in operation and maintenance of the facility.

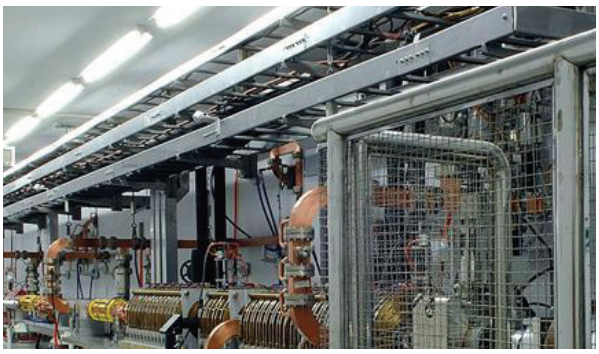

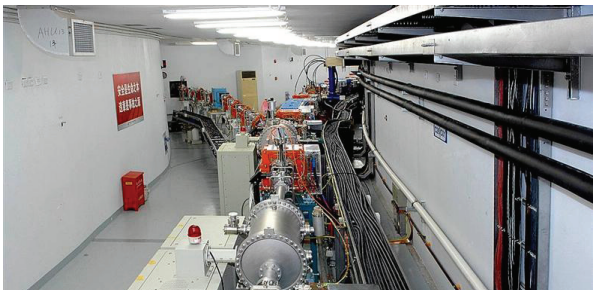

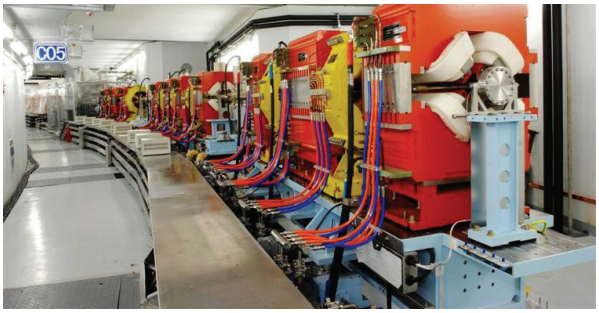

束流测量与控制技术

束流测量与控制技术部　冷用斌

束流测量与控制技术部专注于粒子加速器先进测控技术的研究。主要工作有：加速器分布式控制/数据采集系统结构设计、优化，新型设备控制器研制及应用研究，新型束流检测探头研制，基于数字信号处理技术的束流诊断技术，新型束流诊断原理的探索及应用。2007–2008 年，本部在上海光源以及 SDUVFEL 装置研制中取得如下成果。

控制组

1　SSRF 控制系统简介

SSRF 控制系统是基于 EPICS 系统、按照标准层次结构建造的大型分布式加速器控制系统。设备控制及机器保护系统采用 VME 64X 系统、PLCs 以及专门的嵌入式控制器，串口服务器用以连接串口设备以及基于串口的仪器，并通过控制系统网络连接所有的设备控制器。经历设计及样机建造阶段，完成系统原型开发及测试，主要包括数字化电源控制、数字化事件定时系统、基于以太网的设备控制系统[1]。所有的控制子系统均已投入运行[2]。另外，各软硬件系统开发及运行环境，以及基于 MatLab 加速器工具箱和中间件的上层物理应用环境，均已成功运用于加速器调束及运行。建立了中央数据库，完成了包括电子日志系统在内的系列配置及运行工具。一个增强的数据存档引擎正在测试，该引擎使用中央数据库存储运行数据和数据库原生的 XML 数据类型，可与各类数据分析软件方便集成。

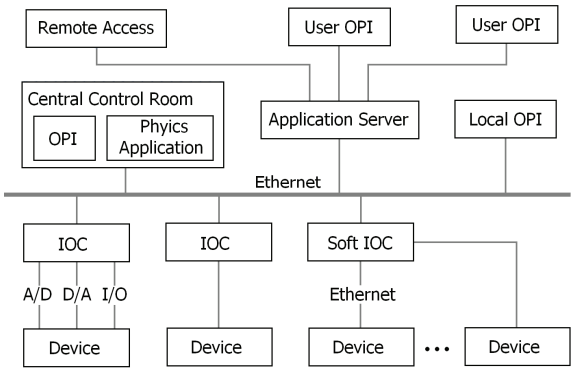

图 1　SSRF 控制系统结构示意图

2　控制系统环境

建立了包括控制系统网络、服务器系统及操作员界面(OPI)系统在内的控制系统开发及运行环境。开发人员及操作员可使用一套帐户系统登录任意终端，共享整个控制系统的资源。

SSRF 控制系统网络为基于 1000Base-T 的以太网，采用主干冗余设计以确保整个控制系统网络的可靠性，并可代替绝大部分设备的控制现场总线。例如，PLC 系统和基于串口设备(协议转换：串口转以太网转换器)的大部分设备直接联入控制系统网络，用异步设备驱动的 Soft IOC 集成到 EPICS 系统中[3]，还有一个集中的多 IOC 配置及管理系统来管理所有的 Soft IOC，可自动监测所有 Soft IOC 的运行情况。在网络设计上，不同子系统由 VLAN (虚拟局部网络)分隔以确保相互间不干扰，并在需要时实施 QOS(服务质量)的能力，并可方便灵活地重组以及划分所有的控制系统网络端口。

3　软件系统

SSRF 控制系统采用 EPICS base 3.14.8.2，OPI 使用了 edm 工具和一些 Python 或 prel 的脚本来实现[4]。上层物理环境使用 Matlab version 2007a，加速器工具箱(Accelerator Toolbox, AT) 和中间件作为上层物理应用的工具，并且配置了 MCA 和 LabCA 的 EPICS 访问工具箱与控制系统连接。建立了中央服务器系统，包括一组软件服务如 IOC 管理、在线电子日志系统、数据存档服务等以及 Oracle RAC 数据库系统。所有 OPI 系统均运行 Linux Fedora 7。

4　设备控制

完成直线加速器、增强器及储存环所有设备控制系统的安装和在线测试、系统联调，顺利投入调束运行。主要包括有电源控制、真空控制、注入引出、主定时、机器保护等。还完成了首批光束线相关的插入件控制系统的设计与建设工作，并建立了音视频监控系统、主机房，机柜温度监测、VME 机箱监控等系统在内的一批辅助系统。

SSRF 控制系统是一个大规模分布式控制系统，经设计、样机研制、设备加工及安装调试等阶段，成功建立了基于 EPICS 的分布式控制系统，完成设备控制系统的建设与调试工作，投入正常运行。系统集成了大量先进技术，性价比高，性能可靠、稳

定。从直线加速器控制系统起算，控制系统的 2 年多时间的运行证明其长时间运行的可靠、稳定性。

束流测量组

1 SSRF 束流诊断系统研制

上海光源束测系统覆盖储存环、增强器和直线加速器，这一综合性电子束流诊断系统，包括束流位置、工作点、束流流强(电荷量)、横向截面形状(尺寸)、束团长度以及束流能谱测量等多个子系统，由 258 套束流探头、212 个输入输出控制器(IOC)以及相应的数据采集处理软件构成。投入运行的束测系统所有关键技术指标均达到或超过设计指标(表 1)[5-6]。

表 1 SSRF 束测系统性能一览表

	测量对象	设计值	实测值
直线加速器/输运线	位置	分辨率 100 μm	33 μm
	截面	分辨率 200 μm	200 μm
	电荷量	相对精度 2%	1%
	能谱	相对精度 0.1%	0.1%
	发射度	相对精度 10%	10%
增强器	位置	分辨率 100 μm	50 μm
	截面	分辨率 200 μm	200 μm
	平均流强	分辨率 50 μA	30 μA
	工作点	分辨率 0.001	0.001
储存环	位置	分辨率 1 μm	200 nm
	截面	分辨率 10 μm	10 μm
	束长	分辨率 2 ps	2 ps
	平均流强	分辨率 10 μA	2 μA
	工作点	分辨率 0.0001	0.0001

该束测系统研制过程中，新型高精度纽扣电极 BPM 探测器、数字 BPM 信号处理器、同步光空间干涉仪、数字化横向反馈、高精度逐束团电荷量测量等先进束流诊断技术均得到验证和应用。

储存环 BPM 探头设计参考了日本 KEK 光子工厂、英国 Diamond 光源、法国 Soleil 光源、美国 SPEAR3 等多家先进光源的设计优化而成，采用陶瓷真空钎焊密封、小电极尺寸(Φ10 mm)、小电极/真空室壁间隙(0.3 mm)、反极性 SMA 接头、跑道型双电极组件的结构，纽扣电极和 feedthrough 部分采用钛加工，而跑道型装配法兰采用 316 L 不锈钢加工，组件整体具有束流阻抗小、定位精度高、磁导率低的特点。

BPM 信号处理器为斯洛文尼亚 Instrumentation Technologies 公司的最新一代数字 BPM 处理器 Libera[4]，其以高速 AD(125 MHz)和 FPGA 芯片为核心，基于带通欠采样、数字下变频、数字滤波技术研制，对束流射频信号直接进行采样处理，可在不同端口提供 ADC 原始数据(百 MHz 采样率)、逐圈束流位置数据(MHz 采样率)、快反馈所需束流位置数据(10 kHz 采样率)以及静态闭轨数据(10 Hz 采样率)，覆盖直线型和环形加速器束流位置测量的所有应用。

工作于可见光波段的空间干涉仪安装在同步光监测实验室中，用空间频率相干技术对束斑截面尺寸的测量分辨率好于 10 μm，此设备可测定储存环的发射度以及强流不稳定性的流强阈值。

采用数字化反馈控制器的横向反馈系统投入使用，对 RF 前端以及反馈滤波算法进行优化后的评估测试结果证明：反馈系统对多束团强流不稳定性引起的横向振荡有明显抑制作用，抑制比好于 40 dB，是储存环稳定运行稳定出光必不可少的关键子系统之一。

储存环逐束团电荷量测量由 BPM 探头和信号完成，数据采集采用周期信号的等效采样技术，从而将量化精度及等效采样率提高到 10 bits/400 GHz 水平，使逐束团电荷量测量的精度达 0.1%。

2 SDUV FEL 装置束测系统关键技术研究

针对 SDUV FEL 装置结构紧凑、安装空间狭小的特点，进行了束测探头小型化以及基于以太网的设备控制器等关键技术的研究，popin 型截面探测器样机、以工业以太网作为现场总线的束测数据采集系统样机等，经实验室测试可满足自由电子激光装置的性能要求。

参考文献

1 SSRF 设计报告, SINAP-Report/20042–6
2 http://www.ssrf.ac.cn
3 J Odagiri, *et al*. EPICS Devices/Driver Support Modules for Network-based Intelligent Controllers, Proc ICALEPCS 2003, 494–496A N
4 http://www.aps.anl.gov/epics/
5 Leng Y B, *et al*. Beam Instrumentation System Development and Commissioning in SSRF, Proc EPAC08
6 Chen Y Z, *et al*. "SSRF Injector Diagnostics commissioning results", Proc EPAC08

LENG Yongbin, Division of Beam Instrumentation and Control

The division focuses on developing advanced technologies for accelerator control and beam diagnostics. The research programs include R&D of distributed accelerator control system architecture, advanced generic device controllers, novel sensors of electron beams, DSP based beam diagnostics technologies, new diagnostics method, etc. In 2007 –2008, the following targets have been achieved in the construction of SSRF and SINAP SDUVFEL facility.

The Control Group

1 Introduction

The SSRF control system is an EPICS-based hierarchical standard accelerator control system. The VME 64X system and PLCs are used for low level devices control and interlocks system. Serial device servers are used to connect serial devices and instrumentation to the Ethernet. System development environment of hardware and software has been set up. Models of most of sub-systems have been set up and tested with devices on schedule, such as the digital power supply control system and event-timing system[1]. The control system has been working satisfactorily even since its installation on the SSRF[2]. The high level physical application environment has been established and tested online using Matlab Accelerator Toolbox (AT) and the middle layer. The SSRF central database and a series of tools, such as configuring tools and alarming handler, have been completed. An enhanced distributed archive engine, which stores data to the central database and using native XML data type with xml schema for data storage, is under test.

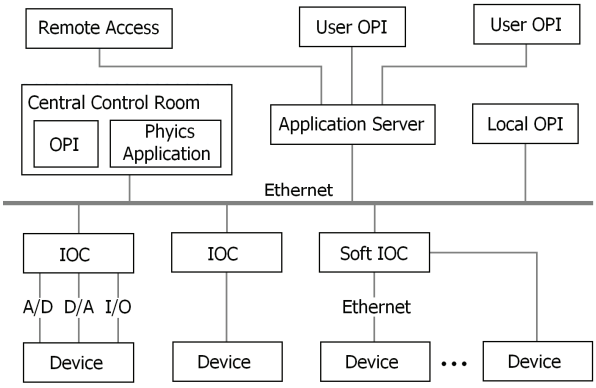

Fig.1 The schema of SSRF control system.

2 The Environment

A runtime environment of the control system has been established and in use. It consists of the network system, server system and OPI system. A developer or operator can login in on any terminal and share resources of the entire environment under one account system.

SSRF uses the 1000Base-T control network. The backbone redundancy design was adopted to ensure the network reliability, and to eliminate field buses for most device controllers. For example, most of the PLC and serial based devices (using protocol translate: serial to Ethernet translator) are connected by the control network directly and integrate with EPICS using soft IOC, which can be managed by multi-IOC running configuring system[3]. The network design is with separate sub-systems to different subnet by VLAN (Virtual Local Area Network), which can be divided and recombined conveniently and flexibly.

3 Software system

The SSRF control system runs on EPICS base 3.14.8.2, and the edm and some strip by Python are used in OPI[4]. Matlab version 2007a, Accelerator Toolbox (AT) & middle layer AT, is used for high level physics application, and MCA/LabCA is used for the control system access. A center server system, together with a series of center services, such as the IOC management system, e-log system, archive and an Oracle 10g system with RAC, is established. The entire OPI system runs on the Linux Fedora 7.

4 Device control

Installation of the device control systems for the linac, booster and storage ring, including the systems for power supplies control, vacuum control, injection/extraction control, timing and machine protection, having been installed and tested online, are in their uses in the SSRF daily operations. In addition, the insertion device control systems, and temperature-monitoring systems of the cable channels, the VME crate monitoring systems, and the audio and video monitoring systems, were completed, and they have been working satisfactorily.

As a large scale real time control system under a high interference working environment, the SSRF control system has been in reliable and stable operation in 2007–2008. Adopting various advanced digital processing systems (such as digital power supplies controller, digital BPM module, digital timing system, digital phasing control etc.), it works effectively with improved accuracy of data measurements without interference. The design of the SSRF control system, integrated a number of advanced computer techniques, such as the XML engine configuration and soft-IOC used for PLC with EPICS. Being cost-effective with good reliability and stability, the entire system provides a good readiness for commissioning the SSRF, and for completion of the SSRF project on time and in budget in the year of 2009.

The Beam Instrumentation Group

1 R&D of SSRF beam diagnostics systems

The beam diagnostics systems for the linac, transport lines, booster and storage Ring of SSRF are of a multi-functional electron beam diagnostics systems, covering the beam position monitors (BPM), tune monitors, average beam current (bunch charge) monitors, beam profile monitors, bunch length monitors, beam energy spectrum monitors, emmitance monitors, transverse feedback etc., and consisting of 258 beam sensors, 212 input/output controllers (IOC) and associate data acquisition software. After four years of development, all design goals have been achieved as shown in Table 1 [5-6].

Table 1 Design specifications of the SSRF beam diagnostics systems, and results achieved in their commissioning.

Systems	Measurement	Specifications	Achieved
LINAC /LTB /BTS	Position	100 μm	33 μm
	Profile	200 μm	200 μm
	Charge	2%	1%
	Energy	0.1%	0.1%
	Emmittance	10%	10%
Booster	Position	100 μm	50 μm
	Profile	200 μm	200 μm
	Average Current	50 μA	30 μA
	Tune	0.001	0.001
Storage Ring	Position	1 μm	200 nm
	Profile	10 μm	10 μm
	Length	2 ps	2 ps
	Average Current	10 μA	2 μA
	Tune	0.0001	0.0001

In construction of the beam diagnostics system, many advanced beam diagnostics techniques, such as high precision button type BPM pickup, digital BPM processor, synchrotron radiation interferometer, digital transverse feedback, high precision bunch-by-bunch beam charge measurement etc., were adopted after considerable evaluations of existing techniques for beam diagnostics.

The button pickup assembly is the most critical component in the ring BPM and orbit feedback system. For better installation accuracy and lower magnetic permeability, the pickup assembly is designed in a pair-button structure of titanium electrodes, two feedthroughs of 50 Ω SMA, and a 316L stainless steel housing flange. The coupling impedance is minimized by using the small-size button (Φ10 mm) and small gap (0.3 mm) between the button and housing.

The beam position monitor system is fully equipped with Libera EBPM processors. It provides the raw ADC data, turn-by-turn (694 kHz @ ring) data, fast application (10 kHz) data and close orbit (10 Hz) data at the same time, and is the most powerful tools during the commissioning and machine study of SSRF.

Synchrotron radiations to the beamlines were diagnosed with visible light. This includes the following five diagnostics measurements: a normal imaging system to monitor electron beam profile; two SR interferometers (horizontal and vertical) to do the precise beam size measurement; a 2D streak camera (HAMAMAZU C5680) for bunch length measurement and multi-bunch instability study; and a fast gated camera (gate width 3 ns) for injection optimization. The imaging system and interferometers, having been commissioned, are ready for regular operation. Results of high current (over 30 mA) beam tests showed that the beam size measurement deviation is about 1 μm. The beam size blowup introduced by small gap of insertion devices could be observed clearly in the measurements.

The FPGA-based digital transverse feedback system was implemented and applied to the storage ring. The current thresholds of instability of the ring were around 45 mA @ vertical and 190 mA @ horizontal, respectively. After applying the transverse feedback, the beam size could be minimized down to normal level. An over 40 dB attenuation of betatron oscillation was achieved, according to beam spectrum calculation from the Libera turn-by-turn data.

Dedicated ring BPM pickups were used to measure bunch-by-bunch beam charge. A PXI-based waveform recorder card (10 bits, 8 GHz sampling rate) was used to acquire the bunch charge data. Appling a new waveform reconstruction algorithm, the equivalent sampling rate of DAQ could be 400 GHz. With this configuration, the bunch charge resolution of 0.1% has been achieved.

2 R&D of SINAP SDUVFEL BI system

Due to compact design and limited installation space of SINAP SDUVFEL facility, the beam instrumentation group has been working on beam sensors minimization and development of LAN-based device controller. Laboratory tests of prototype pop-in profile monitor and DAQ system, which is based on industrial Ethernet field bus, indicate that they are fully qualified for the FEL facility.

References

1 SSRF Design report, SINAP-Report/20042–6

2 http:// www.ssrf.ac.cn

3 J Odagiri, *et al.* "EPICS Devices/Driver Support Modules for Network-based Intelligent Controllers", Proc ICALEPCS 2003, 494–496A N

4 http://www.aps.anl.gov/epics/

5 Leng Y B, *et al.* "Beam Instrumentation System Development and Commissioning in SSRF", Proc EPAC08

6 Chen Y Z, *et al.* "SSRF Injector Diagnostics commissioning results", Proc. EPAC08

机械部 2008 年项目进展

机械部　殷立新

2008 年机械工程部主要承担并完成了上海光源工程低温系统建设调试、插入件研制、设备安装等工作。

2007 年液氦低温系统的 2 次调试曾出现设备故障，2008 年初重新设计了常温氦气管道，按洁净气体管道标准进行施工，通过对全过程施工质量控制，保证了管道的洁净度。3 月中旬开始对制冷机进行调试，到 4 月底制冷机各项参数达到设计指标。8 月初，低温系统开始稳定地向超导高频腔提供制冷功率，投入加速器正式运行中。

上海光源椭圆激化波荡器主体机架制造工期由于承制单位的原因出现延误。3 月份开始，从磁铁组、机械组和维护车间抽调 4 名技术人员进驻生产厂家，协助厂家进行主体机架的组装和调试工作。7 月份完成出厂验收，运抵上海光源现场。磁铁组与机械维护车间紧密配合，于 10 月完成了该椭圆激化波荡器的磁体安装、磁测和垫补工作并通过了设备验收。在磁间隙 33 mm 时垂向磁场峰值大于 0.6 T，相位误差小于 4°。10 月底该波荡器被安装到储存环中供光束线调试使用。光束线光谱测试表明，第一台自行设计和制造的椭圆激化波荡器取得成功。

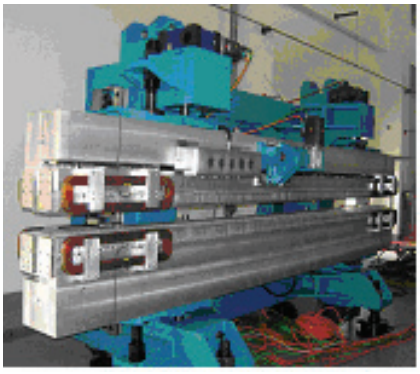

椭圆激化波荡器 EPU100

上海光源 2 台真空波荡器原计划整机从国外进口。2008 年初工程经理部接到承制公司报告的交货延期消息后，判断该进口真空波荡器已难以满足工程总体进度的要求，决定紧急启动自行研制 2 台真空波荡器供工程使用。真空波荡器结构复杂，工艺难度高，是集高精度磁体技术、超高真空技术、精密机械传动和控制技术等多项高技术于一体的先进设备。上海光源经理部从各相关系统抽调技术骨干组成项目组，于 3 月初开始集中力量进行真空波荡器研制。在对国外装置资料和国内技术条件进行全面分析的基础上开展设计工作，到 7 月中旬，项目组完成了方案设计和工程设计，并通过了经理部组织的工程设计评审。7 月下旬开始非标设备制造和标准设备采购。在作好人员、设备和技术等充分准备的情况下，于 10 月下旬在光源现场的工艺车间进行设备组装和测试。在首台组装测试过程中，发现、解决或处理了多项设计、技术、工艺问题。到 2009 年 1 月 27 日完成了第 1 台波荡器研制，2 月 25 日完成第 2 台波荡器。在磁间隙 7 mm 时磁场峰值 0.94 T，相位误差分别小于 3.1°和 2.2°。2009 年 1 月 28 日和 2 月 26 日 2 台真空波荡器分别被安装到储存环中开始为光束线调试供光。根据光束线光谱测试推算 2 台真空波荡器均达到设计指标，满足光束线调试和运行要求。

在完成上海光源工程设备研制工作的同时，机械工程部各专业组还组织完成了数次加速器机械设备的安装、加速器准直复测和维护工作，参与了深紫外自由电子激光装置等的建设工作，以及超导波荡器研制项目的调研、课题申请和前期设计工作。

真空波荡器 IVU25B

Progresses in Mechanical Engineering for the SSRF Project

YIN Lixin, Division of Mechanical Engineering

The Mechanical Engineering Division has made great efforts in the research and development of the insertion devices, and installation and commissioning of the cryogenic system of the SSRF project.

In 2007, during commissioning of the liquid-helium cryogenic system, the equipment went wrong twice. In 2008, the warm helium pipelines were redesigned, and the construction was conducted according to standard of cleaning gas pipelines. With ensured cleanliness of the pipelines through quality control of the entire construction process, the cryogenic system commissioning was started in mid March, and the refrigerating specifications were achieved at the end of April. In August, the cryogenic system started to provide refrigerating power to the super-conducting RF cavities, and it has been in stable operation since then.

The main frame manufacturing for the SSRF elliptical polarized undulator (EPU) was delayed due to the manufacturer's reasons. In March, four engineers and technicians from the magnet group, the mechanical group, and the maintenance workshop were sent to the manufacturing site, and stayed there for three months, to help the manufacturer in the main frame's assembly and test. In July, after the factory acceptance, the main frame was delivered to the SSRF site. The magnet group coordinated with the maintenance workshop closely, finished the magnet blocks installation, magnetic field measurement, and shimming for the EPU until October, when the acceptance passed. The peak magnetic field in vertical direction was more than 0.6 T and the phase error was less than 4° at the magnetic gap of 33 mm. At the end of October, this EPU was installed in the storage ring for the beamline commissioning. The light spectrum obtained on the beamline indicates that the first EPU development is successful.

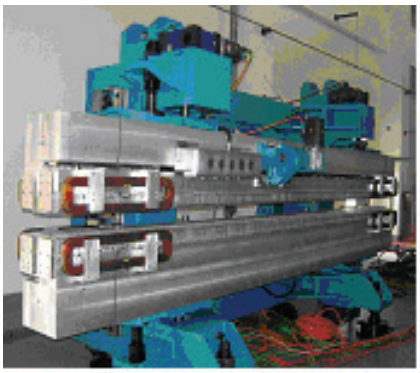

The elliptical polarized undulator EPU100.

At the beginning of 2008, a foreign manufacturer, who was contracted with SSRF for providing the two in-vacuum undulators (IVU), sent a notice of delay in delivery of the two IVUs. This would become an apparent obstacle to the in-schedule completion of the project, and SSRF decided to develop the two IVUs in house.

An IVU is of very complicated structures, and its manufacturing requests integrated high technologies of high-precision magnet technology, ultra high vacuum technology, precise mechanical transmission and control technology etc. The SSRF established a task force consisting of key scientists and engineers from relevant sectors.

All the resources available were concentrated on developing the two IVUs from the beginning of March. The design began with an overall analysis of existing devices in foreign synchrotron radiation facilities and technical conditions in China. In mid July, we completed the design, which passed the design review organized by SSRF in late July, when we started to manufacture the non-standard equipment and purchase the standard equipment.

With sufficient preparation of manpower, equipment, and technology, the equipment assembly and test was carried out in the maintenance workshop from late October. Many designing and technical problems were found and solve during the assembly and test of the first IVU. The development of the IVUs was completed after 3 months. Their test results showed that the peak magnetic field was over 0.94T and the phase error was less than 3.1° and 2.2°, respectively, at the magnetic gap of 7mm. On January 28, and February 26, 2009, the two IVUs were installed in the storage ring, respectively, and started to provide light for commissioning of the beamlines. It was predicted, from the spectrum obtained on the beamlines, that both IVUs could meet the requirements for beamline commissioning and operation.

In addition to completion of the SSRF equipment developments, each group of the division organized and completed several equipment installations and maintenance for the accelerators. Also, they took part in the construction of DUV-FEL project, and investigation and application of research programs, including the research and development of a super-conducting undulator.

The in-vacuum undulator IVU25B.

X 射线成像光学研究进展

X 射线成像光学组　肖体乔

成像光学组主要致力于 SSRF 首批光束线站之一的“X 射线成像及生物医学应用光束线站”的设计建设工作，该线站可开展动态 X 射线同轴位相衬度成像、显微断层成像(μ-CT)和其它新型成像技术的应用。

2007 年完成该线站的调整初步设计报告[1,2]和总体设计，以及光束线部件和实验站设备的设计、订购和加工等。

2008 年 9 月底完成光束线各部件和实验站设备的离线测试、整体安装集成、数据采集软件的编制及测试等。2008 年 10 月开始带光在线调试，并于年底前完成所有验收指标的内部测试，测试结果均达到验收指标。

在发展新型 X 射线成像技术方面，我们分析了同轴相衬成像中影响成像质量的若干因素[3]，开展了强吸收介质内低 Z 材料结构的 X 射线相衬成像研究[4]，以及 X 射线相衬成像在中药材显微鉴定中的应用研究[5]。我们在 X 射线成像及生物医学应用光束线站上开展了多种样品的相衬 CT 实验研究，获得了理想的三维重构像，与上海交通大学徐学敏研究组合作，开展了肿瘤形成早期钙化、新生血管形态学等实验研究。

完成了国家自然科学基金项目“具有原子分辨率的硬 X 射线全息术研究”，开展了形状记忆合金 $Ti_{50}Ni_{44}Fe_6$ 随温度变化的相变过程的荧光全息成像的实验研究，首次揭示了该材料在母相和低温公度相时的原子排列结构存在微小差异，为研究二阶相变提供了关键信息[6-8]。

2008 年开始执行国家自然科学基金项目“基于同步辐射的三维 X 射线荧光 CT 研究”(青年科学基金)。争取中的研究项目包括国家自然科学基金和上海市重点基金的合作项目、973 项目课题—临床医学影像和治疗关键技术及新型成像方法研究、X 射线相干衍射成像研究、X 射线相衬 CT 的重构算法研究和实验研究等。

参考文献

1 肖体乔，谢红兰，邓彪，杜国浩. X 射线成像及生物医学应用光束线站调整初步设计报告, 2007

2 胡雯，谢红兰，杜国浩，肖体乔. 高能物理与核物理， 2007, **31**(6): 597

3 刘丽想，杜国浩，胡雯，谢红兰，肖体乔. 物理学报，2007, **56**(8): 4556

4 师绍猛，陈荣昌，薛艳玲，任玉琦，杜国浩，邓彪，谢红兰，肖体乔. 物理学报, 2008, **57**(10): 6319

5 薛艳玲，肖体乔，杜国浩，刘丽想，胡雯，徐洪杰. 光学学报，2008, **28**(9): 1828

6 谢红兰，胡雯，罗红心，杜国浩，邓彪,，陈荣昌，薛艳玲，师绍猛，肖体乔. 物理学报, 2008, **57**(11): 7044

7 Hu Wen, Kouichi Hayashi, Naohisa Happo, Shinya Hosokawa, Tomoyuki Terai, Takashi Fukuda, Tomoyuki Kakeshita, Xie Honglan, Xiao Tiqiao. Journal of Crystal Growth, 2009, **311**: 982

8 Hu Wen, Kouichi Hayashi, Tokujiro Yamamoto, Naohisa Happo, Shinya Hosokawa, Tomoyuki Terai, Takashi Fukuda, Tomoyuki Kakeshita, Xie Honglan, Xiao Tiqiao, Motohiro Suzuki. Phys Rev B, 2009, **80**: 060202(R)– 060202-1~4

Progresses in Research of X-ray Imaging Optics

XIAO Tiqiao, Group of X-ray Imaging Optics

In 2007–2008, the X-ray imaging optics group focused on design and construction of the X-ray imaging and biomedical application beamline, which is one of the Phase I beamlines of SSRF, and on which novel imaging techniques of dynamic X-ray in-line phase contrast imaging, micro-CT imaging (μ-CT) and others can be done.

The improved R & D design[1,2] and the master design were completed in 2007, and the beamline components and the experimental station instruments were designed, ordered or manufactured.

By September 30, 2008, off-line tests of the beamline equipment and experimental station instruments, their installation and integration, and compilation and test of the data acquisition software had been completed. In October, the on-line commissioning with X-rays from the beamline was started. As of the end of the year, the in-house tests were completed and all the design specifications were achieved.

For developing the new technology of X-ray imaging, studies were carried out on factors affecting image quality of the in-line phase contrast imaging[3], on X-ray phase contrast imaging of low Z materials structure in strong absorption medium[4], and on microscopic identification of Chinese herbal medicine using X-ray phase contrast imaging[5]. Phase contrast CT experiments of several kinds of samples were performed on the X-ray imaging and biomedical application beamline, and ideal 3D images were reconstructed. In addition, we collaborated with Professor Lisa XU of Shanghai Jiaotong University in the research on early formation calcification of tumors and angiogenesis morphology.

In 2008, we completed a program supported by the Natural Science Foundation of China (NSFC), i.e. Hard X-ray Holography with Atomic Resolution, in which temperature-caused phase transition process of $Ti_{50}Ni_{44}Fe_6$, a shape-memory alloy, was studied using X-ray fluorescence holographic imaging method. It was found for the first time that there exists a little difference in atomic arrangement structure of $Ti_{50}Ni_{44}Fe_6$ between the parent phase and low temperature commensurate phase, and this provides key information for studying the second phase transition[6–8].

The NSFC program of 3D X-ray Fluorescence CT Based on Synchrotron Radiations was granted to us in 2008. And our efforts were made to gain supports for research programs of Coherent X-ray Diffraction Imaging (an NSFC program), Construction Algorithm and Experiment of X-ray CT with Phase Contrast (a key project of the Science and Technology Commission of Shanghai), and Studies on Key Clinic Imaging and Treatment Technologies and Novel Imaging Methods, a sub-project of the Major Programs for China's Development in Basic Research (the 973 Program).

Reference

1 Xiao Tiqiao, Xie Honglan, Deng Biao, Du Guohao, Regulative Original Design Report of X-ray Imaging and Biomedical Application Beamline, 2007

2 Hu Wen, Xie Honglan, Du Guohao, High Energy Physics and Nuclear Physics, 2007, **31**(6): 597

3 Liu Lixiang, Du Guohao, Hu Wen, Xie Honglan, Xiao Tiqiao, Acta Physics Sinica, 2007, **56**(8): 4556

4 Shi Shaomeng, Chen Rongchang, Xue Yanling, Ren Yuqi, Du Guohao, Deng Biao, Xie Honglan, Xiao Tiqiao, Acta Physics Sinica, 2008, **57**(10): 6319

5 Xue Yanling, Xiao Tiqiao, Du Guohao, Liu Lixiang, Hu Wen, Xu Hongjie, Acta Optica Sinica, 2008, **28**(9): 1828

6 Xu Hongjie, Hu Wen, Luo Hongxin, Du Guohao, Deng Biao, Chen Rongchang, Xue Yanling, Shi Shaomeng, Xiao Tiqiao, Acta Physics Sinica, 2008, **57**(11): 7044

7 Hu Wen, Kouichi Hayashi, Naohisa Happo, Shinya Hosokawa, Tomoyuki Terai, Takashi Fukuda, Tomoyuki Kakeshita, Xie Honglan, Xiao Tiqiao. Journal of Crystal Growth, 2009, **311**: 982

8 Hu Wen, Kouichi Hayashi, Tokujiro Yamamoto, Naohisa Happo, Shinya Hosokawa, Tomoyuki Terai, Takashi Fukuda, Tomoyuki Kakeshita, Xie Honglan, Xiao Tiqiao, Motohiro Suzuki. Phys Rev B, 2009, **80**: 060202(R)– 060202-1~4

波荡器自发辐射理论研究

同步实验部　陈鸣之　何建华

波荡器自发辐射光谱模拟计算方法研究

波荡器(Undulator)是第三代同步辐射光源的关键部件，其性能直接影响同步辐射光源性能。我们在已有的理论基础上建立了一套完整的由波荡器磁场分析其光谱特性的方法：模拟电子在磁场中轨迹，考虑电子束空间分布、角发散、能散的影响，积分计算波荡器光谱。这种方法的优点是可用模拟磁场或实测磁场参数进行计算，通用性强，可对多种波荡器进行分析，用实测磁场参数的计算结果能很好预测波荡器的光谱。这套方法对波荡器的物理设计、加工制造与验收都有辅助作用，同时也可作为波荡器自发辐射理论研究的工具。

锥形 Apple-II 波荡器的自发辐射特性研究

我们研究了锥形 Apple-II 波荡器的主要的自发辐射特性。研究表明，使 Apple-II 波荡器的磁隙作线性变化，可有效加宽波荡器辐射带宽，且增宽能量范围内的辐射特性依然良好。因此，使 Apple-II 波荡器的磁隙作线性变化，可为能量扫描实验提供便利。

参考文献

1 Chen Mingzhi, He Jianhua. Investigation of a method to calculate spontaneous radiation spectra from relativistic electrons in undulators, Chinese Physics C, 2009, 58–64

2 Chen Mingzhi, He Jianhua. Spontaneous radiation from relativistic electrons in a tapered Apple-II undulator, Nuclear Science and techniques, 2009, 5–9

Theoretical Studies on Spontaneous Radiations in Undulators

CHEN Mingzhi HE Jianhua

Division of Synchrotron Radiation Experiments

A new method to calculate spontaneous radiation spectra from relativistic electrons in undulators

Undulators are key devices to produce brilliant synchrotron radiations at a synchrotron radiation facility. We developed a numerical method, and the computer code, to simulate the electron trajectory in an undulator and calculate spontaneous radiations from the relativistic electrons. The effects of electron beam emittance and energy spread are taken into account. Comparing with other computation methods available currently, this method is advantageous in several aspects. Either measured or simulated 3D magnetic field, or arbitrary electron beam pattern, can be used for the calculation, and it can analyze undulators of any magnetic structures. It predicts precisely the practical radiation spectrum of an undulator.

Spontaneous radiation from relativistic electrons in a tapered Apple-II undulator

We studied most properties of radiations from a tapered Apple-II undulator. It was found that tapering an Apple-II undulator linearly can broaden the harmonic bandwidth and the performance of polarization is excellent in the broadened energy range. So Apple-II undulator can be tapered to provide convenience for energy scan experiment with the undulator.

References

1 Chen Mingzhi, He Jianhua. Investigation of a method to calculate spontaneous radiation spectra from relativistic electrons in undulators, Chinese Physics C, 2009, 58–64

2 Chen Mingzhi, He Jianhua. Spontaneous radiation from relativistic electrons in a tapered Apple-II undulator, Nuclear Science and techniques, 2009, 5–9

单色仪转角重复精度的位相板衍射准直方法测量

上海同步辐射光源实验部　巩志华　陈 敏　王 勇　严 睿　郜仁忠

第三代同步辐射光源对传输过程光学元件的机械精度提出了很高要求。上海光源的首批七条光束线之一的软 X 射线谱学显微光束线，采用变包含角平面光栅单色仪，其机械结构精度直接影响出射光束的能量分辨率及稳定性。由于测量原理的限制，激光干涉仪及自准直仪难以进行单色仪转角重复精度的测量，需发展新的测量方法。本组设计了半导体激光单模光纤和位相板相结合的衍射准直方法，进行高精度转角重复精度的测量，其结果明显优于商用的 ELCOMAT 3000 自准直仪。

准直激光束通过一维π阶跃位相板时将产生衍射图样，经分束后分为参考光和测量光。参考光由FT透镜聚焦在CCD靶面上形成参考光斑，测量光由平面镜反射后到达分束镜，由FT透镜聚焦到CCD上形成测量光斑。通过面阵CCD探测光斑信号，并将其转换为数字信号由计算机进行数据处理。

我们对装置的分辨率和量程的静态稳定性测试表明，其分辨率小于 0.02″，量程为 17.77′，静态稳定性良好(与自准直仪接近)；在平面镜单独运动和平面镜与光栅联动两种模式下，测得的变包含角平面光栅单色仪转角重复精度优于 ELCOMAT 3000 自准直仪。

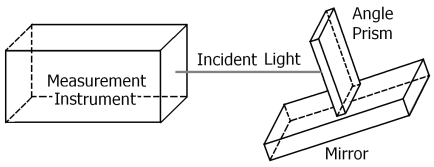

图1　面镜转角重复精度的测量原理图

在平面镜转轴上安装角棱镜(图1)，第一、二、三、四镜面分别对应于角棱镜从上往下的4个面，相邻两面的角度差为2°，在测量每一棱镜面时，调节自准直仪读数为零，使滑台下行10 mm，返回记录点纪录该点数据；然后从记录点上行10 mm，再返回纪录点纪录该点数据。重复测量5次。位相板衍射准直方法的测量步骤同自准直仪的测量步骤。结果表明，在相同的测量条件下，两种方法的测量结果很接近，说明本装置测量平面镜的转角重复精度与自准直仪基本相同。

将自准直仪和反射镜各置于平面镜一侧(图2)，自准直仪发出的光经光栅、平面镜、反射镜反射后，再次经平面镜和光栅反射而回到自准直仪，平行转动平面镜和光栅，测量角度变化，测量步骤同上文所述，选取其中四个角度测量点。位相板衍射准直装置的测量方法同自准直仪的测量方法。

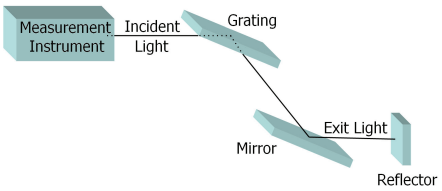

图2　联动时转角重复精度的测量原理图

结果表明，在相同的测量条件下，位相板衍射准直法测量的转角重复精度明显优于自准直仪。软X射线单色仪通常工作在掠入射模式下，平面镜和光栅的转角范围为–0.1°~7.5°，而ELCOMAT 3000自准直仪采用的LED光源光斑尺寸为32 mm，当掠入射角为4°时，若光全部照射在平面镜上，要求平面镜和光栅的长度为459 mm，而其实际长度仅为450 mm和170 mm，也即有近2/3的光子损失，导致自准直仪的信噪比严重偏低。而位相板衍射准直法能较好地实现掠入射条件下的转角重复精度的高精度测量。且自准直仪测量要求平面镜和光栅替代镜的面型精度好、反射率高，则制作成本很高；而位相板衍射准直装置采用稳定的准直激光束作测量基准，光束直径小于1 mm，当掠入射角为4°时所需平面镜和光栅替代镜的长度仅为15 mm，镜子制作成本大为降低。

该方法结合位相板衍射准直技术和半导体单模光纤技术，采用直径小于1 mm的激光束，可实现掠入射情况下变包含角平面光栅单色仪的转角重复精度的高精度测量。该装置测量平面镜和光栅联动时单色仪的转角重复精度可达±0.1″，优于商用的ELOMAT 3000自准直仪的测量精度，该法可用于SSRF中其他光束线的光学元件转角重复精度的测量。目前，该装置只能测量一个方向的角度变化，自准直仪可同时测量两个方向的角度变化，下一步工作将设计能同时测量*X*、*Y*方向角度变化的装置。

参考文献

1　巩志华，陈敏，王勇，严睿，郜仁忠. 单色仪转角重复精度的位相板衍射准直方法测量，光学学报，2009，**29**(10): 2813-2817

2　李直，赵洋，李达成. 光学学报，2001, **21**(9)：1079–1083

Measurement of Monochromator Angle Repeatability by Phase Plate Diffraction Collimation Method

GONG Zhihua CHEN Min WANG Yong YAN Rui TAI Renzhong
Division of Experimental Stations

In order to measure the mechanical angle repeatability of the variable-included-angle plane-grating-monochromator used in the soft X-ray spectromicroscopy beamline at SSRF, a new method was proposed based on the phase plate diffraction collimation. This system was designed combining laser diode fiber with phase plate diffraction collimation technique. A 2-dimension CCD was adopted to collect the images, which has been used to measure the displacement of the light spot, and thus the angle repeatability of the plane mirror and the grating could be determined. The results shows that this method could be used to measure the monochromator's angle repeatability in a higher precision estimated to be ±0.1″, which is better than that measured by the commercial ELCOMAT 3000 Auto collimator used in a same condition.

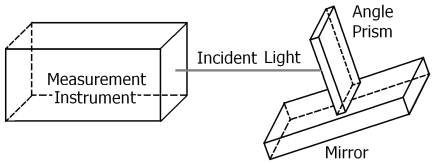

Fig.1 Principle of measuring the plane-grating–monochromator.

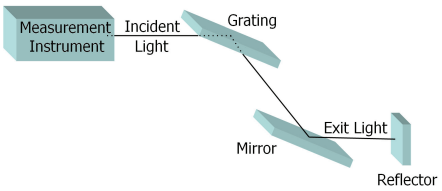

Fig.2 Schematics of the angle repeatability measurement of the monochromator.

Referencs

1 Gong Zhihua, Chen Min. Wang Yong, Yan Rui, Tai Renzhong. Journal of Optics, 2009, **29**(10): 2813–2817

2 Li Zhi, Zhao Yang, Li dachneg. Journal of Optics, 2001, **21**(9): 1079–1083

上海光源首批光束线站安全联锁控制系统

束线工程部　龚培荣　朱周侠

1　光束线站安全联锁控制系统概述

上海光源光束线站安全联锁控制系统包括人身安全联锁系统与设备保护联锁系统，前者在光束线站运行时确保棚屋内运行和实验人员不受到同步辐射的意外伤害，后者则确保光束线站诸设备的安全运行。

安全联锁系统的设计，因棚屋结构和线站设备而异。而棚屋设计中，有辐射防护要求的棚屋数目不等(1 个、2 个或 3 个)，人身安全联锁系统须针对任何棚屋结构保障所有实验人员的人身安全。唯当规定的联锁条件得以满足，方能打开光闸引入同步光进行实验；并有严格的逻辑关系和保障措施，以实现人身安全保护。

设备保护系统分为前端区设备控制联锁和束线设备联锁保护。前端区设备控制联锁系统根据前端类型分为插入件前端和弯铁前端两种系统，它们所涉信号量和工作状态参量不同，要根据具体情况编写控制程序以实现前端设备的控制和联锁保护。束线设备联锁保护系统因束线而异，须满足光束线的具体工作需求，实现光学设备的保护。

2　光束线站安全联锁控制系统的设计

在安全联锁系统的设计过程中，主要解决的技术问题是系统信号的可靠性，我们采用了关键部件使用双信号判断原则、失效即保护原则以及冗余控制技术。设计采用 Allen-Bradley 公司的 ControlLogix 系列 PLC，通过 Ethernet/IP 以太网工业协议实现与上位机 IOC(I/O Controller)通信，由上位机与 PLC 通信实现实验条件下棚屋门和相应光闸的开关控制及其状态的指示。通过网络传递，安全联锁系统的状态可以十分便捷地在 EPICS 软件环境下的 OPI 上显示，并实现人机对话。

此外，系统还采用触摸屏技术显示系统的运行状态以及故障报警。实验人员可在触摸屏上方便地查看设备运行状态、报警信息并进行相关操作。PLC 的高可靠性和稳定性与触摸屏的友好互动性的结合，能可靠地实现人身与设备的安全保护，最大限度地满足实验人员的需求。

3　安装、调试和运行情况

人身安全联锁保护系统从 2007 年 6 月初开始启动设计工作。2008 年 2 月 15 日，第 1 套光束线站 BL16B 人保系统设备进场安装、调试；3 月 17 日，BL14B 的人保系统设备进场安装调试。4 月 15 日，两光束线站的人保系统通过 SSRF 内部验收，满足了光束线站的人身保护要求，为光束线站的调束打下了基础。随后，承建公司的安装调试人员和控制组的技术人员共同努力，顺利完成了其余五条线站人身保护系统的安装调试工作。2008 年 7 月 22 日，通过 SSRF 组织的整体验收。

前端区设备控制和联锁保护系统从 2007 年 9 月开始启动方案设计。11 月 26 日开始安装，12 月 18 日，七条光束线前端控制电缆全部安装到位，同时临时联锁方案也完成信号接线和调试工作，满足了加速器储存环的调束要求，实现了前端设备在储存环调束期间的联锁保护。2008 年 3 月 27 日，完成了除 BL08U 以外 6 条光束线前端设备的束流测试工作，相关设备都经历了 50 mA 束流下的运行考验，完成了前端光路的测量工作。之后，工作重心转向正式联锁方案的接线和调试，以及配合前端部件带光测试的准备。至 08 年 6 月底，七条光束线正式联锁方案的切换全部完成。2008 年 7 月 22 日，通过 SSRF 组织的七条光束线前端控制系统的内部验收。

光束线设备保护系统设计工作开始于 2008 年 2 月初，经过调研和讨论，完成了 BL16B、BL14B 两条光束线设备保护方案，2008 年 4 月 7 日通过了该设备保护方案的内部评审，开始工程实施。2008 年 5 月 7 日，完成了 BL16B 光束线设备保护系统的调试工作，为 BL16B 的调束提供了保障。5 月 31 日，BL14B 光束线设备保护系统的安装调试工作结束，保证了 6 月初 BL14B 调束工作的顺利进行。另外 5 条光束线设备保护系统的设计、安装和调试工作，也在此后开始并按期完成。

注：光束线设备保护系统已于 2009 年 4 月 13 日通过了 SSRF 内部验收。整个安全联锁系统运行状况良好。2009 年 4 月 29 日召开的 SSRF 国际评审会议中，安全联锁系统得到了与会评委的认同。

The Beamline Interlock System of SSRF

GONG Peirong ZHU Zhouxia, Division of Beamline Engineering

1 Introduction

The beamline interlock system includes personal safety systems (PSSs) and equipment protection systems (EPSs). The PSSs are to set up a logical action by using the searching buttons, door switches, emergency buttons etc. to interlock the photon shutters and to keep the staff and users from unexpected radiation hazard, while the EPSs are to monitor operation device parameters, such as temperature, vacuum and water flow, to protect them from possible damage when a parameter goes over its pre-set threshold. The beamline interlock system has been working properly even since their starting operation in July 2008.

The design of a PSS varies with the hutch structure and number of the hutches that need radiation protection. The design must ensure the personal safety when synchrotron radiations (SR) are emitted into a hutch of any type. Only when all the conditions of an interlock system are met, can the shutters be opened to let the SRs go to the experiment station. Any non-standard operation is regarded as illegal and cannot operate shutters.

The EPSs include front-end equipment control and interlock system and beamline equipment protection system. The EPS designs vary from front-end to front-end, e.g. the front ends of an insertion device or a bending magnet differ greatly from each other in their signals and parameters. A beamline equipment protection system must satisfy requirements to protect optical components of the beamline.

2 Design of the Interlock Systems

Because signal reliability is of the top importance for an interlock system, the principles to design the system are: redundant control, fault-failure and dual signals to determine the status of key components.

As the heart of a system, the Allen-Bradley PLC of ControlLogix5561 is of high reliability and stability. And separately isolated input/output modules can reduce possible interference among signals. The PLC communicates with the I/O controller by Ethernet/IP for status control of the hutch door and corresponding shutters. And status of the interlock system can be displayed on OPI programmed by EPICS, via a friendly human-machine interface. A beamline interlock system has a Panel View touch screen displaying the status and alarm information, and this facilitates a user to check all the status details and operate the panel for switching on/off the vacuum valves and photon shutters. All these provide high reliability and stability, and great convenience and flexibility, meeting the user demands the uttermost.

3 The System Installation, Commissioning and Operation

The PSSs design was start in June 2007. In February to April of 2008, the first two PSSs were installed and commissioned successively on the BL16B and BL14B beamlines. Meeting the protection requirements, the two PSSs were checked and accepted on April 15 by the SSRF project, as a prelude for commissioning the first two SSRF beamlines and obtaining monochromatic SR lights. Subsequently, between the joint efforts of the installation and commissioning team and the beamline control group, the PSSs for the other five beamlines were completed. On July 22, 2008, the entire work on PSSs of the seven Phase I beamlines was checked and accepted by the SSRF project.

Designs of the front-end equipment control and interlock systems began in September 2007, and installation of the interlock systems began on November 26. By December 18, all control cables of the seven front-ends had been installed, while completing the temporary interlock signal wiring and tests to realize interlock protections required for beam-tuning of the storage ring. As of the end of March 2008, online tests of 50 mA beam current for all the front-ends of beamlines except BL08U were completed. In the next three months, the temporary wiring works were transformed into permanent ones, and the interlock programming and optical test preparation were completed. On July 22, 2008, front-ends equipment control and interlock systems of the seven Phase I beamlines were checked and accepted by the SSRF project.

Design of the beamline equipment protection systems was initiated in early February 2008, and extensive survey and discussions were carried out for the BL14B and BL16B equipment protection scenario, which was reviewed and approved by the SSRF project on April 7. The equipment protection system of BL16B was completed, and was commissioned on May 7, two days before beam-testing of the beamline. The equipment protection system of BL14B were completed and commissioned as of the end of May. And works on the other beanlines were conducted smoothly in the following months.

The beadmline interlock system began operation in July 2008. It works reliably an communicates smoothly with other interlock systems and control systems.

---

* The entire work of beamline equipment protection systems was checked and accepted by the SSRF project in April 2009, and was appreciated by the international review committee of the SSRF in April 2009.

安全、健康与环境保护

技术安全技术部　夏晓彬

技术安全技术部集研究、工程设计与建设、以及安全技术支撑为一体，从事辐射安全/核安全及相关研究。主要工作包括：设计、建设、运行以及评价辐射安全系统；提供辐射安全与核安全、消防安全、生物/化学品使用安全、特种气体和特种机械设备使用安全等必要的技术保障；提供工作环境安全、人员健康和园区周边环境保护相关的技术支持和监督；提供放射性危害因素检测评价、放射防护项目预评价和控制效果评价技术服务。

辐射安全

1　辐射防护研究

2008 年度重点开展了高能粒子辐射防护研究。高能粒子与物质的相互作用过程复杂，难以用实验方法作系统研究，数值模拟法成为高能粒子辐射防护研究的重要手段。建立了复杂几何条件的辐射屏蔽数值模拟计算系统，对高能电子、质子和重离子加速器设施的辐射源相、辐射场分布进行了系统研究，并应用于辐射屏蔽效果评价。图 1 为上海光源的束流垃圾桶的辐射剂量分布的模拟结果，为其辐射安全性分析提供了计算依据。

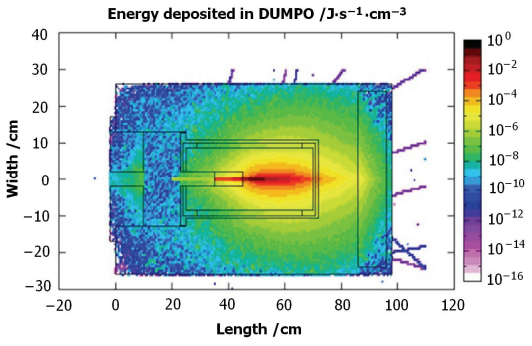

图 1　上海光源束流垃圾桶周围辐射剂量分布

2　上海光源辐射安全工程设计与建设

2008 年度建设完成了上海光源辐射安全系统，并全面投入运行。该系统包括辐射屏蔽系统、人身安全联锁系统、辐射剂量监测系统及束流损失探测系统。图 2 为 2008 年投入运行的上海光源的辐射安全系统中央控制界面。

完成了上海光源调束期间各加速器的辐射监测、光束线站棚屋检漏及光束线站的辐射安全评估；起草了《上海光源个人外照射监测与管理暂行办法》、《上海光源辐射安全管理规程》、《上海光源用户辐射安全管理规定》等辐射安全管理规定；完成了《上海光源辐射安全分析专题报告》；协助完成了放射工作人员的辐射安全培训等，为顺利获得国家环境保护部颁发的上海光源辐射安全许可证作了充分的技术准备。

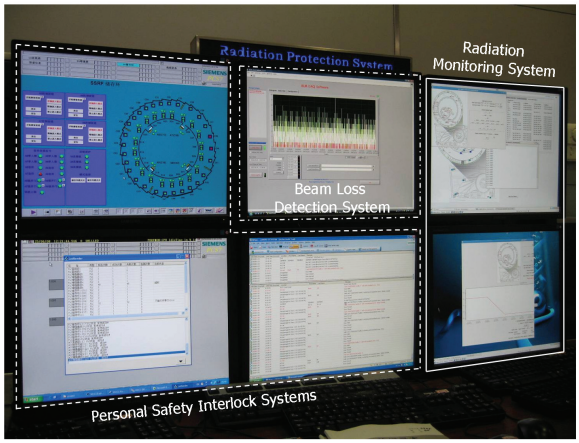

图 2　上海光源的辐射安全系统中央控制界面

3　辐射安全监测与环境保护技术支撑

负责制定辐射安全监测计划和实施。监测内容包括放射工作人员和用户的个人剂量监测、放射工作场所监测、园区内非放射性工作区及园区周边环境辐射监测。完成两园区放射工作人员的个人剂量监测、工作场所及园区周边环境的伽马及中子剂量率监测、环境样品 (流出物、地面水、土壤、植物、气溶胶) 中放射性的总 α、总 β 测量及 γ 能谱分析。

负责上海光源辐射安全系统的运行与维护、组织或协助辐射安全教育与培训、参与辐射事故和应急处置等工作。

完成嘉定园区皮秒/飞秒加速器辐射屏蔽改进和屏蔽效果评估监测；完成嘉定园区 2×6 MeV 加速器退役的辐射剂量调查；完成 101 大楼的环境辐射剂量水平调查。参加我所两座辐射加工钴源的源棒退役和加源工作，承担其中的辐射安全任务。

4 职业卫生技术服务

设立在本部门的“辐射安全检测中心”持有《上海市职业卫生技术服务资质证书》[沪卫职技字(2008)第 0023 号，放射线和放射性同位素放射卫生防护评价(乙 A 级)]，以及上海市质量技术监督局资质认定并颁发的“计量认证证书”(证书编号 2009090755L)，依法进行放射性危害因素检测与评价， 以及职业病危害(放射防护)项目预评价和控制效果评价。目前从事以下项目的对外技术服务：

(1) 环境、生物和建筑材料样品中放射性核素的 γ 能谱分析；(2)环境、工作场所和个人外照射剂量的热释光剂量测定与评价；(3)样品中放射性核素的总 α、总 β 活度水平测定与评价；(4)环境和场所 χ-γ 辐射剂量率监测与评价；(5)工作场所中子剂量率检测与评价；(6)样品中纯 β 放射性核素 ^{3}H、^{14}C 等活度水平测定与评价；(7)工作场所 α、β 表面沾污监测与评价

2008 年共出具各类检测报告 143 份；职业病危害（放射防护）预评价及控制效果评价报告 29 份。

5 职业健康监督与管理

组织完成了 1626 人的常规健康体检及 254 人的放射工作人员体检。

消防及其它技术安全

负责嘉定和张江园区的消防安全、生物/化学、特种机械设备和特种气体使用安全。

6 消防技术安全

上海光源运行时产生辐射，造成加速器隧道中消防安全上的特殊性，要求消防立足于防，为此，采取多种方式防止火灾发生，即使发生火情也要在最早期被探测到，以及时采取停机、停电措施。该消防设备体系包括消防报警系统、消防联动系统和消防水系统。

上海光源消防安全实行全年 24 小时连续值班制度，配有专用号码报警手机，遇紧急情况可及时报警。为使张江园区的整个消防报警和联动设备均处于正常稳定的工作状态，多次测试了的所有火灾探测器，检测了所有联动设备进行，更换了消防器材，多次进行水压喷淋试验。制订了消防安全规章制度，实验用户消防及安全管理制度、消防器材使用管理规定等一系列规章制度。

7 特种机械设备

张江园区有大小吊车 16 台，主体建筑内环型行吊 2 台(16 吨), 大小电梯 5 台。对这些设备落实了有资质的维修单定期进行维护保养和检修。嘉定园区有几台年久失修的行吊设备，请有关单位进行了检测，作了必要的维修和保养。制订了特种设备安全管理规定，落实了专人使用，并做好使用记录。

8 生物/化学和特种气体的安全

2008 年度招聘专业人员开始对化学、生物和特种气体安全进行系统、规范管理。制订了《实验室安全环保管理规定》、《使用特种气体安全管理规定》、《用户实验潜在危险性样品（临时）使用方案》、《上海光源生化实验室应急程序》等规章制度。定期对生物实验室的废水池进行抽样检查，以确定可否将剩余废水排入园区污水管道，确保不造成环境污染。

空白页

核物理与核技术

Nuclear Physics and Nuclear Techniques

相对论重离子对撞物理研究

核物理研究室　马余刚

格点量子色动力学预言了在高温高密的条件下会发生强子物质到夸克胶子等离子体(QGP)的相变。这样的物质状态存在于宇宙大爆炸百万分之一秒后，因而研究这种新物质和相变对于了解宇宙演化有着非常重要的意义。目前，通过相对论重离子对撞产生夸克胶子等离体，是唯一可能的实验手段。位于美国布鲁克海文国家实验室相对论对撞机(RHIC)，可进行高达 200 GeV 质心能量金核-金核对撞，从而有可能制造出这种新物质。本课题组于 2001 年加入 RHIC-STAR 合作组以来，主要关注奇异性、重味夸克、多粒子关联等方面的实验研究。与此同时也在理论上利用唯象模型对相对论重离子对撞动力学进行研究。

RHIC-STAR 实验研究

利用 RHIC-STAR 实验探测器进行了多方面的实验研究。首次测量了 200 GeV 能量下中心快度横向动量达 5 GeV/c 的 φ (1020)介子的自旋取向[1]。通过 φ->K^++K^-这个衰变道对质心能量为 62.4、130 和 200 GeV 的金核-金核和 200 GeV 的质子-质子，氘核-金核对撞中产生的 φ 介子进行了系统实验测量[2]。在系统性分析中，观察到 Au+Au、Cu+Cu 碰撞中 φ 介子的产额明显高于 p+p 碰撞中。通过进一步的分析，φ 介子的增强不能简单地归于小系统中 φ 介子产生的正则抑制机制，而是由于热密物质的产生从而导致的增强[3]。在 RHIC 对撞实验中世界上首次观测到了反超氚核[4]。分析了 200 GeV 的质子-质子对撞产生的中心快度非光子性电子的产额[5]。利用 RHIC-STAR 探测器测量了金核-金核对撞中质子和 K 介子比率的涨落。

RHIC 物理唯象动力学研究

用多相部分子输运模型(AMPT)研究了双强子方位角关联的横向动量和赝快度依赖性，促进了对 RHIC 物理中部分子和强子相互作用性质的了解[6]。利用多相部分子输运模型也研究了双强子关联相对于反应平面的依赖性，研究结果反映了高能量粒子穿过高温部分子物质的能量损失的路径效应[7]。而我们建议双强子关联的系统尺寸依赖性可以作为寻找 QCD 相变的探针[8]。也发现由于强烈的部分子级联产生的很强的纵向流是金核－金核中心对撞实验上观测到的双强子关联的纵向展宽的原因[9]。建议利用可辨别粒子的椭圆流的组份夸克标度律的破缺来作为 RHIC 上低能量扫描中寻找 QCD 相变临界点的一个有力的探针[10]。利用 3+1 维的流体力学模型计算了夸克胶子相，强子相，以及初始非热性产生分别对光子的产额的贡献[11]。在流体力学的框架下考虑的集体粘滞系数对体系演化的影响，和剪切粘滞系数对双轻子产生的影响[12]。在夸克组合产生强子机制的框架下，通过不同超子的横向动量分布，例如 Ω 和 φ 的价夸克横动量分布，提出了组分夸克在强子化时刻的部分子分布[13]。用多相部分子输运模型和动力学组合模型的研究发现，超氚核、氦核、质子和 Λ 的关系可以反映重子和奇异性之间的关联，这一信号可作为探索夸克-胶子等离子体(QGP)相变的重要探针[14]。另外，用相对论输运模型(ART)发现在兰州近代物理所的 CSR 能区重离子碰撞中有可观的超氚核产额，可满足对超核结合能和衰变寿命的精确测量。上述研究为我国大科学工程的物理实验提供了指导。

参考文献

1 Abelev B I, *et al.* (for the STAR Collaboration) Phys Rev C, 2008, **77**: 061902
2 Abelev B I, *et al.* Phys Rev C, 2009, **79**: 064903
3 Abelev B I, *et al.* Phys Lett B, 2009, **673**: 183
4 Chen J H (for the STAR Collaboration). Nucl Phys A, 2009, **830** : 761c; The STAR Coll. Science, 2010, **328**: 58
5 Jin F. J Phys G: Nucl Part Phys, 2009, **36**: 064051
6 Zhang S, *et al.* Phys Rev C, 2007, **71**: 064904
7 Li, W, *et al.* Phys Rev C, 2009, **80**: 064913
8 Zhang S, *et al.* J Phys, G: Nucl Part Phys, 2009, **37**: 094058
9 Ma G L, *et al.* Eur Phys J C, 2008, **57**: 589
10 Tian J, *et al.* Phys Rev C, 2009, **79**: 067901
11 Long J L, *et al.* Chin Phys Lett, 2008, **25**: 3188
12 Guan N N, *et al.* Phys Rev C, 2009, **80**: 014908
13 Chen J H, *et al.* Phys Rev C, 2008, **78**: 034907; J Phys G, Nucl Part Phys, 2009, **36**: 064016
14 Zhang S, *et al.* Phys Lett B, 2010, **684**: 224

Researches on Relativistic Heavy-ion Collisions

MA Yugang, Division of Nuclear Physics

Lattice QCD theory predicted a transition of quark-gluon plasma (QGP) at high temperature or density. It is important to search for the new matter and phase transition experimentally, because the transition is believed to occur at 10^{-6} s after the Big Bang. However, the only experimental way is by relativistic heavy ion collisions. The Relativistic Heavy Ion Collider (RHIC) at Brookhaven National Laboratory can provide colliding heavy-ion beams at 200 GeV per nucleon pair. Since 2001 when we joined the STAR collaboration at RHIC, the RHIC physics about strangeness, heavy flavor, multi-particle correlation etc have been our focus in the experiments, while phenomenological models have been used to understand the partonic dynamics in relativistic heavy-ion collisions.

Experimental researches at RHIC-STAR

Taking advantages of the STAR detector at RHIC, we have made the first analysis on spin alignment measurements for the φ(1020) vector mesons produced at mid-rapidity with transverse momentum up to 5 GeV/c for Au+Au collisions at $S_{NN}^{1/2}$= 200 GeV[1]. We have done a systematic measurement of φ meson production via its charged kaon decay channel φ->K^++K^- in Au+Au collisions at $S_{NN}^{1/2}$=62.4, 130, and 200 GeV, and in p+p and d+Au collisions at $S_{NN}^{1/2}$=200 GeV[2]. The φ meson yields in nucleus–nucleus collisions are found to be enhanced relative to those from p + p collisions. The source of enhancement of strange hadrons is related to the formation of a dense partonic medium in high energy nucleus-nucleus collisions and cannot be alone due to canonical suppression of their production in smaller systems[3]. We have observed anti-hypertriton for the first time in the world in heavy-ion collisions at RHIC[4]. We have done an analysis of mid-rapidity non-photonic electron (NPE) production in p+p collisions at 200 GeV[5]. We measured the fluctuation on p/K multiplicity ratio from Au+Au collisions using the RHIC-STAR detector.

Phenomenological study on partonic dynamics in relativistic heavy-ion collisions

The transverse momentum (p_T) and pseudorapidity (η) dependences of di-hadron correlation have been studied by using a multi-phase transport (AMPT) model, which can shed light on the knowledge of both partonic and hadronic interactions at RHIC[6]. Di-hadron azimuthal correlations relative to the reaction plane have been investigated in Au +Au collisions at $S_{NN}^{1/2}$ = 200 GeV by using AMPT model, which indicates path-length effect of energy loss in hot partonic medium[7]. The system size dependence of di-hadron correlation provides us a potential probe for locating the QCD phase boundary[8]. We found that the longitudinal broadening of near side in di-hadron correlation is generated by a longitudinal flow induced by strong parton cascade in central Au+Au collisions[9]. Number-of-Constituent-Quark (NCQ) scaling for the identified-particle elliptic flow is proposed as a probe for studying phase change in low-energy data taken at RHIC[10]. We have computed photons from the quark phase, hadronic phase and initial non-thermal contributions by a 3+1 D relativistic hydrodynamic model[11]. We have investigated the effect of bulk and shear viscosity on system evolution and production of di-lepton in hydrodynamics[12]. We proposed a new method to extract the parton distribution at hadronization with the help of the quark coalescence mechanism. For instance, the strange quark distribution can be obtained by the yield ratio the Ω and φ in the same transverse momentum of valence quark[13]. With the help of AMPT model and dynamical coalescence model, we found the information on baryon-strangeness correlation can be obtained by hypertrion, ^{3}He, p and Λ which can be a probe of quark-gluon phase transition[14]. In addition, we predicted that the yield of hyperons by ^{12}C+^{12}C at CSR energies is measurable at Lanzhou-CSR in near future, and its binding energy and life time can be learned from such measurements.

References

1 Abelev B I, *et al.* (for the STAR Collaboration) Phys Rev C, 2008, **77**: 061902
2 Abelev B I, *et al.* Phys Rev C, 2009, **79**: 064903
3 Abelev B I, *et al.* Phys Lett B, 2009, **673**: 183
4 Chen J H. (for the STAR Collaboration). Nucl Phys A， 2009，**830** : 761c; The STAR Coll. Science, 2010, **328**: 58
5 Jin F. J Phys G: Nucl Part Phys, 2009, **36**: 064051
6 Zhang S, *et al.* Phys Rev C, 2007, **71**: 064904
7 Li W, *et al.* Phys Rev C, 2009, **80**: 064913
8 Zhang S, *et al.* J Phys, G: Nucl Part Phys, 2009, **37**: 094058
9 Ma G L, *et al.* Eur Phys J C, 2008, **57**: 589
10 Tian J, *et al*, Phys Rev C, 2009, **79**: 067901
11 Long J L, *et al.* Chin Phys Lett, 2008, **25**: 3188
12 Guan N N, *et al.* Phys Rev C, 2009, **80**: 014908
13 Chen J H, *et al.* Phys Rev C, 2008, **78**: 034907; J Phys G: Nucl Part Phys, 2009, **36**: 064016
14 Zhang S, *et al.* Phys Lett B, 2010, 684: 224

低中能重离子碰撞物理与中微子国际合作

核物理研究室　马余刚

在当前国际核物理的一些前沿领域的实验与理论研究中，包括质子–质子关联函数与丰质子奇异核结构、同位旋标度率与核物质状态方程、低中能核反应中轻碎片椭圆流的核子数标度率与光子的产生、中微子国际合作(CUORE)项目等，我们得到了一些有意义的科研成果。

质子-质子关联函数与丰质子奇异核结构

完成了在日本理化学研究所 RIPS 束线上进行的丰质子核 ^{23}Al 动量分布和核反应总截面同时测量实验的数据分析工作，得到了 ^{23}Al, ^{22}Mg, ^{21}Na 等核的动量分布和核反应总截面实验结果。结合少体 Glauber 理论分析得到了 ^{23}Al 的价核子分布正常，但核芯可能有增大现象[1]。为进一步研究 ^{23}Al 的奇特结构，又在 RIPS 上进行了质子–质子关联函数测量，希望通过这一实验，找到 ^{23}Al 以及临近核的结构特征的更多证据。

同位旋标度率与核物质状态方程

同位旋效应是低中能核反应的一个重要现象。用统计擦碎模型研究了弹核碎裂反应的同位旋效应及其同位旋标度现象，并且从同位旋标度规律和对称能的关系中提取了对称能系数，计算的结果显示对称能系数和系统的激发能相关，随激发能的增加有所减小[2]。用晶格气体模型计算了平衡热源中轻碎片的同位旋效应，并提取了对称能项，发现它对温度的依赖性不强，但对密度有明显的幂指数规律[3]。用统计衰变模型(GEMINI)研究了平衡热源发射碎片的同位旋效应，研究了同位旋标度率参数与发射源大小，源的同位旋不对称性及激发能的依赖性。提取出的对称能系数约为23 MeV，其中包括体积项和表面项的贡献，表面项的贡献约占25%的贡献，说明在分析有限核和核物质的同位旋效应时是不同的，有限核的表面效应不可忽略，对称能中的表面效应也不能忽略，在综合考虑体积和表面效应的情况小，提取的对称能系数要小于只考虑体积效应的31 MeV[4]。

轻碎片椭圆流的核子数标度率与光子的产生

在中能重离子碰撞中，集体流形成于反应的重叠区，对热核的性质以及确定核态方程的软硬具有重要意义。通过对核子和轻碎片的椭圆流研究，提出了低中能核反应中的轻碎片的椭圆流的核子数标度率。进一步发现四级流与椭圆流的平方比是1/2, 并建议它可以作为反映热化程度的探针[5]。在核反应过程中，高能光子有别于强子探针，它基本不参与与周围介质发生其它的相互作用，它传达了非失真的发射源信息，从而为重构核反应过程中的核物质性质提供了可能性。通过BUU模型的模拟研究第一次发现在中能重离子碰撞中，高能光子存在象核子一样的方位角各向异性发射，无论是直接流还是椭圆流，与同一反应产生的核子流正好存在反关联，它们可能具有相同的产生源，只是产生机制不同。因此，我们期待高能光子可象核子一样—甚至更好地—来探测核反应中各阶段核物质的性质[6]。

中微子国际合作(CUORE)

CUORE (Cryogenic Underground Observatory for Rare Events)目前主要的研究目标是测量 ^{130}Te 的无中微子双 beta 衰变事件，通过无中微子双 beta 衰变的半衰期测量，进而得到中微子的质量谱。探测器材料采用 TeO_2 晶体，在 CUORE 合作中我们负责该探测器单元晶体的本底辐射、原材料纯度和宇宙射线本底测量。主要通过等离子体质谱仪(ICP-MS)测量 Te 金属，TeO_2 等原材料中的微量元素如 Ag、Au、Pt、Pb、Bi、Th 和 U 的含量，保证这些微量元素的杂质含量在实验允许值之下；研制了进行低本底 γ 测量的探测器和宇宙射线探测器。正在研制新的探测器测量和数据获取系统，能够在硬件上实现符合测量。

参考文献

1 Fang D Q, Guo W, Ma W C, *et al*. Phys Rev C, 2007, **76** : 031601(R)

2 Fang D Q, Ma Y G, Zhong C, *et al*. J Phys G, 2007, **34**: 2173

3 Su Q M, Ma Y G, Tian W D, *et al*. Chin Phys Lett, 2008, **25**: 2000

4 Tian W D, Ma Y G, Cai X Z, *et al*. Phys Rev C, 2007, **76**: 024607

5 Yan T Z, Ma Y G, Cai X Z, *et al*. Chin Phys Lett, 2007, **24**: 3388

6 Liu G H, Ma Y G, Cai X Z, *et al*. Phys Lett B, 2008, **663**: 312

Low and Intermediate Energy Heavy Ion Collision Physics, and International Collaboration of Neutrino Research

MA Yugang, Division of Nuclear Physics

Experimental and theoretical studies were conducted at SINAP on the following subjects: proton-proton correlation function and structure of proton-rich nuclei, isoscaling and nuclear equation of state (EOS), number-of-nucleon scaling of elliptic flow for light particles and photon production, and international collaboration of neutrino research.

Proton-proton correlation function and structure of proton-rich nuclei

The experiment was performed on the RIPS beam line of RIKEN, Japan. Experimental data were analyzed for measuring simultaneously the momentum distribution and reaction cross section of ^{23}Al. The momentum distribution and reaction cross section for ^{23}Al, ^{22}Mg, ^{21}Na etc were obtained. The valence proton distribution in ^{23}Al is normal, while an enlarged ^{22}Mg core is deduced to explain both the momentum distribution and reaction cross section data within framework of the Few-Body Glauber model[1]. For further investigation on the exotic structure of ^{23}Al and the neighboring nuclei, an experiment on RIPS was done again to measure the proton-proton correlation function.

Isoscaling and nuclear equation of state

Isospin effect is an important phenomenon in heavy ion collisions at intermediate energy. The isospin effect and isoscaling behavior in projectile fragmentation reactions were studied using the statistical abrasion-ablation model. The excitation energy dependence of the symmetry energy coefficient Csym is extracted from the isoscaling parameters[2]. Isospin effect of the light fragments from the equilibrated thermal sources was studied by the lattice gas model. The deduced symmetry energy from the isoscaling parameters shows little dependence on temperature but follows the power-law dependence on the freeze-out density[3]. With the statistical sequential decay model (GEMINI), the isoscaling effect from and equilibrium hot source was studied, and the dependence of isoscaling parameters on source size, source isospin asymmetry and source temperature was analyzed. Our results show that the symmetry energy coefficient Csym is about 23 MeV around the saturate density which the surface effect contributing 25% to the extract symmetry energy coefficient. This indicates that the surface contribution should be included in the symmetry energy term in finite nuclei system.

Number-of-nucleon scaling of elliptic flow for light particles and photon production

In heavy ion collisions at intermediate energies, the collective flow comes from the overlap zone of the colliding nuclei. This is important for studying the property of thermal nuclei and nuclear equation of state. We found that there is a number-of-nucleon scaling for the transverse momentum dependent elliptic flow for light particles. We also investigate the behavior of the elliptic flow (v2) and the 4th order anisotropic flow (v4), versus transverse momentum for the light fragments. v4 seems to be scaled by the square of v2 and the ratio between v4 and v2 is 1/2. This ratio value reflects that the collision system reaches to thermal equilibrium[5]. In nuclear reactions at intermediate energies, energetic photons are different from hadronic probes which can deliver an undistorted picture of the emitting source. Using the BUU model, we have found that anisotropic emission of energetic photons like nucleon also exists in the intermediate energy heavy-ion collisions for the first time. Not only directed transverse flow but also elliptic flow is anti-correlated with that of nucleon. It indicates that they are coming from the same source but different mechanism. Therefore energetic photons can serve as a good probe to nuclear matter properties[6].

Neutrino international collaboration

CUORE (Cryogenic Underground Observatory for Rare Events) mainly aim currently at the measurement of neutrinoless double beta decay (0νDBD). By the half life measurement of 0νDBD, one can get the neutrino mass scale. The main work of our group within the CUORE collaboration is to observe the low background of intrinsic radioactive contamination, purity measurement of original materials, and Cosmic ray background measurement. To guarantee the content of these elements are under the experimental background permit, the elements such as Ag，Au，Pt，Pb，Bi，Th and U were measured by ICP-MS method in Te metal and TeO_2 powder. We also developed a low background gamma detector system to monitor the gamma radiation in TeO_2 powder, and two new cosmic ray detectors to measure the cosmic flow in lab region.

References

1 Fang D Q, Guo W, Ma W C, *et al*. Phys Rev C, 2007, **76** : 031601(R)

2 Fang D Q, Ma Y G, Zhong C, *et al*. J Phys G, 2007, **34**: 2173

3 Su Q M, Ma Y G, Tian W D, *et al*. Chin Phys Lett, 2008, **25**: 2000

4 Tian W D, Ma Y G, Cai X Z, *et al*. Phys Rev C, 2007, **76**: 024607

5 Yan T Z, Ma Y G, Cai X Z, *et al*. Chin Phys Lett, 2007, **24**: 3388

6 Liu G H, Ma Y G, Cai X Z, *et al*. Phys Lett B, 2008, **663** : 312

荷能粒子束与纳米结构相互作用机制的理论研究

核物理室　朱志远

离子及电子等荷能粒子束已成为制备纳米结构器件、调整纳米材料结构和性质的重要手段，了解和掌握荷能粒子与纳米结构物质的相互作用机制，尤其是粒子辐照下纳米结构中的缺陷产生、迁移和自修补机制，对于实现控制辐照诱导的纳米材料结构转变和性质调节，具有重要意义。我组致力于荷能粒子与碳纳米结构相互作用机制的理论研究，利用分子动力学、蒙特卡罗及第一性原理方法，对该领域开展了大量研究工作，取得了一些重要成果。

离子辐照碳管过程中的化学侵蚀作用

以往观点认为，化学键能通常远小于入射离子能量，故相互作用的化学方面对离子辐照下碳纳米管中的缺陷产生机制几乎没有影响。我们对多种离子辐照下单壁碳纳米管中的损伤产生机制的分子动力学研究表明，在 25–1000 eV 能区，同非成键离子如 Ne 和 Ar 相比，C、B、N 和 Si 等离子的化学成键作用显著加强了它们对碳管的损伤能力，使损伤产额随离子质量的变化不再是单调的。离子与碳管原子间的成键相互作用，实系一种化学侵蚀过程；而质量效应仅来源于物理碰撞过程。我们的结果表明，在 1 keV 以下能区，化学侵蚀过程对于离子诱导的损伤产生机制的重要性不亚于物理碰撞过程。

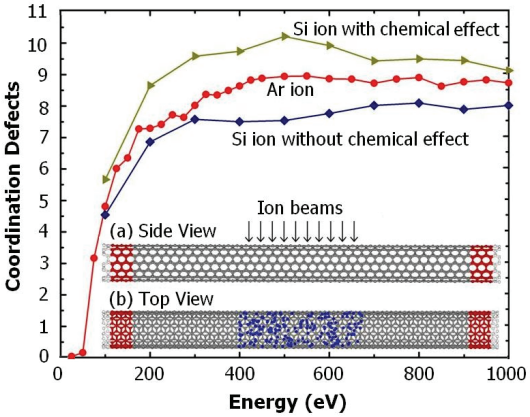

碳管半径和手性对离子辐照下碳管稳定性的影响

在粒子束与碳纳米管的相互作用机制中，碳管半径和手性的影响和作用是一个重要问题。我们发现，相对于电子束辐照下碳管半径和手性对辐照损伤机制的影响，离子束辐照下碳管的稳定性随管半径和手性的变化展现出一些奇异行为。在 1 keV 以下，碳离子辐照下的碳管稳定性不再随半径的减小，而出现反常的上升行为，使(5, 5)管的辐照稳定性优于(7, 7)管。我们还发现，在离子辐照下，锯齿型碳纳米管的稳定性优于相同半径的扶手椅型碳管。这些稳定性行为，与弯曲石墨面对外来作用的抵抗力、碳管缺陷的自修补能力以及碳管石墨网络中的成键结构的差异有关。

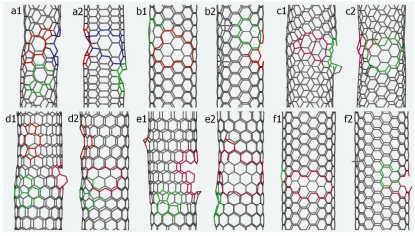

离子轰击碳管产生的各种缺陷示意图

离子在碳纳米管中的沟道效应研究

碳纳米管的优良的结构、力学性质和抗辐射能力，使人们意识到可以用其传导粒子束。我们用蒙特卡罗模拟研究了碳纳米管传导不同粒子束时，由于粒子的质量和核电荷数不同而引起的传导效应的差别。对入射粒子 He、Ar 以及 C 的两种同位素的研究发现，碳纳米管俘获入射粒子束的临界角不仅仅与入射粒子的质量存在依赖关系，且与核电荷数也有依赖关系。将入射粒子发生碰撞时的动量守恒和能量守恒关系结合考虑，推导出的广义临界角公式能解释不同原子及不同同位素在单壁碳纳米管沟道中入射临界角的差别。

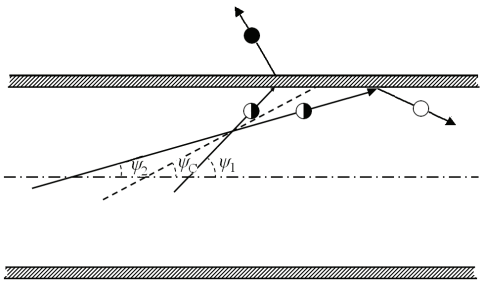

参考文献

1　Xu Zijian, Zhang Wei, Zhu Zhiyuan, *et al*. Nanotechnology, 2009, **20**: 125706

2　Xu Zijian, Zhang Wei, Zhu Zhiyuan, *et al*. J Appl Phys, 2009, **106**: 043501

3　Zheng Liping, Zhu Zhiyuan, Li Yong, *et al*. J Phys Chem C, 2008, **112**: 15204

Interaction Mechanism of Energetic Particles with Nanostructures

ZHU Zhiyuan, Department of Nuclear Physics

Irradiation with particle beams, such as ions and electrons, has been a standard and important approach for fabricating nanoscale devices and modifying the structure and properties of nanomaterials. Thus, knowledge of the interaction mechanisms between energetic particles and nanostructures, especially the defect production, mobility and self-healing mechanisms, is important for controlling the ion-induced structure transformations and property modulations of nanostructures. Our theoretical group has been concentrated in studying interaction mechanisms between ions and carbon nanostructures, using molecular dynamics, Monte Carlo simulation and ab initio methods to carry out researches on a number of subjects in this field. Some significant results have been achieved.

Chemical erosion effect of ions on CNTs

It was widely believed that chemical aspect of interactions is of no importance to the ion-induced defect production mechanism in CNTs, as the chemical bonding energy is usually much less than the incident ion energy. However, our MD study on the damage production in SWCNTs irradiated by various ion species indicated that, in the energy range of 25–1000 eV, the chemical bonding action of C, B, N and Si ions significantly enhances the damage capability of the ions to CNTs, compared to non- bonding ions such as Ne and Ar, and the defect production no longer changes monotonically with the ion mass. The bonding interaction between the ion and CNT atoms is actually a kind of chemical erosion process, in contrast to the physical collision processes governed by the mass effect. Our results indicate that in the energy range below 1 keV, the chemical erosion process plays an equally important role as the physical collision process to the ion-induced damage production mechanism in CNTs.

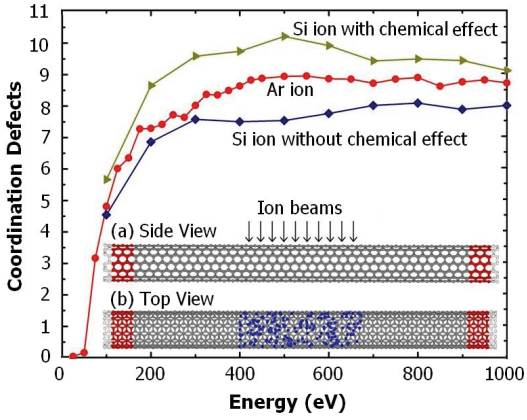

Effects of tube diameter and chirality on the stability of CNTs under ion irradiation

The role of tube diameter and chirality in the interaction mechanism between particle beam and CNTs is an important issue. Our study indicated that, in contrast to the electron irradiation results, the dependence of CNT stability under ion irradiation on the tube diameter and chirality shows strange behaviors. It was found that, under irradiation of C ions at below 1 keV, the monotonic decrease of CNT stability with radius decreasing is no longer true, and the stability of (5, 5) CNT is better than that of (7, 7) CNT. We also found that under ion irradiation, the stability of a zigzag CNT is better than that of an armchair CNT of the same diameter. These stability behaviors are closely related to the defect self-mending ability of CNTs, the resistance of curved graphite surface to the incoming actions and the bonding structure differences of CNT graphite networks.

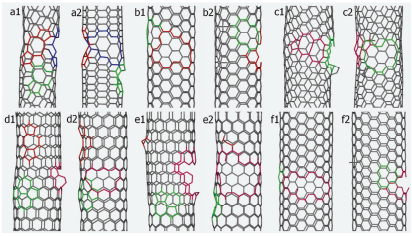

Schematics of different defects in ion-irradiated CNTs

Ion channeling in CNTs

CNTs, which possess excellent structural, mechanical and radiation shielding properties, may be considered as ideal conduction channels for particle beams. Using Monte Carlo method,we studied channeling effect in CNTs with ion species of different masses and charge numbers. By simulations with He, Ar and two isotopes of C, we found that, the incidence critical angle of ions captured by a CNT depends not only on the ion mass but also on the charge number. Combining energy conservation with momentum conservation in the process of ion collision on the CNT wall, we established a general critical angle formula to explain the differences of incidence critical angle in an SWCNT between different incident atoms and isotopes.

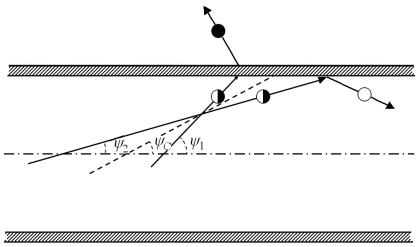

References

1 Xu Zijian, ZhANG Wei, Zhu Zhiyuan, *et al*. Nanotechnology, 2009, **20**: 125706

2 Xu Zijian, Zhang Wei, Zhu Zhiyuan, *et al*. J Appl Phys, 2009, **106**: 043501

3 Zheng Liping, Zhu Zhiyuan, LI Yong, *et al*. J Phys Chem C, 2008, **112**: 15204

应用理论物理研究

计算物理组　方海平

本组从事理论物理学与生物学的交叉研究，主要是纳米生物学和纳米尺度界面水的特性研究。本组以上海光源和我所重要研究方向为导向，与相关实验组密切结合开展应用基础理论研究，并建设相关的模拟计算平台，为实验提供模拟计算支持。已与所内多个实验组合作，并取得成功；也开展一些建立基本理论的探索性研究。

纳米水通道的电学开关特性

2003 年，美国科学家彼得·阿格雷博士因发现了允许水分子出入的细胞膜蛋白水通道而荣获当年度诺贝尔化学奖。但是，细胞膜蛋白水通道的具体工作机制仍然不完全清楚。蛋白水通道和周围的水溶液中都有电荷存在。蛋白水通道由于热噪音引起电荷移位是否会影响蛋白水通道的开或关状态？在有效电信号下，通或关的状态是否迅速响应？

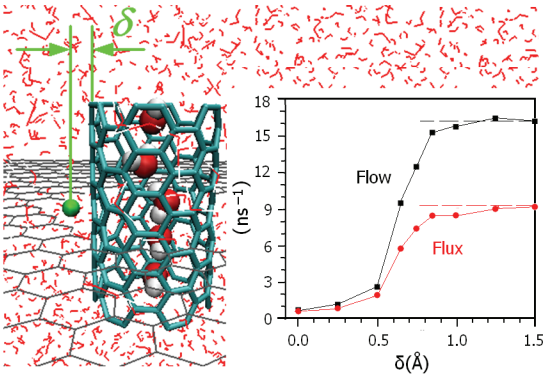

我们利用具有合适半径的纳米碳管作为生物膜蛋白水通道的简化模型，通过分子动力学模拟，在我们前期发现纳米水通道具有优异力学开关特性(J. Am. Chem. Soc. 2005,**127**, 7166–7170)的基础上，进一步发现这种纳米水通道具有优异电学开关特性。这个优异特性主要来源于限制于这种纳米水通道中的一维水链的特殊性质和水分子与电荷相互作用的局域性。该研究成果有助于理解生物分子在信号传递过程中如何保持极好信噪比的分子机制，并对设计人工分子机器也具有一定的启示性。

细胞膜蛋白水通道启发的纳米水泵

分子机器是人类的一个梦想，但目前很难做出像生物分子机器那样精细复杂的结构并实现其高级功能。我们运用分子动力学模拟方法，参考生物水通道中分布在重要氨基酸残基上的电荷分布，利用特定半径的纳米碳管，设计出纳米尺度水泵。该工作的核心是限制于这种纳米水通道中的水表现出沿着纳米水通道轴向的准一维水链，并在通道内形成准一维氢键网络的特性。在特定的电荷分布引起的非对称电场作用下，这样的准一维水链在保持特定的氢键方向的同时，又维持相对低的通透阻尼，使水分子定向地从纳米管道的一端流向另一端。

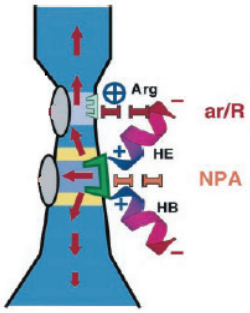

生物水通道示意图

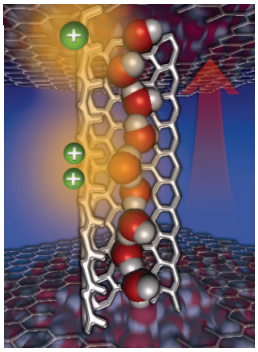

设计的纳米水泵

外界微环境对纳米碳管中水分子传输行为的影响

在宏观尺度上，当我们考虑管道内水流的时候，习惯上只关心管道大小、形状和内表面结构。但在纳米和分子尺度，情况会完全不一样。我们发现，不同的外界微环境导致通过单壁纳米管内的水流量可以有两倍的差异。这主要是单壁纳米管内水与管外原子的相互作用造成的。该研究成果有助于高速传输水的分子机器的设计，也有利于理解水分子穿过生物水通道时外界磷脂层对其传输行为的影响。

参考文献

1　Gong Xiaojing, Li Jingyuan, Lu Hangjun, Wan Rongzheng, Li Jichen, Hu Jun*, Fang Haiping*. NATURE Nanotechnology, 2007, **2**: 709–712 (Highlighted in NATURE Nanotechnology "News & Views", "NATURE China", "New Scientist")

2　Li Jingyuan, Gong Xiaojing, Lu Hangjun, Li Ding, Fang Haiping*, Zhou Ruhong*. Proc Natl Acad Sci USA, 2007, **104**: 3687

3　Gong Xiaojing, Li Jingyuan, Lu Hangjun, Zhang He, Fang Haiping*. Phys Rev Lett, 2008, **101**: 257801

Theoretical Physics for Nanobiology and Interfacial Water

FANG Haiping, Group of Computational Physics

The group is engaged in interdisciplinary studies on theoretical physics and nanobiology, focusing on molecular dynamics simulation and other computational studies on biomolecules and interfacial water. These provide theoretical assistance to synchrotron radiation studies and other experimental research programs at SINAP. Collaborating well with the experimental groups, the group has made remarkable progresses. It works on other fundamental researches, too, such as nanobubbles, nanochannels, biological channels and the structure of biomolecules.

Electrostatic Gating of a Nanometer Water Channel The transportation of water molecules across nanometer water channels in membranes plays a key role in biological activities. In this study, a single-walled carbon nanotube (SWNT) is used as a prototype to study water permeation across a nanochannel under the influence of an external charge with molecular dynamics simulations. This designed nanopore shows an excellent on-off gating behavior by a single external charge (+1.0 e), being sensitive to the charge signal when it is closed (less than a critical distance of 0.85 Å or about half the size of a water molecule), and effectively resistant to the charge noise. The effect on the flow and net flux across the channel was found to be negligible when the charge is over 0.85 Å away from the nanopore wall. This critical distance can be estimated from the interaction balance for the water molecule in the SWNT closest to the imposed charge with its neighboring water molecules and with the charge. The flow and net flux decay exponentially with respect to the difference between the two interaction energies when the charge gets closer to the SWNT wall, and reaches a very small value once the charge crosses the wall, suggesting a dominating effect on the permeation properties from local water molecules near the external charge.

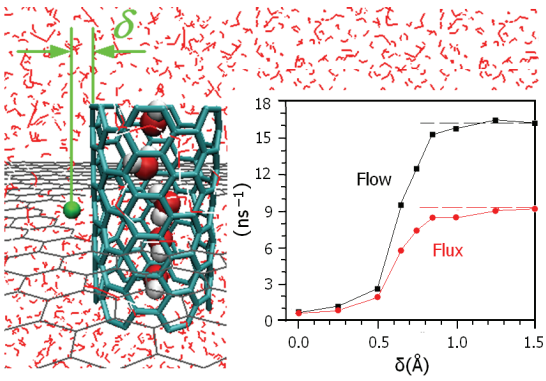

A Charge Driven Molecular Water Pump Inspired by Structure of Aquaprins Understanding and controlling the transport of water across nanochannels is of great importance for designing novel molecular devices, machines and sensors, and it has wide applications, including the desalination of seawater. Nano-pumps driven by electric or magnetic fields can transport ions and magnetic quanta, but water is charge-neutral and has no magnetic moment. On the basis of molecular dynamics simulations, we propose a design for a molecular water pump. The design uses a combination of charges positioned adjacent to a nanopore, and is inspired by the structure of channels in the cellular membrane that conduct water in and out of the cell (aquaporins). The remarkable pumping ability is attributed to the charge dipole-induced ordering of water confined in the nanochannels where water can be easily driven by external fields in a concerted fashion. The findings may provide possibilities for developing water transport devices that function without osmotic pressure or a hydrostatic pressure gradient.

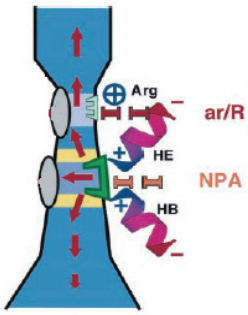

Schematics of AQP1

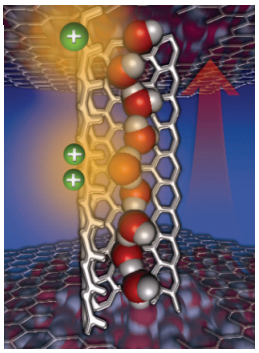

Designed Nanopump

Enhancement of Water Permeation across a Nanochannel by the Structure outside the Channel We used molecular dynamics simulation to study the effect of the external structure on water permeation across a single-walled nanochannel. In contrast to the macroscopic scenario, the outside structure greatly affects the water transport across the nanochannel. Remarkably, the ratio of maximal to minimal flux reached a value of about two for different outside structures. The findings are expected to be helpful in design of high-flux nanochannels and provide an insight into the contribution of the lipid membrane to water permeation across biological water channels.

References

1 Gong Xiaojing, Li Jingyuan, Lu Hangjun, Wan Rongzheng, Li Jichen, Hu Jun*, Fang Haiping*. NATURE Nanotechnology, 2007, **2**: 709–712 (Highlighted in NATURE Nanotechnology "News & Views", "NATURE China", "New Scientist")

2 Li Jingyuan, Gong Xiaojing, Lu Hangjun, Li Ding, Fang Haiping*, Zhou Ruhong*. Proc Natl Acad Sci USA, 2007, **104**: 3687

3 Gong Xiaojing, Li Jingyuan, Lu Hangjun, Zhang He, Fang Haiping*. Phys Rev Lett, 2008, **101**: 257801

激光-电子-伽玛光源预研

核物理研究室 SLEGS 组　徐 望

上海激光电子 γ 源(Shanghai Laser Electron Gamma Source, SLEGS)将建于 SSRF 上[1]，采用极化 CO_2 激光与 SSRF 贮存环中的 3.5 GeV、200–300 mA 相对论电子束发生康普顿散射，可得到 1–22 MeV 准单色的极化 γ 射线束，强度可达 10^{9-10} photons/s。SLEGS 建成后，可在其上开展如核物理、粒子物理及核天体物理等基础研究，也可开展工业、医学等应用研究。

为建设 SLEGS 光束线提供参考和研制依据，2005 年在中国科学院知识创新工程方向性项目(项目经费 300 万元)、中国科学院百人计划项目、上海应用物理研究所百人计划项目和上海市浦江人才计划项目的资助下，我们开始在我所现有的 100 MeV 高性能直线加速器上，建立一个低能 X 射线站作为 SLEGS 的样机，并利用它开展电子束与激光束碰撞的原理性实验研究。

在 SLEGS 样机小组全体成员，所 100 MeV 直线加速器部分人员及中科院上海光机所的参与人员的共同努力下(共约 15 人)，2008 年 4 月底，在该直线加速器上完成了 SLEGS 样机实验装置的建设。SLEGS 样机实验装置布局见图 1，主要组成部分有：多角度激光康普顿散靶室、探测器远程遥控装置、时间同步、位置同步、探测器及屏蔽、电子学和数据获取系统、激光器及光学系统、真空系统和电子动量谱仪。

2008 年 5 月和 10 月，我们共进行了两期激光康普顿散射的原理性实验，即 SINAP I 和 SINAP II。两期实验所用的 Nd:YAG 激光器其功率分别为 10 MW 和 200 MW，脉宽分别为 21 ns 和 8 ns。实验所用的电子束能量均为 108 MeV，束团宽度为 2.5 ns。SINAP I 和 SINAP II 的电子束流强分别为约 0.1 nC 和 0.01 nC。两期实验成功地实现了 ns-ns 级的电子和强激光 40°的碰撞，用 Si(Li)探测器及数据获取系统成功获得 30 keV 左右的激光康普顿 X 射线能谱。这是在国内首次测得激光与自由电子 Compton 散射光子能谱。SINAP I 和 SINAP II 的 X 射线 LCS(laser-Compton scattering)光源强度为分别是 500/s 和 50 000/s。另外，通过该电子直线加速器上的 WCM(**wall-current monitor**)等束测元件，测量得到电子的能散分辨率为 0.4 ‰左右。

SLEGS 样机实验的顺利进行，为即将在上海光源开展 SLEGS 的研究打下了坚实的基础，例如：探索和实现 SLEGS 的激光与电子的时间同步；空间重合以及碰撞模式（斜碰或正碰）等。另外，在今后两年内，上海深紫外自由电子激光装置即将建成。此装置将可实现激光与加速器电子的时间同步精度达 100 fs，提供的电子束的宽度(FWHM)为 2–3 ps。基于此装置，我们将采用高功率激光器(20 TW)研究相对论光学区（激光的归一化矢势振幅 a_0>1）的激光康普顿散射 (SINAP III)。通过 SINAP III，期望观察非线性康普顿，研究激光加速电子和新型相干光。

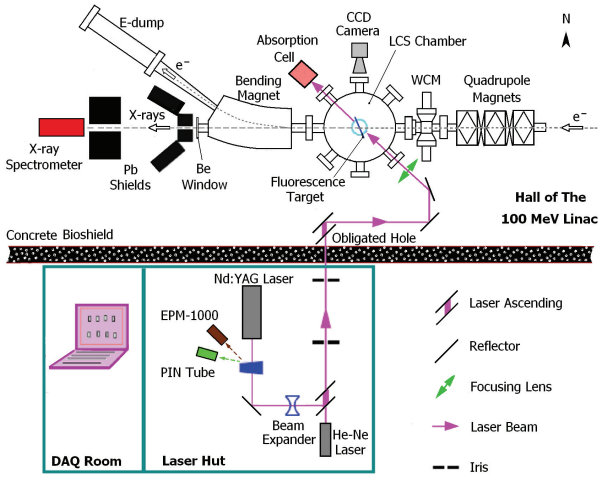

图 1　SLEGS 样机实验装置布局图

参考文献

1　Guo W, Xu W, Chen J G, *et al*. Nucl Instr Meth, 2007, **578**(A): 457

Pre-study of the Shanghai Laser-Electron Gamma Source

XU Wang, the SLEGS Group, Department of Nuclear Physics

The Shanghai Laser-Electron Gamma Source (SLEGS) [1], which will be built on SSRF, is based on laser-Compton scattering (LCS). The collision of a polarized CO_2 laser with the 3.5 GeV 200–300 mA relativistic electron bunches in the storage ring will generate high intensity (10^{9-10} photons/s) quasi-monochromatic and polarized γ-rays of tunable energies from 1 MeV to 22 MeV. These γ-rays can be used to carry out experiments for basic researches of nuclear physics, particle physics and nuclear astrophysics, and for industrial and medical applications as well.

In order to pave ways for constructing the SLEGS beam line, an experimental group was established in 2005 at SINAP to carry out principle-proof experiments of laser and electron beam collision, funded by the Chinese Academy of Sciences under the Knowledge Innovation Project (¥ 3M) and the Hundreds Talents Project, the Shanghai city under the Pujiang Talent Project of Municipal Committee of Science and Technology, and SINAP under supplementary funding to the CAS Hundreds Talents Project. Between the joint efforts of SINAP (the SLEGS group and the 100 MeV linac group) and Shanghai Institute of Optics and Fine Mechanics, which were contributed by about 15 scientists and engineers, a prototype laser-electron gamma source (LEGS), i.e. an X-ray beam line, was established in April 2008 at SINAP on the high-performance 100-MeV linac. Layout of the prototype LEGS is shown in Fig.1. It consists of mainly the multi-angle scattering Compton chamber, the X-ray detector and the remote position-control system, the synchronization system, the pulse-width overlapping system, the data acquisition system, the laser and optical system, the vacuum system, and the electron momentum spectrometer.

In May and October 2008, two principle-proof LCS experiments, i.e. SINAP I and SINAP II, were performed on the prototype LEGS, using a Q-switched Nd:YAG laser in pulse width of 21 and 8 ns (FWHM) and peak power of 10 and 200 MW for SINAP I and SINAP II, respectively, and 108 MeV E-beam bunches in 2.5 ns (FWHM) macro-pulse width. E-beam charges of about 0.1 and 0.01 nC/pulse were provided for SINAP I and SINAP II, respectively. The experiments were successful at the collision angle of about 40° between the laser and electron beams. Spectra of the generated X-ray around 30 keV were recorded by the Si(Li) detector data acquisition system. And the experimental results agreed well with theoretical predictions.

According to experimental data of SINAP I and SINAP II, in which the X-ray generation by LCS and its spectrum were observed for the first time in China, the total LCS X-ray fluxes of 500 Hz and 50,000 Hz were achieved. During the experiments, the E-beam energy spread was measured at about 0.4‰ by the wall current monitors on the linac.

The SINAP I and SINAP II experiments are of help for the SLEGS construction, with the progresses in especially synchronization of the electron and laser beams, spatial overlapping of the E-beam and laser pulses, and the interaction scheme (slanting or head-on collision).

Meanwhile, the Shanghai Deep-UV free electron laser (FEL) facility, which will be built at SINAP in two years, can provide an E-beam in macro-pulse width of 2–3 ps, hence the synchronization of ≤ 100 fs between the electron and laser beams. These will enable studies on Compton scattering in the relativistic optical region (normalized laser vector potential amplitude of a0>1), with a high peak power (such as 20 TW) laser. This will be the LCS experiments of SINAP III, in which some fundamental researches, e.g. the observation of nonlinear effects in Compton scattering and the researches of laser-accelerated electron, and a new coherent light source, will be carried out on the FEL facility.

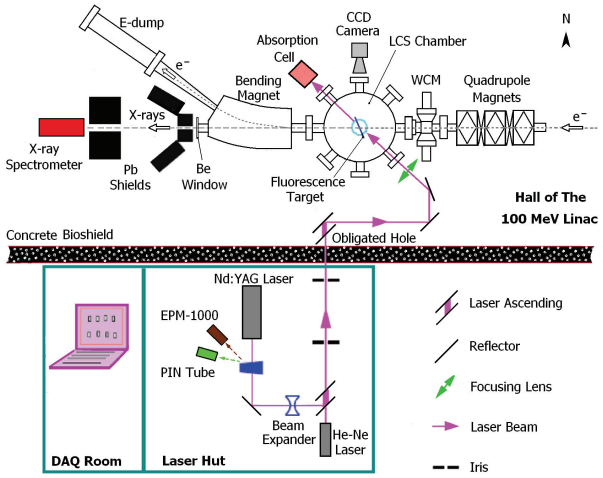

Fig.1 Layout of the prototype laser-electron gamma source.

References

1 Guo W, Xu W, Chen J G, *et al*. Nucl Instr Meth, 2007, **578**(A): 457

核分析技术在大气环境健康研究中的应用

核分析科学与技术研究室分子环境组　李 燕

上海市大气细颗粒物的污染特征

上海是中国的经济中心，2010 年的世博会还将使其成为世界关注的中心，上海市大气质量的优劣已经成为中国乃至世界关注的焦点。上海市经过多年不懈的努力，确保了基于 API3 指数的上海市大气优质率高达 84%以上，但如果上海市大气质量的评价基准由 API3 上升为 API3+细颗粒物(PM 2.5)时，上海市大气优良率将从 84%降至 50%。可见，上海市大气颗粒物污染以细颗粒物污染为主，上海市大气质量的好坏取决于大气细颗粒物的浓度。为了给上海市有关环境部门在制定大气细颗粒物防治措施上提供科学依据，保护市民的身体健康，我们用基于同步辐射的透射 X 射线显微镜(SR-TXM)、X 射线荧光分析(SR-XRF)和 X 射线吸收精细结构谱(XAFS)，以及基于 SR-XRF 和扫描质子微探针(SPM)的单颗粒指纹法和同位素比(铅、碳)的示踪法，研究了上海市大气细颗粒物的三维结构、富集元素含量的粒径分布特征、元素化学形态的粒径分布特征以及大气细颗粒物的来源。

结果表明，上海市大气颗粒物的三维结构为：汽车尾气颗粒由轻元素组成的表面和一些支撑支架构成，支架内含有数十纳米大小的铁氧化物颗粒；燃煤烟尘主要由碳等轻元素组成圆球表面，在颗粒内和表面上有很多空洞，还有少量实心碳小球；钢铁烟尘主要为附有一些实心小球的实心大球。大气颗粒物中元素粒径分布特征与其来源直接相关：来自地面扬尘和建筑尘元素(Fe、Ca、Mg、Al、Sr、Ba、U)显单一粗模态，来自工业活动元素(Pb、Cd、Se、Bi)显单一细模态；来源化学燃烧和气粒转化元素(S、As、Ag、Au、Cu、Cr、Co、Cs、Mn、Mo、K、Zn、Ni、 Na、Ga、Rb、Ti、V、W)显多模态(粗、细、超细)。大气颗粒物中元素化学形态有昼夜差异、粒径分布特征，如大气颗粒物中的铁白天以 Fe_2O_3 为主，晚上则主要以 Fe_3O_4 的形式存在；硫的质量主要集中在细颗粒中，细($PM_{2.5}$)和超细(<100 nm)颗粒物中 S 主要以硫酸盐形态存在，但超细颗粒中也还存在着一些还原态的低价态 S；中心城区颗粒物碳质成分较高。上海市大气颗粒物质量浓度的粒径谱集中在 0.611–0.380 μm 的主模态，2.38 μm 的次要模态，以细颗粒为主；由单颗粒物指纹法和同位素比示踪法估算得到上海市大气细颗粒物的主要来源是燃煤和机动车尾气，其中机动车尾气更大。

大气颗粒物和重金属的毒理学

大气颗粒物的毒性与颗粒物的大小、颗粒物中重金属含量等有关。纳米颗粒物由于体积小，易于进入人体深部，因而它的毒性可能大于粗和细颗粒物。用放射性核 ^{125}I 标记研究超细颗粒物在活体大鼠中肺和血液、脏器间的转运结果显示：超细颗粒物能从肺向血液、肝、心、肾、胃和脾等转移；有肺部炎症的大鼠，其转运程度成倍增加。由此提示：患肺部炎症、咳嗽、哮喘等人群更容易受到大气颗粒物的侵害。^{59}Fe 标记的纳米颗粒物在大鼠肺部的清除过程研究表明：不溶性超细颗粒更易通过高血压动物肺部进入体内，但较难排出体外，超细颗粒物对心血管疾病病人(如高血压)的危害比正常人群更大。

铅是对人体高度有毒的元素，但使用无铅汽油后城市儿童血铅的起源尚不清楚。为促使城市儿童血铅水平的下降，很有必要搞清影响血铅的污染源。通过铅污染来源、存在形式等的系统研究，我们发现上海市儿童血铅水平和上海大气颗粒物中铅浓度呈强的正相关，相关系数为 0.979，后者又和上海市煤的年耗量呈正相关，相关系数为 0.857。通过比较各自的铅同位素比(图 1)，我们发现燃煤烟尘可能是目前影响城市儿童血铅的主要污染源。这些燃煤烟尘应该是儿童呼吸和手接触它的沉积物经嘴进入血液。铅一旦进入血液，可能可以穿过血脑屏障后，进入海马等中枢神经系统，从而影响动物的智力，这一推断已在我们的用 SR-XRF 研究铅染毒大鼠海马中多种元素分布中得到证实。

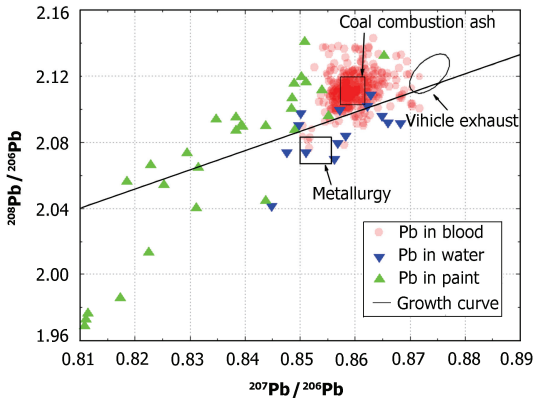

图 1 上海市儿童全血和涂料、饮水、煤飞灰、汽车尾气、冶金尘等污染源中的 $^{207}Pb/^{207}Pb$ 和 $^{208}Pb/^{206}Pb$ (Environ. Sci. Tech. 2010, 44, 4760–4765)

Application of Nuclear Analytical Technique in Atmospheric Environment and Health

LI Yan, Center for Nuclear Analytical Science and Techniques

Characteristic of fine airborne particulate matter in Shanghai

Shanghai, an economic center in China, and venue of the World Expo 2010, attracts worldwide attentions. And air quality of the city has been a worldwide focus, too. We carried out a series of studies on fine airborne particulate matter in Shanghai using synchrotron radiation-based techniques of transmission X-ray microscopy (SR-TXM), X-ray fluorescence (SR-XRF) and X-ray absorption fine structure (XAFS), together with scanning proton microprobe (SPM, for single aerosol particle fingerprint database) and isotopic tracer method. Three dimensional structure of the fine airborne particulate matter was investigated. Carbon and lead isotopic compositions and size-distribution of trace metals enriched in the airborne particulate matter were determined. Chemical speciation of some trace elements and originations of the airborne particulate matter were studied. The findings are summarized as follows.

Particles from vehicle exhaust are structured with a light element surface supported by frames consisting of iron oxides in nano-meter sizes. Particles from coal combustion are of holed spherical balls consisting of carbon and other light elements, while some of the particles, in little amount, are solid. Metallurgic dust particles are mainly formed by a large solid particle with small particles attached to it. Size distributions of trace metals are related to their sources. Metals in re-suspended road dust and cement dust, such as Fe, Ca, Mg, Al, Sr, Ba and U, show monomodal with the peak in coarse particulate matter. Metals from industrial activities (Pb, Cd, Se and Bi) are monomodal with the peak in fine particulate matter. And those from both chemical combustion and gas-particle conversion (S, As, Ag, Au, Cu, Cr, Co, Cs, Mn, Mo, K, Zn, Ni, Na, Ga, Rb, Ti, V and W) show significantly multi-modal with the peaks in coarse, fine and ultra-fine particulate matter. Chemical speciation of the trace element shows diurnal variation and size distribution. Fe exists mainly as Fe_2O_3 in daytime while as Fe_3O_4 in nighttime. Sulfur exists mainly as sulfate in fine (PM2.5) and ultra-fine (<100 nm) particulate matter, but some reducible sulfur with low valence can be found in the ultra-fine particulate matter. According to the single aerosol particle fingerprint database based on SPM and the isotopic tracer method, coal combustion and vehicle exhaust are major sources of fine airborne particulate matter in Shanghai, with the vehicle exhaust being the largest origination.

Toxicities of airborne particulate matter and heavy metal

Toxicity of airborne particulate matter may be related to its size and contents of heavy metal. Nano-particles, which access deep into the body easily due to their small sizes, show greater toxicities than coarse and fine particulate matters. Radioactive ^{125}I-labeling studies with rats revealed metastasis of the lung-inhaled ultra-fine particles into the blood, liver, heart, kidney, stomach and spleen. Another study on ^{59}Fe-labeled nano-particles being cleared off from rat lungs show that, while organisms have self-cleaning function, ultra-fine particles do more harm to cardiovascular disease (such as high blood pressure) patients.

Lead is a highly toxic element to human body, but the origin of blood lead in children is still un-clarified after phasing out of leaded gasoline. Therefore, it is necessary to find pre-dominate source of lead exposure to blood so as to control blood lead level of children. By long-term experiments, we found that blood lead concentration of children in Shanghai strongly correlates with lead content in atmospheric particles with a correlation coefficient of r=0.979, and the atmospheric lead content correlates with the coal consumption in r=0.857. Comparing lead isotopic composition in the children blood with that of each end-member of paint, water, coal fly ash, automobile exhaust, metallurgical dust (Fig.1), it can be concluded that the coal fly ash is a predominant source of Pb exposure to children in Shanghai. Once lead enters the blood, it may pass through the blood-brain barrier into central nervous system to affect the intelligence. This has been confirmed in our SR-XRF study on elemental distribution and micro-structural changes in the hippocampus of lead-poisoned rats.

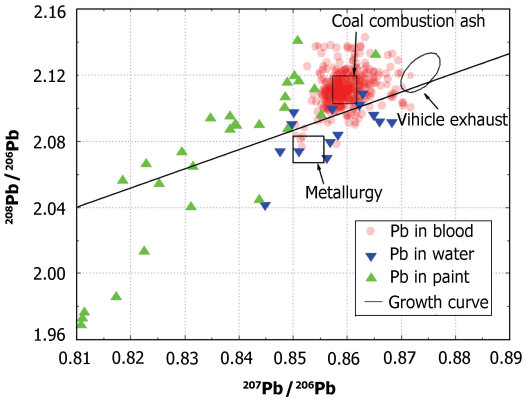

Fig.1 Lead isotope ratios of $^{207}Pb/^{206}Pb$ and $^{208}Pb/^{206}Pb$ in children's blood, paint, water and major emission sources of coal combustion ash, vehicle exhausts, and metallurgical dust. (Feng Liang, Guilin Zhang, Mingguang Tan, *et al*. Environmental Science & Technology, 2010 **44**(12), 4760-4765).

离子束驱动的碳材料的制备和性质

核分析科学与技术研究室材料组　　周兴泰

碳材料结构和性质上的多样性一直是材料科学的一个研究焦点，尤其是一些新型碳材料（如富勒烯、碳纳米管、金刚石薄膜和磁性碳）极大地扩展了碳材料的研究领域，并且，这些新型碳材料有很多潜在的应用前景，所以这些新型碳材料受到广泛地关注。

通常，碳材料是在平衡态或准平衡态条件下制备的。不过，目前很多新型碳材料是在远离平衡态的条件下制备和改性的。离子束辐照和等离子处理是典型的非平衡技术，且这两种技术能对碳材料的性质有很多有效的改进。例如，离子束辐照是一种有力的驱动碳纳米材料自组织生长和调节碳材料性质的工具[1]。离子束还能以可控的方式聚焦扫描样品。微波等离子体在制备材料过程中具有低反应温度、短的反应时间和高生产率等特点。

材料组聚焦在利用离子束和等离子体等技术来制备和改性一些新型碳材料的研究上。研究这些新型碳材料的性质，并对其潜在应用进行探索研究。我们的研究分为如下三部分: (1) 离子束驱动的碳纳米管网络的构建和性质; (2) 利用等离子体化学气相方法制备金刚石纳米结构; (3) 离子束注入诱导的磁性碳材料的研究。

离子束驱动的碳纳米管网络的构建和性质

用 40 keV Si 离子束在不同温度和不同剂量的条件下辐照多壁碳纳米管，用透射电镜观察辐照的碳纳米管的结构变化。发现在高温辐照的相邻的碳纳米管分享共同的石墨层，也就是形成碳纳米管结[2]，如图 1 所示。我们的实验表明，在 5×10^{16} ions/cm^2 注量条件下，在 600–850 K 的温度范围内，碳纳米管结都保持很好的石墨有序结构。碳纳米管结的形成是离子束辐照和高温共同作用的结果，也就是说，离子束辐照的碳纳米管焊接是高温下碳纳米管中的缺陷产生和复合共同导致的结果。

还研究了辐照的碳纳米管薄膜的导电性。厚度为 2 μm 的碳纳米管薄膜在不同温度下用 Ar 和 H 离子束进行辐照，发现在 800 K 辐照的碳纳米管薄膜的导电性能提高~30%。其导电性的提高是由高温离子束辐照的碳纳米管形成的共价键连接造成的。

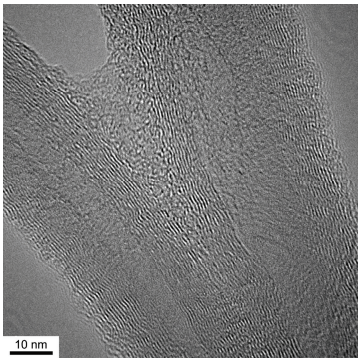

图 1　在 600 K、5×10^{16}/cm^2 Si 离子束辐照下形成的碳纳米管焊接的高分辨透射电镜图像

用等离子体化学气相方法制备金刚石纳米结构

一维纳米结构(管、线、带等)具有的特殊性质和潜在应用前景，使该类结构受到极大关注[3,4]。我们改进了微波等离子体化学气相沉积金刚石的工艺。此研究方向主要是制备金刚石纳米结构。在温度为 850℃，气压为 80 Torr(10.7 kPa)，2.45 GHz 微波频率的条件下，利用 Ar/N_2/H_2/CH_4 混合气体，在硅衬底上合成出了金刚石纳米棒。

作为亚稳态一维纳米结构，金刚石纳米棒只能在某些临界条件下生长。这些临界条件必须同时符合亚稳态热动力学和一维纳米结构生长条件。实验发现，在我们的掺氮、富氩、高功率微波等离子体环境中，高浓度的甲烷气体对于形成一维纳米金刚石极为有利(图 2a)。在这种环境下，往往形成内核为金刚石，外层为石墨带的复合型一维碳纳米结构。

实验还发现，在未掺氮的富氩气等离子体环境下(只有 Ar/H_2/CH_4)，金刚石纳米棒(图 2b)也能生长。在无氮的情况下，形成一维结构的主要原因归结为聚乙炔链的形成。由于 Ar+或 Ar* 对气体分子的碰撞，激发出多种复杂的有机分子结构，其中包括过渡态的聚乙炔分子和多环芳烃[5]，这些过渡态有机分子结构帮助形成了一维碳纳米结构（一维碳纳米结构经重组形成金刚石纳米棒）。氮的添加对于沉积物的结构有很大影响，而对形貌影响很有限，并且在一维形貌的产物中没有氮的掺杂。据此推测，一维结构的形成跟氮的掺杂没有太大关系，更大的关联性是在于与氮添加有相似作用的气相表面化学和动力学行为[6]。

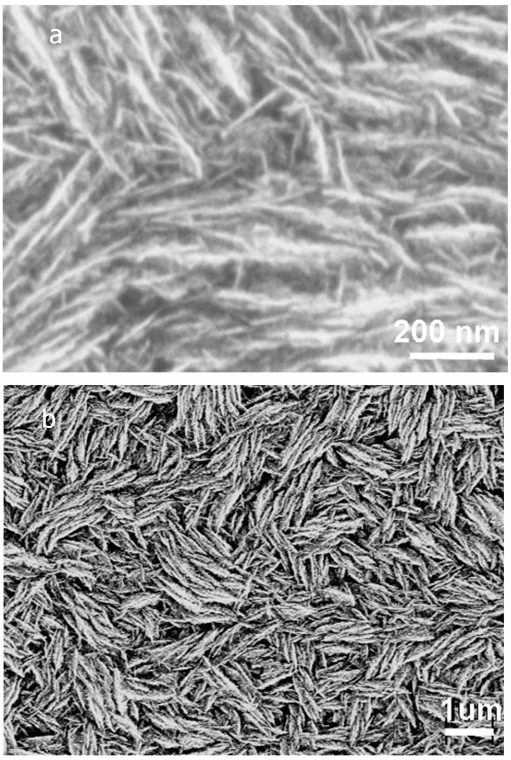

图 2 添加氮(a)与不添加(b)氮(b)的微波等离子体条件下生长的金刚石纳米棒薄膜的正面 SEM 照片

离子束注入诱导的磁性碳材料的研究

对纯碳室温磁性的报导[7,8]引起了人们对在这些材料中磁性起源及应用的前景的研究。在室温下用$^{12}C^{+}$辐照的方法在高序热解石墨中诱导出了宏观磁性，磁化强度高达9.3 emu·g^{-1}。发现样品的铁磁临界温度T_c约为460 K。注入引起的磁矩能通过改变注量来改变。

图3为室温测得的样品磁性。其中，图3(a)为空白(○)和注量为2×10^{15}/cm^2 (◆)时样品从–0.1 T~0.1 T的低磁场下的磁滞回线。注入样品的磁滞回线表明铁磁性的明显存在。图3(b)为样品在每次注入后在–1.0 T 到1.0 T的外场下测得的磁矩。图3(c)是饱和磁矩随注量的变化。注量为3×10^{14}–2×10^{15}/cm^2，饱和磁矩随注量增加。但当注量增至5×10^{15}/cm^{2}时，饱和磁矩明显降低。这表明进一步增大注量可能使缺陷密度过高，从而导致磁矩的减小[9]。缺陷密度的增加以及晶格变形的程度增加甚至非晶化可能使能带结构以及载流子的浓度偏离磁有序所需要的状态[10,11]。这说明在一定的范围内，可以调节注量来调节高序热解石墨的磁化强度。

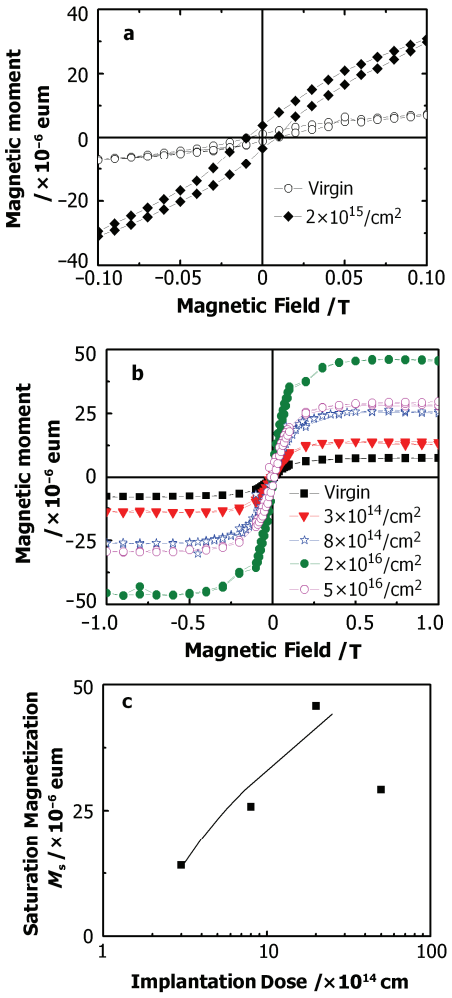

图 3 300 K 下高序热解石墨的磁矩

参考文献

1 Krasheminnikov A V, Banhart F. Nature Mater, 2007, **6**: 723–733

2 Ni Z C, Li Q T, Yan L, *et al*. Carbon 2008, **46**: 376–378

3 Zheng W P, Zu R D, Wang Z L. Science, 2001, **291**: 1947–1949

4 Zhang Y J, ZHU J. Micron, 2002, **33**: 523–534

5 Aggadi N, Arnas C, Benedic F, et al. Diamond Relat Mater, 2006, **15**: 908–912

6 CAO G Z, Schermer J J, van Enckevort W J P, *et al*. J Appl Phys, 1996, 79: 1357–1359

7 Azevedo A F, Ramos S C, Baldan M R, *et al*. Diamond Relat Mater, 2008, **17**: 1137–1142

8 Birrell J, Gerbi J E, Auciello O, *et al*. J Phys Condens Matter, 2006, **18**: S1771–S1776

9 Zhang Y, Talapatra S, Kar S, *et al*. Phys Rev Lett, 2007, 99: 107201–107204

10 Esquinazi P, Spemann D, Hohne R, *et al*. Phys Rev Lett, 2003, **91**: 227201–227204

11 Barzola-Quiquia J, Esquinazi P, Rothermel M, *et al*. Phys Rev B, 2007, **76**: 161403R–161406R

Fabrication and Properties of Carbon Materials Irradiated by Ion Beams

ZHOU Xintai YAN Long XIA Huihao YU Guojun

Materials group, Center for Nuclear Analytical Science and Techniques

Carbon materials are a focus of material science due to their various structures and properties. The field of research on carbon materials has been greatly extended ever since the discoveries of a series of new carbon materials, i.e. C_{60}, carbon nanotubes (CNTs), diamond films and magnetic carbon, which are extensively attractive with their special properties for many potential applications in advanced materials.

Usually, the carbon materials are processed in equilibrium or quasi-equilibrium states, but many novel carbon materials can be fabricated and modified in far-from equilibrium states. Ion beam irradiation and plasma treatment are typically non-equilibrium techniques to synthesize the new carbon materials, due to their effects on the carbon materials. For instance, the ion beam irradiation is a powerful tool for driving self-assembly of carbon nanostructures, with controlled property changes of the carbon materials[1]. Moreover, the ion beams can be focused onto spots of a few nanometers in diameter, and scanned in a controllable way over the material surface. Also, modification with microwave plasma is advantageous in terms of low reaction temperatures, short reaction time and high production rate.

The materials group focuses on fabrication and modification of novel carbon materials by ion beam and plasma techniques, and investigations on their improved properties towards potential applications of the carbon materials. The fields of research include (1) fabrication and properties of carbon nanotube networks by ion beam irradiation, (2) fabrication of nano diamond structures by plasma enhanced chemical vapor deposition, and (3) magnetic carbon materials by ion beam irradiation.

Fabrication and properties of CNT networks by ion beam irradiation

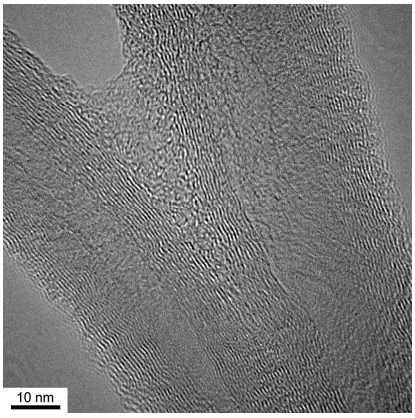

Fig.1 HRTEM images of the welding of the MWCNTs irradiated at the dose of 5×10^{16} ions/cm^2 at 600 K.

Multi-walled carbon nanotubes (MWCNTs) were irradiated to different doses by 40 keV Si ion beams at different temperatures. The radiation-induced structural change of MWCNTs and formation of MWCNT junctions were characterized by transmission electron microscopy (TEM). MWCNT junctions are formed when two adjacent MWCNTs share a common grapheme (Fig.1)[2]. Implanting the MWCNTs to 5×10^{16} ions/cm^2 at 600–850 K, the MWCNT junctions have a well-ordered structure, indicating that the MWCNT junction formation is caused by both ion beam irradiation and the heating effect by the bombardment. That is, the MWCNT welding is a result of defect production and recombination at elevated temperatures.

Microwave plasma chemical vapor deposition (MPCVD) fabrication of nano diamond structures

The main objective is to fabricate diamond nanostructures. Particularly, one-dimensional nanostructures (tubes, wires, ribbons, etc.) are in intensified studies for understanding mechanism of dimensionalities and the space-confined phenomena, and for potential applications as well [3,4]. MPCVD was used to synthesize diamond nanowires (DNRs). The synthesis was performed on (100) n-type silicon (Si) wafers using $Ar/N_2/H_2/CH_4$ mixtures, in a 2.45 GHz microwave plasma system, at the substrate temperature of 850°C and plasma pressure of 80 Torr.

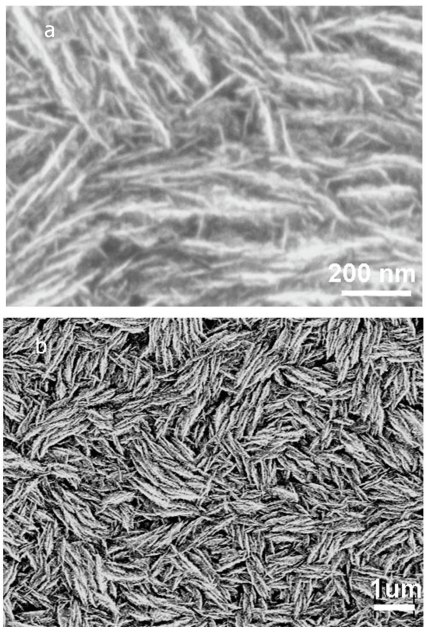

Fig.2 SEM images of high density DNRs with (a) and without (b) nitrogen addition.

As a metastable 1D nanostructure, DNRs can only grow in a critical condition for both the metastable thermodynamic and 1D growth. It was found that high concentration

methane was a major factor leading to favorable conditions for DNRs synthesis in Ar-rich environment using high microwave power (Fig.2a). The composite has high sp^3 carbon content in the nanorods along with graphite sheet surrounding the rods.

Also, DNRs were grown without nitrogen addition with $Ar/H_2/CH_4$ only (Fig. 2b). The formation of 1-dimensional nanostructure can be carried out by polyacetylene chains like C-H in the Ar rich plasma in the absence of nitrogen. The excitation processes due to collisions between Ar ions led to the formation of a complex mixture of organic molecules including trans-polyacetylene and polycyclic aromatic hydrocarbons[5], which helped to form the nanostructures. The N_2 addition is more influential in terms of structural changes than morphology changes. Any dependence of the N_2 addition on morphology is not a result of nitrogen incorporation, but a result caused by nitrogen related surface processes with changes in gas phase chemistry and surface kinetics[6].

Magnetic carbon by ion beam irradiation

The magnetism of pure carbon materials[7,8] have stimulated research interest in determining the origin of magnetism of the materials and exploring prospective applications. We have worked out an experimental method to induce macroscopic magnetization (as large as 9.3 emu·g^{-1}) at RT in highly oriented pyrolytic graphite (HOPG) samples by using $^{12}C^+$ ion implantation. It was found that the ferromagnetic critical temperature, T_c, of the sample is about 460 K. The implantation-induced magnetic moments in the sample could be tuned simply by changing the implantation dose. Fig.3 shows the measured magnetic moments of the HOPG sample at 300 K.

Fig.3(a) shows the magnetic hysteresis loops, in a low field from –0.1 T to 0.1 T, of the HOPG sample before (○) and after (◆) implantation with 2×10^{15}/cm^2 of $^{12}C^+$ ions. The loop of the implanted sample clearly shows ferromagnetic behavior. Fig. 3(b) shows the magnetic moments measured after each implantation stage for an applied magnetic field cycled between –1.0 T and 1.0 T. Fig.3(c) depicts the measured saturation magnetic moment as a function of the implantation dose. For the doses ranging from 3×10^{14} /cm^2 to 2×10^{15}/cm^2, the saturation magnetic moment increases with the dose. However, increasing the dose to 5×10^{15}/cm^2 decreases substantially the saturation magnetic moment. This indicates that further increase of the implantation dose may create too high a defect density, resulting in reduction of the magnetic moments induced by the defects[9], and the lattice disorder, perhaps even amorphous zones in the lattice, may destroy the band structure and carrier density that are necessary for magnetic coupling[10,11]. This suggests a dose window that can be used to tune the magnetization in HOPG.

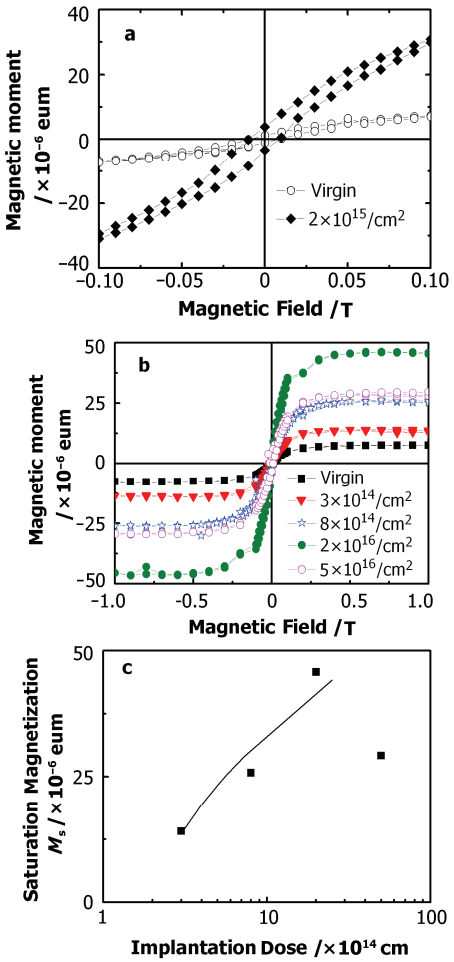

Fig.3 Magnetic moments of HOPG sample measured at 300 K.

References

1 Krasheminnikov A V, Banhart F. Nature Mater, 2007, **6**: 723–733

2 Ni Z C, Li Q T, Yan L, *et al*. Carbon 2008, **46**: 376–378

3 Zheng W P, Zu R D, Wang Z L. Science, 2001, **291**: 1947–1949

4 Zhang Y J, Zhu J. Micron, 2002, **33**: 523–534

5 Aggadi N, Arnas C, Benedic F, *et al*. Diamond Relat Mater, 2006, **15**: 908–912

6 Cao G Z, Schermer J J, van Enckevort W J P, *et al*. J Appl Phys, 1996, **79**: 1357–1359

7 Azevedo A F, Ramos S C, Baldan M R, *et al*. Diamond Relat Mater, 2008, **17**: 1137–1142

8 Birrell J, Gerbi J E, Auciello O, *et al*. J Phys Condens Matter, 2006, **18**: S1771–S1776

9 Zhang Y, Talapatra S, Kar S, *et al*. Phys Rev Lett, 2007, **99**: 107201–107204

10 Esquinazi P, Spemann D, Hohne R, *et al*. Phys Rev Lett, 2003, **91**: 227201–227204

11 Barzola-Quiquia J, Esquinazi P, Rothermel M, *et al*. Phys Rev B, 2007, **76**: 161403R–161406R

太赫兹光谱技术研究

核分析科学与技术研究室　朱智勇

太赫兹波(0.1–10 THz)位于红外和微波之间，是电磁波谱中有待深入研究的最后一个频率窗口。太赫兹时域光谱技术是近 20 年前发展起来的实验技术，可同时获得振幅和相位信息，具有无损和高信噪比等特点。本课题组致力于太赫兹时域光谱技术及其应用研究，目前工作包括太赫兹成像技术研究、化合物及生物大分子太赫兹特征光谱测量研究、纳米及纳米复合材料的太赫兹光谱性质研究以及利用辐照技术研制太赫兹波发射晶体等工作。

太赫兹成像技术研究

THz 波透过物品后携带大量信息，如何利用这些信息进行成像是目前的关键问题。本组用太赫兹时域光谱装置进行物品的二维扫描式成像研究，内容包括：(1)混合物成分分布成像研究(图 1)，建立并发展了 THz 波段混合物成分分析方法。通过引入样品表面透射系数的影响使分析精度提高了一倍以上。(2)轮廓成像研究，提出了利用峰值劈裂现象实现轮廓成像的方法。此方法可以准确鉴别出物品的外部轮廓，相对于传统成像方法具有更高的空间分辨率和更好的信噪比。(3)不同数据处理方法对于 THz 成像质量的影响。

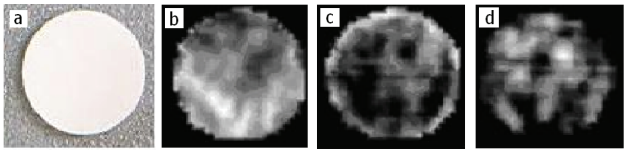

图 1　混合物(a)中的苯甲酸(b)、邻甲苯甲酸(c)和间甲苯甲酸(d)的空间分布图

分子结构太赫兹特征光谱的测量研究

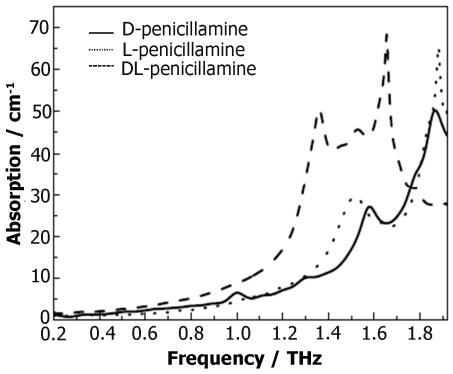

图 2　D-, L-和 DL-青霉胺室温下的 THz 吸收光谱

物质在 THz 波段的光谱吸收包含有丰富的物理化学信息。本组用 THz 时域光谱技术实现了不同结构化合物的分析检测，其中包括同分异构体、手性药物及多晶药物等。所涉及的生物分子有：糖类、氨基酸、蛋白质、DNA 碱基及修饰核苷等。利用量子化学理论计算对实验所获 THz 光谱进行了解析。探索了用 THz-TDS 技术开展有关固态化学反应的研究。结果显示，THz 光谱与分子结构、组成、相互作用及环境变化密切相关(图 2)，THz 时域光谱技术能用于不同化合物鉴定及药物合成的在线检测与质量控制，并有助于化学反应动力学研究。

碳纳米材料及其复合材料太赫兹光谱性质研究

测定了碳纳米管、C_{60}、石墨以及不同结构的碳黑材料与聚乙烯组成的复合材料的 THz 光谱性质，获得了它们的吸收系数和折射率等参数随碳的种类和含量的变化关系，并结合德拜偶极子理论对结果进行了分析。研究发现，复合材料对太赫兹波的吸收程度随碳种类的不同有很大的区别，其中 C_{60} 对太赫兹波的吸收最弱，碳纳米管则表现出非常强的相互作用。高结构碳黑和低结构碳黑与聚乙烯组成的复合材料在 0.2–1.6 THz 区域呈现不同的色散关系。在同样的掺杂浓度下，碳纳米管直径增加一倍可使复合材料对太赫兹波的吸收提高三倍。研究工作还利用有效介质理论提取了碳材料的介电参数。

离子注入制备太赫兹波发射晶体

获取具有尽可能短的载流子寿命、高的载流子迁移率和介质耐击穿强度的光电导晶体材料是提升光电导天线太赫兹脉冲发射能力的关键所在。我们用 2 MeV He 离子束注入半绝缘砷化镓(SI-GaAs)晶体，制备出与低温外延生长的砷化镓(LT-GaAs)太赫兹发射性能相当的太赫兹发射晶体。发现 2 MeV He 离子辐照产生太赫兹波发射的最佳注量在 $10^{16}/cm^2$ 左右，过高注量会使材料非晶化而丧失太赫兹波发射能力。此外，还发现用 He 离子辐照可有效修复高电压电击穿的太赫兹发射光电导天线。

参考文献

1　Zhang Zengyan, Yu Xiaohan, Zhao Hongwei, *et al*. Optics Communications, 2007, **277**: 273–276

2　Ge Min, Zhao Hongwei, Ji Te, *et al*. Chin J Chem, 2007, **25**: 272–277

3　Chen Xiliang, Ma Mingwang, Yan Xiaomin, *et al*. ACTA Physico-Chimica Sinica, 2008, **24**(11): 1969–1974

THz Spectroscopic Technique and Applications

ZHU Zhiyong, Center for Nuclear Analytical Science and Techniques

Terahertz (THz) wave band locates between far infrared and microwaves. It is the last band in the electromagnetic spectrum yet to be explored. Terahertz time-domain spectroscopy (THz-TDS) technique is becoming an attractive technique because of its unique advantages. The group is engaged in researches of THz-TDS spectroscopic technique and its applications, including THz imaging technique, specific THz spectra of compounds and bimolecular, dielectric properties in the THz range of nanometer materials and their composites with polymers, and THz emission crystal development based on irradiation technique.

THz imaging techniques

The rich information taken by THz wave transmitted through samples can be used for imaging. Based on a THz-TDS setup we carried out researches of two dimensional scanning imaging of various materials. Spatial component distributions of a mixture can be revealed (Fig.1). Integrated THz absorption spectra in the whole measuring range were taken as fingerprints of compounds. It was found that analytic precision could be improved by a factor of two, considering the transmission coefficient at the sample surface. Outline imaging by THz-TDS was proposed. Spectroscopic splitting at interface was studied. Different data processing methods were tried to optimize THz imaging quality.

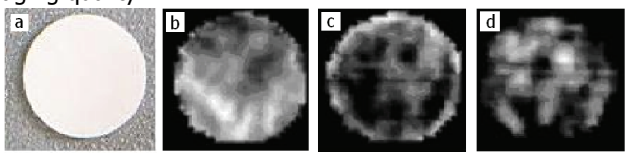

Fig.1 A mixture sample (a) and spatial distribution of its components: the benzoic acid(b), o-toluic acid(c) and m-toluic acid(d).

Specific THz spectra of molecular structure

THz wave is sensitive to different molecular species and the change of environment. On the THz-TDS setup, we carried out researches on pharmaceutical identification and analysis, including various structural compounds, isomers, chiral enantiomers and polymorphism of drug molecules. A series of important bimolecular such as saccharides, amino acids, protein, DNA bases and modified nucleoside derivatives have also been investigated. To understand the physical origins of the low frequency resonant modes, theoretical calculation, such as density functional theory (DFT), was adopted. In addition, some solid state chemical reactions were investigated. The studies demonstrate that THz-TDS is a promising and efficient tool for both qualitative and quantitative analysis of molecular structures.

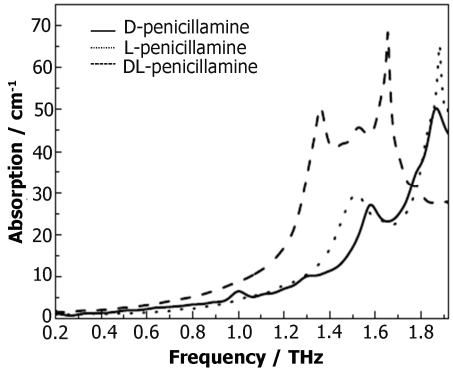

Fig.2 THz absorption spectra of L-, D- and DL-penicillamine.

THz spectra of nanometer materials and their composites

The spectroscopic properties of composites formed by filling carbon materials (including MWNT, C60, graphite and carbon black) into HDPE were studied using THz-TDS technique. It was found that the composites with different carbon materials possess vary different dielectric properties in the THz range. The HDPE/C60 has very low absorption, while the HDPE/MWNTs absorbs strongly. Under the same filler concentration, increasing the MWNTs diameter by a factor of two can lead to a three-time increase in the THz wave absorption of the HDPE-MWNTs composite. Dielectric properties of carbon materials were extracted by using the effective medium theory.

THz wave emission crystal made by MeV ion implantation

Producing a terahertz emitter of higher performance requires photoconductive materials that are of shorter carrier lifetime, reasonably good carrier mobility and high resistivity. Ion-implantation is an attractive way to modify the properties of photoconductive materials. We have successfully prepared some terahertz photoconductive antenna by implanting around 1016/cm2 He ions at 2 MeV into SI-GaAs. It was also found that the THz emission ability of an electrically break-down emitter could be recovered by the He ion implantation.

References

1 Zhang Zengyan, Yu Xiaohan, Zhao Hongwei, *et al*. Optics Communications, 2007, **277**: 273–276

2 Ge Min, Zhao Hongwei, Ji Te, *et al*. Chin J Chem, 2007, **25**: 272–277

3 Chen Xiliang, Ma Mingwang, Yan Xiaomin, *et al*. ACTA Physico-Chimica Sinica, 2008, **24**(11): 1969–1974

单分子探测与操纵研究

单分子探测与操纵组　胡　钧

以 AFM 为研究手段，在探测单个 DNA 分子的行为特征上，着重于研究 DNA 与蛋白质在固相表面上的相互作用。目的在于揭示不同外力作用下对 DNA 行为的影响。包括：对 DNA 分子本身结构的影响(如是否会引起碱基的缺失、突变)；对 DNA 分子在执行功能过程中的影响(如对 DNA 与蛋白质相互作用速率的影响)；以及是否可通过纳米操纵的手段对 DNA 与蛋白质的反应位点进行人为控制，最终达到在单分子水平上合成 DNA 分子的目的。

基于纳米操纵和单分子成像以及分析技术的 DNA 与 DNase I 相互作用的机械生化过程和动力学研究

在单分子水平上仅仅 pN 的机械力作用于单个分子就将极大影响反应的实际进程。运用外力是否对酶与机械力拉伸的单个 DNA 分子相互作用有影响，以及随后导致其动力学过程变化对于研究生物体系的机械生化过程有着重要的生物学意义。利用原子力显微镜的重定位成像，对反应前后不同拉伸程度 DNA 分子的酶切产生缺口情况进行单分子统计分析，在一定拉伸范围内揭示了该反应速率的动力学信息，并且发现在小力区适度拉伸的范围内 DNase I 酶切速率存在显著的机械活化增强现象。单个 DNA 分子在不同拉伸程度下与 DNase I 相互作用的机械生化过程对于生物分子多次反复相互作用的研究体系具有代表性意义。

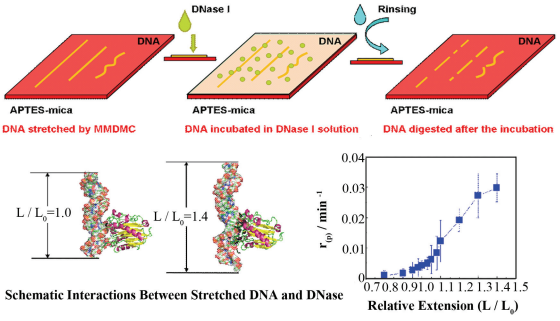

DNA 与 DNase I 的机械生化过程和动力学研究

疏水聚合物衬底上的高效率转印

疏水聚合物衬底具有柔软、重量轻、稳定性好和制备成本低等优点，在此类衬底上制作电路，是一条能便宜地获得大面积电子器件的途径，引起了人们的极大兴趣。虽然真空沉积和光刻法已在刚性的半导体基材上成功地制备图案，但是聚合物材料会在高温下降解，还能与有机溶剂或蚀刻液反应，这一方法不能用于在聚合物衬底上制备图案。如何使其他方法制备的图案转移到聚合物衬底上，是低成本制备大面积的柔性电子器件的核心问题。

我们提供了一个简单的方法来解决这个问题，即所有的转印操作都在有机溶剂气氛中进行。通过这个方法，实现了在疏水聚合物衬底上对水性‘墨水’的高效率转印。在疏水衬底凝结的有机溶剂层的作用下，分别得到了在聚二甲基硅氧烷，聚苯乙烯，和聚乙烯基对苯二甲酸酯衬底上转印的牛血清蛋白图案。同时，这个方法也可和我们以前发明的刻蚀技术(级联微缩吸附纳米刻蚀技术)相结合，以实现对其它方法制备的图案进行进一步的微缩。

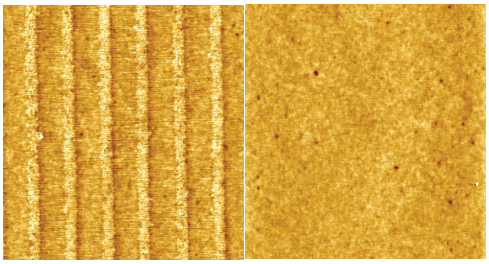

BSA在PDMS衬底上的转印

可控“蘸笔”纳米刻蚀探针修饰方法

采用改进的 AFM 探针修饰方法 —AFM 可控蘸针法替代通常的将探针浸入“墨水”的直接蘸针法，可控制“墨水”吸附在探针的针尖末端，有效避免纳米点制造过程中非定位沉积的干扰。利用该方法修饰的探针可在 DNA 分子上可控制备氯化铜溶液纳米点阵，为生物大分子的局部修饰、加工和改造提供有效途径。

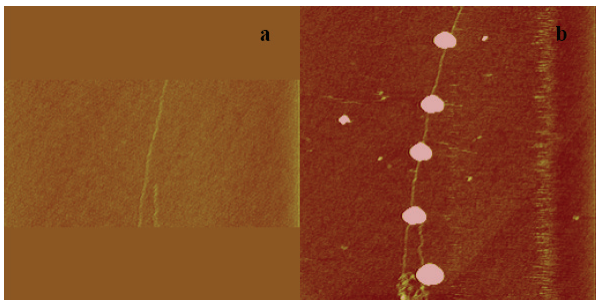

氯化铜纳米阵列

Progresses in Single Molecule Research

Hu Jun, Group of Single Molecule Detection and Manipulatioin

The ongoing research in our group focuses on single DNA molecular behaviors, especially interaction between DNA and protein, on solid surfaces using AFM. The aim of research is to explore some information on DNA behavior under extra force. This includes the force influence on the DNA structure, e.g. base deletion and mutation; and the force influence on DNA function processing, e.g. the rate of reaction between protein and DNA. It is hoped that DNA synthesis can be finally realized at the single molecule level through positioning techniques by nano-manipulation based on AFM.

Mechanochemical Activation and Kinetics in DNase I Digestion Revealed by Nanomanipulation and Single-Molecule Imaging & Analysis

The tension of only a few piconewtons acting on single biomolecules, where the distinct states are not blurred by bulk averaging, should lead to totally different mechanochemical processes. Whether an applied force affects enzymes acting on the mechanically stretched DNA molecules and subsequently cleavage rate or not, is a focus with its significance in biology. The atomic force microscopy (AFM) *ex situ* imaging & analysis were used to measure the cleaved gaps on these DNA molecules with different stretching extents before and after the digestion. Detailed kinetic profiles of the reaction have been revealed at the lower tension, and a mechanochemical activation in DNase I digestion was discovered. Crystallographic studies on the DNase I-DNA complex indicated that the stretching resulted in wider minor grooves on DNA molecule, which may be more accessible for the enzyme to recognize and afterward cut the DNA. As a whole, it seems very clear that the minor groove had more probability to open during the initial DNA stretching in our experimental conditions. The molecular dynamics (MD) simulations demonstrated the close relationships between the locally conformational changes of those stretched DNA molecules in the small-tension regime and the mechanochemical activation in DNase I digestion.

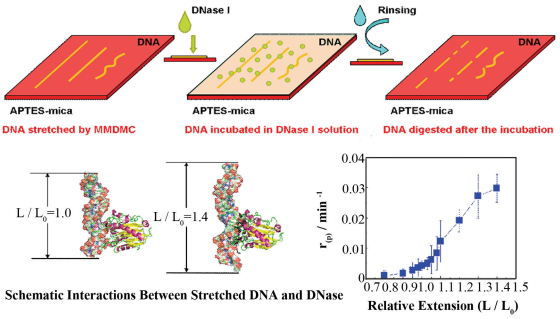

The interaction between DNA and DNase I

Transfer printing on hydrophobic polymer substrate with high efficiency

How to transfer patterns made by photolithography or other methods onto polymer substrate is the central issue on obtaining large-area, flexible electro-device at low cost.

A facile route to solve this problem was provided to realize transferring aqueous inks onto hydrophobic polymer substrate with high efficiency by operating in organic solvent atmosphere. Under the assistance of condensed solvent on the substrate, bovine serum albumin (BSA) were desirably transferred onto untreated poly(dimethylsiloxane) (PDMS), polystyrene (PS) and poly(ethylene terephthalate) (PET) hydrophobic substrate as a proof-of-concept experiment. Moreover, combining this method with SCAN (stepwise contraction and adsorption nanolithography) could be an alternative way to further miniaturize patterns prepared by other methods.

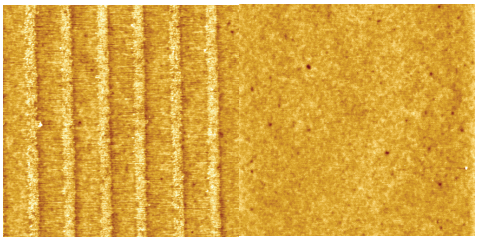

BSA transferred on PDMS

A new method of coating AFM tip for positioning ink deposition

A coating AFM tip method to facilitate the dip-pen nanolithography (DPN) processes was presented. The small amount of ink could be limited to the apex of atomic force microscope (AFM) tip by adjusting AFM operation parameters. With this automatic AFM-engaging system overloading ink, usually disturbing imaging and manipulating, could be avoided. Thereby, a uniform nanoarray of $CuCl_2$ was constructed on a DNA molecule. The unique technique could provide a novel approach to precisely modify biological molecule at the nano-meter scale.

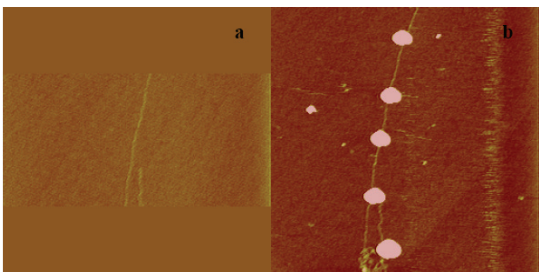

$CuCl_2$ nanopattern on a single DNA molecule

生物传感器研究

生物传感器组　樊春海

主要从事纳米生物传感器、微流控生物芯片、生物光子学与生物电化学、分子机器、DNA 纳米技术与 DNA 计算等研究。研究组依托上海光源和物理生物学实验室，与相关课题组紧密合作，以生物分子自组装、生物传感检测、生物分子机器等为主要研究方向，旨在发展可用于分子诊断、环境检测和生物安全防御发展的新一代高灵敏度、高特异性、廉价、快速、便携的集成化生物传感器与生物芯片。

电化学生物传感器

以金电极为检测平台，在金表面进行有序组装 DNA 茎环结构，在固体界面上成功地实现了捕获探针与信号探针的集成，使 DNA 识别、DNA 分子折叠和电子传递三者耦联起来。同时引入酶催化反应使E-DNA 传感器的灵敏度提高了三个数量级(J. Am. Chem. Soc., 2008, 130, 6820–6825)。

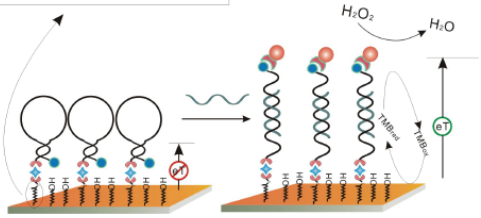

酶催化E-DNA传感器

纳米荧光细胞探针

荧光生物探针在研究细胞行为领域具有重要意义。我们发展了具有良好水分散性、生物相容性、高荧光强度和优异光稳定性的新型硅纳米微球。其制备的荧光生物探针对细胞的实时、长程荧光标记，大大优于基于荧光染料的传统生物探针(Angew. Chem. Int. Ed., 2009, 48, 128–132, 内封面)。

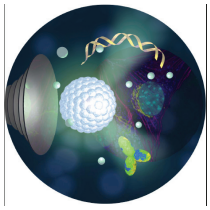

硅纳米微球荧光探针

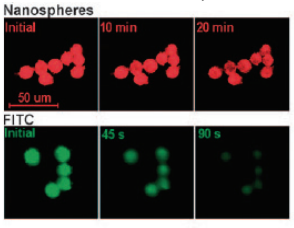

不同荧光探针标记细胞后的荧光变化

纳米复合探针

将 DNA 和蛋白质在纳米金界面上进行共组装，制成多功能纳米生物复合探针。如 AuNP-DNA-HRP 探针可实现对 100 pM 靶 DNA 分子的目视快速检测(血清体系)。该类 AuNP-DNA-蛋白质复合探针可根据检测需求进行调制，通过组装过程中对 DNA 和蛋白质的种类、数量和比例等的精确调控，实现对基因及蛋白质目标的检测，具有广泛的通用性 (Adv. Mater., 2008, 20, 497–500, 内封面)。

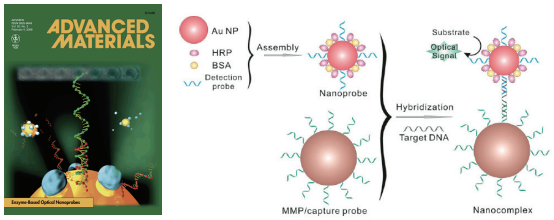

多功能纳米生物复合探针的制备及应用

纳米探针与核酸适体结合用于小分子检测

建立基于核酸适体和纳米金的 ATBR 策略(Aptamer-Target Binding Readout)。利用靶分子会引起 DNA 构象变化以及金纳米粒子可以区分单、双链及其它构象 DNA 探针的特点，实现靶分子的快速灵敏检测。其特异性好，灵敏度高，廉价快速，在环境监测、疾病诊断等领域具有较大应用潜力(Adv. Mater., 2007, 19, 3943–3946)。通过对核酸适体进行设计，使 DNA 构象变化更明显，可提高对可卡因检测的灵敏度并拓宽应用范围(Small, 2008, 4, 1196 –1200，封面)。利用微流控技术发展了基于纳米金探针的汞离子检测方法，实现对汞离子的现场、目视检测(Chem. Commun., 2008, 4885–4887, 封面)。

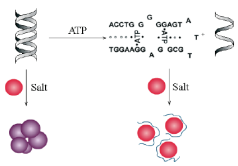

ATBR 策略

微流控芯片

可卡因检测

参考文献

1 Liu G, Wan Y, Gau V, Zhang J, Wang L, Song S, Fan C. An enzyme- based E-DNA sensor for sequence-specific detection of femtomolar DNA targets, J Am Chem Soc, 2008, **130**: 6820–6825 (IF 7.885)

2 He Y, Kang Z, Li Q, Tsang C H A, Fan C, Lee S T. Ultrastable, highly fluorescent and water-dispersed silicon-based nanospheres as cellular probes, Angew Chem Int Ed, 2009, **48**: 128–132 (IF 10.03)

3 Wang J, Wang L, Liu X, Liang Z, Song S, Li W, Li G., Fan C. A gold nanoparticle-based aptamer target binding readout for ATP assay, Adv Mater, 2007, **19**: 3943–3946 (IF 8.191)

4 Zhang J, Wang L, Pan D, Song S, Boyer F Y, Zhang H, Fan C. Visual cocaine detection with gold nanoparticles and rationally engineered aptamer structures, Small, 2008, **4**: 1196–1200 (IF 6.408)

5 He S, Li D, Zhu C, Song S, Wang L, Long Y, Fan C. Design of a gold nanoprobe for rapid and portable mercury detection with the naked eye, Chem Commun, 2008, 4885–4887 (IF 5.14)

Progresses in Biosensor Researches

FAN Chunhai, Group of Biosensors

The group is aimed at developing next generation sensors to meet China's requirements for molecular diagnostics, environmental monitoring and biological safety. The next generation biosensors are meant to have high sensitivity and selectivity, and to be cost-effective with rapid detection time and capable of further devising them into portable biochips. Current interests of the group include nano-biosensors, microfluidic biochip, bio-photonics and bio-electrochemical DNA computation, and DNA machine.

Electrochemical DNA Sensors We developed an enzyme-amplified electrochemical DNA sensor on Au electrodes. The Au electrodes were modified with a hairpin DNA probe, which functions as both the capture and signal probes. With the aid of redox enzyme label, this electrochemical sensor integrates DNA recognition, DNA folding and surface electron transfer on a single chip. The sensor sensitivity can be 1000 times higher than traditional E-DNA sensors. (JACS, 2008, **130**: 6820–6825)

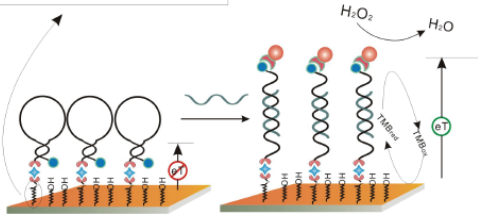

Enzyme amplified E-DNA sensors.

Fluorescent Cellular Nanoprobes Fluorescent cellular probes are powerful tools for studying cellular morphology, behavior, and physiological functions. We developed novel nontoxic silicon nanospheres as cellular probes with good water dispersibility, high photoluminescence, and excellent photostability. Cellular experiments indicate that the as-prepared nanospheres are remarkably efficacious for real-time and long-term cell imaging. (Angew. Chem. Int. Ed., 2009, **48**: 128–132, Inside Cover)

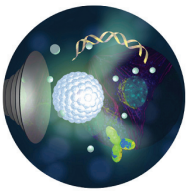

Silicon nanospheres as cellular probes.

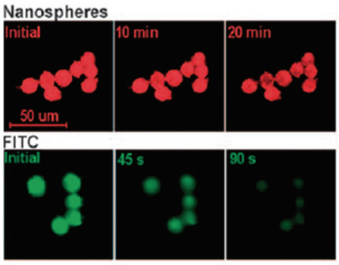

Fluorescence of cells labeled with the Si nanospheres (top) and FITC (bottom).

Multicomponent Nanoprobes We designed a multicomponent nanoprobe by co-assembling thiolated oligonucleotide (detection probe), horseradish peroxidase (HRP, signal amplification), and bovine serum albumin (BSA, non-specific blocker) at the surface of 15 nm Au NPs. This novel multifunctional nanoprobe enables the visual detection of target DNA (in serum) with detection limit as low as 100 pM. In addition, by precisely controlled surface modification of the nanoprobes, this method is of general implication for gene or protein detection. (Adv. Mater., 2008, **20**: 497–500, inside cover)

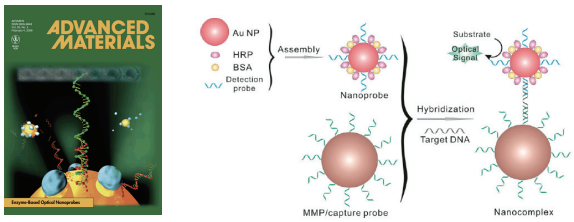

Optical DNA detection based on multicomponent nanoprobes.

Small Molecule Detection Based on Aptamer and Bare Au Nanoparticles For small molecule detection, we designed an aptamer-target binding readout (ABTR) strategy, based on target-induced aptamer conformational change and the ability of Au nanoparticles to differentiate ss-, ds- and other DNA structures. The visual assay is of high sensitivity and selectivity, and exhibits great potential in environmental pollution monitoring and clinical diagnostics (Adv. Mater., 2007, **19**: 3943–3946). For example, by rational design of anti-cocaine aptamer, a visual assay for cocaine detection with improved sensitivity was achieved (Small, 2008, **4**: 1196–1200, Cover). Also, combining ABTR strategy with microfluidic technology, a fully portable, power-free and cost-effective device was designed to enable rapid, sensitive and selective detection of mercury ions with the naked eyes.

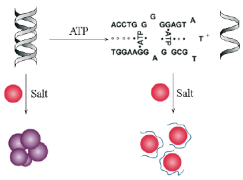

ABTR strategy.

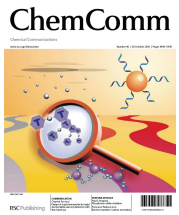

Microfluidic device for Hg^{2+} detection.

Visual cocaine detection.

References

1 Liu G., Wan Y, Gau V, Zhang J, Wang L, Song S, Fan C. An enzyme- based E-DNA sensor for sequence-specific detection of femtomolar DNA targets, J Am Chem Soc, 2008, **130**: 6820–6825 (IF 7.885)

2 He Y, Kang Z, Li Q, Tsang C H A, Fan C, Lee S T. Ultrastable, highly fluorescent and water-dispersed silicon-based nanospheres as cellular probes, Angew Chem Int. Ed., 2009, **48:** 128–132 (IF 10.03)

3 Wang J., Wang L., Liu X., Liang Z., Song S., Li W., Li G., Fan C. A gold nanoparticle-based aptamer target binding readout for ATP assay, Adv Mater, 2007, **19**: 3943–3946 (IF 8.191)

4 Zhang J, Wang L, Pan D, Song S, Boyer F Y, Zhang H, Fan C. Visual cocaine detection with gold nanoparticles and rationally engineered aptamer structures, Small, 2008, **4**: 1196–1200 (IF 6.408)

5 He S, Li D, Zhu C, Song S, Wang L, Long Y, Fan C. Design of a gold nanoprobe for rapid and portable mercury detection with the naked eye, Chem Commun, 2008, 4885–4887 (IF 5.14)

纳米材料的生物效应研究

物理生物效应组　黄 庆

本课题组的研究瞄准纳米技术、核技术、与生物科学领域的交叉领域。研究内容包括：纳米材料的合成和表征，纳米材料与生物大分子的相互作用，纳米材料的细胞生物学效应及其分子机理，纳米材料的整体动物毒性及体内分布，同步辐射技术在纳米生物效应中的应用。

纳米材料的细胞生物效应研究

纳米材料的比表面大、吸附活性高，我们提出建立纳米材料细胞生物学效应检测的新方法。通过对几种碳纳米材料与细胞培养液中血清蛋白和指示剂酚红的相互作用研究，表明这些平时不必特殊关注的细胞培养液中的一些成分，在纳米颗粒生物学效应中起了不容忽视的作用，需要特别注意。

量子点作为新一代生物探针，具有亮度高、不易淬灭等特点，受到研究者的广泛关注。尤其是目前研究较为成熟的 CdTe 量子点，其具有荧光信号，同时，由于其 Cd 元素的存在而能为同步辐射 X-ray 显微技术所观测，因此，是一种应用前景广泛的新型生物探针。

我们用 K562 和 HEK293T 细胞系，考察了一系列水相直接合成的量子点的细胞生物学效应。发现 CdS 的包被在一定的程度上减小了细胞毒性，而 ZnS 的包被则非常显著地提高了量子点的生物相容性，为其应用于细胞生物学标记奠定了基础。

纳米颗粒的整体动物毒性研究

考察了二氧化钛(3 nm)重复多次滴注小鼠后的系统毒性，包括小鼠体重及各组织器官的变化，组织病理学考察，生化参数变化及组织分布情况。结果表明，滴注到肺部的 TiO_2 纳米颗粒可以穿过肺泡-毛细血管屏障进入血液，进而被转运至其他器官，引起肺外组织的损伤。

研制了纳米颗粒的气溶胶呼吸暴露装置，利用自然呼吸法对生产 20 nm 锐钛矿型 TiO_2 纳米颗粒过程中可能对工人产生的呼吸安全性进行了研究。发现，小鼠长期吸入原始粒径为 20 nm 的锐钛矿型 TiO_2 纳米颗粒不仅对呼吸系统产生毒性，而且会影响小鼠的血液循环系统。

富勒烯衍生物的合成及在医药领域的应用研究

除了纳米颗粒生物安全性和毒性研究外，我们还研究了纳米颗粒的生物效应及其在医药领域的潜在应用。在 SK 神经上皮瘤细胞的急性帕金森病模型中，发现富勒醇能减小 MPP^+引起的细胞毒性，抑制氧化损伤；避免 MPP^+引起的线粒体功能紊乱。提示富勒醇有望成为一种线粒体营养剂，有效预防和延缓帕金森病的发生。在四氯化碳(CCl_4)诱导的肝损伤的大鼠模型中，实验揭示富勒醇能够降低肝和肾的化学氧化损伤。另外，实验发现富勒烯连接了糖皮质激素后在保持原有药理活性同时，降低了糖皮质激素的毒副作用，尤其是明显减少药物对神经系统的损伤。

我们合成了具有高度水溶性的 MMFCA(多羟基亚甲基富勒烯羧酸衍生物): $(OH)_{16}C_{60}CHCOOH$。这种新的衍生物有可能成为一种介导疏水的 C_{60} 衍生物进入水的载体。

参考文献

1 Ying Zhu, Wenxin Li, Qingnuan Lie, *et al*. Carbon, 2009, **47**: 1351–1358.
2 Yuanyuan Su, Yao He, Haoting Lu, Biomaterials, 2009, **30**, 19–25
3 LI Yufeng, LI Jungang, YIN Jilei, *et al*. J Nanosci. Nanotechnol (accepted)
4 CAI Xiaoqing, JIA Haiqun, LIU Zhongbo, *et al*. J NeuroSci Res, 2008, **86**(16): 3622–3644
5 ZHU Engao, LIU Ruili, LV Min, *et al*. J Nanosci Nanotechnol

Biological Effects of Nanomaterials

HUANG Qing, Laboratory of Physical Biology

The research of the group is focused on interdisciplinary studies combining nanotechnology, nuclear techniques and biological science. The research programs conver preparation and characterization of nanomaterials, interactions of nanomaterials with, cellular biological effects of nanomaterials and the molecular mechanism, toxicity and bio-distribution of nanomaterials in animals, and using synchrotron radiations to study the bio-effect of nanomaterials.

Cellular bio-effects of nanomaterials

Because of the large surface area and adsorption ability of nanomaterials, we proposed to establish new methods for evaluating cytotoxicity of nanomaterials. The interaction of carbon nanomaterials with serum proteins and phenol red (a pH indicator) in cell culture medium was investigated. It was found that special attentions should be paid to some components of the culture medium, which are regarded as biologically active in common molecular biology, but show observable effects on the biological interactions of nanomaterials.

Quantum dots (QDs), as new optical probes with high brightness and little fluorescence **quenching**, have attracted a great deal of research interest. CdTe, a particular type of QDs that are studied widely on not only their fluorescent properties, but also their detection by synchrotron radiation microscopy with characteristic X-rays of Cd element, can be a new type of biological probes with good application prospects.

We evaluated the cytotoxicity of a series of QDs synthesized in aqueous phase with a variety of cell lines including K562 and HEK293T. We have demonstrated that epitaxial growth of a CdS layer reduced the cytotoxicity of QDs to a small extent. However, the presence of a ZnS outlayer improved greatly the biocompatibility of QDs. Our investigation clearly shows that the structured QDs are highly promising biological fluorescent probes for cellular imaging.

The toxicity of nanomaterials in animals

The systematic influence of 3-nm TiO2 nanoparticles (NPs) in mice after repeated intratracheal instillation of the NPs was studied. Changes in the tissues and organs, body weight, biochemical parameters, histopathology, and the tissue and organ distribution of the TiO2 NPs were assayed. The results indicate that the intratracheally instilled 3-nm TiO2 NPs induced significant lung toxicity, and also they could penetrate capillary–blood barrier, even blood-brain barrier, to reach the extrapulmonary tissues, resulting in extrapulmonary tissues toxicity and growth inhibition.

An aerosol inhalation exposure chamber was designed to study the respiratory toxicity induced in mice by anatase TiO2 NPs in 20 nm of primary size. It was found that long-time inhalation of the TiO2 NPs would cause lung damage to the mice, and the function of blood circulation system would be affected, too.

Preparation and application of fullerene derivative in the medicine field

In addition to securities and toxicity of nanomaterials, we also studied bio-effects and potential application of nanomaterials in medicine. We examined the protective effects of the fullerene derivative C60(OH)24 in a MPP+-induced acute cellular Parkinson's disease model in human neuroblastoma cells. Pretreatment with C60(OH)24 showed significant protective effects on MPP+-induced loss in cell viability, with decreased mitochondrial function and increased levels of reactive oxygen species and oxidative damage. The results suggest that C60(OH)24 may be a mitochondrial protective antioxidant and can prevent Parkinson's disease effectively.

The protective effects of C60(OH)24 on oxidative stress and dysfunction in the liver and kidney, induced by CCl4 were investigated in Sprague-Dawley rats model. The results indicate that C60(OH)24 can protect the liver and kidney tissues against CCl4-induced oxidative stress. Another experiment revealed that C60-glucocorticoid decreased the original toxicity of glucocorticoid while the pharmacological activity of glucocorticoid was kept. In particular, they reduced significantly the damage of drug to the nervous system.

Finally, a new multihydroxylated methanofullerene carboxylic acid (MMFCA) derivative, (OH)16C60CHCOOH, with high aqueous solubility was synthesized. This new MMFCA derivative might be a potential vehicle for the introduction of hydrophobic C60 derivatives into water or a hydrophilic environment.

References

1 Ying Zhu, Wenxin Li, Qingnuan Lie, *et al.* Carbon, 2009, **47**: 1351–1358.

2 Yuanyuan Su, Yao He, Haoting Lu, Biomaterials, 2009, **30:** 19–25

3 LI Yufeng, LI Jungang, YIN Jilei, *et al.* J Nanosci. Nanotechnol

4 CAI Xiaoqing, JIA Haiqun, LIU Zhongbo, *et al.* J NeuroSci Res, 2008, **86**(16): 3622–3644

5 ZHU Engao, LIU Ruili, LV Min, *et al.* J Nanosci Nanotechnol

咪唑离子液体的辐射效应

辐射化学与辐照技术研究室

吴国忠　陈仕谋　付海英　龙德武　沙茂林　戚明颖　黄卫　刘玉胜　窦强

室温离子液体[1, 2]，亦称室温熔融盐，是一类完全由特定阳离子和阴离子构成的特殊软物质。由于其阴、阳离子体积较大又极不对称，仅靠静电力无法使阴、阳离子在微观尺度上紧密堆积，则整个有序的晶体结构遭到破坏、离子间作用力较小，从而使此类化合物的熔点大幅下降，甚至不能结晶，在室温或接近室温下呈现液态。离子液体的导电性和强极性，热稳定性较好，并可重复使用，在萃取、化学合成、催化、核废料回收等领域广受关注。

碳纳米填充离子液体的相行为

本课题组首次证实了离子液体在多壁碳纳米管中的结晶行为。在研究中发现当受限于多壁碳纳米管内部时，离子液体 1-丁基-3-甲基咪唑四氟化硼([bmim][BF_4])将会经历一个完全不同的相转变和结晶过程，而形成熔点高于 200°C.的稳定多晶态，分析认为这种奇特的结晶行为归因于碳纳米管对离子液体结构的纳米效应。

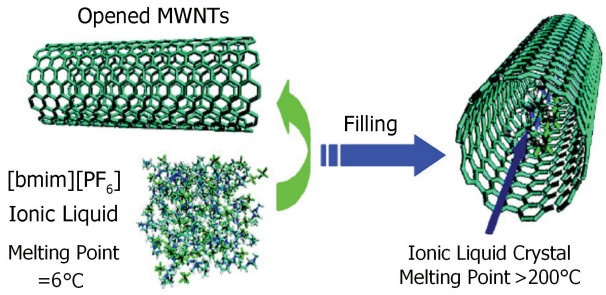

咪唑离子液体的辐射效应

离子液体在核燃料循环方面的应用是近年来研究热点，这只要与辐射场下离子液体的辐照稳定性密切相关[3-5]。研究表明，γ 辐照导致离子液体紫外吸收的增强，但不影响其玻璃化温度。拉曼光谱分析表明，[bmim][BF_4]的辐射裂解导致烷基链的断裂和咪唑环上 H 原子的断裂，而对阴离子 BF_4^-的影响不大。在不同剪切速率和温度下，测定了[bmim][BF_4]和[bmim][PF_6]辐照前后的粘度。剪切压力对剪切速率的变化曲线表明，辐照前后的[bmim][BF_4]都属于牛顿流体。辐照后[bmim][BF_4]的粘度随温度不断降低，且符合阿累尼乌斯方程。

瞬态反应动力学

以蒽醌(AQ) 作为探针分子，用激光光解研究了咪唑型离子液体 1-丁基-3-甲基咪唑六氟化磷([bmim][PF_6])与乙腈(MeCN)混合体系的瞬态吸收光谱和光诱导电子转移过程。随着[bmim][PF_6]的增加，杜醌激发三线态的瞬态吸收峰的位置出现一定的蓝移，杜醌激发三线态的表观衰减速率常数 k_{obs} 随[bmim][PF_6]/MeCN 比例呈现特殊的变化规律。若[bmim][PF_6]的比例足够大，杜醌三线态与 TMPD 之间的电子转移被抑制。研究结果揭示了一些不同于纯的离子液体或有机溶剂中的一些特殊属性。

分子动力学模拟

我们用分子动力学方法详细模拟了室温离子液体一丁基三甲基咪唑六氟磷酸盐在疏水石墨表面的微观结构。结果发现吸附在石墨表面的离子液体，不管是质量密度还是电子密度都是呈现震荡曲线.吸附底层里的离子液体阳离子的咪唑环和丁基链都平躺在石墨表面。

参考文献

1 Gannon T J, Law G, Watson P R, Gamichael A J, Seddon K R. Langmuir 1999, **15**: 8429
2 Hardacre C, Holbrey J D, McMath E J, Bowron D T, Soper A K. J Chem Phys, 2003, **118**: 273
3 Berg R W, Deetlefs M, Seddon K R, Shim I, Thompson J M. J Phys Chem B, 2005, **109**: 19018
4 Binnemans K. Chem Rev, 2005, **105**: 4148
5 Dujardin E, Ebbesen T W, Hiura H, Tanigaki K. Science, 1994, **265**: 1850
6 Chen S M, Wu G Z, Sha M L, Huang S R. J Am Chem Soc, 2007, **129** (9): 2416–2417
7 Qi M Y, Wu G Z, Chen S M, Liu Y D. Radiat Res, 2007, **167**: 508–514
8 Sha M L, Zhang C F, Wu G Z,Fang H P, Wang C L, Chen S M. J Chem Phys, 2008, **128**: 134504
9 Zhu G L, Wu G Z, Sha M L, Long D W, Yao S D. J Phys Chem A, 2008, **112**: 3079–3085
10 Long D W, WuG Z, Wu A B, J Phys Chem C, 2008, **112**: 13000–13003
11 ShaM L, Wu G Z, Fang H P, Zhu G L, Liu Y S. J Phys Chem C, 2008, **112**: 18584–18587

Radiation Effect of Imidazolium Ionic Liquids

WU Guozhong CHEN Shimou FU Haiying LONG Dewu SHA Maolin QI Mingying
HUANG Wei LIU Yusheng DOU Qiang,
Center for Radiation Chemistry and Radiation Processing

As an important green solvent, ionic liquids (ILs) have been widely used in chemistry, chemical engineering, hydrometallurgy and preparation of new materials. Being non-inflammable, non-volatile and property-adjustable, an ionic liquid can be a better solvent than volatile organic compounds, and a higher efficient extractant or modifier than conventional adsorbents or resins in metal extraction and separation [1-2].

Nanoparticle Polymerization

For the first time we demonstrated the crystallization behavior of ILs inside MWNTs (multi-walled carbon nano-tubes). It was found that [bmim][PF6] confined in MWNTs underwent a fully different phase transition and crystal formation, leading to the formation of a stable polymorphous crystal with a melting point of above 200°C. This novel crystallization behavior is explained by size effect of carbon nanotubes on structure of the ionic liquid.

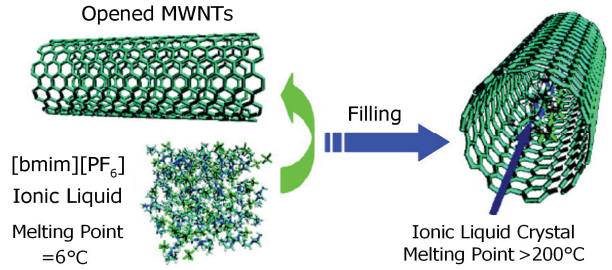

Radiation Effect

The application of room temperature ionic liquids (RTILs) in nuclear fuel cycle and radiation chemistry mainly depends on comprehensive knowledge of their stability and chemical properties under radiation conditions[3-5]. It was found that irradiation increased UV absorption of the ionic liquids, but did not change its glass transition point. Raman spectra of irradiated [bmim][BF_4] indicate that the irradiation induced detectable destruction of alkyl-chain and scission of H-atoms in the ring of imidizolium cation, but relatively small changes of the BF_4^- anion. Viscosities of the irradiated [bmim][BF_4] samples were measured at different shear rates and temperatures, and compared with irradiated [bmim][PF_6] samples. The plots of shear stress against shear rate show that the irradiated [bmim][BF4] remains a Newtonian fluid.

Spectroscopy Analysis and Kinetics

The transient absorption spectra and photoinduced electron transfer process of duroquinone (DQ) in mixed binary solution of [bmim][PF_6] and acetonitrile (MeCN) were investigated by laser photolysis at the excitation wavelength of 355 nm. A spectral blue shift of 3DQ* was observed by comparing the IL/MeCN mixtures and MeCN. At lower VIL(volume fraction of IL), the interaction between DQ and solvent is dominant and the decay rate constant (kobs) of 3DQ* increases steadily with the VIL, whereas at higher VIL, the network structures due to hydrogen-bond and viscosity are dominant and the decay rate constant decreases obviously with increasing VIL. A critical point (turnover) was observed at VIL =~ 0.30. The dependence of the observed growth rate (kgr) of the photoinduced electron transfer (PET) products on VIL is complex and shows a special down-up-down change.

Molecular Dynamic Simulation

Microscopic structures of [bmim][PF6] on hydrophobic graphite surfaces were studied by molecular dynamics (MD) simulation. The results show that both the mass and electron densities of the surface adsorbed ionic liquid are oscillatory, and the first peak adjacent to the graphite surface is considerably higher than others, corresponding to a solid-like IL bottom layer of 6 Å. Three IL layers are indicated between the graphite surface and the inner bulk ionic liquid. The simulation also indicates that the imidazolium ring and butyl tail of the cation (bmim+) of the IL bottom layer are lying flat on the graphite surface.

References

1 Gannon T J, Law G, Watson P R, Gamichael A J, Seddon K R. Langmuir 1999, **15**: 8429
2 Hardacre C, Holbrey J D, McMath E J, Bowron D T, Soper A K. J Chem Phys, 2003, **118**: 273
3 Berg R W, Deetlefs M, Seddon K R, Shim I, Thompson J M. J Phys Chem B, 2005, **109**: 19018
4 Binnemans K. Chem Rev, 2005, **105**: 4148
5 Dujardin E, Ebbesen T W, Hiura H, Tanigaki K. Science, 1994, **265**: 1850
6 Chen S M, Wu G Z, Sha M L, Huang S R. J Am Chem Soc, 2007, **129** (9): 2416–2417
7 Qi M Y, Wu G Z, Chen S M, Liu Y D. Radiat Res, 2007, **167**: 508–514
8 Sha M L, Zhang C F, Wu G Z,Fang H P, Wang C L, Chen S M. J Chem Phys, 2008, **128**: 134504
9 Zhu G L, Wu G Z, Sha M L, Long D W, Yao S D. J Phys Chem A, 2008, **112**: 3079–3085
10 Long D W, WuG Z, Wu A B, J Phys Chem C, 2008, **112**: 13000–13003
11 ShaM L, Wu G Z, Fang H P, Zhu G L, Liu Y S. J Phys Chem C, 2008, **112**: 18584–18587

高温辐射交联 PTFE 的研究进展

辐射化学与辐射技术研究室　王谋华　吴国忠

聚四氟乙烯(PTFE)的热稳定性和化学稳定性优异，应用非常广泛；但其耐磨擦性能差、对高能射线异常敏感，这些缺点使其在某些特殊领域的应用受限。上世纪 80 年代发现辐射法可实现 PTFE 直链分子的交联。辐射交联 PTFE 的某些性能发生巨大改变，其中最引人注目的是耐磨擦性能和耐辐射性能的提高[1,2]。耐磨性能的改善使其在减摩领域具有潜在应用价值，耐辐射性能的提高则可使其应用范围拓宽到航空航天等强辐射场领域。

研究表明，PTFE 的辐射交联条件非常苛刻。用 γ 射线或电子束进行 PTFE 辐射交联时，温度须控制在 330℃附近，即稍高于 PTFE 的熔点(327℃),气氛则要求无氧惰性气氛或真空[3]。辐照温度稍低于 327℃，会使 PTFE 链断裂，导致降解，力学性能降低（低温辐射降解 PTFE 作为制备 PTFE 超细粉的技术，早已为人熟知）。当辐照温度高于 340℃时，则会引起 PTFE 的高温裂解，温度越高裂解越快，也得不到交联 PTFE。电子束会使被辐照物快速升温，电子束辐射交联 PTFE 的关键技术，是如何控制辐照温升。

为此，本课题组对束下装置进行了三次设计改进，终于在惰性气氛中成功实现了 PTFE 的电子束高温辐射交联，辐照温度控制在 335±5℃。辐射交联 PTFE 的透明度增加，随着辐照剂量的增加，熔点和结晶热逐渐降低[4]。

用环-环和环-块摩擦仪进行的交联 PTFE 片材的干摩擦行为研究结果表明， 辐射交联 PTFE 样品的摩擦系数略为增大(~5%)，但其耐磨擦性能有巨大提高，如 150 kGy 交联 PTFE 样品的摩擦失重可减至原来的 1‰以下，即耐磨擦性能提高 3 个数量级以上。摩擦面的扫描电镜图像显示，未交联 PTFE 的摩擦面光滑，有明显划痕，而辐射交联后的 PTFE 摩擦面变得粗糙，无明显划痕。可以认为，由于 PTFE 的直链结构照交联为三维网状结构，PTFE 分子链作用力加大，链段间难以相对滑动，不会因摩擦而离去，故耐磨性能大幅度提高。

此外，我们还在进行交联 PTFE 的电性能和耐辐射性能研究。

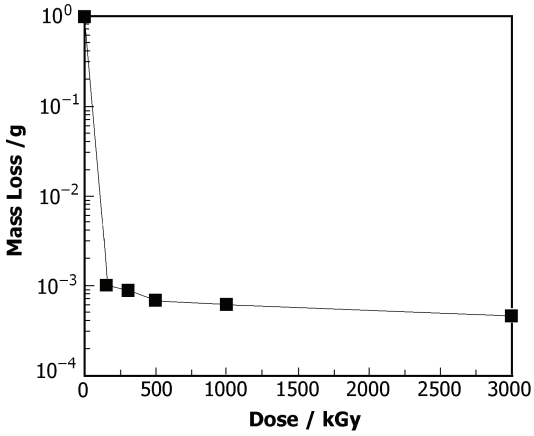

图 1　交联剂量对摩擦失重的影响

参考文献

1　Sun J. Radiation crosslinking of PTFE. Polymer Communications 1994, **35**(13): 2881–2883

2　Oshima A, Tabata Y, Kudoh H, Seguchi T. Radiation induced crosslinking of polytetrafluoroethylene. Radiation Physics and Chemistry 1995, **45**(2): 269–273

3　Seguchi T, Yagi T, Ishikawa S, Sano Y. New material synthesis by radiation processing at high temperature - polymer modification with improved irradiation technology. Radiation Physics and Chemistry, 2002, **63**(1): 35–40

4　唐忠锋, 王谋华, 吴国忠, 赵燕凝. PTFE 的辐射交联及其应用, 有机氟工业，2008, **3**: 3–6

Progress in High Temperature Radiation Cross-linked PTFE

WANG Mouhua WU Guozhong, Centre for Radiation Chemistry and Radiation Processing

Polytetrafluoroethylene (PTFE) is a well known engineering plastic material with superior chemical and thermal stability. However, its poor wear resistance and extreme radiation sensitivity are major hindering factors for PTFE application in certain areas. It was found in 1980s that radiation cross-linked PTFE (X-PTFE) changed dramatically in its physical properties, and of particular interest, the abrasion and radiation resistances could be improved substantially [1,2]. The outstanding wear resistance of X-PTFE makes it possible to use it as a special lubricant additive or in its application in extreme conditions, such as the space environment.

As reported in literatures, the irradiation conditions for preparing X-PTFE are strict. PTFE in molten state can be cross-linked by electron beam or γ-ray irradiation in an inert gas atmosphere or vacuum. Irradiating PTFE at temperatures under the melting point (327°C), chain scission occurs and the mechanical properties degrade and crystalline fraction increases with the irradiation dose; while at temperatures over 330°C, thermal decomposition increases with the irradiation temperature [3]. For E-beam irradiation, where the beam heating effect is obvious, the key to preparing X-PTFE is to control temperature rising of the PTFE during the irradiation. In order to improve the temperature control, we redesigned the under-beam device for three times.

Based on the technical improvement, PTFE sheets were cross-linked by electron beam irradiation at 335±5°C in a nitrogen gas atmosphere[4]. With increasing doses, the PTFE sheets became transparent, and the melting point and crystallization heat decreased gradually. Tribological behavior of the X-PTFE sheet was investigated on a ring-on-ring tribometer and a block-on-ring friction tester under dry friction conditions. It was found that the friction coefficient of X-PTFE increased slightly, but wear resistance of X-PTFE was improved substantially. As shown in Fig. 1, the mass loss of X-PTFE in the tribological test decreased by 3 orders of magnitude at 150 kGy. Scanning electron microscopy (SEM) images of the wear-tested samples show that surface of the virgin PTFE sheet was smooth, while surface of X-PTFE was rough. The three-dimensional network of X-PTFE is responsible for its excellent wear resistance behavior.

Studies on the electrical properties and the radiation resistance of X-PTFE are in progress.

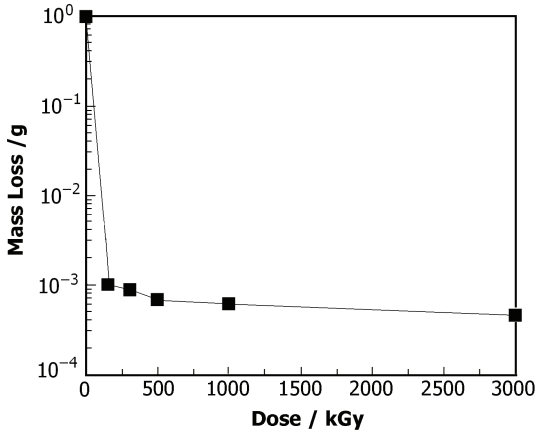

Fig.1 Abrasion loss of X-PTFE as a function of the irradiation dose.

References

1 Sun J. Radiation crosslinking of PTFE. Polymer Communications 1994, **35**(13): 2881–2883

2 Oshima A, Tabata Y, Kudoh H, Seguchi T. Radiation induced crosslinking of polytetrafluoroethylene. Radiation Physics and Chemistry, 1995, **45**(2): 269–273

3 Seguchi T, Yagi T, Ishikawa S, Sano Y. New material synthesis by radiation processing at high temperature-polymer modification with improved irradiation technology, Radiation Physics and Chemistry, 2002, **63**(1): 35–40

4 Tang Zhongfeng, Wang Mouhua, Wu Guozhong, Zhao Yanning. Radiation crosslinked PTFE and its application. Organo-Fluorine Industry, 2008, **3**: 3–6

改性膜材料及其应用研究

辐射化学与辐照技术研究室　李景烨

高分子粉体的预辐射接枝

利用辐射接枝技术对高分子膜材料粉体进行接枝改性，从而获得具有功能性支链的接枝聚合物。特别是实现了多种非水溶单体的水相接枝聚合[1]，具有潜在的产业化价值。将接枝聚合物制备成各种致密或多孔的分离膜，研究了其传质性能与接枝链结构及接枝率的关系，拓展了功能膜的使用范围和应用领域。

辐照后高分子粉体的水相接枝聚合

质子交换膜

用聚偏氟乙烯(PVDF)粉体作为基材，通过辐射接枝苯乙烯后，经溶液铸膜或热压成膜后磺化得到厚度为 30–70 μm 的质子交换膜，其质子交换容量从 0.5–1.5 meq/g 可控[2]。

与传统的以膜为基材进行接枝改性不同，以粉体为基材进行接枝后成膜可有效地提高接枝链段分布的均匀性，获得大面积均匀、高强度的质子交换膜。特别是跨膜方向的接枝链分布，在低接枝率下，以膜为基材接枝改性获得的质子交换膜，其支链富集于表面，而中心部分未接枝，因此，电导率极低。而以粉体为基材，则可在低接枝率下保证跨膜方向的接枝链均匀分布。

热压成膜获得的质子交换膜表现出高于商品化全氟磺酸膜的质子传导率，其阻醇性能及其在燃料电池中的伏安曲线等性能也有改善。

抗污染滤膜

研究以聚偏氟乙烯(PVDF)或聚醚砜(PES)粉体作为基材，通过辐射接枝亲水性丙烯酸类单体后，经相转化法得到具有非对称结构的微滤或超滤膜。改性后的滤膜，由于亲水性的提高，其水通量较为改性滤膜有显著提高。另外，基于电荷排斥机理及接枝链段中的极性基团与水分子形成大量氢键作用，提高了改性后滤膜抗蛋白质污染的能力，在过滤蛋白质溶液时获得更高的效率。同时，表面红外光谱研究也发现，为改性滤膜经蛋白质污染后，表面黏附较多蛋白质分子，而改性滤膜表面的蛋白质黏附量极小。

由于接枝链为弱酸弱碱性的聚电解质，因而改性滤膜在不同 pH 值下水通量不同，具有 pH 响应的特点。其原因是接枝链电离与否改变了其回转半径，从而改变了滤孔的大小[3,4]。

旋转式厌氧膜生物反应器

与好氧膜生物反应器不同，厌氧膜生物反应器(AnMBR)更适合于处理复杂和有机含量更高的废水；同时，在厌氧微生物处理有机物时还能产生能源性氢气及甲烷气体，实现了“变废为宝”。但目前厌氧膜生物反应器绝大多数为外置错流式，其膜污染严重、动力消耗大、生物活性易受损。通过创新性地将动态旋转膜分离组件及抗污染滤膜引入厌氧膜生物反应器系统，设计加工了旋转式厌氧膜生物反应器。该旋转式厌氧膜生物反应器用于处理食品废水，设计日处理能力 20 吨。在这一系统中，可以系统地研究和优化厌氧过程，并筛选不同的抗污染滤膜，从而进一步提升系统性能，扩展其应用领域。

参考文献

1　李景烨，邓波，谢雷东等，专利申请号 200810040814.2
2　吉玉玲，李林繁，于洋等，辐射研究与辐射工艺学报，2009, **27**(2): 79–83
3　Deng B, Li J Y, Hou Z C, *et al*. Radiat Phys Chem, 2008, **77**: 898–906
4　Deng B, Yang X X, Xie L D, *et al*. J Membrane Sci, 2009, **330**: 363–368

Functional Membranes of Copolymers Modified by Radiation Grafting

LI Jingye, Department of Radiation Chemistry & Radiation Processing

Pre-irradiation graft copolymerization

Functional monomers were grafted onto polymer powder. Especially, water-insoluble monomers were grafted in water under shear dispersion[1]. The graft copolymers were fabricated into dense or porous functional membranes, which showed much better performance than the pristine membranes. Dependence of membrane properties on degree of grafting and structure of graft chains were studied.

Graft polymerization performed in water dispersion

Proton exchange membrane

Styrene grafted poly(vinylidene fluoride) (PVDF) powder was fabricated into dense membranes of different thicknesses from 30–70 μm by solution casting or hot- pressing. Proton exchange membranes (PEMs) were obtained by sulfonating the dense membranes, and the ion exchange capacity (IEC) value ranges from 0.5–1.5 meq/g.

The powder grafting technique is advantageous in developing large area PEMs over traditional ways using as-prepared membranes for graft polymerization. Using this novel routine, the graft chains are well-distributed, especially in transmembrane direction even at very low degree of grafting.

Proton conductivity of the PEMs fabricated via hot-pressing is superior to that of perfluorosulfonic acid PEMs commercially available. The alcohol permeability and fuel cell performance of the synthesized PEMs were tested, with encouraging results.

Antifouling filtration membrane

Hydrophilic acrylic monomers were grafted onto PVDF or polyethersulfone (PES) powder by pre-irradiation induced graft polymerization technique, and asymmetric microfiltration or ultrafiltration membranes were prepared from the grafted polymer powder under phase inversion method. Because of the improvement in hydrophilicity, the modified filtration membranes showed better water flux under the same conditions. The electric charge repulsion between charged graft chains and protein molecules, and hydrogen bond formation with water molecules, are two main reasons for elevated antifouling performance of the modified filtration membranes, which resulted higher efficiency in filter protein-containing solutions.

Because the graft chains are polyelectrolyte, the gyration radius of graft chains is dependent on pH value, therefore, the modified filtration membranes are also endowed with pH sensitivity[3,4].

Rotating anaerobic MBR

Unlike aerobic membrane bio-reactor (MBR), anaerobic membrane bio-reactor (AnMBR) is suitable for treating complex and dense organic pollution water. Also, hydrogen and methane gas are the main products by anaerobic microorganisms that decompose organic wastes, hence a more economic and attractive system with AnMBR. External cross-flow type is the most popular one in current applications. However, serious membrane pollution, high power consumption and damage to microorganisms are the major shortcomings. In our novel rotating AnMBR system, a rotating filtration membrane unit was designed and antifouling filtration membranes were used to improve the performance. This rotating AnMBR system is used to treat waste water in food industry with a capacity of 20 ton/day. The anaerobic bioprocess is under studying and optimizing in this system and further improvement in the performance is expected.

References

1 Li J Y, Deng B, Xie L D, *et al*. Chinese Patent, application number: 200810040814.2

2 Ji Y L, Li LF, Yu Y, *et al*. J Radiat Res & Radiat Proc, 2009, **27**(2): 79–83 (in Chinese)

3 Deng B, Li J Y, Hou Z C, *et al*. Radiat Phys Chem, 2008, **77**: 898–906

4 Deng B, Yang X X, Xie L D, *et al*. J Membrane Sci, 2009, **330**: 363–368

辐射技术处理水体中有机物和金属离子

辐射化学与辐照技术研究室 王 敏

20 世纪 70 年代起大型钴源和电子加速器技术的发展，改善了在辐射技术应用中的辐射源问题。从此，利用辐射技术处理环境污染物的研究也逐步引起各国关注。目前，这一领域的应用研究主要集中在电子束烟气脱硫脱硝、废污水的辐照治理、污泥的辐照处理以及饮用水的深层净化[1]。废气和废水中的持久性有机污染物的辐射降解和治理也广受关注[2]。本组开展了污染物辐射降解及其降解机理的研究，以及辐射改性制备重金属吸附材料研究。

有机污染物降解机理

含苯环、芳香族硝基类有机物是一种典型的污染物。辐照几种有机物的水溶液，通过有机物的降解率、溶液 TOC 去除率，考察有机物的降解和矿化效果。设计各种辐照体系，研究了水辐解产生的各种活性粒子对有机物的降解效果。结果表明，辐照法是一种去除水体中含苯环有机物的有效方法，其降解率在不同体系中均可达 100%，高剂量下的 TOC 去除率达 30%以上。用脉冲辐解研究了几种有机物与•OH 和 e_{aq}^-反应生成中间产物的瞬态吸收光谱，测得相应反应速率常数。用 GC、HPLC-MS 分析了降解产物，推测了几种有机物的降解机理。

辐射改性材料吸附水体中的重金属

重金属污染是危害最大的水污染之一[3]。目前对水中重金属污染的传统处理方法主要采用物化吸附法和絮凝沉淀法。随着高分子材料科学发展，开发和研制新型的有机功能材料是当前重金属水处理研究的一大热点。用 ^{60}Co γ 射线预辐照接枝和化学改性的方法，在高分子材料聚偏氟乙烯(PVDF)上引入胺基，制备了胺基吸附材料，并研究了该吸附材料对重金属离子的吸附性能。

PVDF 材料具有耐高温、韧性好、机械性能良好和化学性质稳定等优点，但由于它表面能低、疏水性强，限制了它在环境、净水等领域的应用。本组用预辐照 PVDF 粉体，在溶液体系和乳液体系中研究了粉体接枝甲基丙烯酸缩水甘油酯(GMA)，制备了含有高活性环氧基团的 PVDF-g-PGMA 的共聚物。用 PVDF-g-PGMA 上环氧基与三乙烯四胺(TETA)胺基间的开环加成反应实现材料胺基化，制备了胺基吸附材料。将其用于吸附水体中的 Cu^{2+}离子。研究了溶液 pH 值、温度、接触时间、Cu^{2+}离子初始浓度等因素对改性材料吸附性能的影响，并探讨了吸附动力学过程。接枝率为 100%时，Cu^{2+}离子的吸附量为 70 mg/g。最优条件下，Cu^{2+}离子的吸附量可达 100 mg/g 以上。研究证明辐射技术对于聚合物改性制备功能材料具有工艺简单、节省能源、易于控制等优点，是一种经济、有效的方法[4]。

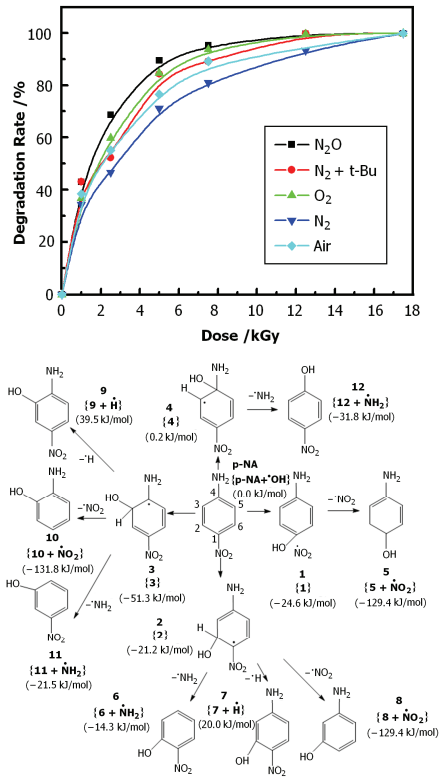

图 1 p-NA 水溶液辐照降解效果和降解主要机理

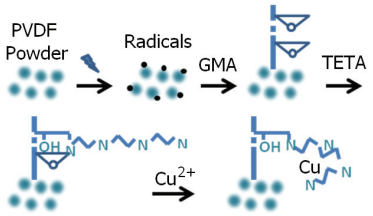

图 2 预辐照 PVDF 接枝 GMA，TETA 改性材料吸附金属

参考文献

1 同位素和辐射技术在环境保护中的应用，国际原子能机构，北京：原子能出版社，1995, 96–137
2 Wojnárovits L. Takács E. Radiat Phys Chem, 77, 225–244
3 Yeow M L, Liu Y, Li K. Journal of Membrane Science 2005, **258** (1-2): 16–22
4 张敬，王敏，蒲长永，等. 核技术，2009, **32**(6): 448–452

Radiation Technology for Organic Pollutants Degradation and Heavy Metal Removal

WANG Min, Department of Radiation Chemistry and Radiation Technology

Based on developments in ^{60}Co and electron beam irradiators, radiation methods for environmental protection have attracted worldwide attentions, especially in E-beam desulfurization and denitration of flue gas, waste water treatment, sludge treatment and drinking water disinfection[1, 2]. The research programs of our group include radiation treatment of heavy metal pollutants in water, radiolysis of some organic pollutants in aqueous solutions, and radiation modification of materials for heavy metal recovery from waste water.

Kinetics and mechanisms of decomposition and mineralization of organic pollutants

Radiation-induced decomposition and mineralization of organic pollutants in aqueous solution were investigated with degradation rate, TOC removal rate, efficiency of denitration and pH of the solutions in different irradiation systems. Complete degradation of the organic pollutants was observed at different doses under diverse irradiation conditions. The transient absorption spectra were recorded after the pulse radiolysis, while different transient species involved were recognized. Besides, the first-order reaction rate constants of organic pollutants with •OH and e_{aq}^- were determined by pulsed radiolysis. The related radiolytic products under various conditions were identified using GC and HPLC-MS analyses. The mechanisms behind the radiolytic degradation of organic pollutants were proposed based on the degradation products observed.

Preparation of metal adsorbent to recover rare metals from waste water

Heavy metals are harmful water pollutants. Generally, toxic heavy metals are removed from water by Conventional treatments such as adsorption and flocculation methods. Novel functional polymer materials can provide a new solution. We prepared rare metal adsorbents by using radiation-induced graft polymerization and subsequent modification to introduce amidoxime groups.

A polyvinylidene fluoride (PVDF), an excellent material for many applications, has its setbacks due to its low surface energy and hydrophobicity[3]. To improve the properties, irradiated PVDF powders were grafted with glycidyl methacrylate (GMA) in methanol solution and water emulsion. Effects of the reaction time and temperature, the dose, and the monomer concentration, on the grafting efficiency were studied. Composition and performance of the grafted powders were analyzed using FTIR and DSC. The grafted PVDF was converted to amine-type adsorbent by chemical modification of triethylenetetramine (TETA). The capability of the amine-type adsorbent was investigated with contact time, temperature, pH, etc. It was found that the TETA-modified PVDF powder can be considered as a promising adsorbent for heavy metal removal. Without organic solvent in the grafting method, the emulsion graft polymerization is a green chemistry [4].

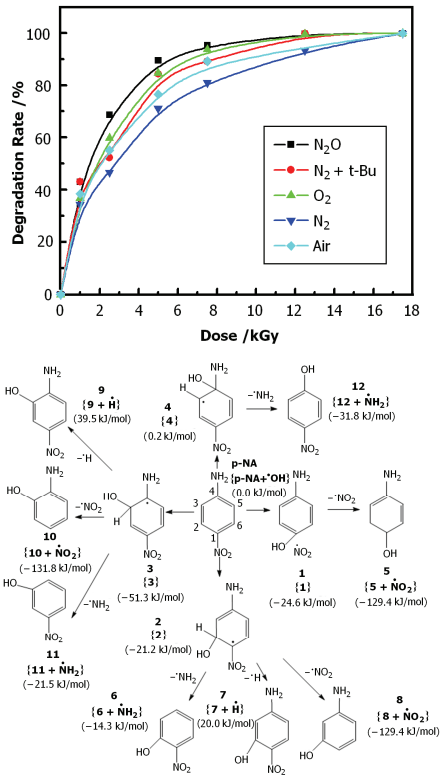

Fig.1 Degradation rates of p-NA aqueous solutions and the suggested degradation mechanism.

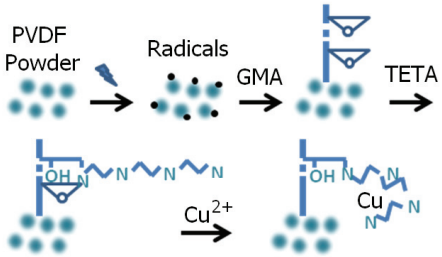

Fig.2 Introduction of diethylamino group into the polymer.

References

1 Applications of isotopes and radiation in conservation of the environment, IAEA. Beijing, Atomic Energy Press, 1995, 96–137

2 Wojnárovits L, Takács E. Radiat Phys Chem, **77**, 225–244

3 Yeow M L, Liu Y, Li K. Journal of Membrane Science 2005, **258** (1-2): 16–22

4 Zhang Jing, Wang Min. Pu Changyong, *et al.* Nucl Tech, 2009, **32**(6): 448–452

快速反应动力学研究

辐射化学与辐照技术研究室　王文锋

快速反应动力学研究，是时间分辨技术在化学、生物学等领域中的应用，以了解相关化学、生物作用过程及机理，是当今世界科学的前沿课题之一, 也是我所的重点发展学科之一。本组用激光光解、电子束脉冲辐解装置以及 ESR 等大型设备，结合快速反应动力学检测装置，研究辐射(光)引发的效应，并跟踪其反应过程。主要研究抗氧化剂的性能及其修复受损伤的 DNA 及其碱基、蛋白质自由基的过程及反应机理、以及光敏剂对生物分子的损伤机理及效率。我们还用 THz 光谱进行化合物结构的分析鉴定、分子间相互作用以及固态化学反应过程监测等研究。

氟代喹诺酮类衍生物的光敏作用

氟代喹诺酮类衍生物是一类在医学临床中有着广泛应用的抗菌消炎药物，上世纪 90 年代发现该类药物具有光致毒性，引起学术界的广泛关注。

我们对依诺沙星(ENX)、诺氟沙星(NFX)和环丙沙星(CPX) 等三种氟代喹诺酮类衍生物的光敏毒性进行了快速反应动力学实验，研究其自身三线态的光化学性质、自猝灭速率常数和各类氨基酸对三种化合物三线态的猝灭速率常数。我们还用脉冲辐解技术测定了这三种化合物阴离子自由基的吸收峰位置。测得 ENX、NFX 和 CPX 三线激发态的最大吸收峰位置分别为 520、610 和 620 nm，它们被氧气猝灭的速率常数 $K_q(O_2)$分别为 2.4×10^9、2.2×10^9 和 2.6×10^9。测得酸酪氨酸、色氨酸、半胱氨酸和精氨酸等四种氨基酸对 ENX 的猝灭速率常数 K_q 分别为 1.9×10^9、2.3×10^9、1.5×10^9 和 1.7×10^9。此类药物的光化学性质和光敏毒性的研究，结合分子结构与光敏毒性的关系研究，能加深和丰富对喹诺酮类衍生物的认识和理解，对于医学和临床也具有一定的理论指导意义。

抗氧化剂作用机理研究

鉴于抗氧化剂在生物体的衰老与疾病中所起的重要作用，其作用机理一直是关注热点。在脉冲辐解和激光光解瞬态吸收光谱装置上，我们研究了硫辛酸清除活性氧自由基(ROS)等的反应特性，得到反应的瞬态吸收光谱和反应速率常数，硫辛酸清除 $HO^{\cdot}$、e_{aq}^{-}、$CO_3^{\cdot-}$、$SO_4^{\cdot-}$、$Br_2^{\cdot-}$的反应速率分别为 7.4×10^9、1.3×10^{10}、9.8×10^8、2.3×10^9、2.0×10^9 $L\cdot mol^{-1}\cdot s^{-1}$，并初步推断了其反应机理。

虾青素和角黄素是具有广泛应用价值的类胡萝卜素，我们还研究了它们的性质。2-萘乙酮三重态与虾青素和角黄素发生激发能量转移，产生虾青素三重激发态(550 nm)和角黄素三重激发态(550 nm)激发三重态。用能量转移法测得虾青素激发三重态和角黄素激发三重态在乙腈中最大吸收波长处的摩尔小光系数分别为 $\varepsilon_{AST,550}$=23500 $L\cdot mol^{-1}\cdot cm^{-1}$，$\varepsilon_{CAN,550}$=11000 $L\cdot mol^{-1}\cdot cm^{-1}$。改变虾青素和角黄素的浓度测得 2-萘乙酮三重态与虾青素(1.25×10^{10} $L\cdot mol^{-1}\cdot s^{-1}$)、角黄素($1.12\times10^{10}$ $L\cdot mol^{-1}\cdot s^{-1}$)激发能量转移速率常数。同时测得虾青素(3.3 μs)和角黄素(3.0 μs)在乙腈中的三重态寿命。

快速反应动力学技术是具有广泛应用领域的研究手段，我们将开展辐射(光）)成的生物分子损伤机理及控制过程，跟踪由脉冲电子束与激光引起的电荷与能量传递过程，重点研究药物分子对生物分子的损伤及抗氧化剂的作用机理；利用极紫外 FEL 光源结合 UV 激光，发展超快的里德堡态氧原子和氮原子的探测方法，用于交叉分子束反应动力学和分子光化学动力学的研究，同时进行分子和原子超激发态的超快动力学等研究；结合研究所的核能发展规划，开展相关的自由基反应过程研究，如室温离子液体为介质的辐射(光)化学行为，与反应堆密切相关的超临界水、受限水以及浓溶液的反应动力学研究以及萃取剂的 520 辐射效益等研究。

参考文献

1 Zhang Z X, Wang W F，Journal of Photochemistry and Photobiology B: Biology, 2008, **92**: 77–82,

2 Shi Y M, Wang W F, MUTAGENESIS，2008, **23**: 19–26

3 Liu G F, Wang W F, Chinese Journal of Chemistry, 2008, **26**: 1257–1261

4 Ge Min, Wang W F, Chemical Physics Letters, 2007, **444**, 355–358

5 ZHU H P, Wang W F, Chinese Journal of Chemistry, 2007, **25**: 1233–1237

6 Zhang Z X, Zhu H P, Wang W F, Science in China Series B-chem，2007, **50**: 84–90

Fast Chemistry Reaction Kinetics

WANG Wenfeng, Center for Radiation Chemistry and Radiation Processing

Radiation chemistry kinetics and radiation biology are of both theoretical and practical importance. The group is engaged in studies on radiation- and light-induced chemical effects of materials. Based on radiation physics and chemistry of biological substance, we have been focused mainly on free radical behaviors and change transfer reaction in biological molecules by using laser photolysis, pulsed radiolysis, EPR and related spectroscopic methods.

Pulsed electron beams, lasers (UV) and ^{60}Co γ-rays are used for investigating the radiation induced phenomena in biological molecules of interest, especially the intra- and inter-molecular energy and charge transfer. Mechanisms of free radical reactions between bimolecular with photosensitizer and antioxidants were studied, and the results are useful for radiotherapy or reduction of biological damage caused by the radiations. Also, THz-TDS was used to investigate low-frequency vibration and rotation behavior of biomolecules, the crystal transformation process, and solid-state reaction.

Transient Species of Fluoroquinolones and Their Reactions with Amino Acids

Photochemistry of fluoroquinolone antibiotics (FQs), i.e, enoxacin (ENX), norfloxacin (NFX) and ciprofloxacin (CPX), were investigated by laser flash photolysis and pulsed radiolysis. Transient absorption spectra of the FQs were observed and transient species were assigned. The absorption maxima (λ_{max}) of primary triplet states of ENX, NFX and CPX were located at 520, 610 and 620 nm, respectively. The secondary triplet states were characterized by λ_{max}=680 nm (ENX), 700 nm (NFX) and 700 nm (CPX). The transient absorption around 440 nm was assigned to cyclohexadienyl anion, and a product was formed by the FQs in a photo-substitution reaction with OH^-. The unimolecular decay rate constant, and bimolecular decay rate constant quenched by the ground state and O_2, were determined. Reactions of the FQ triplet states with amino acids (tyrosine, tryptophan, cysteine and arginine) were investigated. Evidences obtained by pulsed radiolysis provide more direct supports for the existence of the cyclohexadienyl anion and reduced radicals of FQs.)

It was also found that the FQs were not able to generate triplet states in nonprotic organic solvent, because of probably intramolecular charge transfer of excited states of the FQs. Photoinduced intramolecular electron transfer could take place in systems with acceptor and donor subunits formally linked by a simple bond, such as twisted intramolecualr charge transfer, wagged intramolecualr charge transfer and rehybridization by intramolecualr charge transfer. Most FQs can be viewed as electron donor-acceptor compound, with the piperazine ring being the ecletron-donating group, and the aromatic ring being the electron-accepting group. Experiments were performed using UV-visible absorption spectra and laser flash photolysis, for elucidating the effects of intramolecular charge transfer on excited states of the FQs.

Transient species and its properties of antioxidants

Pulsed radiolysis and laser flash photolysis were used to study the reactions between LA (α-lipoic acid) and ROS (reactive oxygen species). Transient spectra of LA radicals were observed and the absorption maxima were assigned. It was found that LA could effectively quench free radicals such as $\cdot OH$, $CO_3^{\cdot -}$, $SO_4^{\cdot -}$, e_{aq}^- and $Br_2^{\cdot -}$ at the rates of 7.4×10^9, 9.8×10^8, 2.3×10^9, 1.3×10^{10} and 2.0×10^9 $L\cdot mol^{-1}\cdot s^{-1}$, respectively. Mechanism of the reactions was studied, too.

Triplet properties of astaxanthin (AST) and canthaxanthin (CAN) were investigated by laser flash photolysis of different deaerated polarity solutions of acetonitrile and benzene at room temperature, using 2-acetonaphthone as a sensitizer. The energy transfer method was used to obtain decay rate constants of the triplet state, which are (in $L\cdot mol^{-1}\cdot s^{-1}$) 1.25×10^{10} (AST) and 1.12×10^{10} (CAN) in acetonitrile, 1.75×10^{10} (AST) and 3.27×10^{10} (CAN) in benzene. The molar extiction coefficient of triplet state was dertermined as (in $L\cdot mol^{-1}\cdot cm^{-1}$) $\varepsilon_{AST,550\ nm}$=23500 and $\varepsilon_{CAN,560\ nm}$=11000.

The fast reaction kinetics study can be applied in many fields of research. More efforts will be made at SINAP on primary and subsequent processes of the radiation induced injury of some major biological targets, and structure and dynamics of reactive transient species of some potential radio- and chemo-protectors and photosensitizers.

References

1 Zhang Z X, Wang W F. Journal of Photochemistry and Photobiology B: Biology, 2008, **92**: 77–82

2 Shi Y M, Wang W F, Mutagenesis, 2008, **23**: 19–26

3 Liu G F, Wang W F. Chinese Journal of Chemistry, 2008, **26**: 1257–1261

4 Ge Min, Wang W F. Chemical Physics Letters, 2007, **444**, 355–358

5 ZHU H P, Wang W F. Chinese Journal of Chemistry, 2007, **25:** 1233–1237

6 Zhang Z X, Zhu H P, Wang W F, Science in China Series B-chem，2007, **50:** 84–90

放射性分子影像探针研究进展和展望

放射性药物研究中心　张 岚　周 伟　张国欣

放射性分子影像探针研究组从事各种放射性核素标记的分子影像探针的设计、制备、生物学评价及其应用研究，重点为单光子发射断层显像(SPECT)和正电子发射断层显像显像(PET)的影像探针；并开展 ^{188}Re 标记放射性治疗药物研制和开发，以及纳米材料制备及其在生物医学领域的应用研究。

作为新兴影像技术，分子影像技术可在分子或细胞水平上对活体生物体内的生理、生化过程进行成像，并可进行空间、时间分辨的定性、定量分析，是生物医学研究的有力工具，并在各种疾病的临床诊断中得到广泛应用。各种用途的分子影像探针是实现分子影像在上述领域中成功应用的基础之一。

新型分子影像探针

主要集中于 ^{18}F 标记的各种 PET 探针(药物)的研究开发，目的在于开发具有临床应用前景的 PET 诊断药物以及可用于生物医学研究的分子影像工具探针。研究方向主要包括：(1) 肿瘤靶向的分子影像探针，如靶向血管活性肠肽受体的 ^{18}F-VIP、靶向碳酸酐酶 IX 的 ^{18}F 标记的小分子探针等。(2) 用于神经退行性疾病的分子影像探针，如用于阿尔兹海默病的 ^{18}FEtPIB 等。

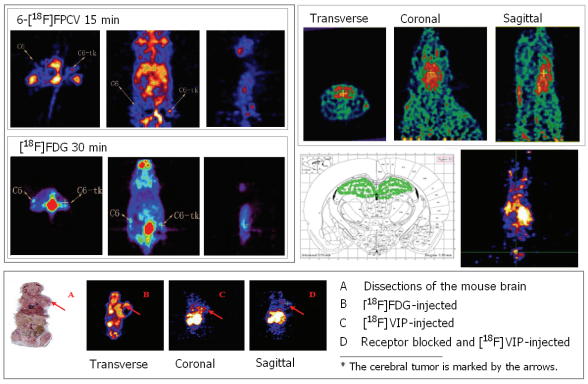

图 1　部分 PET 探针的 MicroPET 影像

分子影像探针制备新技术

针对当前放射性核素标记的 PET、SPECT 探针制备中的主要问题，采用模块化设计，分别构建具有肿瘤靶向作用的多肽模块和放射性核素标记模块，应用链接化学反应，实现多肽模块和标记模块的偶联，组装成放射性核素标记的多肽 PET/SPECT 探针，在此基础上，对获得的探针进行体内外生物学研究，评价其作为肿瘤靶向分子影像探针的可行性，以探索解决链接化学在分子影像探针制备中应用的关键问题，建立一种基于模块化设计思路和链接化学技术的放射性核素标记多肽类分子影像探针制备新技术。

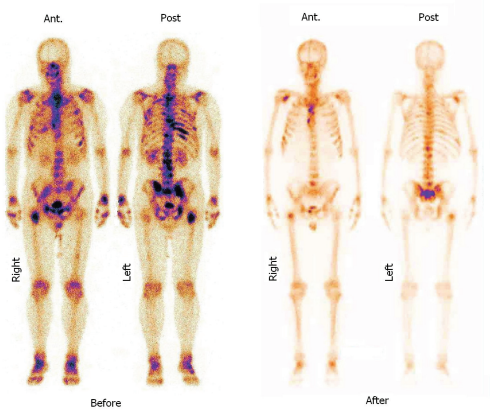

图 2　^{188}Re-HEDP 治疗前后病人的 SPECT 影像

^{188}Re 标记放射性新药研究

前期开发的 ^{188}Re-HEDP 2008 年完成 I 期临床试验，试验结果表明该药物安全、有效，正准备开展临床 II 期试验并完成成果转化。^{188}Re-铼硫混悬液临床前研究和 ^{188}Re 标记新技术研究进展良好。

纳米药物合成及应用

磁纳米药物合成　出靶向生物分子(羊抗兔 IgG、CEA 单抗等)偶联磁纳米粒的“磁–生物”双靶向纳米药物。标记放射性治疗核素后，可得磁纳米放射性药物；以结合放射性标识物为目的，可用作放射免疫分析试剂。

荧光量子点　制成性能良好的 II-VI 及含氧酸盐荧光量子，为合成新型磁性荧光纳米药物奠定了基石。正开展的研究有：分子影像探针合成新技术—链接化学中磁纳米粒模块化研究；磁纳米粒形貌对其血循环影响研究；量子点细胞毒性研究。

参考文献

1　Cheng Dengfeng, Yin Duanzhi, Zhang Lan, *et al*. Nucl Med Comm, 2007, **28**(6): 501–506
2　Zheng Mingqiang, Yin Duanzhi, Zhang Lan, *et al*. Acta Pharmacologica Sinica, 2008, **29**(5): 548–554
3　Zhang Guoxin, Wang Yongxian, Zhang Chunfu, *et al*. J Nanopart Res, 2009, **11**(2): 441–448

Progresses and Prospects in Radioactive Molecular Imaging

ZHANG Lan ZHOU Wei ZHANG Guoxin

Center for Radiopharmaceuticals Research

The radioactive molecular imaging group focuses on designing, preparation, biological evaluation and application of radioisotope-labeled molecular imaging probes (PET and SPECT). Also, we are developing ^{188}Re-labeled radiopharmaceuticals and working on nano materials and their applications in medicine.

As an emerging new imaging technology, molecular imaging can visualize physical or biochemical functions *in vivo* at molecular or cellular level, and further qualitative or quantitative analysis can be realized based on the images obtained. Molecular imaging has become a powerful tool for biological or medical studies and has been widely applied in clinical diagnosis of many diseases. Molecular imaging probes for different purpose are one of the legs which facilitate the development of molecular imaging.

Molecular imaging probes

The research programs are mainly focused on ^{18}F-labeled PET probes, aimed at developing new radiopharmaceuticals for PET diagnosis or providing tools for researchers. Current interests include: 1. Tumor targeted PET probes, such as ^{18}F-VIP targeting vasoactive intestinal peptide, and ^{18}F labeled ligands for carbonic anhydrase IX; 2. PET probes for neurodegenerative diseases, such as ^{18}FEtPIB for Alzheimer's disease.

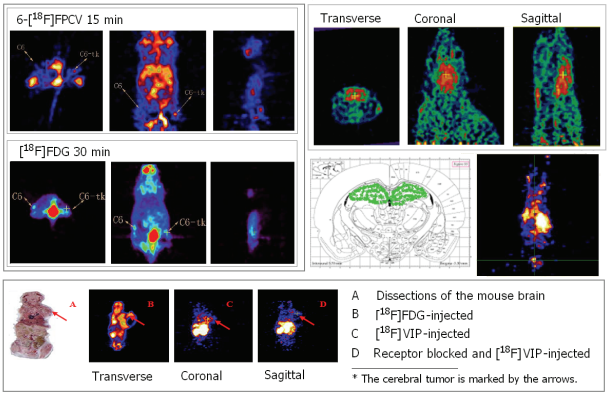

Fig.1 The PET-imaging probes developed by our group.

Novel techniques for preparing molecular imaging probes

This program is focused on major issues in molecular imaging probe preparation, especially radiolabeled peptide probes for PET and SPECT applications. Based on modu**larized design**, tumor targeting peptide modules, and ^{18}F- or ^{125}I-labeled modules, are synthesized. And using **click chemistry**, the modules are linked together to form different PET or SPECT probes. The obtained probes are evaluated *in vitro* and *in vivo* to find their feasibility as a tumor targeting molecular imaging probes.

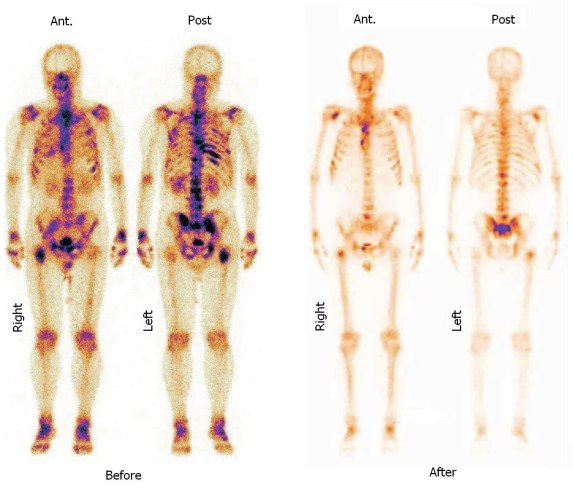

Fig.2 SPECT Images before and after ^{188}Re-HEDP therapy.

^{188}Re labeled new radiopharmaceuticals

^{188}Re-HEDP, a new radiopharmaceutical developed by our group has accomplished its Phase I clinical trials, which showed that it is safe and efficient. Now, we have been collaborating with a company to push forward the Phase II trials. Besides, ^{188}Re-sulfide suspension and novel Re- labeling techniques have been in good progresses.

Synthesis and application of nano-drugs

Magnetic nano-drug Magnetic nanoparticles are coupled with bio-molecular target (goat-anti-rabbit IgG, CEA monoclonal antibody, etc.) to form magnetic-biological double targeted nano-drug. Magnetic radiopharmaceutical is obtained by radioisotope labeling. Nano-drug can act as the radioimmunoassay reagent for the purpose of combining with radioactive markers.

Fluorescence quantum dots (QDs) The II-VI QDs and oxysalt QDs of better properties are prepared, providing basis for synthesis of novel magnetic fluorescent nano-drugs. Researches in progresses include: the new synthesis technology of molecular imaging probe—magnetic nanoparitcles modular of click chemistry, studies on effects of magnetic nanoparticle morphologies on their blood circulation, and QDs toxicity quantum in cells.

References

1 Cheng Dengfeng, Yin Duanzhi, Zhang Lan, *et al*. Nucl Med Comm, 2007, **28**(6): 501–506

2 Zheng Mingqiang, Yin Duanzhi, Zhang Lan, *et al*. Acta Pharmacologica Sinica. 2008, **29**(5): 548–554

3 Zhang Guoxin, Wang Yongxian, Zhang Chunfu, *et al*. J Nanopart Res, 2009, **11**(2): 441–448

基于树状分子、雌激素受体及 β-榄香烯的放射性药物研究

放射性药物中心　沈玉梅

为提高放射性诊断和治疗药物的有效性和安全性，我们开展了基于树状分子、雌激素受体及 β-榄香烯的 ^{99m}Tc 和 ^{188}Re 的同位素标记、构效关系探讨、体内生物分布及小动物 SPECT 显像研究。研究结果表明，同位素标记化合物在肿瘤部位有不同程度的浓集，在血液、肌肉和内脏组织的分布则有所降低。

β-榄香烯胺类、醚类衍生物及铼配合物的合成及抗肿瘤活性

合成了 β-榄香烯胺类、醚类、铼的系列衍生物，并观察了对人宫颈癌细胞 HeLa 细胞株的抑制活性以及药物对细胞周期和周期调节蛋白的影响。发现胺类衍生物和铼配合物的抗癌活性有显著提高，且通过调节周期调控蛋白 CyclinD1、Rb、PRb 的表达使细胞周期阻滞于 G_1 期。我们借助 ^{99m}Tc 研究了铼配合物在荷瘤鼠体内脏器和肿瘤部位的分布情况，来考察铼配合物的肿瘤靶向性。

β-榄香烯-[Re(CO)$_3$(H$_2$O)$_3$]+化合物的锝标记及体内分布和 SPECT 成像

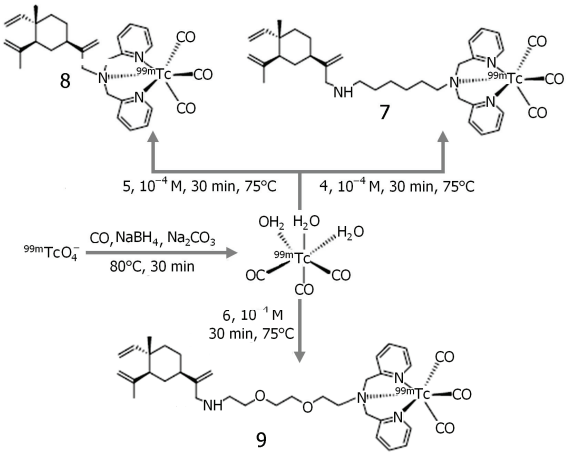

Scheme 1　β-榄香烯-[Re(CO)$_3$(H$_2$O)$_3$]+化合物的合成和放射标记

对合成的系列衍生物进行抗癌活性初筛后，对抗肿瘤活性较好的铼配合物进行 ^{99m}Tc 标记，Scheme 1 中，7、8、9 三种标记化合物的辛醇-水分配系数分别为 13.17±1.05、11.54±1.05、9.54±1.07，配合物的水溶性明显提高；荷瘤鼠体内分布(图 1，图 2)表明，在 Lewis 肺癌 LLC 细胞荷瘤鼠的肿瘤部位有一定浓集。因此，如何对化合物进行肿瘤靶向结构修饰，治疗效果，是的今后努力方向。

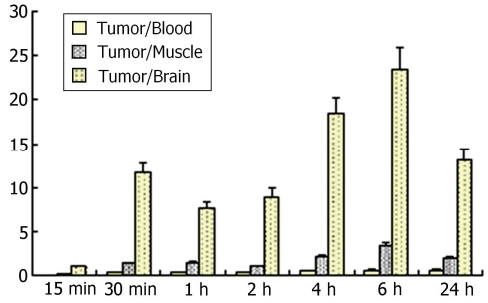

Fig.1　Tumor/blood, tumor/muscle and tumor/brain ratios in LLC(Lewis lung cancer)-bearing mice.

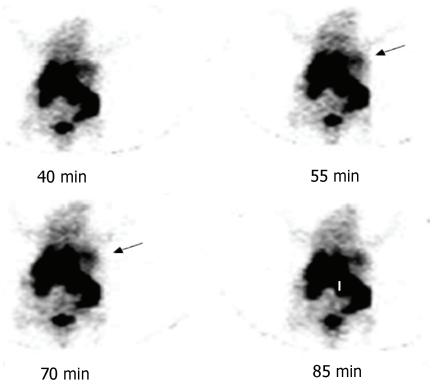

Fig.2　Micro-SPECT images of an LLC-bearing mouse.

参考文献

1　Cheng K M, *et al*. Chinese Journal of Organic Chemistry, 2008, 65–68

2　Ren Y F, *et al*. Acta Chemica Sinca, 2008, **66**(4): 459–464

3　Sun Y H, *et al*. Bioorganic & Medicinal Chemistry, 2009, **17**: 1118–1124.

4　Sun Y H, *et al*. Journal of Biological Inorganic Chemistry, 2009, **14**：899–904

5　Ren Y F, *et al*. Journal of Labelled Compounds and Radio-pharmaceuticals,　2009, **52**: 139–145

6　Huang L L, *et al*. *Steroids*, 2009, **74**: 701–706

7　Huang L L, *et al*. Journal of Organometallic Chemistry, 2009, **10**: 1016

8　Liu G F, *et al*. Medicinal Chemistry Research, 2009-MS#MCRE-270

9　Zhu H, *et al*. Synthetic Communications, LSYC-2009- 2818

Radiopharmaceuticals Studies Based on Dendrimer, Estrogen Receptor and β-elemene

SHEN Yumei, the Radiopharmaceuticals Center

For obtaining high quality radiopharmaceuticals and effective imaging agents, rhenium and technetium radiolabelling, biodistricution and micro-SPECT imaging studies based on dendrimer, estrogen receptor and β-elemene were conducted at SINAP. By modifying their structures, the radiolabelled compounds accumulated much more in tumor, while the concentration decreased in blood, muscle, liver etc.

Synthesis and *in vitro* Anti-proliferative Activity of β-elemene Monosubstituted Derivatives

β-elemene monosubstituted amine, ether and rhenium coordinated complex were synthesized. Their IC50 on HeLa cell lines, cell cycle and protein expression of G_1 phase (CyclinD1, Rb, P-Rb) were detected, respectively, by the methods of WST-1, flow cytometry and Western Blot. The results showed that the *in vitro* anti-proliferative activity of β-elemene monosubstituted amine and $Re(CO)_3$-β-elemene derivatives in human cervix epitheloid carcinoma HeLa cells were improved significantly, compared with ether derivatives and parent β-elemene. The derivatives could reduce Rb phosphorylation and cyclinD1 protein expression to arrest the cell cycle at G_1 phase. β-elemene-$^{99m}Tc(CO)_3(H_2O)_3^+$ conjugates (Scheme 1) were synthesized to study their tumor-targeting ability and water solubility.

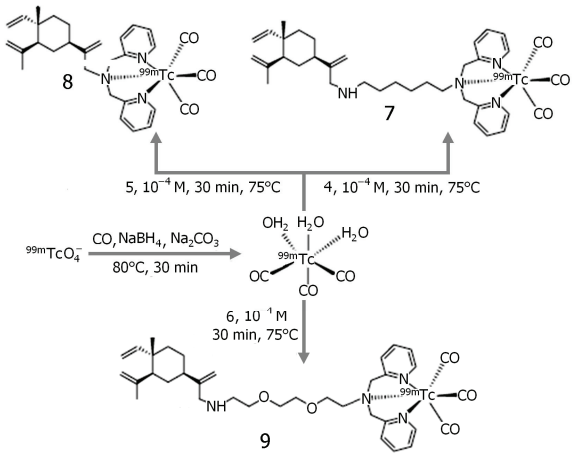

Scheme 1 Radiosynthesis of β-elemene-$^{99m}Tc(CO)_3$ Conjugates.

Radioactive Synthesis and Bio-distribution of β-elemene-$^{99m}Tc(CO)_3$ Conjugates

Aqueous solubility of the complexes can be evaluated by the octanol/water partition coefficients, which were determined as 13.17±1.05, 11.54±1.05 and 9.54±1.07, for Complex 7, 8 and 9, respectively. Compared with the reported P = 199.5 ± 4.12 of β-elemene, the oil-water partition coefficients of β-elemene-$^{99m}Tc(CO)_3(H_2O)_3^+$ decreased over 20 times than the parent β-elemene, and the water solubility was improved, too. Biodistribution of Compound 9 was studied using micro SPECT imaging with LLC(Lewis lung cancer)-bearing mice. The results (Figs. 1 and 2) show that β-elemene-$^{99m}Tc(CO)_3(H_2O)_3^+$ conjugate has certain accumulation in tumor after intravenous administration to the LLC-bearing mice. At 6 h post-injection, the tumor/muscle ratios in LLC-bearing mice reached 3.38 , but the radio distributions in non-target tissues are fairly high. Further efforts will be made to solve this problem.

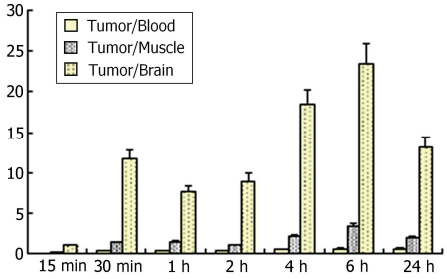

Fig.1 Tumor/blood, tumor/muscle and tumor/brain ratios in LLC(Lewis lung cancer)-bearing mice.

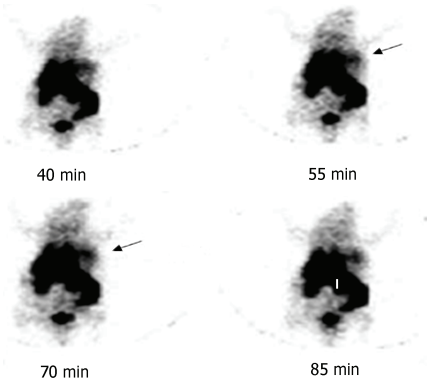

Fig.2 Micro-SPECT images of an LLC-bearing mouse.

References

1 Cheng K M, *et al*. Chinese Journal of Organic Chemistry, 2008, 65–68

2 Ren Y F, *et al*. Acta Chemica Sinca, 2008, **66**(4): 459–464

3 Sun Y H, *et al*. Bioorganic & Medicinal Chemistry, 2009, **17**: 1118–1124

4 Sun Y H, *et al*. Journal of Biological Inorganic Chemistry, 2009, **14**: 899–904

5 Ren Y F, *et al*. Journal of Labelled Compounds and Radiopharmaceuticals, 2009, **52**: 139–145

6 Huang L L, *et al*. Steroids, 2009, **74:** 701–706

7 Huang L L, *et al*. Journal of Organometallic Chemistry, 2009, **10**.1016

8 Liu G F, *et al*. Medicinal Chemistry Research, 2009, MS#MCRE-270

9 Zhu H, *et al*. Synthetic Communications, LSYC-2009- 2818

生物特征识别技术及应用研究

先进探测仪器研究中心　李勇平　敖新宇　黄跃峰

生物特征识别技术作为21世纪改变世界的十大高科技之一，在反恐与社会公共安全领域有广泛的应用。本课题组致力于生物特征识别的算法、技术应用和标准化检测技术的发展研究，重点针对人脸和指纹两种生物特征及融合识别技术及应用开展深入的探索研究。课题组长目前担任全国安防标委会生物识别应用技术分会(SAC/TC100/SC2)委员兼副秘书长，负责标准化体系的研究与制定。

生物特征识别算法研究

在人脸识别算法方面提出了基于二维 Gabor 特征(Gaborface)矩阵的人脸表征方法并对两种运用方式：整体 Gaborface 表征(EGFR)和多通道 Gaborface 表征(MGRF)进行了研究，采用二维 PCA 人脸识别算法在 ORL 和 YALE 数据库进行了实验，识别率分别达到 100%和 98.89%，该结果表明了该方法的有效性和可行性。对人脸姿态估计与校正重点研究了特征变换方法的有效性和适用性；对视频人脸识别的光照影响则采用平面光场分布拟合进行补偿，提高了算法的稳定性。在指纹识别方面提出了基于频域分析的奇异点区域提取算法，实现了指纹图像采集的同时获得奇异点区域，这样 2DPCA 能够得以有效快速地应用。在多模生物特征融合识别方面，提出了基于 FAR 归一化的分类器融合法则，提高了融合识别的可靠性和稳定性。

生物特征证照技术研究与应用

图 1　生物特征电子护照功能模块

根据国际民航组织(ICAO)新一代生物特征的电子护照规范 Doc9303，研究并实现了以 Java 卡为基础的的生物特征电子护照演示性平台。在该平台设计实现了具备通用接口的 Java 卡上文件类型，为护照信息在卡上的管理提供了有效手段；完成了 Java 卡上的电子护照基本功能程序设计，包括发卡和验证这两个阶段的写卡和读卡功能，通过了第三方软件的通用性测试；实现了 Passive Authentication 对系统数据进行加密，用 EF.SOD 来保障数据的安全和有效。另外，根据浮点数标准 IEEE754，设计了卡上单精度浮点运算环境，并成功地将该 CS-LDA 算法移植到 Java 卡，实验结果表明达到了应用要求。

指纹识别产品标准测试平台研制

根据全国安防标委会(SAC/TC100)研究制定的“指纹防盗锁通用技术条件”行业标准(标准号：GA701-2007)，受公安部安防报警产品质量检测中心委托，研制了基于该标准技术要求的指纹模块测试平台，建立了测试指纹数据库并编制了测试软件。实验结果表明，该平台能够满足标准的检测需求，现已通过公安部组织的验收并正式投入使用。

图 2　指纹模块测试平台

参考文献

1　Wang Lin, Li Yongping, *et al*. Image and Vision Computing, 2008, **26**: 820
2　Wang Chenbo, Li Yongping, *et al*. Intern J Computer Science and Network Security, 2008, **8**: 250
3　Zhang Hongzhou, Li Yongping, *et al*. Intern. J. Computer Science and Network Security, 2007, **7**: 89
4　牟晓生，戎玲，李勇平，等．“指纹防盗锁通用技术条件”GA701-2007
5　杨振宇，李勇平，等．计算机工程与科学, 2008, **30**(1): 49–51
6　金莉莉，李勇平，等．计算机工程，2008, **34**(7): 215–217
7　鲍强，敖新宇，李勇平，等．计算机工程，2009, **35**(5): 259–261

Biometrics Technique and Applications

LI Yongping AO Xinyu HUANG Yuefeng,
Center for Advanced Detection and Instrumentation

Biometrics, as one of the 10 emerging technologies to shape the world in the 21st century, has many potential applications in anti-terrorism and public security. The group devotes on related algorithm for face and fingerprint recognition (and their fusion), the standard measurement and the technique applications. And the group head is deputy secretary-general of the biometric application sub-committee (SAC/TC100/SC2) under the National Public Security Committee, being in charge of designing and establishing systematic architecture of the sub- committee standards.

Biometrics recognition algorithm

We proposed a scheme based on the linear correlation criterion to select optimized Gabor filter bank. In addition, by using 2D Gaborface matrices rather than transformed 1D feature vectors, two strategies to use the Gaborface bank are proposed, i.e. the ensemble Gaborface representation (EGFR) and multichannel Gaborface representation (MGFR). The feasibility of our method is proved by the experimental results on the ORL, Yale and FERET databases. The MGFR-based $(2D)^2$PCA method achieves 100% recognition accuracy for the ORL database, and 98.89% for the Yale database.

Estimation and correctness of face pose were focused on effectiveness of the feature transformation, while the processing on video-based face was focused on restoring the original illumination condition to improve the stability of recognition. Both the approaches achieve better results than most approaches in common uses.

Algorithm on singular point extraction based on analysis on frequency domain was proposed to obtain the singular point area right on capturing the fingerprint image, and based on this the 2DPCA could be applied. On the multiple biometrics, fusion algorithm based on FAR score normalization was performed, with good stability and feasibility of fusion recognition.

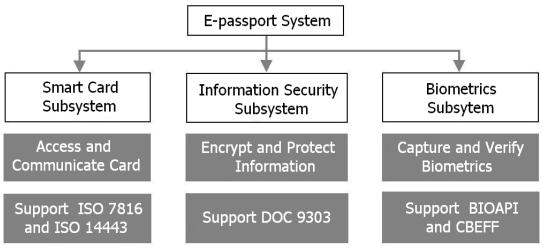

Fig.1 E-passport function modules.

Biometrics passport

According to ICAO's Doc9303 criterion on new generation e-passport, a demo platform of e-passport based on biometrics, PKI and RFID was implemented using Java card. The file-system in compliance with passport specifications was designed. It provides the means for information management on the Java. The primary functions of e-passport, such as passport issuing and verifying, were realized. The procedures were tested with the third party. Passive authentication was implemented, and EF.SOD was used to protect the data security and effectiveness. A floating-point data processing library on Java card was established according to the floating point standard IEEE-754, and the face verification algorithm CS-LDA was adapted for the Java card environment. Experimental results showed that basic Match-On-Card functionality requirements were fulfilled.

Testing platform for fingerprint lock

According to the GA701-2007 industrial standard established by the National Public Security Committee (SAC/TC100), a fingerprint recognition module testing platform was developed with the consignment of Quality Test Center for public security products of the Ministry of Public Security. A related fingerprint database was built to support various kinds of fingerprint modules. Integrated GUI software was developed for users to perform routine tests. Extensive experiments demonstrated that platform could meet the test requirements. It was checked and accepted in September 2008 by the Ministry of Public Security, and has been in regular use since then.

Fig.2 Testing platform for anti-burglary fingerprint lock.

References

1 Wang Lin, Li Yongping, *et al*. Image and Vision Computing, 2008, **26**: 820

2 Wang Chenbo, Li Yongping, *et al*. Intern J Computer Science and Network Security, 2008, **8**: 250

3 Zhang Hongzhou, Li Yongping, *et al*. Intern J Computer Science and Network Security, 2007, **7**: 89

4 Mo Xiaosheng, Rong Lin, Li Rongping, *et al*. National Standard for Fingerprint Lock GA-701, 2007

5 Yang Zhenyu, Li Yongping, *et al*. Computer Engineering and Science, 2008, **30**(1): 49–51

6 Jin Lili, Li Yongping, *et al*. Computer Engineering, 2008, **34**(7): 215–217

7 Bao Qiang, Ao Xinyu, Li Yongping, *et al*. Computer Engineering, 2009, **35**(5): 259–261

离子迁移率(IMS)技术及应用

先进探测仪器研究中心　蒋大真　李勇平

本课题组重点开展高灵敏度 IMS 检测技术研究以及测试平台研制。在前端探测技术方面，研制成两种类别的离子门结构和不同管径的 3 种系列共 7 套高性能的漂移管；后端数据采集与处理则针对室外移动和室内固定应用，分别开展基于不同处理器的信号采集与处理系统。与前端飘逸管结合，可以组装成微型、便携式、台式的离子迁移检测仪器。

离子门控制技术研究

离子门控技术是提高电离效率和检测灵敏度的关键，在原有专利技术—双脉冲门控技术的基础上，开展了 B-N 结构门控技术研究并应用于飘移管内，比对表明，两种结构的门控技术的效果均较满意。

不同管径的漂移管设计与实现

为扩展 IMS 的应用领域，仿真设计并制成直径 6、14 和 54 mm 等不同管径/长度比的飘移管，可满足不同的检测灵敏度和应用环境的要求。

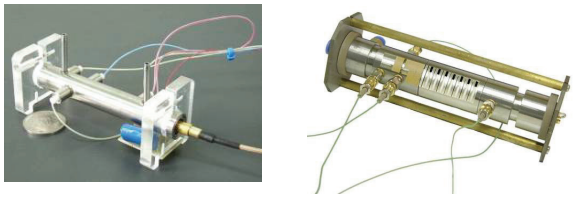

图 1　Φ6 mm (左)与 Φ14 mm (右)漂移管

数据采集与处理平台研究

图 2　基于工控机的一体化 IMS 检测平台

在 LabView 开发环境下完成了基于工控一体机、手提电脑和 PXI 控制器的数据采集和处理平台：基于 TI 数字处理控制器(DSC) F28335 的特定功能微型平台和基于 DSC 和 ARM 的多功能小型平台研究。

实际检测应用研究

除常规毒品和爆炸物检测外，重点开展了军用毒气、食品添加剂有毒物质和农药残留检测(图 3)，表 1 列出了部分物质的检测灵敏度结果。

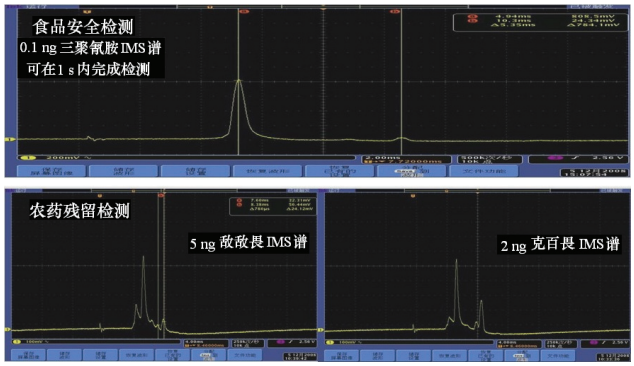

图 3　三聚氰胺和农药残留检测 IMS 图

表 1　部分物质的检测灵敏度结果

有毒物质	灵敏度 /ng
三聚氰胺 Melamine	< 1
敌敌畏 Dichlorvos	< 1
克百威 Carbofuran	< 1
盐酸克伦特罗 Clenbuterol	< 0.1
莱克多巴胺 Ractopamine	< 0.1

交流合作

与防化研究院建立了合作关系，我们的检测平台成功地检测出沙林气体和芥子气等毒剂。将就平台稳定性、可靠性和灵敏度以及仪器型号化方面作进一步改进与完善。2008 年，作为我国第一家单位加入国际 IMS 学会，并在第 17 届 IMS 国际年会(加拿大渥太华)上作“哈德玛得变换在 IMS 中的应用”口头报告，受到大会的广泛关注。

参考文献

1　Jiang Dazhen, Wei Yongbo, Li Yongping. The Application of Hadamard Transform in Ion Mobility Spectrometry, Int Conf on IMS, July 20–25, Ottawa, Canada

Ion Mobility Spectrometry

JIANG Dazhen LI Yongping

Center for Advanced Detection and Instrumentation

The group focuses on high sensitive IMS technique and applications with a prototype IMS developed at SINAP. In the front-end of detection, two types of ion-gating structures and various diameter/length drifting-tubes were developed to have a family of seven high-performance drift tubes. According to different requirements and environment, different back-end systems for data acquisition and processing, based on various processors, were developed for outdoor and indoor applications, and micro-, portable and desktop IMSs were designed with the drift-tubes.

Ion-gating control

Ion gating control plays important role for enhancing ionization efficiency and detection sensitivity of IMS. The B-N gate structure was studied based on our patented twin-pulse gating structure, and implemented in the drift tube successfully. Both the gating control techniques were tested in experiments with satisfying results.

Drift-tubes

After theoretical simulation, drift tubes of 6, 14 and 54 mm in diameter (with suitable length) were developed, for different requirements of sensitivity and environment.

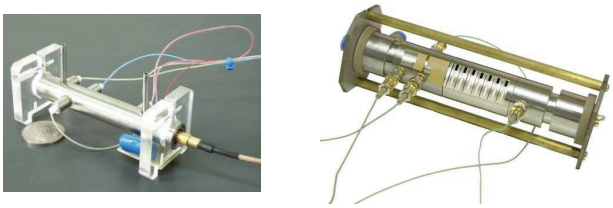

Fig.1 The Φ6 mm (left) and Φ14 mm (right) drift-tubes.

Data acquisition and processing systems

Fig.2 The prototype all-in-one IMS.

Platforms based on industrial control PC, laptop and PXI controllers were built up with LabView SDK. Efforts were made to use the recent TI digital signal controller (DSC) F28335 for functionality-specific mini-platform and general purpose multi-function small platform based on dual DSC and ARM processors.

IMS applications

In addition to detection of narcotics and explosives, the prototype IMS was applied to detect military toxic gas, food additives and pesticide residues, with encouraging results in experimental tests (Fig 3 and Table 1).

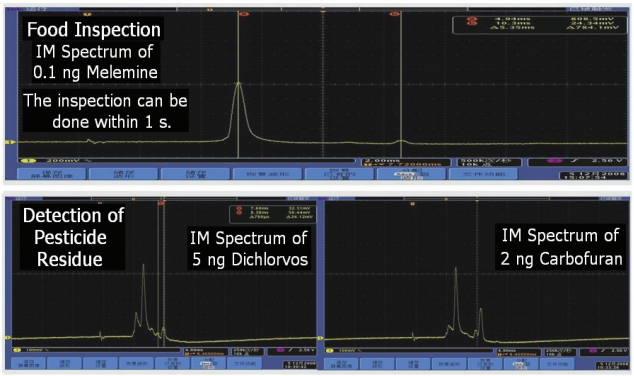

Fig.3 Melamine and pesticide spectra by the prototype IMS.

Table 1 Detection limit of the prototype IMS.

Harmful or Toxic Substances	Detection Limits /ng
Melamine	< 1
Dichlorvos	< 1
Carbofuran	< 1
Clenbuterol	< 0.1
Ractopamine	< 0.1

Academic exchange

In 2008, SINAP joined the International Society on IMS (ISIMS). We attended the 17th International Conference on IMS in Ottawa, Canada on July 20–25, 2008, and made an oral presentation entitled The Application of Hadamard Transform in Ion Mobility Spectrometry.

Reference

1 Jiang Dazhen, Wei Yongbo, Li Yongping. The Application of Hadamard Transform in Ion Mobility Spectrometry, Int Conf on IMS, July 20-25, Ottawa, Canada

生物医学分子影像物理与技术研究

先进仪器研究中心　漆玉金

本课题组的研究瞄准快速发展的新兴交叉学科分子影像领域，发展多模态的分子影像技术。分子影像是利用无创影像技术在生物活体内对特定的生物分子或靶向药物分子参与的生理过程进行可视化的表征与定量描述，对未来在分子或细胞层次上的疾病早期诊断与治疗以及新药研发模式变革具有重要意义，其科学研究价值和潜在的产业价值倍受关注与重视。课题组从事的分子影像技术包括：单光子发射计算机断层成像(SPECT)、正电子发射断层成像(PET)和 X 射线计算机断层成像(CT)。我们的研究目标是发展多模态的活体小动物分子影像技术，目前主要开展 micro-SPECT 成像与 micro-CT 及 MRI 融合的分子影像技术研究，具体的研究课题有：先进成像探测器的研发、成像系统的模拟与开发、精确定量的三维图像重建与处理技术研究以及运用这些分子影像技术为其他研究组提供服务等。

高分辨模块化成像探测器技术研究

成像探测器是构建影像系统的核心部件，高分辨模块化成像探测单元是发展先进成像设备的关键。利用先进的阵列闪烁晶体和位置灵敏光电倍增管成功地研制出了多款高分辨的小型伽玛相机模块，开发出了具有自主创新特色的阵列探测器简化读出电子学电路，取代传统的读出电子学电路，在不增加读出及处理电子学的复杂性的情况下，可以显著地提高了探测器的内在分辨，同时增大探测器的有效成像视野。

下一步研究将集中发展强磁场下的新型 SPECT 和 PET 模块探测器技术，思路是采用新兴的半导体位置灵敏光电倍增管技术，开发新型高分辨 SPECT 和 PET 成像探测器模块。

Micro-SPECT 与 micro-CT 成像系统研发

采用针孔准直器技术来代替常规的平行孔准直器技术，精确的蒙特卡洛模拟用于针孔准直器的优化设计与系统样机设计，成功地开发了 2 台高分辨的小动物 micro-SPECT 成像系统。一台基于上述高分辨小型伽玛相机探头；另一台基于改造临床使用的商用伽玛相机探头。两台 micro-SPECT 系统都达到了亚毫米的成像分辨，并成功地应用于多项小动物成像实验研究，取得了用户满意的成像效果。

小动物 micro-CT 的设计基于锥束成像几何的系统构建，采用微聚焦光斑的 X 射线管(~45 μm)和较大视野的 CMOS 平板探测器(~12 cm)来发展高分辨的成像系统，同时设计了一个机械快门以有效降低成像物体的吸收剂量。对小动物能实现较快的(5–6min)断层成像扫描，成像分辨可达 100 μm 左右。

下阶段研究将开展 micro-SPECT 与 micro-CT 同机系统集成研究；同时开展能与 MRI 成像融合的新型 micro-SPECT 或 micro-PET 样机系统研究。

三维断层图像重建与处理技术研究

研究主要集中在开发精确定量的三维图像重建与系统校正技术。针对针孔 SPECT 与锥形束 CT 成像的几何相似性，开发利用了统一的数学方法来估定成像系统的几何校正的新颖算法，把多模态 micro-SPECT/CT 系统的图像配准融合算法有机地结合起来；成功地开发了针孔 SPECT 成像的统计迭代三维图像重建技术，把系统响应修正加入统计迭代算法显著地改善了图像的重建质量，系统成像分辨率提高到亚毫米。还在常规圆规道针孔 SPECT 成像的基础上，开发了螺旋轨道的针孔 SPECT 成像技术，可显著地改善常规圆轨道针孔 SPECT 成像的轴向分辨，增大了其轴向视野。

下一步研究将集中在开展多针孔 SPECT 成像方法研究，在保持高分辨成像的同时，提高成像的探测效率，缩短成像时间；同时还要加强多模态分子影像的图像融合技术研究。

参考文献

1 张猛蛟, 漆玉金. 核技术，2007, **20**(7): 629–632
2 代秋声, 漆玉金. 原子能科学技术，2008, **42**(6): 535–539
3 赵翠兰, 漆玉金, 施亮, 等. 原子核物理评论，2010, **27**(1): 63-67
4 Qi Y J, Zhang M J, Zhao C L, *et al*. Record of the 2007 IEEE Nuclear Science Symposium & Medical Imaging Conference, M19-67, 3725–3728
5 Zhang X Z, Dai Q S, Qi Y J. Record of the 2008 IEEE Nuclear Science Symposium & Medical Imaging Conference, M10-416, 5255–5259
6 代秋声, 漆玉金. 物理学报，2010, **69**(2): 1769–1778
7 张雪竹, 漆玉金. 科学通报，2010, 55(18):1846–1855

Biomedical Molecular Imaging Physics and Technology

QI Yujin, Center for Advanced Detection and Instrumentation

The group is focused on developing multi-modality molecular imaging technologies, a fast growing field of research world wide. Molecular imaging uses non-invasive imaging technologies to visualize and characterize specific molecular events and targets *in vivo*. Currently, the group's research interest covers single photon emission computed tomography (SPECT), positron emission tomography (PET), and X-ray computed tomography (CT), aimed at developing multi-modality molecular imaging techniques for small animal imaging, and exploring integration of micro-SPECT imaging with micro-CT and MRI systems. Specifically, research programs of the group include the development of new or improved imaging detectors, system simulation and development of novel imaging system; the study of accurate quantitative 3D image reconstruction algorithms with image degradation corrections; and application of the imaging techniques in studies involving small-animal imaging experiments.

Novel imaging detectors

A detector is a basic unit to build an imaging system. High resolution modularized detectors are the key for developing advanced imaging system. We used pixellated scintillation crystal array with position sensitive photomultiplier tube to develop a modular gamma camera. A novel subtractive resistive readout was developed to replace the conventional resistive readout to improve the detector performance while keeping the simplicity of the signal processing electronics. The intrinsic resolution and effective field-of-view (FOV) of the detectors are significantly improved with the novel readout electronics.

The next program is to develop a new type of modularized detector for SPECT and PET. Based on the newly emerged silicon photomultiplier technique, the detector shall work effectively in strong magnetic field of an MRI.

Small-animal micro-SPECT and micro-CT imaging systems

Two micro-SPECT systems were developed successfully by utilizing pinhole collimation, instead of the conventional parallel-hole collimation. The collimator and system designs were optimized using Monte Carlo simulations. One system was based on the above modular gamma camera, while the other was upgraded from a conventional gamma camera for clinic use. With sub-millimeter spatial resolution, both the micro-SPECT systems have been used in many small-animal imaging experiments.

A small-animal micro-CT system we developed is based on cone-beam imaging geometry. A micro-focus X-ray tube (~45-μm focal spot) and a CMOS flat-panel X-ray detector with a 12-cm field of view (FOV) were used. A mechanical shutter to reduce the dose absorbed in the imaging objects. This system can perform fast CT imaging (5–6 minutes) with a spatial resolution of about 100 μm.

Efforts will be made in integrating the multi-modality molecular imaging systems of micro-SPECT and micro-CT, and in exploring the integration of micro-SPECT or micro-PET imaging with MRI system.

3D image reconstruction and processing

This program is to develop accurate quantitative 3D image reconstruction algorithms with image degradation correction techniques. Based on the high similarity between pinhole and cone-beam geometry, we developed a unified mathematical optimization method to determine the complete geometric and registered parameters for both cone-beam CT and pinhole SPECT for misalignment calibration and image registration. A 3D pinhole SPECT image reconstruction with statistically iterative OSEM algorithm was developed. The system response was implemented into the algorithm, and this improved significantly the reconstructed image quality, with sub-millimeter image resolution recovery. We also developed the helical pinhole SPECT imaging technique, in addition to the conventional pinhole SPECT with circular orbit scan. The helical pinhole SPECT provides significant improvement in the axial imaging FOV and resolution, being very useful for whole body small animal imaging.

Further work is targeted to developing multi-pinhole SPECT imaging technique to increase detection efficiency while keeping the high spatial resolution and reducing the imaging scan time. Efforts will also be made in studying image co-registration and fusion techniques for multi-modality imaging.

References

1 Zhang M J, Qi Y J. Nucl Tech, 2007, **20**: 629–632
2 Dai Q S, Qi Y J. Atomic Energy Science & Technology, 2008, **42**: 535–539
3 Zhao C L, Qi Y J, Shi L, et al., Review of Nuclear Physics, 2010, **27**(1):63-67
4 Qi Y J, Zhang M J, Zhao C L, *et al*. Record of the 2007 IEEE Nuclear Science Symposium & Medical Imaging Conference, M19-67, 3725–3728
5 Zhang X Z, Dai Q S, Qi Y J. Record of the 2008 IEEE Nuclear Science Symposium & Medical Imaging Conference, M10-416, 5255–5259
6 Dai Q S, Qi Y J. Acta Physica Sinica, 2010, **69**(2): 1769–1778
7 Zhang X Z, Qi Y J. Chinese Science Bulletin, 2010, **55**(18): 1846–1855

700–800 kV/150 mA×2 电子辐照加速器研制

应用加速器研究室　李德明　张宇田

电子束辐照燃煤锅炉烟道气脱除 SO_2 和 NO_x 方法由日本荏原公司于 20 世纪 70 年代提出，其原理为用电子束辐照烟道气体，激发产生自由基与加入的氨进行反应生成硫酸氨和硝酸氨达到脱除环境污染物 SO_2 和 NO_x，这些硫酸氨和硝酸氨经进一步加工可作为农用化肥。相对于化学法脱硫脱硝,该技术具有可同时脱除两种污染物，并且副产物是化肥，也无二次污染，具有明显的技术优势。

电子束烟气脱硫脱硝装置中的关键设备是大功率电子加速器。这种低能大功率的电子加速器具有广泛的潜在市场需求，日本已研制成功并投入试用，俄罗斯、美国、法国等国家也在加紧研制。

在中国科学院知识创新重大项目“核技术应用关键技术研究”的支持下(子课题 3—燃煤烟气电子束净化关键技术研究及国产化示范应用)，我们瞄准技术领域前沿，设计并研制了这种低能大功率的低能加速器。2008 年 11 月，中国科学院组织专家组对该大功率电子加速器进行了测试，测试结果表明，其以达到如下技术指标：

电子束能量/ keV	750 (空载)
	700 (负载)
电子束流强 / mA	150 × 2
能量不稳定度 / %	±5
束流不稳定度 / %	±5
扫描宽度 / mm	2000
扫描频率 / Hz	100
扫描不均匀度 / %	± 10

该机高压发生器采用 SF_6 气体绝缘工频变压器，具有体积小，电能转换效率高达 90%以上。模块化设计使得制造和检修维护均极为方便。电子枪阴极采用 LaB_6 晶体，电子发射能力强，性能稳定可靠。加速器整体性能达到国际同类加速器先进水平，是当前国内引出束流最大、单机功率最大的低能电子辐照加速器。该机的研制成功，将为推动我国核技术和电子束辐照技术在环境保护和辐射加工领域中的应用，产生积极作用。

Development of 700–800kV/150 mA×2 E-beam Irradiator for Radiation Processing

LI Deming ZHANG Yutian, Division of Applied Accelerators

The technology of electron beam flue gas treatment (EBFGT) for removal of SO_2 and NO_x in the fumes produced by coal-fired installation was brought up by Ebara Corporation in 1970s. Irradiating the flue gases with electron beams produces highly reactive free radicals, which oxidize the SO_2 and NO_x components of the flue gas into corresponding acids, and the acids react with the ammonia sprayed into the flue gases to form ammonium sulfate and ammonium nitrate. The byproducts of the treatment are collected for further treatment to become farming fertilizers. Comparing to the chemical process for denitration and desulfuration, the electron beam process can remove both pollutants simultaneously, create useful by-product as agricultural chemical fertilizer, while no secondary pollution. It has technical advantages obviously. The critical equipment for EBFGT is the high power electron accelerator. The low-energy high power electron accelerator has widely potential market demand, which is successfully developed and trial used in Japan and developing rapidly in countries as Russia, America, France and etc.

Supported by the Knowledge Innovation Project of the Chinese Academy of Sciences under the contract of Key Technologies in EBFGT and Its Demonstrational Application in China, which is part of the CAS project of Key Technologies in Applications of Nuclear Techniques, and aimed at frontier technologies in EBFGT, we have developed the powerful low energy E-beam irradiator. According to measurements in November 2008 by the CAS-organized expert team to test the accelerator for checking and accepting the project, the accelerator performed satisfactorily with the following specifications.

Beam energy / keV	750 (without load) 700 (loaded)
Beam current / mA	150×2
Energy instability / %	±5
Beam current instability / %	±5
Beam scan width / mm	2000
Beam scan frequency / Hz	100
Beam scan non-uniformity / %	±10

The high voltage is generated by using a power frequency transformer of SF_6 gas insulation, hence it small size and high power conversion efficiency (over 90%). Adopting the method of modularized design, the accelerator is convenient to manufacture and to do the maintenance. With the cathode made of crystal LaB_6, the electron gun provides strong electron emission and its performance is stable and reliable. Entire performance of the accelerator has reached advanced level achieved by similar E-beam irradiators in the world. It is the low energy E-beam irradiator of the highest beam current and power in China. The successful development will certainly promote of nuclear technique applications in China, especially E-beam application in environment protection and other areas of radiation processing.

附录 1 2007–2008 年学术论文统计

Papers Published in 2007–2008

上海光源 Shanghai Synchrotron Radiation Facility

1 冷用斌, 周伟民, 陈永忠, 等. 上海光源储存环直流流强监测系统设计, 核技术, 2007, **30**(7): 477–480

2 刘学, 朱毅, 朱伟忠, 等. 内衬弹簧冷却槽晶体的热缓释研究, 核技术, 2007, **30**(10): 808–810

3 朱毅, 王纳秀, 夏绍建, 等. 上海光源插入件光束线水冷四刀狭缝设计, 核技术, 2007, **30**(6): 481–485

4 李纪堂, 郑丽芳, 胡勇, 等. 同步辐射光束线前端真空快保护系统, 核电子学与探测技术, 2007, **27**(2): 257–259

5 柯明, 殷立新, 董岚. 北京同步辐射装置准直测量控制网的设计与优化, 测绘科学, 2007, **32**(2): 122–124

6 胡勇, 郑丽芳, 李纪堂. 基于 EPICS 的运动控制系统, 核电子学与探测技术, 2007, **27**(6):

7 袁启兵, 谷鸣, 陈志豪, 等. 基于 PLC 的 110 MW 脉冲调制器控制器设计, 核技术, 2007, **30**(10) 864－867

8 袁启兵, 谷鸣, 王锐萍, 等. The control system for SSRF injection and extraction, Nuclear Science and Technology, 2007, **18**(6): 326–329

9 彭程程, 谷鸣, 刘波, 等. Measurement system for SSRF pulsed magnets, Nuclear Science and Technology, 2007, **18**(6): 321–325

10 彭程程, 谷鸣, 刘波, 等. 模拟有源积分器在脉冲磁场测量中的分析和应用, 核技术, 2007, **30**(9): 725–729

11 李长兴, 谷鸣, 陈志豪, 等. 脉冲调制器机柜屏蔽效能分析测试, 核技术, 2007, **30**(2): 81－86

12 唐俊龙, 许瑞年, 陈焕光, 等. Virtual instrument for controlling and monitoring digitalized power supply in SSRF, Nuclear Science and Technology, 2007, **18**(3): 129–134

13 韩毅昂, 后接, 刘桂民, 等. Analysis on transmission efficiency of SSRF electron beam transfer lines, Nuclear Science and Technology, 2007, **18**(2)

14 韩毅昂, 刘桂民, 李德明. Magnet lattice design of SSRF electron beam transfer lines, Nuclear Science and Technology, 2007, **18**(4)

15 曹红萍, 陈焕光, 许瑞年, 等. 皮秒加速器的安全联锁设计, 核技术, 2007, **30**(10): 721–724

16 李瑞, 卢宋林, 胡志敏, 等. 高效率隔离型准谐振 24V 1A 开关电源实现, 核技术, 2007, **30**(2): 93–96

17 李瑞, 卢宋林, 陈焕光, 等. 新型 PID 校正技术在 2Hz 动态开关电源中的运用, 核电子学与探测技术, 2007, **27**(5): 833－835

18 唐俊龙, 许瑞年, 陈焕光, 等. Lab VIEW 在 SSRF 数字电源研制中的应用, 核电子学与探测技术, 2007, **27**(1): 35–40

19 孙启龙, 林国强, 戴志敏, 等.加速器物理与射频, 基于碳纳米管场致发射的电子枪的初步研究, 高能物理与核物理, 2007, **31**(3): 296–299

20 孙启龙, 王兴涛, 林国强, 等. 碳纳米管光场致发射新型电子枪的初步方案设计, 核技术, 2007, **30**(11): 947－951

21 储建华, 赵振堂. 偏轴双腔互比型腔式束流位置监测器, 强激光与粒子束, 2007, **19**(10): 1717–1721

22 邓海啸, 王兴涛, 李东国, 等. 上海深紫外自由电子激光的非线性谐波辐射研究, 强激光与粒子束, 2007, **19**(10): 1603–1607

23 张猛, 赵明华. 上海同步辐射装置次谐波聚束腔中二次电子倍增效应的模拟, 核技术, 2007, **30**(5): 403–406

24 于成浩, 柯明, 赵振堂. 由三维坐标值计算两点距离的精度分析及应用, 测绘科学, 2007, **32**(1): 73–74

25 于成浩, 柯明, 赵振堂. 提高激光跟踪仪测量精度的措施, 测绘科学, 2007, **32**(2): 54–56

26 张海鸥, 王志山. 上海光源(SSRF)输运线真空系统设计, 真空科学与技术学报, 2007, **27**(6): 553–556

27 李宇, 阎和平, 周巧跟. 脉冲线测量波荡器磁场的研究, 核技术, 2007, **30**(10): 815

28 邓彪, 余笑寒, 徐洪杰. 同步辐射微束 X 射线荧光 CT 的计算机模拟, 核技术, 2007, **30**(1): 5–11

29 邓彪, 余笑寒, 徐洪杰. 同步辐射硬 X 射线微束技术, 核技术, 2007, **30**(5): 397–402

30 邓彪, 余笑寒, 徐洪杰. 若干因素对同步辐射微束 X 射线荧光 CT 图像质量的影响研究, 核电子学与探测技术, 2007, **27**(2), 260–264

31 邓彪, 余笑寒, 徐洪杰. Influence of sampling interval and number of projections on the quality of SR-XFMT reconstruction, 高能物理与核物理, 2007, **31**(4): 409–413

32 邓彪, 余笑寒, 徐洪杰. Nondestructive analysis by combined X-ray tomography on a synchrotron radiation facility, Nuclear Science and Techniques, 2007, **18**(5): 257–260

33 张增艳, 余笑寒, 肖体乔, 等. 化学混合物成分的太赫兹光谱分析, 光子学报, 2007, **36**(2): 290–293

34 郭智, 邰仁忠, 徐洪杰, 等. X-ray probe of the polar nanoregions in the relaxor ferroelectric 0.72Pb($Mg_{1/3}Nb_{2/3}$)O_3-0.28$PbTiO_3$, Applied Physics Letters, 2007, **91**(8): 081904–1–081904–3

35 郭智, 郃仁忠, 徐洪杰,等. Study of the Microscopic Structures in 0.72Pb($Mg_{1/3}Nb_{2/3}$)O_3-0.28 $PbTiO_3$ relaxor ferroelectrics by means of X-ray Diffraction, Journal of Applied Physics, 2007, **101**(5): 053505-1- 053505-6

36 郭智, 严睿, 张祥志, 等. 0.72Pb($Mg_{1/3}Nb_{2/3}$)O_3-0.28 $PbTiO_3$ 弛豫铁电体中纳米极化区域温度特征实验研究, 核技术, 2007, **30**(10): 801–804

37 胡雯, 谢红兰, 杜国浩, 等. 同步辐射 X 射线成像光束线劳厄双晶单色器设计, 高能物理与核物理, 2007, **31**(6): 597–601

38 张增艳, 余笑寒, 赵红卫, 等. Component analysis to isomer mixture with THz-TDS, Optics Communications, 2007, **277**(2): 273–276

39 刘丽想, 杜国浩, 胡雯, 等. 同步实验部, X 射线同轴轮廓成像中影响成像质量的若干因素研究, 物理学报, 2007, **56**(8): 4556–4564

40 骆玉宇, 肖体乔, 陈敏, 等. 利用同步辐射扭摆器光源研究 X 射线同轴轮廓成像质量, 核技术, 2007, 30(2): 97–104

41 徐春艳, 宋佳平, 丁澦, 等. Crystallization and preliminary X-ray analysis of Sau3AI/E64A Mutant Protein, Protein and Peptide Letters, 2007, **14**: 505–506

42 马广明, 赵振堂, 刘建飞. Design of a higher harmonic cavity for the SSRF storage ring, 中国物理 C, 2008, **32**(4): 275–279

43 马广明, 赵振堂. Studies on high order mode of bell-shaped prototype cavities, 中国物理 C, 2008, **32**(12): 1012–1015

44 尹成科, 戴志敏, 刘建飞, 等. A non-IQ sampling controller in low level RF system, 中国物理 C, 2008, **32**(10): 862–856

45 赵玉彬, 尹成科, 张同宣, 等. Digital prototype of LLRF system for SSRF, 中国物理 C, 2008, **32**(9): 758–760

46 张同宣, 赵振堂. 腔体带通滤波器设计, 核技术, 2008, **31**(6): 401–404

47 张同宣, 赵玉彬, 尹成科, 等. 上海光源数字化低电平控制系统的硬件设计与实现, 强激光与粒子束, 2008, **20**(6): 1048–1052

48 陈明, 封自强, 赵申杰, 等. 上海光源储存环高频功率源, 中国物理 C, 2008, **32**(S1): 197–199

49 赵玉彬, 赵振堂, 尹成科, 等. 在现场可编程门阵列中的高频反馈数字化算法, 强激光与粒子束, 2008, **20**(12): 579–579

50 田顺强, 后接, 陈光玲, 等. Analysis of sextupole effects on beta function beating in the SSRF storage ring, 中国物理 C, 2008, **32**(7): 576–579

51 田顺强, 后接, 陈光玲, 等. New chromaticity compensation approach and dynamic aperture increase in the SSRF storage ring, 中国物理 C, 2008, **32**(8): 661–664

52 田顺强, 刘桂民, 张文志, 等. Calibration of the linear optics in the SSRF storage ring, Nuclear Science and Technology, 2008 **19**(5): 257–265

53 后接, 孙小影, 陈光玲, 等. Excitation curve calibration for the SSRF Booster Magnets and applications in the commissioning, Nuclear Science and Technology, 2008, **19**(4): 204–208

54 后接, 刘桂民, 李浩虎, 等. Sorting of bending magnets for the SSRF booster, 中国物理 C, 2008, **32**(4): 285–289

55 陈建辉, 赵振堂, 戴志敏, 等. Study of closed orbit response to magnet vibrations at the SSRF storage ring, 中国物理 C, 2008, **32**(7): 589–592

56 冀瑞敏, 田顺强, 后接, 等. 高频噪声对上海光源储存环束流品质的影响, 核技术, 2008, **31**(5): 321–324

57 张满洲, 后接, 李浩虎, 等. Optimal sorting method and application to SSRF booster dipoles, 中国物理 C, 2008, **32**(11): 924–927

58 张文志, 刘桂民, 赵黎颖, 等. 上海同步光源定时系统物理设计, 中国物理 C, 2008, **32**(S1): 109–111

59 邓海啸, 戴志敏. Design of cascading two stages of high gain harmonic generation scheme based on Shanghai deep ultraviolet free electron laser, 中国物理 C, 2008, **32**(3): 236–242

60 邓海啸, 戴志敏. Gain of harmonic generation in high gain free electron laser, 中国物理 C, 2008, **32**(4): 297–392

61 邓海啸, 戴志敏. Harmonic operation of high gain harmonic generation free electron laser, 中国物理 C, 2008, **32**(7): 593–598

62 邓海啸, 戴志敏. On harmonic operation of Shanghai deep UV free electron laser, Nuclear Science and Technology, 2008, **19**(1): 7–12

63 邓海啸, 王兴涛, 戴志敏. Short-pulse length effects of the seed laser in high-gain harmonic generation free-electron laser, Phys Rev ST Accel Beams, 2008, **11**(4): 040732

64 邓海啸, 李东国, 戴志敏. Field evolution of harmonic radiation in an HGHG FEL, Nuclear Science and Technology, 2008, **19**(5): 266–273

65 邓海啸, 戴志敏. High gain harmonic generation free electron laser seeded by few-cycle laser, J Phys D: Appl

Phys, 2008, **41**(11): 115503

66 卑华, 戴志敏. Theoretical and numerical analysis of coherent Smith-Purcell radiation, 中国物理 C, 2008, **32**(11): 916–923

67 卑华, 林栩凌, 戴志敏. Design of Smith-Purcell emitter in femtosecond accelerator, 中国物理 C, 2008, **32**(12): 1007–1011

68 卑华, 戴冬东, 戴志敏. Simulation of smith-purcell radiation from compact terahertz source, 强激光与粒子束, 2008, **20**(11): 2067–2072

69 储建华, 童德春, 赵振堂. RF measurements of position a C-band cavity beam monitor, 中国物理 C, 2008, **32**(5): 385–388

70 于成浩. 3 维准直测量技术在上海光源中的应用研究, 测绘学报, 2008, **37**(4): 531

71 WANG Xiao, CHEN Liang, DU Hanwen, *et al*. Measurement of underground motion at SSRF site, Journal of Synchrotron Radiation (Impact factor 2007: 2.978), 2008, (15): 350–354

72 WANG Xiao, CHEN Liang, YAN Zhongba, *et al*. Mechanical stability for magnet girder assembly at SSRF, Journal of Synchrotron Radiation(Impact factor 2007: 2.978), 2008, (15): 385–391

73 王晓, 曹云, 陈亮, 等. SSRF 中 BPM 支撑的机械稳定性分析, 中国物理 C, 2008, **31**(增刊): 28–30

74 冯忠俊, 王晓, 杜涵文，等. 上海自由电子激光工程地基振动研究, 核技术, 2008, **31**(4)；245–249

75 安双利, 蒋迪奎, 郭盘林. 上海电子束离子阱真空控制系统, 核技术, 2008, **31**(2): 109–113

76 何志义, 许皆平, 崔剑. 移动式氦液化器控制系统升级改造, 核技术, 2008, **31**(3): 233–236

77 安双利, 蒋迪奎, 郭盘林. 上海 EBIT 装置微量气体注入系统的研制, 真空科学与技术, 2008, **27**(1): 1–4

78 安双利, 蒋迪奎, 蒋罗荣, 等. 上海光源 TSP&NEG 复合电源的研制, 真空, 2008, **44**(4): 72–74

79 王宏飞, 陆杰, 周巧根, 等. 翻转线圈系统在波荡器积分场测量中的应用, 强激光与粒子束, 2008, **20**(5): 320

80 魏向军, 雷勇 , 孙天希, 等. Elemental depth profile of faux bamboo paint in forbidden city studied by synchrotron radiation confocal m-XRF, X-ray Spectrometry, 2008, **37**(6): 595–598

81 严睿, 郭智, 郜仁忠. Observation of long-range correlation dynamics in $BaTiO_3$ near TC by Photon Correlation Spectroscopy, Applied Physics Letters, 2008, **93**(19): 192908-1–192908-3

82 朱伟忠, 吴衍青, 陈敏, 等. 13.4 nm 软 X 射线干涉光刻透射光栅的优化设计, 光学学报, 2008, **28**(7): 1225–1230

83 朱伟忠, 吴衍青, 郭智, 等. 大面积 10000 线/毫米软 X 射线金属型透射光栅的设计、制作与检测, 物理学报, 2008, **57**(10):, 6387–6392

84 朱伟忠, 吴衍青, 史沛熊, 等. 基于高级硅刻蚀和硅氧化工艺的软 X 射线干涉光刻分束, 核技术, 2008, **31**(6): 415–419

85 振孙晖, 罗红心, 肖体乔, 等. 动对长程面型仪静态稳定性的影响, 核技术, 2008, **31**(9): 658–662

86 师绍猛, 陈荣昌, 薛艳玲, 等. 强吸收介质内部低 Z 材料结构的 X 射线显微成像研究, 物理学报, 2008, **57**(10): 6319–6328

87 师绍猛, 陈荣昌, 薛艳玲, 等. 激光核聚变靶的 X 射线相衬显微成像研究, 核技术, 2008, **31**(7): 524–528

88 张增艳, 肖体乔, 赵红卫, 等. 核苷混合物的太赫兹谱定量分析, 光谱学与光谱分析, 2008, **28**(9): 1990–1993

89 谢红兰, 胡雯, 罗红心, 等. X 射线荧光全息术中消除光源偏振效应和孪生像的重构新算法, 物理学报, 2008, **57**(11): 7044–7051

90 红兰, 胡雯, 罗红心, 等. 双能量 X 射线荧光全息图重构算法消除孪生像的模拟研究, 核技术, 2008, **31**(8): 571–576

91 薛艳玲, 肖体乔, 杜国浩, 等. 西洋参和高丽白参的 X 射线显微鉴定研究, 光学学报, 2008, **28**(9): 1828–1832

92 席再军, 余笑寒, 肖体乔, 等. Study of terahertz pulses at an edge, Chinese Optics Letters, 2008, **6**(9): 1－3

93 陈焕光, 李瑞, 郭春龙, 等. PSI 数字化电源控制器在上海光源大功率电源上的应用及创新, 核技术, 2008, **31**(10): 726–730

94 陈焕光, 许瑞年, 沈天健. 基于 FPGA 的 Manchester 编解码及快速数字化电源通信的实现, 核电子学与探测技术, 2008, **28**(3): 637–640

95 许升辉, 许瑞年, 柯新花, 等. 嵌入式操作系统 μC/OS-II 数字化电源控制卡上的移植研究, 核技术, 2008, **3**1(12): 895

96 柯新花, 卢宋林, 许瑞年, 等. 一种使用的高精度 ADC 测试方法, 核技术, 2008, **31**(5): 374

97 柯新花, 卢宋林, 李瑞, 等. A novel testing approach for SSRF digital power supply controllers, Nuclear Science and Technology, 2008, **19**(4): 209–21

98 许瑞年, 陈焕光, 沈天健, 等. 国产数字化电源控制器在 SSRF 直线电源上的应用, 中国物理 C, 2008, **32**(增刊): 124–126

99 李烜, 赵明华, 汪宝亮, 等. 任意模式电耦合波导耦合器的 CST 仿真, 核技术, 2008, **31**(8): 561–564
100 张猛 , 赵明华. Study of Multipacting effect in superconducting cavity, Chinese Physics C (HEP&NP) , 2008, **32**(10): 846–848
101 顾强, 赵振堂, 童德春, 等. RF gun for an intense THz radiation source, Chinese Physics C (HEP&NP) , 2008, **32**(8): 657–660
102 汪宝亮, 赵明华, 侯汨, 等. 上海光源次谐波聚束器的优化设计及测试, 强激光与粒子束, 2008, **20**(6): 1053–1056
103 顾强, 戴建枰, 戴志敏, 等. 100 MeV 电子直线加速器的物理设计, 强激光与粒子束, 2008, **20**(1): 135–139
104 顾强, 陈永中, 戴志敏, 等. Preliminary results of a femto-second electron bunch facility, 强激光与粒子束, 2008, **20**(4): 585–588
105 米清茹, 郑丽芳, 刘松强. EPICS 控制系统软件开发环境的研究, 核技术, 2008, **31**(1): 39451
106 阎映炳, 冷用斌, 杨嵩. EPICS 在线数据分析软件包研制及应用, 核技术, 2008, **31**(3): 170–173
107 阎映炳, 冷用斌, 刘德康, 等. EPICS interface to libera electron beam position monitor, Nuclear Science And Techniques, 2008, **19**(2): 65–73
108 杨嵩, 冷用斌, 阎映炳, 等. 基于 EPICS 及虚拟仪器技术的 Libera 测试系统研制, 核技术, 2008, **31**(6): 410–414
109 许姗姗, 叶恺容, 陈永忠, 等. SSRF 直线加速器束流发射度测量, 核技术, 2008, **31**(3): 174–177
110 韩利峰, 袁任贤, 俞路阳, 等。 Front-end signal analysis of the transverse feedback system for SSRF, Nuclear Science And Techniques, 2008, **19**(5)
111 韩利峰, 袁任贤, 叶恺容. 横向反馈系统数字滤波算法及系统仿真, 核技术, 2008, **31**(7): 489–492
112 韩利峰, 袁任贤 , 俞路阳, 等. FPGA 横向反馈数字板在 SSRF 储存环的应用, 核技术, 2008, **31**(10): 736–739
113 戴兴, 叶恺容, 陈杰, 等. 基于Lab VIEW的同步光数据采集及处理系统, 核技术, 2008, **31**(5): 325–329

核物理 Nuclear Physics

1 STAR 合作. Measurement of transverse single-spin asymmetries for dijet production in proton-proton xollisions at $\sqrt{S_{\rm NN}}$=200, Phys Rev Lett, 2007, **99**: 142003
2 STAR 合作. Transverse momentum and centrality sdpendence of high-pT Nonphotonic electron suppression in Au +Au collisions at, Phys Rev Lett, 2007, **99**: 192301
3 STAR 合作. Scaling properties of hyperon production in Au+Au collisions at $\sqrt{S_{\rm NN}}$=200 GeV, Phys Rev Lett, 2007, **98**: 62301
4 STAR 合作. Rapidity and species dependence of particle production at large transverse momentum for *d*+Au collisions at $\sqrt{S_{\rm NN}}$=200 GeV, Phys Rev C, 2007, **76**: 54903
5 STAR 合作. Global polarization measurement in Au+Au collisions, Phys Rev C, 2007, **76**: 24915
6 STAR 合作. Strangelet search in Au+Au collisions at $\sqrt{S_{\rm NN}}$ = 200 GeV, Phys Rev C, 2007, **76**: 011901(R)
7 STAR 合作. Strange particle production in p+p collisions at $\sqrt{S_{\rm NN}}$=200 GeV, Phys Rev C, 2007, 0556–2813
8 STAR 合作. Energy dependence of $\pi^{\pm}$, p and transverse momentum spectra for Au+Au collisions at $\sqrt{S_{\rm NN}}$= 63 and 200 GeV, Phys Lett B, 2007, **605**: 104
9 STAR 合作. Forward lambda production and nuclear stopping power in d+Au collisions at $\sqrt{S_{\rm NN}}$= 200 GeV, Phys Rev C, 2007, **76**: 64904
10 STAR 合作. Mass, quark-number, and $\sqrt{S_{\rm NN}}$ dependence of the second and fourth flow harmonics in ultrarelativistic nucleus-nucleus collisions, Phys Rev C, 2007, **75**: 34901
11 STAR 合作. Two particle correlation on transverse momentum and momentum dissipation in Au+Au collisions at $\sqrt{S_{\rm NN}}$ = 130 GeV, J Phys G, 2007, **34**: 799
12 STAR 合作. The energy dependence of p_t angular correlations inferred from mean-p_t fluctuation scale dependence in heavy ion collisions at the SPS and RHIC, J Phys G, 2007, **34**: 451
13 STAR 合作. Delta_φ-Delta η correlations in central Au+Au collisions at $\sqrt{S_{\rm NN}}$ = 200 GeV, Phys Rev C, 2007, **75**: 34901
14 STAR 合作. Partonic flow and meson production in Au+Au collisions at $\sqrt{S_{\rm NN}}$ = 200 GeV, Phys Rev Lett, 2007, **99**: 112301
15 方德清, 郭威, 马春旺, 等. Examining exotic structure of proton-rich nucleus ^{23}Al, Phys Rev C, 2007, **76(**3): 031601r
16 方德清, 马余刚, 钟晨, 等. Systematic study of isoscaling behavior in projectile fragmentation by the statistical abrasion-ablation model, J Phys G, 2007, **34**: 2173

17 方德清, 马余刚, 马春旺, 等. Systematic behavior of isospin effect in fragmentation reactions, 高能物理与核物理, 2007, **31(**1): 59

18 GUO W, XU W, CHEN J G, *et al*. A high intensity beam line of γ-rays up to 22 MeV energy based on Compton backscattering, Nuclear Instruments and Methods in Physics Research Section A Accelerators, Spectrometers, Detectors and Associated Equipment, 2007, **578(**3): 457

19 CHEN J G, XU W, GUO W, *et al*. An X-ray source based on Compton backscattering of CO_2 laser and, Nuclear Instruments and Methods in Physics Research Section A Accelerators, Spectrometers, Detectors and Associated Equipment, 2007, **580**: 1184

20 ZHONG Chen. 100 MeV electrons, Eur Phys JC, 2007, **49(**1): 389–391

21 ZHONG Chen. Scaling of the charm cross-section and modification of charm ρ_T spectra at RHIC, J Phys G, 2007, **34**: S741

22 TIAN W D, MA YG, CAI X Z, *et al*. Isospin effect in statistical sequential decay, Phys Rev C, 2007, **76**: 24607

23 TIAN Wendong, MA Yugang, CAI Xiangzhou, *et al*.Isoscaling in statistical sequential decay model, Chin Phys Lett, 2007, **24(**2): 385

24 LONG J L, HE Z J, Ma Y G, *et al*. Evolution and photons of a chemically equilibrating quark–gluon plasma at finite baryon density, J Phys G, 2007, **34**: 847

25 MA Erjun, MA Yugang, CAI Xiangzhou, *et al*. Differential cross sections of elastic electron scattering from CH_4, CF_4 and SF_6 in the energy range 100–700 eV, Chinese Physics Letters, 2007, **16(**11): 1009

26 YAN T Z, MA Yugang, CAI Xiangzhou, *et al*. Phenomenological Scaling of Rapidity Dependence for Anisotropic Flows in 25 MeV/nucleon Ca+Ca by Quantum Molecular Dynamics Model, Chinese Physics, 2007, **27**: 3388

27 YAN T Z, MA Yugang, CAI Xiangzhou, *et al*. Scaling of anisotropic flows and nuclear equation of state in intermediate energy heavy ion collisions, Chinese Physics Letters, 2007, **16(**9): 2676

28 MA Yugang, CAI Xiangzhou, CHEN J G, *et al*. Nucleon-nucleon momentum correlation function for light nuclei, Nuclear Physics A, 2007, **790**: 299c

29 MA Yugang, YAN T Z, CAI Xiangzhou, *et al*. Scaling of anisotropy flows in intermediate energy heavy ion collisions, Nuclear Physics A, 2007, **787**: 611c

30 ZHANG Song Zhang, Ma Guoliang, Ma Yugang, *et al*. Centrality, transverse momentum and pseudorapidity dependences of \mach-like"correlations in a partonic transport model, International Journal of Modern Physics E, 2007, **16(**7): 2029,

31 SHI Xinghua, MA Guoliang, MA Yugang, *et al*. "Temperature" fluctuation and heat capacities of quarks and meson, International Journal of Modern Physics E, 2007, **16(**7): 1912

32 ZHANG Song, Ma Guoliang, Ma Yugang. Transverse momentum and pseudorapidity dependences of Mach-like correlations for central Au+Au collisions at $\sqrt{S_{NN}}$ = 200 GeV, Phys Rev C, 2007, **76**: 14904

33 MA Guoliang, ZHANG Song, MA Yugng. Two-and three-particle correlations in a partonic transport model, J Phys G, 2007, 0954－3899

34 MA Guoliang, SONG Zhang, MA Yugang. Hadron azimuthal correlations and mach-like structures in a partonic/hadronic transport model, Nucl Phys A, 2007, **783**: 515

35 MA Guoliang, MA Yugang, Song Zhang. Three-particle correlations from strong partonic cascade in the AMPT model, Phys Lett B, 2007, **647**: 122

36 ZUO Jiaxu, CAI Xiangzhou, CHEN Jinhui. Anisotropic flows of omgea baryon due to parton casvade, International Journal of Modern Physics E, 0218-3013, SINAP, **16,** 7, 1870

37 MA Yugang. Experimental observables on nuclear liquid gas phase transition, Journal of Fudan University (Natural Science), 2007, **46**: 33

38 CHEN Jinhui, *et al*. Spin alignment of K* and phi mesons in Au+Au and p+p collisions at $\sqrt{S_{NN}}$ =200 GeV, J Phys G, 2007, **34**: S331

39 XU Y, XU W, MA Y G. A new study for $^{16}O(\gamma, \alpha)^{12}C$ at the energies of nuclear astrophysics Oðg; aÞ interest: The inverse of key nucleosynthesis reaction, Nuclear Instruments and Methods in Physics Research A, 2007, **581**: 866

40 SHEN W Q. High-energy nuclear physics in China, J Phys G, 2007, **34:** S173

41 弓晓晶, 李敬源, 陆杭军, 等. A charge driven molecular water pump, Nature Nanotechnology, 2007, **2:** 709

42 李朝霞, 张雪花, 张立娟, 等. A nalysis of the gas states at a Liquid/Solid Interface Based on Interactions at the microscopic Level, Journal of physical chemistry B, 2007, **111**: 9325

43 李华兵, 张超英, 吕晓阳, 等. An improved method on

two-dimensional lattice Boltzmann simulations with moving boundaries, Chinese Physics Letters,2007, **24**: 3458

44 李朝霞, 张立娟, 伊厚会, 等. Theoretical study on the capillary force between an atomic force microscope tip and nanoparticle, Chinese Physics Letters, 2007, **24**: 2289

45 李鼎, 狄勤丰, 李敬源, 等. Large slip length over a nanopatterned surface, Chinese Physics Letters, 2007, **24**: 1021

46 张立娟, 陈郝, 李朝霞, 等. Long lifetime of nanobubbles due to a high inner density, Science in China Series G-Physics and Astronomy, 2007, **37**: 556

47 伊厚会, 陈艳燕, 李华兵. Lattice boltzmann simulations of a dumbbell moving in a poiseuille flow, Chinese Physics Letters, 2007, **16(**8): 2444

48 左光宏, 胡钧, 方海平. Proteing folding under mediation of ordering water: an off-lattice Go-Like model study, Chinese Physics Letters, 2007, **24**: 2426

49 潘瑞芹, 许子健, 朱志远, 等. Thermal conductivity of functionalized single-wall carbon nanotubes, Nanotechnology, 2007, **18(**28): 285704

50 勇振中, 王震遐, 胡建刚, 等. Carbon nitride nanowires with an onion-like cross-linked microstructure, Carbon, 2007, **45(**10): 2134

51 勇振中, 朱志远, 王震遐, 等. One dimensional carbon nanotube-FexCy nanocrystal composite, Nanotechnology, 2007, **18(**10): 105602

52 许子健, 韩家广, 朱志远, 等. Valence of D_{5h} C_{50} fullerene, J PHYS CHEM A, 2007, **111(**4): 656

53 潘瑞芹, 许子健, 朱志远. Length dependence of thermal conductivity of single-walled carbon nanotubes, Chinese Physics Letters, 2007, **24**: 1321

54 勇振中, 巩金龙, 王震遐, 等. Field emission enhancement of carbon nanotubes by surface modification, Chinese Physics Letters, 2007, **24**: 233

55 郑里平, 王呈斌, 许子健, 等. Channeling of low energy light and heavy ions in single-wall nanotubes, Nuclear Instruments and Methods in Physics Research Section B, 2007, **260**: 513

56 郑里平, 李斗星, 许子健, 等. 用双粒子模型研究微量元素与 Ni 在 Ni3Al 晶界共富集现象, 物理学报, 2007, **56**: 1520

57 郑里平, 许子健, 朱志远, 等. X 射线在碳纳米管(绳)和 Fullerites 晶体内的传输, 核技术, 2007, **30(**2): 125

58 王晓峰, 许子健, 朱志远. Reversible mechanical bistability of carbon nanotubes under radial compression, Chemical Physics, 2007, **334**: 144-147

59 STAR 合作. System-size independence of directed flow measured at the BNL relativistic heavy-ion collider, Phys Rev Lett, 2008, **101**: 252301

60 STAR 合作. Forward neutral-pion transverse single-spin asymmetries in p+p collisions at $\sqrt{S_{\rm NN}}$=200 GeV, Phys Rev Lett, 2008, **101**: 222001

61 STAR 合作. Longitudinal double-spin asymmetry for inclusive jet production in p-p collisions at at $\sqrt{S_{\rm NN}}$=200 GeV, Phys Rev Lett, 2008, **100**: 232003

62 STAR 合作. Spin alignment measurements of the K*0(892) and phi(1020) vector mesons in heavy ion collisions at $\sqrt{S_{\rm NN}}$ =200 GeV, Phys Rev C, 2008, **77**: 061902(R)

63 ρ_0 photoproduction in ultraperipheral relativistic heavy ion collisions at $\sqrt{S_{\rm NN}}$ =200 GeV, Phys Rev C, 2008, **77**: 34910

64 STAR 合作. Centrality dependence of charged hadron and strange hadron elliptic flow from $\sqrt{S_{\rm NN}}$ = 200 GeV Au+Au collisions, Phys Rev C, 2008, **77:** 54901

65 STAR 合作. Enhanced strange baryon production in Au+Au collisions compared to p+p at $\sqrt{S_{\rm NN}}$ = 200 GeV, Phys Rev C, 2008, **77**: 44908

66 CHEN J H, JIN F, Gangadharan D, *et al*. Parton distributions at hadronization from bulk dense matter produced in Au+Au collisions at $\sqrt{S_{\rm NN}}$ = 200, Phys Rev C, 2008, **78**: 34907

67 LIU G H, MA Y G, CAI X Z. Azimuthal asymmetry of direct photons in intermediate energy heavy-ion collisions, Phys Lett B, 2008, **663**: 312

68 马国亮, 张松, 马余刚, 等 Longitudinal broadening of near-side jets due to parton cascade, The European Physical Journal C - Particles and Fields, 2008, **57(**3): 589

69 左嘉旭, CHEN J Y, CAI X Z, *et al*. Partonic effect on anisotropic flows of Omega baryon for Au + Au at 62.4 and 200 GeV/c, The European Physical Journal C - Particles and Fields, 2008, **55**: 463

70 靳富, 马余刚, 马国亮, 等. Baryon-strangeness correlations in parton/hadron transport model for Au+Au collisions at $\sqrt{S_{\rm NN}}$ = 200 GeV, J Phys G: Nucl Part Phys, 2008, **35**: 44070

71 左嘉旭. Baryon to meson ratios on the near and away-side of jets and their centrality dependence at STAR, J Phys G: Nucl Part Phys, 2008, **35**: 44027

72 陈金辉. Spin alignment of K0892 and 1020 mesons in

Au+Au and p+p collisions, J Phys G: Nucl Part Phys, 2008, **35**: 44068

73 陈金辉. System size and energy dependence of f-meson production at RHIC, J Phys G: Nucl Part Phys, 2008, **35**: 04053

74 TIAN W D, MA Y G, CAI X Z, *et al*. Dynamical and sequential decay effects on isoscaling and density dependence of the symmetry energy, International Journal of Modern Physics, 2008, **17(**9): 1705

75 LIU G H, YAN T Z, MA Y G. Anisotropic flows of nuclear clusters and hard photons in intermediate energy heavy ion collisions, International Journal of Modern Physics E, 2008, **17**: 1850

76 MA C W , FU Y, FANG D Q, *et al*. Isospin effect and isoscaling phenomenon in projectile fragmentation, International Journal of Modern Physics E, 2008, **17**: 1669

77 LONG Jiali, HE Zejun, MA Yugang, *et al*. Photons from quark and hadron phases in Au + Au collisions, Chin Phys Lett, 2008, **25(**9): 3188

78 王宏伟, 马余刚, 蔡翔舟, 等. Structure study of light unbound nuclei near drip line, Chinese Physics C, 2008, **32(**S2): 38

79 陈金根, 徐望, 王宏伟. Transmutation of nuclear wastes using photonuclear reactions triggered by compton backscattering photons at the Shanghai laser electron gamma source, Chin Phys C, 2008, **32(**8): 677

80 郭威, 徐毅, 陈金根, 等. Shanghai laser electron gamma source and its applications, Chin Phys C, 2008, **32(**S2): 190

81 TIAN Wendong, WANG Hongwei, MA Yugang, *et al*. Isospin effect of projectile fragment yields, Chinese Physics C, 2008, **32(**S2): 89

82 MA C W, FU Y, FANG D Q, *et al*. A possible experimental observable for the determination of neutron skin thickness, Chin Phys B, 2008, **32(**17): 1216

83 FANG D Q, GUO W, MA C W, *et al*. Studies on the exotic strucutre of ^{23}Al, Chin Phys C, 2008, **32(**S2): 34

84 ZUO Jiaxu, Sorensen Paul, CAI Xiangzhou, *et al*. Particle correlation in P+P Collision $\sqrt{S_{\rm NN}}$ =200 GeV in PYTHIA , Chin Phys C, 2008, **32(**S2): 13

85 管娜娜, 贺泽君, 龙家丽, 等. Dileptons from a cenically equilibrating Quark-Gluon Plasma at finite baryon density, Chin Phys Lett, 2008, **25(**11): 3916

86 MA Erjun, MA Yugang, CAI Xiangzhou. Electron scattering by C_4H_{10} and C_6H_6 in the energy range 100–1000 eV, Chin Phys Lett, 2008, **25(**1): 97

87 牛冬校, 冯晓录, 周星飞, 等. 应用 Fe^{3+}在裸云母表面制作 DNA 分子的 AFM 样品的方法, 电子显微学报, 2008, **27**: 151

88 牛冬校, 冯晓录, 蔡翔舟. 利用软印刷结合扩散制作纳米颗粒样品的方法, 核技术, 2008, **31**: 307

89 原子核高 K 同质异能态的诱发 gamma 辐射, 原子核物理评论, 1007-4627, SINAP, **25,** 4, 332, 石钰, 田文栋, 马余刚, 9, 田文栋, 2008

90 潘强岩, 徐望, 陈金根, 等. 上海激光电子 γ 源, 原子核物理评论, 2008, **25(**2): 129

91 范功涛, 徐望, 马余刚. Measurement of electric polarizabilities of light nucleus(nucleons), Chinese Physics C, 2008, **32(**2): 169

92 弓晓晶, 李敬源, 陆杭军, 等. Enhancement of water permeation across a nanochannel by the structure outside the channel, Phys Rev Lett, 2008, **101**: 257801

93 陆杭军, 李敬源, 弓晓晶, 等. Water permeation and wavelike water density distributions inside narrow nanochannels, Phys Rev B, 2008, **77**: 174115

94 李松焱, 修鹏, 陆杭军, 等. Water permeation across nanochannels with defects, Nanotechnology, 2008, **19(**10): 105711

95 方海平, 万荣正, 弓晓晶, 等. Dynamics of single-file water chains inside nanoscale channels: physics and biological significance and applications, J Phys D, 2008, **41(**10): 103002

96 李华兵, 伊厚会, SAHN Xiaowen, 等. Lattice boltzmann model of vesicle deforming and moving in fluid, Europhys Lett, 2008, **81**: 54002

97 弓晓晶, 方海平. Enhancement of water permeation across nanochannels by partial charges mimicked from biological channel, Chin Phys B, 2008, **17(**7): 2739

98 王春雷, 李朝霞, 李敬源, 等. High density gas state at water/graphite interface studied by molecular dynamics simulation, Chin Phys B, 2008, **17(**7): 2646

99 曾立, 左光宏, 弓晓晶, 等. Water and ion permeation through electrically charged nanopore, Chin Phys Lett, 2008, **25(**4): 1486

100 陆杭军, 弓晓晶, 王春雷, 等. Effect of vibration on water transport through carbon nanotubes, Chin Phys Lett, 2008, **25(**3): 1145

101 万帆, 韩家广, 朱志远. Dielectric response in ferroelectric $BaTiO_3$, Physics Letters A, 2008, **372(**12): 2137

102 郑里平, 朱志远, 李勇, 等. Isotopic mass effects for

low-energy ion channeling in single-wall carbon nanotubes, Journal of Physical Chemistry C, 2008, **112(**39): 15204

103 郑里平, 朱志远, 李勇. Ion mass dependence for low energy channeling in single-wall nanotubes, Nuclear Instruments and Methods in Physics Research Section B, 2008, **266(**5): 849

104 郑里平, 李勇, 朱志远, 等.低能粒子与 X 射线在碳纳米管(绳)内传输研究的现状, 原子核物理评论, 2008, **25(**3): 265

105 王呈斌, 朱志远. Phenomenological study of He-3 photodisintegration up to 150 MeV, Chinese Physics Letters, 2008, **25(**8): 2831

106 闫树华, 李宾. 一种实现可控纳米定位沉积的探针修饰新方法, 核技术, 2008, **31(**3): 237–240

核分析技术 Nuclear Analysis Techniques

1 李勤涛, 倪志春, 杨树敏, 等. 离子束诱导碳圆锥室温生长锥角的可控性研究, 核技术, 2008, **30**: 956–960

2 LI Qintao, NI Zhichun, GONG Jinlong, *et al*. Enhanced field emission from nano-graphite coated carbon nanotubes, Nucl Sci Tech, 2007, **18**: 276–281

3 NI Zhichun, LI Qintao, YAN Long, *et al*. Intensive irradiation of carbon nanotubes by Si ion beam, Nucl Sci Tech., 2007, **18**: 137

4 WANG S, YU G J, GONG J L, *et al*. Large-area uniform nanodot arrays embedded in porous anodic alumina, Nanotechnology, 2007, **18**: 15303

5 NI Zhichun, LI Qintao, GONG J L, *et al*. Structural change of carbon nanotubes produced by Si ion beam irradiation, Nuclear Instruments and Methods in Physics Research B, 2007, **260**: 542

6 YU Guojun, Wang Sen, GONG J L, *et al*. Fabrication and characterization of nanostructured iron antidots on porous anodic alumina, Solid State Phenomena, 2007, **121**–**123**: 131

7 WANG Sen, YU Guojun, GONG J L, *et al*. Large-scale synthesis of bamboo-like carbon nanotubes over zeolites by catalytic decomposition of acetonitrile, Solid State Phenomena, 2007, **121**–**123**: 167

8 ZHANG Zhaoxia, WANG Wenfeng, *et al*. SDS-page study on photooxidation damage of lysozyme induced by riboflavin, Science in China Series B-chem, 2007, **50**(1): 84

9 GE Min, WANG Wenfeng, *et al*. Substituent effects on the low-frequency vibrational modes of benzoic acid and related compounds, Chinese Journal of Chemistry, 2007, **25(**3): 272

10 郝淑梅, 王文锋, 等. 杜醌诱导溶菌酶的光敏损伤研究, 辐射研究与辐射工艺学报, 2007, **25(**3): 161

11 GE Min, WANG Wenfeng, *et al*. Characterization of crystal transformation in the solid-state by terahertz time-domain spectroscopy, Chemical Physics Letters, 2007, **444**(4): 355

12 ZHU, Hongping, WANG Wenfeng, *et al*. Study on the interaction of colloidal gold with Taq DNA polymerase, Chinese Journal of Chemistry, 2007, **25**: 1233

13 郝淑梅, 王文锋, 等.太赫兹光谱技术在自由基检测中的应用, 核技术, 2007, **30**(5): 442

14 LIU Guifeng, WANG Wenfeng, *et al*. Qualitative and quantitative study of isomeric compounds of aminophenol by THZ-TDS, Proc of SPIE, 2007, **6840**: 68400D-1

15 MA Shihua, WANG Wenfeng, *et al*. Study on THz spectra of the active ingredients in the TCM, Proc of SPIE, 2007, **6840**: 68400P-1

16 ZHANG Yi, LU Junhong, LI Minqian, *et al*. A Strategy for ordered single molecule Sequencing based on nanomanipulation(OsmSN), Int J Nanotechnology, 2007, **4**(1/2): 163–169

17 ZHANG Lijuan, Zhang Yi, ZHANG Renjie, *et al*. In situ AFM investigation on degradation of self-assembled monolayers on mica :effect of humidity, Colloids and Surfaces A: Physicochem Eng Aspects, 2007, **293**: 195–200

18 WANG Huabin, ZHOU Xingfei, AN Hong-jie, *et al*. Effects of substrate hydrophobicity / hydrophilicity on height measurement of individual DNA molecules, Chinese Physics Letters, 2007, **24**(3): 644

19 WANG Ying, ZHANG Yi, LI Bin, *et al*. Capturing and depositing one nanoobject at a time: Single particle dip-pen nanolithography, Applied physics letters, 2007, **90s**: 133102

20 LI Hai, ZHANG Feng, ZHANG Yi, *et al*. Organic Solvents Mediate Self-assembly of GAV-9 Peptide on Mica Surface, Acta Biochimica et Biophysica Sinica, 2007, **39**(4): 285–289

21 LI Bin, ZHANG Yi, YAN Shuhua, *et al*. Positioning scission of single DNA molecules with nonspecific endonu-

clease based on nanomanipulation, Journal of the American Chemical Society, 2007, **129**: 6668–6669

22 LI Hai, ZHANG Xiaodong, ZHANG Yi, *et al*. Fabrication of true-color micropatterns by 2D stepwise contraction andadsorption nanolithography(scan), Surface Review and Letters, 2007, **14**(1): 129–134

23 李海, 武海萍, 黄一波, 等. 用于多组分微图形制备的级联缩微方法及影响因素研究, 电子显微学报, 2007, **26(**2): 130–137

24 申梓刚, 黄一波, 等. 水和乙醇对DNA分子二维操纵的机制研究, 核技术, 2007, **30**(9): 793–796

25 汪颖, 张益, 李宾, 等. 基于“纳米蘸笔技术“的单个纳米颗粒在不同基底表面的转移, 电子显微学报, 2007, **26**(5), 484–487

26 WNAG Peng, LI Hai, YANG Haijun, *et al*. Glycerol facilitates the disaggregation of recombinant adeno-associated virus serotype 2 on mica surface, Colloids and Surfaces B, 2007, **60**: 264–267

27 MI Lijuan, ZHU Hongping, ZHANG Xiaodong, *et al*. Mechanism of the interaction between Au nano-particles and polymerase in nanoparticle PCR, Chinese Science Bulletin, 2007, **52(**17): 2345–2349

28 米丽娟, 李宾, 周化岚, 等. 纳米粒子 PCR 产物的纯化及 AFM 观察, 核技术, 2007, **30(**10): 876–879

29 WANG Huabin, ZHANG Lijuan, ZHANG Feng, *et al*. Investigation on the morphology of precipitated chemicals from TE buffer on solid substrates, Surface Review and Letters, 2007, **14**(6): 1121–1128

30 LI X, YUE W, Iida A, A study of the origin of individual $PM_{2.5}$ particles in Shanghai air with synchrotron X-ray fluorescence microprobe, Nucl Instr And Meth B, 2007, **260**: 336–342

31 WANG Yinsong, LI Aiguo, ZHAN Yuanxun, *et al*. Speciation of elements in atmospheric particulate matter by XANES, J Radioanal Nucl Chem, 2007, **273**: 247–251

32 CHEN Jianmin, TAN Mingguang, ZHANG Guilin, *et al*. Radiolabeling and in vitro evaluation of the polystyrene particles as a promising probe in biomedical sciences, J Radioanal Nucl Chem, 2007,**272**(2): 387–390

33 Aerosol-induced lung injuries observed by synchrotron radiation X-ray phase-contrast imaging technique, Nucl Instr And Meth B, 2007, **262**: 304–312

34 YUE Weisheng, LI Xiaolin, LIU Jiangfeng, *et al*. Source tracing of chromium-, manganese-, nickel- and zinc-containing particles (PM10) by micro-PIXE spectrum, J Radioanal Nucl Chem, 2007, **274**(1): 115–121

35 张元勋, 王荫淞, 张勇平, 等. Investigation of elemental distribution in human femoral head by PIXE and SRXRF microprobe, Nucl Instr and Meth B, 2007, (**B260)**: 178–183

36 杨永兴, 李晓林, 李玉兰, 等. 上海市大气气溶胶中铂元素污染状况调查, 环境科学学报, 2007, **27**(5): 810–816

37 杨永兴, 李玉兰, 谈明光, 等. 微波消解电感藕合等离子体质谱法测定大气气溶胶的铂元素, 分析科学学报, 2007,**23**(3), 249–252

38 李晓林, 包良满, 刘江峰, 等. 上海 2004 年冬季城市大气气溶胶含 Pb 单颗粒物的来源查证, 中国科学院研究生院学报, 2007, **24**(5): 688–691

39 李晓林, 毛雪瑛. 大气气溶胶中痕量贵金属元素 Pt 的仪器中子活化分析初步研究, 核技术, 2007, **30**(4): 370–372

40 刘江峰, 岳伟生, 万天敏, 等. 扫描质子微探针扫描系统优化与分辨率测定, 核技术, 2007, **30**(1): 21–26

41 梁峰, 李超, 赵金镯, 等. ^{59}Fe 标记的纳米颗粒物从大鼠肺部的渗透过程, 核技术, 2007, **30**(9): 763–767

42 张元勋, 王荫淞, 杨传俊, 等. 核分析相关技术用于上海市大气污染特征研究, 核技术, 2007, **30**(4): 366–369

43 张元勋, 杨传俊, 陆文忠, 等. 室内气溶胶纳米颗粒物的粒径分布特征研究, 中国科学院研究生院学报, 2007, **24**(5): 705–709

44 张元勋, 曹同, Iida A, *et al*. 同步辐射 X 荧光分析用于苔藓植物大气污染的初步研究, 核技术, 2007, **30**(9): 730–734

45 XU Jingying, LI Qingnuan, LI Jungang, *et al*. Biodistribution of ^{99m}Tc-$C_{60}(OH)_x$ in Sprague-dawley rats after intratracheal instillation, Carbon, 2007, **45**: 1865–1870

46 GUO Jinxue, ZHANG Xiao, LI Qingnuan, *et al*. Biodistribution of functionalized multiwall carbon nanotubes in mice, Nuclear medicine and Biology, 2007, **34**: 579–583

47 LI Jungang, LI Wenxin, XU Jingying, *et al*. Comparative study of pathological lesions induced by multiwalled carbon nanotubes in lungs of mice by intratracheal instillation and inhalation, Environmental toxicology, 2007, **22**: 415–427

48 LI Jungang, LI Qingnuan, XU Jingying, *et al*. Comparative study on the acute pulmonary toxicity induced by 3 and 20 nm TiO_2 primary particles in mice, Environmental toxicology and pharmacology, 2007, **24**: 239-244

49 YU Bozhang, YANG Jianshe, LI Wenxin. In vitro capabil-

ity of multi-walled carbon nanotubes modified with gonadotrophin releasing hormone on killing cancer cells, Carbon, 2007, **4**: 1921

50 刘瑞丽, 尹娟娟, 马继飞, 等. C_{60}-糖皮质激素荧光特性研究, 光谱学与光谱分析, 2007, **27(**6): 1161–1163

51 刘瑞丽, 赵红卫, 张兆霞, 等. C_{60}-地塞米松的激光光解研究, 物理化学学报, 2007, **23**(7): 1127–113

52 韩博, 李晴暖, 吴胜伟, 等. 甘草苷和异甘草苷与多壁碳纳米管的非共价相互作用, 药学学报, 2007, **42**(11): 1221–1226

53 诸颖, 冉铁成, 李宇国, 等. 多壁碳纳米管(MWNTs)对梨形四膜虫的生长促进作用, 核技术, 2007, **30**(8): 689–693

54 冉铁成, 刘瑞丽, 诸颖, 等. ^{125}I-C_{60} 吡咯烷苯氮芥的制备和生物分布, 核技术, 2007, **30**(4): 373–375

55 徐晶莹, 李俊纲, 冉铁成, 等. 气管滴注 ^{99m}Tc-$C_{60}(OH)_x$ 大鼠的 SPECT 显像观察, 核技术, 2007, **30**(5): 448–453

56 YANG J, LI Wenxin, LI Q, *et al*. Oxygen adsorption by carbon nanotubes and its application in radiotherapy, IET Nanobiotechnology, 2007, **1**(1): 010–014

57 LIU Qi, ZHU Zhiyong, YANG Xiaomin, *et al*. Temperature-sensitive porous membrane production through radiation co-grafting of NIPAAm on/in PVDF, Rad Phys Chem, 2007, **76**: 707–713

58 SONG Yufeng, LIU Qi, SUN Youmei, *et al*. Color center formation in a-Al_2O_3 induced by high energy heavy ions, Nucl Instru Meth(B), 2007, **254**: 268–272

59 宋玉峰, 朱智勇, 吉特, 等. 聚乙烯－碳黑复合材料的太赫兹时域光谱测量研究, 物理化学学报, 2007, **23**(2): 177–180

60 宋玉峰, 朱智勇, 孙友梅,等. 高能铁离子辐照三氧化二铝产生的色心研究, 核技术, 2007, **30**(2): 114–118

61 杨小敏, 刘崎, 付海英, 等. P VA/PVP/ws-chitin 水凝胶伤口敷料的辐射制备及性能表征, 核技术, 2007, **30**(4): 356–360

62 陈西良, 张聪, 付海英, 等. HDPE/EVA/CB 体系流变学性质及其辐照响应, 核技术, 2007, **30**(4): 361–365

63 刘崎, 杨小敏, 付海英, 氮－异丙基丙烯酰胺温敏凝胶的辐射合成与性能表征, 核技术, 2007, **30**(8): 652–656

64 ZUO Xiaolei, SONG Shiping, ZHANG Jiong, *et al*. A Target-responsive electrochemical aptamer switch (TREAS) for reagentless detection of nanomolar ATP, JACS, 2007, **129**(5): 1042–1043

65 LIU Xingfen, Tang Yi, WANG Lihua, *et al*. Optical detection of mercury(II) in aqueous solutions by using conjugated polymers and label-free oligonucleotides, Advanced Materials, 2007, **19**(13): 1471–1474

66 WANG Jing, WANG Lihua, LIU Xingfen, *et al*. A gold nanoparticle-based aptamer target binding readout for ATP assay, advanced materials, 2007, **19**(13): 3943–3946

67 LAO Ruojun, WANG Lihua, WAN Ying, *et al*. Interactions between cytochrome c and DNA strands self-Assembled at gold electrode, International Journal of Molecular Sciences, 2007, **8**: 136–144

68 ZHANG Jiong, SONG Shiping, WANG Lihua, *et al*. A gold nanoparticle-based chronocoulometric DNA sensor for amplified detection of DNA, nature PROTOCOL, 2007, **2(**11): 2888–2895

69 ZHANG Jiong, WANG Lihua, PAN Dun, *et al*. DNA hybridization “turns on” electrocatalysis at gold electrodes, Chem Commun, 2007, **11**: 1154–1156

70 张炯, 万莹, 王丽华, 等. 电化学 DNA 生物传感器, 化学进展, 2007, **19**(10): 1576–1584

71 PAN Dun, ZUO Xiaolei, WAN Ying, *et al*. Electrochemical Interrogation of Interactions between surface-confined DNA and methylene blue, Sensors , 2007, **7:** 2671–2680

72 SONG Shiping, LI Bin, WANG Lihua, *et al*. A cancer protein microarray platform using antibody fragments and its clinical applications, Mol BioSystem, 2007, **3**: 151–158

73 左小磊, 陈浩德, 张兰勇, 等. 电化学过氧化氢传感器, 分析试验室, 2007, **26**(增刊): 128–129

74 张娟, 王丽华, 宋世平, 等. 基于纳米金自组装探针的凝血酶分析, 分析试验室, 2007, **26**(增刊): 191–192

75 宋世平, 樊春海. 纳米金生物复合探针的构建及其在生物分析中的应用, 分析试验室, 2007, **26**(增刊): 193–194

76 刘兴奋, 武海萍, 李玉兰, 等. 一种高灵敏度、高特异性检测重金属 Hg^{2+}的比色生物传感方法, 核技术, 2007, **30(**5): 467–472

77 闫树华, 李宾. 一种实现可控纳米定位沉积的探针修饰新方法, 核技术, 2008, **31**(3): 237–240

78 Wang Peng, Yang HaiJun, WANG Huabin, *et al*. Modification of AFM Tips for facilitating picking-up of nanoparticles, Chin Phys Lett, 2008, **25**(7): 2407–2409

79 WANG Huabin, ZHOU Xingfei, AN Hongjie, *et al*. Study of Radial compression elasticity of single xanthan molecules by vibrating scanning polarization force microscopy, Journal of Nanoscience and Nanotechnology, 2008, **8**(9): 1–4

80 SHEN Guangxia, ZHANG Xuehua, MING Ye, *et al*. Photocatalytic induction of nanobubbles on TiO_2 surfaces,

Journal of Physical Chemistry C, 2008, **112(**11): 4029–4032

81 WANG Peng, WANG Xinyan, YANG Haijun, *et al*. Dispersion and Fixation of adeno-associated virus with glutaraldehyde for AFM studies, Surface Review and Letters, 2008, **15**(5): 1–4

82 WANG Huabin, AN Hongjie, ZHANG Feng, *et al*. Study of substrate-directed ordering of long double-stranded DNA molecules on bare highly oriented pyrolytic graphite surface based on atomic force microscopy relocation imaging, J Vac Sci Technol B, 2008, **26**(5): 41–43

83 王鹏, 吕军鸿, 王鑫艳, 等. 戊二醛交联固定病毒颗粒及其在衬底表面上分散的研究, 核技术, 2008, **31**(7): 557–560

84 杨海军, 李海, 王鹏, 等. EDTA 应用于微接触印刷法制备高密度蛋白微阵列的研究, 核技术, 2008, **31**(12): 946–950

85 王化斌, 安红杰, 杨海军, 等. 单个黄原胶分子的样品制备与原子力显微镜检测, 核技术, 2008, **31**(12): 951–954

86 HE Ya, KANG Zhenhui, LI Quansong, *et al*. Ultrastable, highly fluorescent, and water-dispersed silicon-based nanospheres as cellular probes, angew. Chem Int Ed, 2008, **47**: 1–6

87 LI Jiang, SONG Shiping, LIU Xinfeng, *et al*. Enzyme-based multi-component optical nanoprobes for sequence-specific detection of DNA hybridization, Adv Mater, 2008, **20**: 479–500

88 HE Shijiang, LI Di, ZHU Changfeng, *et al*. Design of a gold nanoprobe for rapid and portable mercury detection with the naked eye, Chem. Commun., 2008, 4885–4887

89 ZHANG Jiong, WANG Lihua, WAN Ying, *et al*. Long-range heterogeneous electron transfer of ferrocene functionalized gold nanoparticles through alkanethiol bridges at gold electrodes, Asian J Chem, 2008, **20**(3): 2275–2282

90 Design of an oligonucleotide-incorporated nonfouling surface and its application in electrochemical DNA Sensors for highly sensitive and sequence-specific detection of target DNA, Anal Chem, 2008, **80**: 9029–9033

91 ZHANG Jiong, WAN Ying, WANG Lihua, *et al*. Switchable charge transport path via a potassium ions promoted conformational change of G-quadruplex probe monolayer, Electrochem Commun, 2008, 1**10**: 1144–1146

92 MI Lijuan, ZHANG, YANG X, *et al*. W Effects of nanomaterials on biomolecular reactions and applications in biosensing and detection, J Nanosci Nanotechnol, 2008

93 WAN Ying, ZHANG Jiong, LIU Gang, *et al*. Ligase-based multiple DNA analysis by using an electrochemical sensor array, Biosensors Bioelectro, 2008

94 SU Shao, HE Yao, ZHANG Mingliang, *et al*. High-sensitivity pesticide detection via silicon nanowires-supported acetylcholinesterase-based electrochemical sensors, Appl Phys Lett, 2008, **93**: 1–3

95 ZHANG Lanyong, SUN Huan, LI Di, *et al*. A conjugated polymer-based electrochemical DNA sensor: design and application of a multi-functional and water-soluble conjugated polyme., Macromol Rapid Commun, 2008, **29**: 1489–1494

96 HE Yao, LU Haoting, SAI Liman, *et al*. Microwave synthesis of water-dispersed CdTe/CdS/ZnS core-shell-shell quantum dots with excellent photostability and biocompatibility, Adv Mater, 2008, **20**: 3416–3421

97 SONG Shiping, WANG Lihua, LI Jiang, *et al*. Aptamer-based biosensors, Trends Anal Chem, 2008, **27**(2): 108–117

98 ZHANG Juan, WANG Lihua, PAN Dun, *et al*. Visual cocaine detection with gold nanoparticles and rationally engineered aptamer structures, Small, 2008, **4**(8): 1196–1200

99 LIU Gang, WAN Ying, Vincent Gau, *et al*. An enzyme-based E-DNA sensor for sequence-specific detection of femtomolar DNA targets, J Am Chem Soc, 2008, **130**: 6820–6825

100 WANG Lihua, ZHANG Juan, WANG Xun, *et al*. Gold nanoparticle-based optical probes for target-responsive DNA structures, Gold Bull, 2008, **41**: 37–41

101 PAN Dun, YAN Juan, WANG Lihua, *et al*. Nanoparticle-based strategies for high-performance biodetection, J Biotechnol, 2008, , **136S**: S760–1

102 GE Min, ZHAO Hongwei, WANG Wenfeng, *et al*. Terahertz time-domain spectroscopic investigation on quinones, Sci China Ser B-Chem, 2008, **50**(4): 354

103 张兆霞, 赵红卫, 王文锋, 等. β-胡萝卜素在乙腈体系中的激光光解研究, 光谱学与光谱分析, 2008, **28**(3): 481

104 ZHANG Zhaoxia, HAO Shumei, 王文锋, 等. Photoreactions of 1,4-naphthoquinone with lysozyme studied by laser flash photolysis and steady-state analysis, Journal of Photochemistry and Photobiology B: Biology, 2008, **92**(2): 77

105 刘桂锋, 马晓菁, 王文锋, 等. Identification of explosives 2, 4-DNT and 2, 6-DNT using terahertz time-domain

spectroscopy, Chinese Journal of Chemistry, 2008, **26**: 1257

106 刘桂锋, 赵红卫, 王文锋, 等. 太赫兹时域光谱技术在危险品检测方面的应用, 光谱学与光谱分析, 2008, **28**(5): 966

107 ZHANG Zhaoxia, HAO Shumei, 等. Photo-oxidation of protein induced by triplet 1,4-naphthoquinone: A mechanism study, Luminescence, 2008, **23**(2): 108

108 ZHANG Peng, SONG Xiyu, WANG Wenfeng, *et al*. Study on photochemistry of fluoroquinolones, 生物化学与生物物理学进展, 2008, **36**: 306

109 SONG Xiyu, ZHANG Peng, WANG Wenfeng, *et al*. Pulse radiolysis and laser flash photolysis studies of lipoic acid, 生物化学与生物物理学进展, 2008, **3L**: 315

110 CHEN Jianmin, TAN Mingguang, LI Yulan, *et al*.Characteristics of trace elements and lead isotope ratios in PM2.5 from four sites in Shanghai, Journal of Hazardous Materials, 2008, **156**: 36–43

111 JIN C, LI Y, LI YL, *et al*. Blood lead: Its effect on trace element levels and iron structure in hemoglobin, Nuclear Instruments and Methods in Physics Research B, 2008, **266**: 3607–3613

112 YANG Y, LI X, LI Y L, *et al*. Platinum concentrations in urban airborne particles from Shanghai, China , Global NEST Journal, 2008, **10**(2): 168–172

113 LUI Wei, MORIIZUMI J, YAMAZAWA H, *et al*. Transformation of Soil Organic Mater in a Japanese Larch Forest: Radiocarbon and stable Carbon Isotope Compositions versus Soil Depth, Journal of nuclear science and technology, 2008, **5**(增): 158–160

114 梁峰, 李玉兰, 陆文伟. 高效液相色谱-电感耦合等离子体质谱联用测定 DNA 分子中 4 种脱氧核苷酸, , 分析化学, 2008, **36**(8): 1097–1100

115 刘江峰, 包良满, 岳伟生, 等. 扫描透射离子显微成像系统的建立和实验研究, 强激光与粒子束技术, 2008, **20**(2): 313–318

116 包良满, 张元勋, 金蝉, 等. 燃煤小锅炉燃烧产物的 SR-XRF 和 XANES 分析, 核技术, 2008, **31**(9): 641–647

117 曹清晨, 张元勋, 娄玉霞, 等. SRXRF 研究苔藓植物对 Pb/Fe/Cr 污染的生物监视和累积特征, 核技术, 2008, **31**(10): 721–725

118 YANG X, LIU Q, CHEN X, *et al*. Investigation of PVA/ws-chitosan hydrogels prepared by combined γ-irradiation and freeze-thawing, Carbohydrate Polymers, 2008, **73**(3): 401–408

119 YANG X, LIU Q, CHEN X, *et al*. Investigation on the formation mechanisms of hydrogels made by combination of γ-ray irradiation and freeze-thawing, Journal of Applied Polymer Science, 2008, **108**: 1365–1372

120 YANG X, ZHU Z, LIU Q, *et al*. Thermal and rheological properties of poly(vinyl alcohol) and water-soluble chitosan hydrogels prepared by a combination of γ-Irradiation and Freeze Thawing, Journal of Applied Polymer Science, 2008, **109**: 3825–3830

121 YANG X, ZHU Z, LIU Q, *et al*. Effects of PVA, agar contents, and irradiation doses on properties of PVA/ws-chitosan/glycerol hydrogels made by γ-irradiation followed by freeze-thawing, Radiation Physics and Chemistry, 2008, **77**(8): 954–960

122 陈西良, 马明旺, 杨小敏, 等. MWNTs/HDPE 复合体系在 THz 波段的光电性质, 物理化学学报, 2008, **24**(11): 1969–1974

123 陈西良, 付海英, 张聪, 等. MWNTs/HDPE 的导电和流变学性质, 高分子材料科学与工程, 2008, **24**(1): 87–90,

124 马晓菁, 赵红卫, 代斌, 等. 次黄嘌呤及其核苷的 THz 光谱, 物理学报, 2008, **57**(6): 3429–3434

125 马晓菁, 赵红卫, 代斌, 等. THz 时域光谱在蛋白质研究中的应用研究, 光谱学与光谱分析, 2008, **28**(10): 2237–2242

126 LIU Yuxia, DU Fuqiang, LIN Wenzhen, *et al*. Photosensitized damage to telomere overhang and telomerase RNA by riboflavin, Progress in Natural Science,2008, **18**(4): 401–404

127 刘玉侠, 杜富强, 林维真, 等. 核黄素光敏损伤端粒 DNA 单链及端粒酶 RNA 亚基机理研究, 自然科学进展,2008, **18**(1): 114–117

128 刘玉侠, 杜富强, 林维真, 等. 蒽醌衍生物与 G-四联体相互作用方式的研究, 辐射研究与辐射工艺学报, 2008, **26**(2): 98-102

129 CAI Xiaoqing, JIA Haiqun, LIU Zhongbo, *et al*. Polyhydroxylated fullerene derivative $c_{60}(oh)_{24}$ prevents mitochondrial dysfunction and oxidative damage in MPP+-induced cellular model of parkinson's disease, J Neurosci Res, 2008, **86**(16): 3622–3644

130 LI Jungang, XUE Yanling, HAN Bo, *et al*. Application of X-ray phase contrast imaging techniquein detection of pulmonary lesions induced by multi-walled carbon nanotubes in rats, Journal of Nanoscience and Nanotechnology,2008, **8**(7): 3357–3362

131 LI J G, LI Q N, XU J Y, *et al*. The pulmonary toxicity of

multi-wall carbon nanotubes in mice 30 and 60 days after inhalation exposure, Journal of Nanoscience and Nanotechnology, 2008, 1–4

132 ZHU Ying, LI Wenxin. Cytotoxicity of carbon nanotubes, Science in China Series B: Chemistry, 2008, **51(**8): 1021–1029

133 SU YY, HE Y, LU H T, *et al*. The cytotoxicity of cadmium based, aqueous phase - synthesized, quantum dots and its modulation by surface coating, Biomaterials, 2008, **30**: 19–25

134 诸颖, 李文新. 碳纳米管的细胞毒性, 中国科学 B, 1006-9240, SINAP, 2008, **38,** 8, 677–684

135 诸颖, 张小勇, 李玉峰, 等. 碳纳米颗粒的放射性 ^{99m}Tc 标记, 原子核物理评论, 2008, **25**: 305–310

136 NI Zhichun, LI Qintao, YAN Long, *et al*. Large-scale fabrication of carbon nanowire networks using kilo-electron-volt ion beam, Diamond and related materials, 2008, **17**: 365–371

137 XIA Huihao, LI Weifeng, SONG You, *et al*. Tunable magnetism in carbon-ion-implanted highly oriented pyrolytic graphite, Adv Mater, 2008, **20**: 4679–4683

138 LI Qintao, NI Zhichun, GONG Jinlong, *et al*. Carbon nanotubes coated by carbon nanoparticles of turbostratic stacked graphenes, Carbon, 2008, **46**: 434–439

139 NI Zhichun, LI Qintao, YAN Long, *et al*. Welding of multi-walled carbon nanotubes by ion beam irradiation, Carbon,2008, **46**: 376–378

140 LI Qintao, NI Zhichun, YANG Shumin, Large-area and high-density silicon nanocone arrays by Ar^+ sputtering at room temperature, Nuclear Instruments and Methods in Physics Research Section B: Beam Interactions with Materials and Atoms,2008, **266**: 197–202

141 YANG Shumin, HE Zhoutong, LI Qintao, *et al*. Diamond films with preferred (110) texture by hot filament CVD at low pressure, Diamond & Related Materials, 2008, **17**: 2075–2079

142 YANG Shumin, WAN Dongyun, HE Zhoutong, *et al*. Highly (111)-textured diamond film growth with high nucleation density, Nuclear Science and Techniques, 2008, **19**: 147–151

143 HE Zhoutong, YANG Shumin, LI Qintao, *et al*. Selective growth of diamond by hot filament CVD using patterned carbon films as mask, Nuclear Science and Techniques, 2008, **19**: 83–87

144 Sobia Allah Rakha, YANG Shumin, HE Zhoutong, *et al*. Synthesis of thin diamond films from faceted nanosized crystallites, Current Applied Physics, 2008

加速器辐照中心 EB Accelerators and Radiation Application

1 刘永好, 王胜利, 李德明, 等. 加速器与辐射研究中心, The status of SMCAMS after recent upgrades, NIM B(Nuclear Inst. And Methods in Physics Research, B), 2007, 62–65

2 王胜利, 刘永好, 李德明, 等. 上海超灵敏小型回旋加速器质谱计分析研究 ^{26}Al 的初步研究, 核技术, 2007

3 陈仕谋, 吴国忠, 沙茂林, 等. Transition of ionic liquid [bmim][PF6] from liquid to high-melting-point crystal when confined in multi-walled carbon nanotubes, J Am Chem Soc, 2007, **129**: 2416–2417

4 黄师荣, 吴国忠, 陈仕谋. Preparation of microporous PVDF membranes by precipitating the casting film in supercritical carbon dioxide, JOURNAL OF MEMBRANE SCIENCE,2007, **293**: 100–110

5 黄师荣, 吴国忠, 陈仕谋. Preparation of open cellular PMMA microspheres by supercritical carbon dioxide foaming, J Supercrit Fluids, 2007, **40**: 323–329

6 戚明颖, 吴国忠, 陈仕谋, 等. Radiolysis of ionic liquid 1-butyl-3-methylimidazolium hexafluorophosphate, Radiat Res, 2007, **167**: 508–514

7 龙德武, 吴国忠, 陈仕谋. Preparation of oligochitosan stabilized silver nanoparticles by irradiation, Radiat Phys Chem, 2007, **76**: 1126–1131

8 龙德武, 吴国忠, 王文峰, 等. Photo-induced interfacial electron transfer from CdSe quantum dots to surface-bound p-benzoquinone and anthraquinone, Res Chem Intermed, 2007, **33**: 655–661

9 徐静静, 吴国忠, 龙德武, 等. Laser photolysis study on photochemical reactions in mixed solutions of [bmim][PF_6] and acetonitrile , Spectroscopy and Spectral Analysis, 2007, **27**: 1936–1938

10 朱光来, 吴国忠, 龙德武, 等. Laser photolysis of ionic liquid [bmim][PF_6], Nuclear Science and Techniques, 2007, **18**: 16–19

11 王敏, 沈忠群, 杨睿媛, 等. 环境污染物的辐射处理应用研究, 辐射研究与辐射工艺学报, 2007, **25**(2): 95–101

12 马红娟, 王敏, 杨睿媛, 等. Radiation degradation of Congo Red in aqueous solution, Chemosphere, 2007, **68(**6): 1098–1104

13 杨睿媛, 王敏, 沈忠群, 等. The degradation and mineralization of 4-chlorophenol in aqueous solutions by electron beam irradiation in the presence of TiO_2 nanoparticles, Radiation Physics and Chemistry, 2007, **76**(7): 1122–1125

14 徐冬梅, 洪军, 姚思德, 等. Size controlling of PEI nanogel induced by Feton reaction, International Journal of Pharmaceutics, 2007, **338** (1-2): 291–2967

15 徐冬梅, 洪军, 盛康龙, 等. Preparation of polyethyleneimine nanogels via photo-Fenton reaction, Radiation Physics and Chemistry, 2007, **76**(10): 1606–1611

16 徐冬梅, 洪军, 姚思德, 等. 以光诱导 Fenton 反应控制 M-PEIs 纳米凝胶的粒径, 高分子学报, 2007, **4**: 389–393

17 宫培军, 孙汉文, 洪军, 等. 加速器与辐射研究中心, In-situ synthesis of PHEMA magnetic nanogels via photochemical method, Science in China Ser-B, 2007, **50**(2): 217–223

18 洪军, 徐冬梅, 宫培军, 等. Facile Synthesis of polymer-enveloped ultrasmall superparamagnetic iron oxide for magnetic resonance imaging, Nanotechnology, 2007, **18**(13): 35608–35608(6pp)

19 洪军, 宫培军, 徐冬梅, 等. Synthesis and characterization of carboxyl-functionalized magnetic nanogel via “Green” photochemical method, Journal of Applied Polymer Science, 2007, **105**(4): 1882–1887

20 洪军, 徐冬梅, 宫培军, 等. Stabilization of α-chymotrypsin by covalent immobilization on amine-functionalized superparamagnetic nanogel, Journal of Biotechnology,2007, **128**(3): 597–605

21 洪军, 徐冬梅, 宫培军, 等. Conjugation of enzyme on superparamagnetic nanogels covered with carboxyl groups, Journal of Chromatography B Analytical Technologies in the Biomedical and Life Science, 2007, **850**(1-2): 499–506

22 洪军, 徐冬梅, 姚思德, 等. 用于 α-胰凝乳蛋白酶固定化的氨基超顺磁纳米凝胶的光化学合成与表征, 高等学校化学学报, 2007, **28**(1): 177–182

23 洪军, 徐冬梅, 宫培军, 等. Covalent binding process of α-chymotrypsin on the magnetic nanogels covered by amino groups, Journal of Molecular Catalysis B: Enzymatic, 2007, **45(**3-4): 84–90

24 付海英, 谢雷东, 窦大营, 等. Storage stability and compatibity of asphalt binder modified by SBS graft copolymer, Construction and Building Materials, 2007, **21**: 1528–1533

25 王胜利, 刘永好, 李德明, 等. Study of ^{26}Al measurement on the Shanghai Mini-cyclotron based AMS, Nucl Instrum Meth B, 2008, **266(**15): 3302–3308

26 郭洪雷, 龚培荣, 刘平, 等. EBS 加速器电源控制系统的研制, 核技术, 2008, **31**(1): 63–66

27 LONG Dewu, WU Guozhong, WU Aibin, *et al*. Photoinduced charge separation in riboflavin/carbon nanotubes superstructures, Journal of physical chemistry C, 2008, **112**(33): 13000–13003

28 SHA Maolin, WU Guozhong, FANG Haiping, *et al*. Liquid-to-solid phase transition of a 1,3-dimethylimidazolium chloride ionic liquid monolayer confined between graphite walls, Journal of physical chemistry C, 2008, **112(**47): 18584–18587

29 SHA Maolin, ZHANG Fuchun, WU Guozhong, *et al*. Ordering layers of [bmim][PF_6] ionic liquid on graphite surfaces:molecular dynamics simulation, Journal of chemical physics, 2008, **128(**13): 134504

30 ZHU Guanglai, WU Guozhong, SHA Maolin, *et al*. Effects of ionic liquid [bmim][PF_6] on absorption spectra and reaction kinetics of the duroquinone triplet state in acetonitrile, Journal of physical chemistry A, 2008, **112**(14): 3079–3085

31 QI Mingying, WU Guozhong, SHE Ying, *et al*. Luoγ-Radiation effect on ionic liquid [bmim][BF4], Radiation physics and chemistry, 2008, **77**(7): 877–883

32 QI Mingying, WU Guozhong, SHA Maolin, *et al*. Radiation induced polymerization of MMA in imidazolium ionic liquids and their mixed solutions with organic solvents, Radiation physics and chemistry, 2008, **77(**10-12): 1248–1252

33 LONG Dewu, WU Guozhong, ZHU Guanglai. Noncovalently Modified Carbon Nanotubes with Carboxymethylated Chitosan: A Controllable Donor-Acceptor Nanohybrid, International journal of molecular sciences, 2008, **9**(2): 120–130

34 王晓兵, 吴国忠, 陈仕谋. 聚四氟乙烯微粉预辐照接枝苯乙烯的研究, 核化学与放射化学, 2008, **30**(4): 238–242

35 BO Deng, LI Jingye, ZHENG Chihou, *et al*. Microfiltration membranes prepared from polyethersulfone powder grafted with acrylic acid by simultaneous irradiation and their pH dependence, Radiation Physics and Chemistry, 2008, **77**(7): 898–906

36 赵君, 王敏, 马红娟, 等. 茜素红的辐射降解研究, 辐射研究与辐射工艺学报, 2008, **26**(1): 13–18
37 董黎, 徐冬梅, 洪军, 等. 辐射制备的 M-PEIs 基因转导载体细胞生物学研究, 核技术, 2008, **31**(6): 465–469
38 ZHAO Jian, LI Dong, LU Bin, *et al*. Down-regulation of osteopontin suppresses growth and metastasis of hepatocellular carcinoma via induction of apoptosis, Gastroenterology, 2008, **135**(3): 956–968

放药中心 Radiopharmaceuticals

1 XU Ronghui, WANG Yongxiang, JIA Guangqiang, *et al*. Zinc blende and wurtzite cadmium sulfide nanocrystals with strong photoluminescence and ultrastability, Journal of Crystal Growth, 2007, **128**(3): 28–33
2 CHENG Dengfeng, YIN Duanzhi, ZHANG Lan, *et al*. Preparation of the novel fluorine-18-labeled VIP analog for PET imaging studies using two different synthesis methods, Journal Of Fluorine Chemistry, 2007, **299**(1): 196–201
3 许荣辉, 汪勇先, 贾广强, 等. 闪锌矿结构 CdS 纳米晶的制备, 高等学校化学学报, 2007, **28**(2): 217–219
4 XU Wanbang, WANG Yongxian, XU Ronghui, *et al*. Synthesis and fluorescence spectrum analysis of CdS nanocrystals, J Mater Sci, 2007, **42**(**1**6): 6942–6945
5 ANG Mingwei, YIN Duanzhi, LI Shiqiang, *et al*. Synthesis of O-(2-[18F]fluoroethyl)-L-tyrosine and its biological evaluation in B16 melanoma-bearing mice as PET tracer for tumor imaging, Science in China Series B:Chemistry, 2007, **50**(2): 279–283
6 CAI Hancheng, YIN Duanzhi, ZHANG Lan, *et al*. Preparation and biological evaluation of 2-amino-6-[^{18}F] fluoro-9-(4- hydroxy-3-hydroxy- methylbutyl) purine (6-[^{18}F]FPCV) as a novel PET probe for imaging HSV1-tk reporter gene expression, Nuclear Medicine and Biology, 2007, **36**(4): 717–725
7 徐万帮, 汪勇先, 梁胜, 等. 水相中荧光 CdSe 纳米晶的优化合成与表征, 无机化学学报, 2007, **23**(7): 1220–1226
8 徐万帮, 汪勇先, 许荣辉, 等. CdS 量子点的优化合成及其在离子检测中的应用, 功能材料, 2007, **38**(8): 1287–1293
9 张春富, 徐万帮, 汪勇先, 等. 荧光 CdTe 量子点和 CdTe/SiO_2 纳米粒子的制备与表征, 功能材料, 2007, **38**: 2174–2176
10 CHENG Dengfeng, YIN Duanzhi, ZHANG Lan, *et al*. Radiosynthesis of ^{18}F-(R8, 15, 21, L17)-VIP and preliminary evaluation in mice bearing C26 colorectal tumors, Nuclear Medicine Communications, 2007, **28**(6): 501–506
11 ZHENG Mingqiang, YIN Duanzhi, SHEN Yumei. Syntheses of 2-(*p*-amino phenyl)-6-substituent-benzothiazoles, Chinese Journal of Organic Chemistry, 2007, **27**: 1369–1373
12 LIANG Sheng, WANG Yongxian, YU Junfeng, *et al*. Surface modified superaramagnetic iron oxide nanoparticles:as a new carrier for bio-magnetically targeted therapy, J Mater Sci:Mater Med, 2007, **18**: 2297–2302
13 成康民, 沈玉梅. β-榄香烯三羰基铼衍生物的放射化学合成, 核技术, 2007, **30**(1): 53–56
14 刘贵锋, 孙艳红, 成康民, 等. β-榄香烯单取代胺衍生物的合成及体外抗肿瘤活性, 中国药科大学学报, 2007, **38**(5): 396–399
15 XU Wanbang, WANG Yongxian, LIANG Sheng, *et al*. Optimized synthesis and fluorescence spectrum analysis of CdSe quantum dots, journal of dispersion science and technology, 2008, **29**(7): 953–957
16 ZHENG Mingqiang, YIN Duanzhi, QIAO Jinping, *et al*. Syntheses and evaluation of fluorinated benzothiazole anilines as potential tracers for *β*-amyloid plaques in Alzheimer's disease, Journal of Fluorine Chemistry, 2008, **129**: 210–216
17 ZHENG Mingqiang, YIN Duanzhi, LEI Bei, *et al*. Biological characters of [^{18}F]O-FEt-PIB in a rat model of Alzheimer's disease using micro-PET imaging, Acta Pharmacologica Sinica, 2008, **29(**5): 548–554
18 武明星, 郭飞虎, 施玲丽, 等. 一种磺胺类碳酸酐酶Ⅸ抑制剂合成, 精细化工, 2008, **25**(9): 850–853
19 武明星, 郭飞虎, 施玲丽, 等. 一种含氟原子和三嗪环的磺胺类化合物的合成, 精细化工, 2008, **25**(10): 945–947
20 施玲丽, 郭飞虎, 王妮, 等. 多肽的 ^{18}F 标记方法, 核技术, 2008, **31**(10): 772–779
21 成康民, 孙艳红, 冯翠兰, 等. β-榄香烯乙二醇衍生物的合成及体外抗癌活性, 有机化学, 2008, **28**(1): 65–68
22 任云峰, 成康民, 刘贵峰, 等. β-榄香烯三羰基铼配合物的合成、放射化学合成及抗癌活性研究, 化学学报, 2008, **66**(4): 459–464

23 任云峰, 刘贵锋, 孙艳红, 等. β-榄香烯-TEG-Re(CO)$_3$配合物的合成、放射性标记及初步生物活性, 高等学校化学学报, 2008, **29**(9): 1765–1768
24 成康民, 沈玉梅, 王谋华, 等. β-榄香烯氨基酸衍生物的合成, 应用化学, 2008, **25**(5): 560–563
25 董墨, 包广粮. 中草药有效成分的氚标记, 同位素, 2008, **21**(3): 161–164

先进探测仪器 Advanced Detectors and Instruments

1 张猛蛟, 漆玉金. 高分辨小型伽玛相机位置读出电路研究, 核技术, 20074, **30**(7): 629
2 王震遐, 潘强岩, 胡建刚, 等. 双离子($^{40}Ar^+$, $C_2H_6^+$)辐照合成金刚石纳米晶颗粒, 物理学报, 2007, **56(**8): 4829–4833
3 张鸿洲, 李勇平, 王琳, 等. Pose insensitive face recognition using feature transformation, Int J of Computer Sciences and Network Security, 2007, **7(**2): 89–957
4 徐慧超, 成诚, 赵翠兰, 等. Characteristics of a prototype CdZnTe detector, Nuclear Science and Technology, 2007, **18**(6): 356–361
5 傅斯翊, 魏永波, 蒋大真. 虚拟仪器技术在离子迁移率谱仪中的应用, 核技术, 2008, **31(**5): 384–387
6 王琳, 李勇平, 王成波, 等. 2D gaborface representation method for face recognition with ensemble and multichannel model, Image Vision Computing, 2008, **26**(6): 820–828
7 王成波, 李勇平, 张鸿洲, 等. Multi-modal biometric verification based on far-score normalization, Int J of Computer Science and Network Security, 2008, **8**(4): 250–254
8 王琳, 李勇平, 王成波, 等. 基于二维 Gabor 小波矩阵表征人脸的识别算法, 计算机工程, 2008, **34**(2): 8–10
9 金莉莉, 李勇平, 汪勇旭,等. 基于二维主成分分析的指纹识别算法, 计算机工程, 2008, **34(**7): 215–217, 220
10 梁平, 唐世标, 蒋连军, 等. HL-2A 中基于 USB 新型多路分时定标器的研制, 核技术, 2008, **31**(1): 71–77
11 代秋声, 漆玉金. 高分辨 micro-SPECT 成像系统针孔准直器的优化设计, 原子能科学技术, 2008, **42**(6): 535
12 赵翠兰, 浦世节. 基于碲锌镉探测器的能谱放大器, 核技术, 2008, **31**(1): 78–80

新技术中心 Membrane Technology

1 侯铮迟, 陈爽, 盛康龙. Distribution of Acrylic Acid-Grafted Chains Introduced into Polyethylene Film by Simultaneous Radiation Grafting Using Water and Ethanol as Solvent, Journal of Applied Polymer Science, 2007, **103**(3): 1570–1577
2 陈爽, 侯铮迟, 张凤英, 等. 接枝丙烯酸聚乙烯表面诱导生成硫化镉及其形貌研究, 辐射研究与辐射工艺学报, 2007, **25**(1): 47–50
3 李晓, 陆晓峰, 段伟, 等. γ 射线辐照接枝丙烯酸改性 PVDF 超滤膜, 膜科学与技术, 2007, **27**(2): 49–52

技术安全室 Technology security

1 方克明, 许浔江, 蔡建华. Calculation and design for SSRF bulk shield, Radiation Measurements, 2007, **41**: S256
2 王建华, ZHANG Hualin. Dosimetric characterization of model Cs-1 Rev 2 Cesium-131 brachytherapy source in water phantoms and human tissues with MCNP5 Monte Carlo simulation, Medical Physics, 2008, **35**(4): 1571–1579
3 王建华, 刘卫, 许浔江, 等. Dosimetric parameters of thepalladium-103 brachytherapy source with Monte Carlo simulation, Chinese Science Bulletin, 2008, **53**(9): 1304–1309
4 王建华, 徐加强, 许浔江, 等. Monte Carlo evaluation for SSRF beam holes shielding eutronsof front end ratchet walls, Chinese physics C, 2008, **32**(增刊 I): 105–108
5 花正东, 许浔江, 方克明, 等. Calculation of gas bremsstrahlung power from straight section of storage ring at SSRF, Chinese physics C, 2008, **32**(增刊 I): 89–92
6 花正东, 许浔江, 王建华, 等. Study of the energy response of high pressure ionization chamber for high en-

ergy γ-ray, Chinese physics C, 2008, **32**(5): 370–372
7 王建华, 凌球, 郭兰英, 等. MB 形容器体积对 BGO 晶体探测效率的蒙特卡罗优化设计, 核电子学与探测技术, 2008, **28**(3): 533–537
8 王建华, 邱小平, 罗志平, 等. ^{60}Co辐照装置剂量场均匀性的优化设计, 辐射研究与辐射工艺学报, 2008, **26(**1): 5–8
9 王建华, 邱小平, 刘卫, 等. ^{131}Cs, ^{125}I 和 ^{103}Pd 近距离治疗源的径向剂量函数研究, 核电子学与探测技术, 2008, **27(**6): 1223–1226

附录 2

2007-2008 年度举办（承办）国际国内重要会议表

No.	会议名称 Conference Name	日期 Dates	规模 Scale
2007			
1	97 期东方科技论坛：同步辐射在医学临床诊断中的应用 Application of Synchrotron Radiation to Medical Clinical Diagnosis	June 29-30	共 54 人：国内专家 49 人；国外专家 5 人
2	104 期东方科技论坛：第三代同步辐射光源恒流注入问题 Top-Up Injection in 3rd Generation Synchrotron Radiation Light Source	Dec.6-7	共 42 人：国内专家 39 人；国外专家 3 人
3	纳米尺度界面水的前沿科学问题国际研讨会 International workshop on Molecular structure and dynamics of interfacial water	Dec.14-18	共 80 人：国外专家 40 人；国内专家 40 人
4	105 期东方科技论坛：同步辐射 X 射线微探针和显微技术及其应用 Synchrotron Radiation X-ray Microprobe, Microscopy and Applications	Dec.16-17	共 62 人：国内专家 50 人；国外专家 12 人
5	同步辐射技术系列研讨会-同步辐射技术与纳米材料 Workshop on Synchrotron Radiation and Nano-materials	Dec.18	共 41 人：国外专家 4 人；国内专家 37 人
6	同步辐射技术系列研讨会-同步辐射技术与环境科学 Workshop on Synchrotron Radiation and Environmental Science	Dec.19	共 46 人：国外专家 2 人；国内专家 44 人
2008			
1	2008 年度 EPICS 国际研讨会 2008 EPICS collaboration meeting and EPICS seminar	Mar.10-14	共 50 人：国外专家 29 人；国内专家 21 人
2	ICFA 束流动力学小型研讨会-“射频偏转腔在加速器中的应用” ICFA Beam Dynamics Mini-Workshop on Deflecting/Crabbing Cavity Applications in Accelerators	Apr.23-25	共 40 人：国外专家 19 人；国内专家 21 人
3	111 期东方科技论坛：同步辐射光源与组合材料表征技术 Combinatorial materials characterization based on synchrotron radiation facility	June17-18	共 30 余人：国内专家 30 余人，国外专家 3 人
4	2008 年度 FNCA 国际研讨会-加速器应用—天然高分子的辐射加工研讨会 FNCA 2008 Workshop on Application of Electron Accelerator- Radiation Processing of Natural Polymers	Oct.27-31	共 80 人：国外专家 17 人；国内专家 63 人
5	生物界面水性质研讨会 Workshop on Water at Biological Interfaces	Oct.27-28	共 45 人：国外专家 11 人；国内专家 34 人
6	119 期东方科技论坛：基于同步辐射光源的显微影像技术在生物学中的应用 Applications of Microscope Imaging Based on Synchrotron Radiation Light Source in Biology	Oct.31-Nov.1	共 50 余人：国内专家 40 余人，国外专家 4 人
7	122 期东方科技论坛：自由电子激光运行模式 Present and Future Free Electron Laser Schemes	Dec.11-12	共 30 余人：国内专家 20 余人，国外专家 6 人

附录 3

2007-2008 年度国际学术会议报告表

Presentations by SINAP scientists at international scientific meetings in 2007–2008

No.	Meetings in 2007	Speaker	Date & Place
1	International Workshop on Hadronic Nuclear Physics 2007 "Quarks in hadrons, nucleus, and matter"	Plenary, 蔡翔舟 Plenary, 郭威 Oral, 马余刚	Feb.21–Mar.1, Korea
2	2007 World Conference on Ageing and Dementia in Chinese Communities	Plenary, 尹端沚 Plenary,郑明强	Mar.6–11, Hongkong, China
3	2007 IEEE Symposium of Foundation of Computational Intelligence	Oral, 李勇平	Mar.27–Apr.7, USA
4	STAR TOF-MRPC Workshop	Oral, 马余刚 Oral, 蔡翔舟	Apr.5–8, China
5	Workshop on Physicists and Biologists Working-Together-Facilitating X-ray Biophotonics	Oral, 肖体乔	Apr.10–15, Australia
6	Italy-Australia Workshop (IAW-3) on Future Directions in Spectroscopy and Imaging with Synchrotron Light: New Light Sources	Invited, 肖体乔	Apr.14, Australia
7	Sino-German High Level Expert Symposium on X-ray Optics	Invited, 余笑寒	Apr.15–19, China
8	The 17th International Symposium on Radiopharmaceutical Sciences	Oral, 汪勇先 Poste, 尹端沚 Poster, 沈玉梅 Poster, 张岚	Apr.28–May.5, Germany
9	The 10th International Conference on Atmospheric Sciences and Applications to Air Quality	Plenary,张元勋	May 13–20, Hongkong, China
10	The 9th International Spring Seminar on Nuclear Physics	Plenary, 马余刚 Plenary, 蔡翔舟	May 18–26, Italy
11	2007 World Congress of Signal and Image Engineering	Oral, 李勇平	May 18–26, UK
12	ICFA Beam Dynamics Workshop on Energy Recovery Linacs	Oral,刘建飞	May 20–26, UK
13	The 3rd China-Singapore Joint Symposium on Research Frontiers in Physics	Oral, 方海平	May 25–27, China
14	ECI Conference on Nanoscience and Nanotechnology for Biological/Biomedical/ Chemical Sensing	Poster, 樊春海 Poster, 宋世平	June 3–9, Hongkong, China
15	2007 International Nuclear Physcis Conference	Plenary, 马春旺	June 2–9, Japan
16	International Conference on Nanoscience and Technology	Plenary, 李宾 Plenary, 龙德武 Poster, 诸颖 Poster, 李民乾 Poster, 王丽华 Poster, 颜娟	June 4–6, China
17	The 4th International Workshop on Radiation Safety at Synchrotron Radiation Source	Oral, 方克明	June 5–10, Canada
18	The 3rd Shanghai International Symposium on Nonlinear Sciencies and Applications (Shanghai NSA '07)	Plenary, 方海平 Plenary, 李华兵	June10, China
19	2007 International Workshop on Nuclear Structure: New Pictures in the Extended Isospin Space	Plenary, 方德清 Poster, 马春旺	June10–15, Japan
20	2007 International Conference on Strangeness in Quark Matter	Plenary, 马余刚 Plenary, 蔡翔舟 Plenary, 左家旭	June 23–30, Slovakia
21	2007 Particle Accelerator Conference	Oral, 赵振堂 Plenary. 周巧根 Plenary, 陈念	June 24–July 7, USA

No.	Meetings in 2007	Speaker	Date & Place
22	Application of Synchrotron Radiation to Medical Clinical Diagnosis	Oral, 徐洪杰	June 29–July 30, China
23	The 4th International Conference on Marterial for Advanced Technologies	Plenary, 李宾	June 30–July 7, Singapore
24	International workshop on nuclear dynamics in heavy-ion collisions andneu-tron stars	Oral, 马余刚	July 7, China
25	Forum for Nuclear Cooperation in Asia 2007 Expert Mission on Application of Electron Accelerator	Oral, 吴国忠	July 11–15, Vietnam
26	The 5th International Conference of Aquaporin	Plenary, 弓晓晶	July 13–16, Japan
27	The 16th International Conference on the Discrete Simulation of Fluid Dy-namics	Oral, 方海平 Oral, 李华兵 Oral, 万荣正	July 22–28, Canada
28	International Program "Computational methods in biomolecular structures and interaction networks"	Oral, 方海平	July 29–Aug.4, Singapore
29	The 1st Annual IEEE International Conference on Nano/Molecular Medicine and Engineering	Oral, 胡钧	Aug.6–9, Macao, China
30	2007 Conference on Medical Applications for Synchrotron Radiation	Oral, 肖体乔	Aug.24–Sept..1, Canada
31	The 29th International Conference on Free Electron Laser	Oral, 戴志敏 Plenary, 周巧根 Plenary, 顾强	Aug.25–Sept.1, Russia
32	The 14th International Conference on Radiation Effects in Insulators	Oral, 朱志勇	Aug.26–Sept..2, France
33	The 10th International Conference on Environmental Science and Technology	Poster, 张元勋 Poster, 李晓林 Poster, 刘卫	Sept.3–11, Greece
34	International Symposium on Isotope Science and Engineering from Basics to Applications	Poster, 刘卫	Sept.17–21, Japan
35	The 7th Japan-China Joint Seminar on Radiopharmaceutical Chemistry	Oral, 尹端沚 Oral, 于俊峰	Sept.26–30, Japan
36	The 11th Biennial International Conference on Accelerator and Large Experi-mental Physics Control Systems	Oral, 刘松强	Oct.14–20, USA
37	Sino-French Workshop on Bioorganic and Medicinal Chemistry	Poster, 刘瑞丽 Poster, 蔡小青	Oct..17–19, China
38	2007 Low-Level Radio Frequency Workshop	Oral, 赵玉彬	Oct.20–Nov.4, USA
39	The 2nd Asia-Oceania Forum on Synchrotron Radiation Research	Oral, 何建华	Oct.31–Nov.5, Taiwan, China
40	2007 Advanced Science Research Symposium	Oral, 吴国忠	Nov.5–10, Japan
41	2007 SPIE Asia Photonic	Plenary, 刘桂峰	Nov.11–16, China
42	The 6th Nuclear and Particle Physics Conference	Oral, 田文栋	Nov.14–22, Egypt
43	The 28th Meeting of the Joint Committee for Cooperation in High Energy Physics	Oral, 徐洪杰 Oral, 赵振堂	Nov.17–23, USA
44	The 3rd Shanghai International Nanotechnology Cooperation Symposium	Invited, 樊春海 Oral, 李海 Poster, 王鹏	Nov.21–23, China
45	International Symposium on EcoTopia Science 2007	Plenary/Poster,夏晓彬	Nov.22–27, Japan
46	UK China Partners in Science II	Oral, 樊春海	Nov.24–Dec.2, UK
47	ISO/TC201 16th Plenary Meeting	Plenary, 黄一波	Nov.28–Dec.2, Japan
48	Top-Up Injection in 3rd Generation Synchrotron Radiation Light Source	Oral, 胡钧 Oral, 郜仁忠 Oral, 万荣正	Dec.6–7, China
49	The 4th National Conference on Synchrotron Radiation	Plenary, 肖体乔 Plenary, 谢红兰 Plenary, 邓彪 Plenary, 魏向军 Plenary, 邹扬	Dec.6–7, China

No.	Meetings in 2007	Speaker	Date & Place
50	International Workshop on Molecular Structure and Dynamics of Interfacial Water	Plenary, 胡钧 Poster, 叶鸣 Poster, 王华兵 Poster, 李海 Poster, 李宾 Poster, 张益	Dec.14–18, China
51	The 5th Singapore International Chemistry Conference	Oral, 樊春海	Dec.17–19, Singapore
52	Synchrotron Radiation X-ray Microprobe, Microscopy and Application	Oral, 徐洪杰 Oral, 黄庆	Dec.17, China
53	Workshop on Synchrotron Radiation and Nano-materials	Oral, 邰仁忠 Oral, 周兴泰	Dec.18, China
54	Workshop on Synchrotron Radiation and Environmental Science	Oral, 李燕 Oral, 黄宇营	Dec.18, China

No.	Meetings in 2008	Speaker	Date & Place
1	The 20th International Conference on Ultra-Relativistic Nucleus Nucleus Collisions	Oral，马余刚 Plenary, 蔡翔舟 Poster, 陈金辉 Poster, 左家旭	Feb.3–11, India
2	The 10th International Workshop on Accelerator Alignment	Oral, 于成浩 Poster, 柯敏	Feb.10–16, Japan
3	The 3rd Environmental Physics Conference	Invited, 张桂林	Feb.16–25, Egypt
4	EPICS collaboration meeting 2008 and EPICS Seminar	Oral, 刘德康 Oral, 沈立人 Oral, 冷用斌 Oral, 许瑞年 Oral, 沈国宝	Feb.12-14, China
5	The 4th International Symposium on Ultrafast Phenomena & Terahertz Waves	Plenary, 马士华 Plenary, 刘桂峰	Mar.29–31, China
6	ICFA Beam Dynamics Mini-Workshop on Deflecting/Crabbing Cavity Applications in Accelerators	Oral, 赵振堂 Oral, 马广明	Apr.23–25, China
7	The 15th International Symposium on Bioluminescence and Chemiluminescence	Poster, 张朝霞	May 13–17, China
8	Biosensors 2008 (The 10th World Congress of Biosensors)	Poster, 宋世平	May 14–16, China
9	The 7th International Conference on the Scientific and Clinical Applications of Magnetic Carriers	Plenary, 汪勇先	May 20–28, Canada
10	International Workshop on Heavy Ion Physics at LHC	Oral, 马国亮	May 21–24, China
11	The 5th International Workshop on Wearable and Implantable Body Sensor Networks, and the 5th International Summer School and Symposium on Medical Devices and Biosensors	Oral, 漆玉金	May 31–June4, Hongkong, China
12	Pohang Accelerator Laboratory- International Advisory Committee Meeting	Oral 赵振堂	June 1–4, Korea
13	International Workshop on Nuclear Structure Physics	Oral, 陈金根	June 1–7, China
14	The 3rd International Symposium on Biomedical Engineering Bio-analysis and Nanotechnology	Plenary,宋世平	June 8–11,China
15	International Workshop on Mechanical Engineering Design of Synchrotron Radiation Equipment and Instrumentation	Plenary, 殷立新 Plenary, 王纳秀 Poster, 王晓	June 9–15, Canada
16	The 11th Biennial European Particle Accelerator Conference (EPAC'08)	Oral, 赵振堂 Plenary, 蒋迪奎 Poster, 冷用斌 Poster，陈永忠 Poster, 缪海峰 Poster, 阎映炳	June 21–28, Italy

No.	Meetings in 2008	Speaker	Date & Place
17	The14th International Conference on the Environment	Oral, 张桂林	June 29–July 5, Canada
18	Hardon and Nuclear Physics 2008	Oral, 马余刚 Oral, 蔡翔舟	June 30, China
19	China-Japan Information and Communications Technology Forum 2008	Poster, 马士华 Poster, 刘桂峰	July 8–9, China
20	American Biological and Lichenological Society Joint Meeting with International Association of Lichenology	Oral, 张元勋	July 12–20, USA
21	17th Annual Conference on Ion Mobility Spectrometry	Oral, 李勇平	July 19–26, Canada
22	International Hydrogen Forum (HyForum 2008)	Plenary, 纪玉玲	Aug.3–6, China
23	The 30th International Free Electron Laser Conference	Poster, 邓海啸	Aug.23–30, Korea
24	The 2nd Asia-Pacific Symposium on Radiation Chemistry (APSRC-2008)	Invited,吴国忠 Invited, 姚思德 Oral,李景烨 Plenary, 马红娟	Aug.28–Sept.2,Japan
25	The International Conference on Nano Toxicology (ICNT2008)	Oral, 褚颖 Poster,苏媛媛 Poster, 蔡小青	Sept.7–10, China
26	Sino-Singapore Symposium on Advanced Materials	Invited, 樊春海	Sept.25–26, China
27	International Conference on Strangeness in Quark Matter 2008	Plenary, 靳富 Plenary, 陈金辉 Poster, 马国亮	Oct.6–10, China
28	Satellite Meeting of the 2nd Sino-German Frontiers of Chemistry Symposium	Invited, 樊春海	Oct.6–10, China
29	The 2nd Asian Triangle Heavy Ion Conference	Oral, 蔡翔舟 Oral, 方德清 Plenary, 马国亮 Plenary, 陈金辉	Oct.12–15, Japan
30	The 13th International Biotechnology Symposium and Exhibition	Invited, 樊春海	Oct.12–17, China
31	The 14th Biennial International Meeting of the Society for Free Radical Research	Poster, 张鹏 Poster, 宋西玉	Oct.17–22, China
32	The 12th International Congress of the International Radiation Protection Association	Plenary, 夏晓彬	Oct.18–26, Argentina
33	2008 Joint Symposium on Molten Salts	Oral, 沙茂林	Oct.18–24, Japan
34	The 7th International Conference on Nano-Science and Technology	Plenary, 杨晓明	Oct.23–27, China
35	Workshop on Water at Biological Interface	Oral, 方海平	Oct.27–28, China
36	FNCA Workshop on Radiation Processing of Natural Polymer	Oral, 吴国忠 Oral, 李德明	Oct.27—31,China
37	The 5th Asia-Pacific Photochemistry Conference	Plenary, 龙德武	Nov.1–4, China
38	The 1st Asia Pacific Conference on Ionic Liquids and Green Processes	Poster, 黄卫 Poster, 刘玉胜 Poster, 窦强	Nov.5–9, China
39	The 2nd IEEE-NANOMED	Invited, 樊春海	Nov.6–9, China
40	Great Wall 2008 International Congress on Medical Physics and the 14th National Annual Meeting of Chinese Society of Medical Physics	Invited, 漆玉金	Nov.23–26, China
41	Photonics and Opto Electronics Meetings 2008	Plenary, 马士华 Plenary, 刘桂峰	Nov.24–27, China
42	The 2nd China-Japan-Korea Joint Seminar on Fluorine Chemistry	Oral, 邓波	Nov.27–28, China
43	The 3rd Asian-Oceania Forum on Synchrotron Radiation Research	Invited,赵振堂 Poster, 黎忠	Nov.30–Dec.6, Australia
44	The 3rd Asian-Oceania Week of the Australian Synchrotron	Invited,何建华	Nov.30–Dec.6, Australia
45	International Workshop on Photon and Jet with ALICE	Oral,马余刚	Dec.4–6, China
46	The 10th International Conference on Control, Automation, Robotics and Vision	Oral, 李景烨 Plenary, 王超	Dec.16–21, Vietnam
47	2008 International Symposium on Information Science and Engineering (ISISE 2008)	Poster, 黄跃峰	Dec.20–22, China

附录 4

2007–2008 所内举办的学术报告

2007

No.	报告	报告人（报告人单位）	日期
1	先进核能系统及综合利用	曹学武 教授(上海交通大学)	Jan.19
2	日本辐射加工研究的过去与现状	濑口忠男 博士(日本原子能研究机构高崎所)	Jan.19
3	Thermal diode and thermal transistor: the art of controlling heat flow	李保文 教授(新加坡国立大学物理系)	Mar.8
4	Studying biomaterials using Nanotechnology	Dr. Umemura Kazuo (Musashi Institute of Technology, Japan)	Mar.5
5	Proteins under force: activation and folding	Frauke Graeter 博士(哥伦比亚大学化学系)	Mar.15
6	Investigation of chemical bonding using surface sensitive techniques	Prof. A.R Chourasia (Department of Physics, Texas A&M University)	Mar.23
7	Novel optical response of highly excited semiconductor quantum wires	怀平 博士 (CREST, JST and Department of Physics, Osaka University, Japan)	Apr.11
8	Radipharmaceutical studies at Institute of Nuclear Chemistry and Technology	Aleksander Bilewicz 教授 (波兰科学院核化学与技术研究所)	Apr.12
9	National laboratories in the context of US R&D and introduction to Argonne Laboratory and APS status	Dr. Robert Rosner (Director, Argonne National Laboratory, USA)	Apr.23
10	Regulation of cell growth and tumor progression by MAP kinase and Raf kinase inhibitory protein	Prof. Marsha R. Rosner (Charles B. Huggins Professor, Director of Ben May Institute for Cancer Research, University of Chicago, USA)	Apr.23
11	材料发现引擎-------组合材料芯片研究新进展	项晓东 博士	May 22
12	M.R. molecular imaging	张春富 博士	May 23
13	关于γ射线激光	张启仁 教授(北京大学物理系)	May 25
14	Cell nano-structured surface interaction	Prof. U. Hartmann (Experimental Physics Department, University of Saarbruecken, Germany)	May 29
15	Optical metrology for nano-biophotonics: Nano-materials and nano-biophotonics for the biophysics of life processes	Dr. Jeeseong Hwang (Optical Technology Division, National Institute of Standards and Technology, USA)	May 31
16	Study on interaction of THz EM field with matters	汪力 研究员(中国科学院物理研究所)	June 4
17	Decay of periodic patterns in a nematic liquid crystal	Dr. Nandor Eber (Institute for Solid State Physics and Optics, Hungarian Academy of Sciences)	June 6
18	The latest developments for Australian synchrotron	Prof. Frank P Larkins (Deputy Vice Chancellor, University of Melbourne, Australia)	June 6
19	Structure and function of ADAMTS13 and VWF	Dr. Hua Jing (Medical School at Houston. The University of Texas, USA)	June14
20	Computer simulations of proteins and nucleic acids: Structure, dynamics and energetics	Nan-Jie Deng 博士 (Accelrys Inc., San Diego, USA)	June14
21	The pathogenesis mechanism investigation of the Alzheimer's disease and ion-channel biosensor	Prof. Tsuneo Urisu (Institute for Molecular Science, Myodaiji Okazaki, Japan)	June 25
22	Nanomagnetics for biomedical applications	Prof. Wang Jianping (Department of Electrical and Computer Engineering, University of Minnesota, USA)	July 4
23	DNA microarray probe design	Shoudan Liang (Depart. of Bioinformatics and Computational Biology, M.D. Anderson Cancer Center, University of Texas, USA)	July 12
24	Phase transitions in isolated nuclear systems	Dr. M. Veselsky (Slovakia Academy of Science)	July 16
25	Correlations and access to dynamics and structure of nuclear systems	Dr. G. Verde (INFN-Catania, Italy)	July 16
26	Partonic collectivity at RHIC	Dr. Nu Xu (Lawrence Bekeley National Lab, USA)	Aug.20
27	Radiation application in industry and agriculture	Dr. T. Kume (日本原子能研究机构高崎研究所)	Aug.31

No.	报告	报告人（报告人单位）	日期
28	Three-dimensional X-ray diffraction microscopy and its applications in nanoscience and biology	Miao Jianwei (University of California at Los Angeles, USA)	Aug.31
29	Proton therapy at Paul Scherrer Institute; Molecular imaging research at the Center of Radiopharmaceutical Science	Prof. Pius August Schubiger (Institute of Pharmaceutical Sciences, ETH/Swiss Federal Institute of Technology)	Sept.3
30	pQCD 框架下的核－核碰撞	萨本豪 研究员 (中国原子能研究院核物理所)	Sept.3
31	[^{11}C]IMPY derivatives as potential radioligands for beta amyloid in AD	蔡利生 博士(美国 NIH staff scientist)	Sept.5
32	Future plan of ERL project and on-going project of J-PARC	Prof. Osamu Shimomura (Director, Institute of Material Structure Science, KEK, Japan)	Oct.10
33	Tumor targeting for imaging and therapy	Lee Zhenghong(Case Western Reserve University, USA)	Oct.10
34	Molecular Imaging: an update	Lee Zhenghong(Case Western Reserve University, USA)	Oct.18
35	Towards the future of structural biology	Prof. Wladek Minor (Department of Molecular Physiology and Biological Physics, University of Virginia, USA)	Oct.22
36	Study of chemical evolution using synchrotron radiation-anisotropy: Introduction to bioorganic molecules by polarized light	Dr.Jun-ichi Takahashi (NTT Science and Core Technology Laboratory Group, Japan)	Oct.26
37	PETRA III —the new third generation light source at DESY	Hermann Franz (DESY, Germany)	Oct.29
38	Computational study of peptide self-assembly	韦广红 教授(复旦大学物理系)	Oct.29
39	Nuclear science with RIBF	Hiroyoshi Sakurai 主任研究员(日本理化学研究所)	Nov.1
40	Use of natural radioactivity radon as a tracer in the atmosphere	饭田孝夫 教授(名古屋大学工学部；日本原子力学会保健物理环境部会长；日本辐射防护报主编)	Nov.1
41	Reaction cross sections to explore exotic nuclei	Mitsunori Fukuda (Dept. of Phys, Osaka Univ., Japan)	Nov.2
42	Computer simulation of biomolecular interactions	Prof. Volkhard Helms (Theoretical Physics Department，University of Saarbruecken, Germany)	Nov.20
43	Geometry and mechanics of carbon nanotubes and gigahertz nano-oscillators	Prof. James M. Hill (School of Mathematics and Applied Statistics, University of Wollongong, Australia)	Nov.28
44	Properties of the superheavy nuclei in the RMF model	Prof. Stefan Gmuca (Institute of Physics, Slovak Academy of Sciences)	Nov.29
45	Accelerator development for photon science at a new SLAC	Robert O. Hettel (Director of Accelerator Systems Dept., Stanford Linear Accelerator Center, USA)	Dec.7
46	Characterization of single crystal using a laboratory and synchrotron X-rays and its application to X-ray optics for study of medicine	Prof. Masami Ando (安藤正海)(Tokyo University of Science, Japan)	Dec.11

2008

No.	报告	报告人（报告人单位）	日期
1	Switching response of DNA conduction under stretching	Song Bo (Institute for Theoretical Physics, University of Regensburg, Germany)	Jan.1
2	QCD Phase Transitions and Signatures of Quark-Gluon Plasma	庄鹏飞 教授 (清华大学物理系)	Jan.10
3	The Australian synchrotron	Dr. Robert Lamb (Director of Australian Synchrotron, Professor of University of Melbourne)	Jan.17
4	Room temperature ionic liquids as solvents: Insights from simulation; Towards understanding the properties of liquid water —Insights from simulations of modified water models	Prof. Ruth M. Lynden-Bell (Chemical Laboratory, University of Cambridge, UK)	Jan.22
5	Photon-in photon-out spectroscopy and the Canadian Light Source	Prof.Tsun-Kong Sham (Department of Chemistry, University of Western Ontario, Canada; Director of Canadian Synchrotron Radiation Facility)	Jan.23
6	Analysis of nanomaterials using synchrotron radiation	Prof. Tsun-Kong Sham	Jan.24
7	Dysfunction of calcium release channels in the pathogenesis of cardiac arrhythmias and heart failure	Xander Wehrens (Assistant Professor, Depart. of Medicine, Division of Cardiology in Baylor College of Medicine, USA)	Jan.25

2008

No.	报告	报告人（报告人单位）	日期
8	投影壳模型在核同质异能态及双 beta 衰变研究中的应用	孙扬 教授 (上海交通大学物理系)	Feb.26
9	利用 Minority Game 市场模型针对价格涨落的市场机制分析 (Analysis of the market mechanism for price fluctuations by using a minority game model)	陈昱 教授(东京大学大学院工学系研究科系统量子工学专攻)	Mar.19
10	Chemically designed nanoparticles and nanowires: Controlled growth, applications and devices	Prof. Sanjay Mathur (Leibniz-Institute of New Materials Saarland University, Saarbruecken, Germany；Department of Chemistry, Wuerzburg University, 97074 Wuerzburg, Germany)	Mar.26
11	PET imaging of agiogenesis	Dr. Xiaoyuan Chen (Assistant Professor, Radiology Department, Molecular Imaging Program at Stanford, Stanford University)	Apr.1
12	整合优势资源 推进疾病基因组研究	王海丰	Apr.8
13	Understanding role of tumor suppressor genes in dosophila oogenesis	李明发 教授(上海交通大学生命科学技术学院)	Apr.8
14	Novel protein scaffolds for molecular probe discovery	Zhen Cheng (Assistant Professor, Radiology Department, Molecular Imaging Program at Stanford, Stanford Univ.)	Apr.14
15	自由电子激光	余理华(美国布鲁克海文国家实验室)	Apr.16
16	The structuring of nanomaterials by electron irradiation	Prof. Florian Banhart (Institut de Physique et Chimie des Matériaux, France)	Apr.24
17	Challenges to metallomics and analytical chemistry solutions	Prof. Ryszard Lobinski	Apr.28
18	软物质物理 物理学的新学科	陆坤权 (中国科学院物理研究所)	Apr.28
19	核技术在海洋环境中的应用	杜金洲 教授 (华东师范大学)	May 5
20	纳米生物传感器	李景虹 教授 (清华大学)	May 16
21	New developments in QEXAFS - experiments and science	Prof. Ronald Frahm(Faculty C/Department of Physics, University of Wuppertal, Germany)	May.16
22	光合作用过程中的水裂解机理研究	苏吉虎 博士(Max Planck Institute for Bioinorganic Chemistry, Germany)	May 26
23	STAR at RHIC	许怒 研究员(LBNL, USA)	May 27
24	临床医学研究与应用医学研究	唐伟 博士(东京大学医学部肝胆胰外科、人工脏器/移植外科)	May 28
25	Development of X-ray microscopy and its application to biomedical sciences	Prof. Hiroshi Kihara (Department of Physics, Kansai Medical University)	May 30
26	Radioactive biodegradable polymers for magnetic targeting	Dr. Urs Häfeli.(Faculty of Pharmaceutical Sciences, The University of British Columbia, Canada)	June 3
27	蛋白质芯片及其应用	陶生策 博士(美国约翰霍普金斯大学)	June 6
28	XAFS and PEEM observations on low-dimensional and nanostructure materials	Prof. Yuji Baba (馬場祐治, 日本原子力研究开发机构)	June 23
29	Solving the problem of absence of detailed balance and unification of dynamics near and far from equilibrium	敖平 博士 (美国华盛顿大学机械工程系和物理系副教授)	June 24
30	日本血吸虫病和包虫病防治的技术创新与瓶颈	冯正 医学博士(中国疾病预防控制中心寄生虫病预防控制所研究员)	June 25
31	Recent progress in constraining the nuclear symmetry energy and its astrophysical impacts	Bao-An Li 教授 (Texas A&M University, USA)	July 2
32	实时操作系统及新型 PLC RTOS 模块在加速器控制系统中的应用	Jun-ichi Odagiri(日本 KEK&JPARC 控制组)	July 2
33	脉冲电子束辐射诱变酵母菌育种	朱虹 博士(同济大学)	July 3
34	High-pT J/Psi at RHIC	许长补 研究员(美国 BNL 国家实验室)	July 17
35	Novel core-shell magnetic nanoparticles: Synthesis, magnetism and biomedical application	You Qiang (Department of Physics, University of Idaho, Moscow)	July 24

No.	报告	报告人（报告人单位）	日期
36	A variational approach to moving contact line hydrodynamics	Qian Tiezheng 教授(香港科技大学)	Aug.28
37	Nanotechnology at the Technical University of Denmark	Dr. Mogens Rysholt Poulsen (Director, DTU Danchip; Acting Director, DTU Nanotech Technical University, Denmark)	Sept.17
38	Multi-scale modeling approaches to understand biological structure and function	Prof. Marcus Elstner(Technical University of Braunschweig, Germany)	Sept.22
39	Ultrafast synchrotron X-ray phase-contrast imaging study of fluids	Dr. Yujie Wang (X-ray Science Division, Advanced Photon Source, Argonne National Laboratory, USA)	Sept.25
40	New horizon of materials science probed by unconventional use of fluorescence XAS	Prof.Hiroyuki Oyanagi (Photonics Research Institute, National Institute of Advanced Industrial Science and Technology, Japan)	Oct.30
41	Overview of laser-plasma acceleration science at LBNL	Dr. Wim Leemans and Dr. Eric Esarey (LOASIS Program, Accelerator and Fusion Research Division, LBNL, USA)	Oct.31
42	Computer simulation of protein-protein association in water	Prof. Volkhard Helms (Saarland University, Germany)	Nov.10
43	Conductivity and electron transfer in DNA	Prof.Tetsuro Majima (Osaka University, Japan)	Nov.10
44	Directed molecular association, folding and macrocyclization	龚兵 教授 (State University of New York at Buffalo, USA)	Nov.14
45	Femtosecond laser beam— linking the ultrafast and ultrasmall worlds	程亚(中国科学院上海光机所强场激光物理国家重点实验室)	Nov.14
46	Illumination Invariant Face Recognition and Robust Technique in Face Processing	Dr. Xuan Zou (Center for Vision Speech and Signal Processing, University of Surrey, UK)	Nov.19
47	T-shaped GaAs quantum-wire lasers and field-effect optical devices	Prof. Hidefumi Akiyama(Institute for Solid State Physics, University of Tokyo, Japan)	Nov.28
49	Nanomedicine based on dendrimer-organized organic/inorganic hybrid nanoparticles	史向阳 教授(东华大学特聘教授)	Dec.12
50	Quest for short x-ray pulses	Dr. Alexander Zholents (Center for Beam Physics, Accelerator and Fusion Research Division, LBNL, USA)	Nov.15
51	Recent progress on X-ray free-electron laser	Dr. Bart Faatz (DESY, Germany)	Nov.15
52	Monte Carlo simulation and its application	Kim Chan Hyeong 教授(韩国汉阳大学核工程学院)	Nov.15
53	Dynamic phases of confined liquids: Why water is so special	Prof. Jacob Klein(Department of Materials and Interfaces Physical and Theoretical Chemistry, Weizmann Institute of Science, University of Oxford, UK)	Nov.16
54	Present status of SPring-8 macromolecular crystallography beamline	Dr. Go Ueno (Technical Scientist, RIKEN SPring-8 Center, Japan)	Nov.18
55	光镊技术的原理、数值计算及应用	任宽芳 教授(法国鲁昂大学)	Nov.19

附录 5

2007–2008 年专利申请授权一览表

NO.	专利名称	申请号	授权号	专利类别
1	一种低拷贝生化反应的方法	200710036291.X		发明
2	绝缘管套	200720066522.7		实用新型
3	β-榄香烯二胺类衍生物及其合成方法和应用	200710037160.3		发明
4	β-榄香烯单取代胺衍生物及其合成方法和应用	200710037161.8		发明
5	一种水凝胶敷料及其制备方法	200710037471.X		发明
6	氨基修饰的磁性纳米粒子及免疫磁性纳米分离试剂的制备方法	200710038353.0		发明
7	一种富勒烯水溶液及其制备方法	200710039329.9		发明
8	碳纳米材料储备液及采用其的碳纳米材料细胞毒性的测定方法	200710039533.0		发明
9	苯并噻唑苯胺类化合物及其制备方法和应用	200710039985.9		发明
10	高压电容器组件	200710040288.5		发明
11	一种[^{18}F]氟标记的嘌呤类化合物及其制备方法和应用	200710103614.2		发明
12	DNA 分子的微/纳米图形的构建方法	200710041865.2		发明
13	一种水凝胶敷料及其制备方法	200710043427.X		发明
14	一种采用茎环结构检测探针的电化学 DNA 检测方法及其试剂盒	200710046090.8		发明
15	β-榄香烯衍生物及其 Re 配合物和***Re 标记物、以及它们的合成方法和应用	200710149900.2		发明
16	β-榄香烯氨基酸衍生物及其合成方法和用途	200710181826.2		发明
17	C_{60} 的多羟基衍生物在防治线粒体损伤相关疾病中的用途	200710046616.2		发明
18	被动式大气气溶胶个人采样器	200710170634.1		发明
19	一种 DNA 的荧光检测方法及其试剂盒	200710048129.X		发明
20	一种检测 DNA 的 i-motif 构象的光学方法	200710048136.X		发明
21	富勒醇在美容护肤品中的应用	200710172972.9		发明
22	一种吡啶类化合物及其制备方法和作为多巴胺 D_4 受体拮抗剂的应用	02110824.2	ZL02110824.2	发明
23	在扫描探针显微镜及其针尖上沉积薄膜的方法	02111906.6	ZL02111906.6	发明
24	[^{18}F]氟标记的吡啶类化合物及其制备方法和作为多巴胺 D_4 受体显像剂的应用	02136016.2	ZL02136016.2	发明
25	管式超滤膜元件卷管、成膜同步连续制备工艺	03141410.9	ZL03141410.9	发明
26	紫外光直接辐照真丝绸形成接枝共聚物的方法	03151467.7	ZL03151467.7	发明
27	C_{60} 的衍生物富勒醇在滋养毛发方面的应用	200410018372.3	ZL200410018372.3	发明
28	医用聚氨酯透气膜及其制备方法和应用	200410025032.3	ZL200410025032.3	发明
29	高分子薄膜与无机晶体涂层复合材料及其制备方法	200410025135.X	ZL200410025135.X	发明
30	一种壳聚糖超细粉末的制备方法	200410089449.6	ZL200410089449.6	发明
31	真丝绸的染色方法	200410093245.X	ZL200410093245.X	发明
32	聚烯亚胺凝胶的光化学合成方法	200510026477.8	ZL200510026477.8	发明
33	聚烯亚胺纳米凝胶及其应用	200510026746.0	ZL200510026746.0	发明
34	MBR 平片膜在线机械擦洗工具	200520047262.X	ZL200520047262.X	实用新型
35	小型 MBR 装置混合液污泥干化处理设备	200520047260.0	ZL200520047260.0	实用新型
36	IMS 检测仪	200520047493.0	ZL200520047493.0	实用新型
37	转动样品架	200620047378.8	ZL200620047378.8	实用新型
38	固体电解质薄膜的测量装置	200820054730.X		实用新型
39	一种用于 DNA 检测的纳米金信号探针及其制备方法和 DNA 检测的方法	200810032870.1		发明

NO.	专利名称	申请号	授权号	专利类别
40	一种基于纳米金与核酸结构的靶分子检测方法	200810036219.1		发明
41	分离与纯化单个病毒的方法	200810036428.6		发明
42	一种苯磺酰胺类化合物及其中间体，及其制备方法和应用	200810037644.2		发明
43	一种苯磺酰胺类羟基衍生物及其中间体及其制备方法和应用	200810037632.X		发明
44	麻醉药品的太赫兹检测方法	200810039967.5		发明
45	利用 THz-TDs 鉴别不同旋光性的麻黄碱	200810040557.2		发明
46	一种非水溶性单体的水相接枝聚合方法	200810040814.2		发明
47	一种水处理用接枝改性的高分子滤膜及其制备方法	200810041112.6		发明
48	一种聚甲基丙烯酸酯及其制备方法和用途	200810041972.X		发明
49	一种放射性铼标记的含 RGD 序列的多肽及其制备方法和用途	200810042679.5		发明
50	滤膜孔径测定仪	200820153336.1		实用新型
51	一种聚乙烯亚胺修饰的碳纳米管及其复合物、制备方法及用途	200810201238.5		发明
52	基于核酸适体的靶物质的检测方法及其固相生物感应器	200810202277.7		发明
53	一种基于纳米金与核酸结构的靶分子检测方法	200810202737.6		发明
54	一种用于重金属离子现场检测的无动力微流控芯片及其制作和使用方法	200810202738.0		发明
55	一种电化学发光系统	200810203100.9		发明
56	一种纳米复合物、该纳米复合物在处理酚类废水中的应用及其应用方法	200810203560.1		发明
57	一种测量水相中碳纳米管吸附苯量的方法	200810204210.7		发明
58	Method for gas storage	US/12/086，939		发明
59	A method for storing gas	EP/O6805231.5		发明
60	气体储藏方法	JP/O88126YJP		发明
61	放射性食管支架及其制作方法	02136015.4	ZL02136015.4	发明
62	用于人体腔道支架上的医用聚氨酯膜及其制备方法	200410017746.X	ZL200410017746.X	发明
63	O-(2-[^{18}F]氟乙基）-L-酪氨酸的合成方法	200510025005.0	ZL200510025005.0	发明
64	电子束烟气脱硫脱硝的方法及其装置	200510025131.6	ZL200510025131.6	发明
65	大孔径聚醚砜膜及其制备方法和用途	200510031066.8	ZL200510031066.8	发明
66	绝缘管套	200720066522.7	ZL200720066522.7	实用新型
67	硅溶胶的制造方法及制得的硅溶胶	200510024230.2	ZL200510024230.2	发明

附录 6

2007–2008 上海应用物理所博士、硕学位授予一览表

2007

No.	学位	学生	专业	导师	论文题目	研究方向
1	博士	宫培军	无机化学	姚思德	用于基因传感检测的特种磁性纳米凝胶的合成	生物纳米材料
2	博士	侯铮迟	无机化学	盛康龙	聚乙烯聚醚砜表面辐射接枝研究	高分子辐射化学
3	博士	王衡东	无机化学	邱士龙	质子交换膜燃料电池 MEA 制备研究	辐射化学
4	博士	林红军	无机化学	陆晓峰	一体式平片膜生物反应器处理污水的性能与应用研究	基于膜分离技术的先进环保和水资源化
5	博士	王敏	核技术及应用	朱志远	染料和氯酚水溶液的辐射降解研究	辐射技术在环境保护中的应用
6	博士	唐俊龙	核技术及应用	李德明	SSRF 数字化电源监控与测试的实验研究	同步辐射光源与束线技术及应用
7	博士	丁建国	核技术及应用	刘松强	EPICS 控制系统中网络技术的研究	加速器控制系统
8	博士	陈永林	核技术及应用	蒋迪奎	上海电子束离子阱(EBIT)装置电子束离子阱系统机构研制	加速器技术及应用
9	博士	梁胜	无机化学	汪勇先	磁靶向纳米药物载体的制备工艺方法学研究及在免疫分析中的初步应用	医用纳米材料
10	博士	刘崎	无机化学	朱智勇	离子径迹蚀刻过程及温敏智能膜的制备研究	功能高分子材料
11	博士	胡建刚	粒子物理与原子核物理	朱志远	带电粒子束作用下碳纳米管结构转变的实验研究	纳米材料
12	博士	陈仕谋	无机化学	吴国忠	碳纳米管的表面功能化及其纳米空间尺寸效应研究	纳米材料
13	博士	张立娟	粒子物理与原子核物理	方海平	纳米尺度固液界面气体的富集	物理与生物的交叉
14	博士	龙德武	无机化学	吴国忠	纳米材料与光敏小分子间界面反应的动力学研究	辐射化学及辐射材料改性
15	博士	李鼎	粒子物理与原子核物理	方海平	人工纳米结构表面的去浸润和对流体的超弱阻尼	表面物理
16	博士	周巧根	粒子物理与原子核物理	徐洪杰	相对论性电子束在螺旋形磁场中相干红外辐射特性的研究	核分析技术及应用
17	博士	徐晶莹	无机化学	李文新	富勒醇的药理毒理学研究	纳米生物医药
18	博士	倪志春	粒子物理与原子核物理	巩金龙	碳纳米管的荷能粒子束改性	粒子束与碳纳米管的相互作用
19	博士	伊厚会	粒子物理与原子核物理	方海平	晶格玻尔兹曼方法对血液流的研究	物理与生物的交叉
20	博士	宋玉峰	无机化学	朱智勇	高能重离子辐照损伤效应的光谱测量研究	离子束辐照改性
21	博士	许荣辉	无机化学	汪勇先	水热法制备强光致荧光 CdS 纳米晶及其性质研究	纳米材料及其生物应用
22	博士	邓彪	粒子物理与原子核物理	徐洪杰	同步辐射微束 X 射线荧光 CT 方法研究	同步辐射光源与光束线站及应用
23	博士	张增艳	粒子物理与原子核物理	肖体乔	以 THz 吸收全谱为特征指纹的混合物成分分析	远红外技术及应用
24	博士	吉特	粒子物理与原子核物理	徐洪杰	THz-TDS 实验方法研究及其应用	太赫兹技术和应用研究
25	博士	刘丽想	粒子物理与原子核物理	肖体乔	X 射线定量相衬成像及其生物医学应用研究	X 射线成像光学
26	博士	许子健	粒子物理与原子核物理	朱志远	富勒烯结构稳定化和碳纳米管机械振动性质的计算模拟研究	纳米结构性质的理论研究
27	博士	郭威	粒子物理与原子核物理	沈文庆	I.中能下 N=10 附近丰质子核的反应截面和弹核碎裂反应产物动量分布研究, II.对上海激光电子伽玛源的蒙特卡罗模拟	粒子物理与原子核物理
28	博士	朱红平	无机化学	姚思德	天然抗氧化剂对蛋白质氧化损伤的保护	自由基化学
29	博士	黄师荣	核技术及应用	吴国忠	用超临界二氧化碳制备微孔聚合物材料	高分子材料制备与加工
31	博士	李海	无机化学	胡钧	生物分子图形的微纳米操纵及其应用	纳米生物学
32	博士	葛敏	无机化学	李文新	化合物结构与相互作用的 THz 时域光谱研究	太赫兹技术应用研究

2007

No.	学位	学生	专业	导师	论文题目	研究方向
33	博士	徐冬梅	无机化学	盛康龙	基因转染载体 M-PEIs 纳米凝胶的合成	纳米材料和纳米医学
34	博士	张炯	无机化学	樊春海	DNA 在金电极表面的分子组装行为及电化学 DNA 生物传感器研究	纳米生物传感器与生物芯片
35	博士	刘兴奋	无机化学	樊春海	基于水溶性共轭高分子的高灵敏度生物传感器研究	生物传感器
36	博士	刘瑞丽	无机化学	李文新	C_{60}-糖皮质激素的制备及其理化性质和药效研究	纳米生物医药
37	博士	程登峰	无机化学	尹端沚	^{18}F 标记的血管活性肠肽 PET 显像剂的研究	放射性药物
38	博士	姜伯承	核技术及应用	赵振堂	上海光源储存环束流集体效应的研究	加速器技术及应用
39	博士	李纪堂	核技术及应用	刘松强	SSRF 光束线中的联锁及保护系统的研究	大型物理装置控制
40	博士	黄国庆	核技术及应用	叶恺容	束流电信号处理技术的研究	加速器束流诊断技术研究
41	博士	安双利	核技术及应用	蒋迪奎	上海 EBTI 及 SSRF 真空控制系统工程研究	同步辐射光源与束线技术及应用
42	博士	郭智	粒子物理与原子核物理	邰仁忠	弛豫铁电体中纳米极化区域的同步光实验研究	同步辐射光源和光束线站
43	博士	殷重先	核技术及应用	刘德康	SSRF 快速轨道反馈系统研究	加速器技术及应用
44	硕士	骆玉宇	粒子物理与原子核物理	肖体乔	基于 X 射线相干特性的成像及其应用研究	X 射线光学显微成像
45	硕士	申梓刚	粒子物理与原子核物理	张益	液体操纵 DNA 分子的机制研究	纳米生物
46	硕士	杨传俊	粒子物理与原子核物理	张元勋	基于 ACCU 方向采样和 WPS 技术的大气污染定位	核分析技术在环境科学中的应用
47	硕士	郝淑梅	无机化学	王文锋	光敏剂对溶菌酶活性的影响研究	自由基生物学
48	硕士	成康民	无机化学	沈玉梅	β-榄香烯衍生物的合成及其 ^{188}Re 三羰基铼化合物的标记	分子标记-诊断药物
49	硕士	杨永兴	无机化学	李晓林	大气颗粒物中铂族元素分析及其污染研究	分析化学
50	硕士	陈爽	无机化学	侯铮迟	辐射接枝聚乙烯薄膜表面无机诱导层生长研究	有机无机复合材料
51	硕士	梁峰	无机化学	李燕	大气颗粒物中纳米氧化铁的毒理效应	大气颗粒物毒理
52	硕士	李长兴	电磁场与微波技术	谷鸣	SSRF 脉冲调制器电磁干扰和抑制的研究	加速器技术、电磁兼容
53	硕士	何志义	信号与信息处理	殷立新	移动式氦液化器控制系统升级改造	计算机应用
54	硕士	张猛蛟	信号与信息处理	漆玉金	MicroSPECT 读出电子学研究	MicroSPECT 成像系统
55	硕士	王良辉	电磁场与微波技术	周巧根	多维霍尔探头恒温技术的研究	多维霍尔探头恒温磁测系统的研究
56	硕士	李华萍	信号与信息处理	龚培荣	上海 EBIT 电源动态控制电路设计	自动控制
57	硕士	祝晴	信号与信息处理	沈立人	分布式 EPICS 系统数据存档引擎	加速器数据存档软件
58	硕士	金莉莉	信号与信息处理	李勇平	指纹识别算法的研究	指纹识别算法
59	硕士	李林	信号与信息处理	沈立人	基于 Web Service 的 SSRF 存档数据服务系统	加速器数据存档
60	硕士	刘学	光学工程	王纳秀	晶体单色器冷却结构优化设计与实验研究	高热载光学系统的缓释技术
61	硕士	汪洋	核技术及应用	巩金龙	基于化学气相沉积方法的碳纳米管组装	碳纳米材料
62	硕士	傅斯翊	信号与信息处理	蒋大真	基于虚拟仪器的数据获取处理系统在离子迁移率谱仪中的实现	数据获取与处理
63	硕士	杨振宇	信号与信息处理	李勇平	生物特征证照系统的嵌入式指纹采集与实时处理	生物特征证照
64	博士	李朝霞	粒子物理与原子核物理	方海平	纳米尺度下气体形态和纳米颗粒之间相互作用的理论研究	纳米技术和单分子生物

2008

No.	学位	学生	专业	导师	论文题目	研究方向
1	博士	潘瑞芹	粒子物理与原子核物理	朱志远	碳纳米结构的热输运性质理论研究	纳米结构的热输运性质
2	博士	张鸿洲	核技术及应用	李勇平	跨姿态人脸识别和姿态估计中的特征转换研究	人脸识别
3	博士	王晓峰	粒子物理与原子核物理	方海平	双链 DNA 解链研究	纳米科技和单分子生物物理
4	博士	李勤涛	粒子物理与原子核物理	巩金龙	基于低能离子沉积和溅射技术的碳与硅纳米结构制备及场发射性能	纳米结构材料
5	博士	米丽娟	无机化学	胡钧	人工纳米生物分子复合体系构建及应用------纳米金 PCR 体系研究	纳米生物学
6	博士	王化斌	无机化学	胡钧	单个生物大分子力学性质研究	纳米生物学
7	博士	孙启龙	核技术及应用	戴志敏	基于碳纳米管阴极的电子枪研究	基于碳纳米管阴极的电子枪研究
8	博士	朱毅	核技术及应用	夏绍建	第三代同步辐射光源光束线若干关键技术研究	同步辐射光源与束线技术及应用
9	博士	李瑞	核技术及应用	李德明	开关型动态大功率磁铁电源系统设计与电源研制	电力电子技术及自动控制
10	博士	赵黎颖	核技术及应用	刘德康	SSRF 主定时系统研究	加速器技术及应用
11	博士	马二俊	粒子物理与原子核物理	马余刚	电子和正电子与奇异原子核及多原子分子弹性散射的理论研究	原子核物理
12	博士	李俊纲	无机化学	李文新	多壁碳纳米管和纳米 TiO_2 的呼吸毒性	纳米生物学
13	博士	左小磊	无机化学	樊春海	几种生物活性小分子的电化学生物传感检测	电化学生物传感器
14	博士	洪军	无机化学	姚思德	手性药物酶促拆分纳米载体研究	生物材料与生物医药
15	博士	卜令山	核技术及应用	赵振堂	上海光源储存环机械共架组件的微振动控制研究	同步辐射光源与束线技术及应用
16	博士	王琳	核技术及应用	李勇平	基于 Gabor 小波的人脸识别算法的研究与应用	信号与信息处理(人脸识别)
17	硕士	郭洪雷	核技术及应用	龚培荣	5 MeV 电子辐照加速器的相关技术研究	加速器自动控制
18	博士	叶寅	核技术及应用	邱士龙	动力型锌镍电池隔膜研制	碱性电池隔膜及其相关材料研究
19	博士	顾强	核技术及应用	赵振堂	基于射频电子直线加速器的高品质电子束的产生	加速器物理与微波技术
20	博士	苏前敏	粒子物理与原子核物理	马余刚	统计模型中的同位旋标度现象及相关实验初探	中低能重离子物理
21	博士	于成浩	核技术及应用	赵振堂	三维准直测量技术在上海光源中的应用研究	同步辐射光源与束线技术及应用
22	博士	陆杭军	粒子物理与原子核物理	方海平	水在纳米通道中的动力学行为研究	水在纳米通道中的性质
23	博士	陈艳燕	粒子物理与原子核物理	方海平	晶格玻尔兹曼方法研究固液界面特性下的血液流	物理与生物交叉
24	博士	朱光来	粒子物理与原子核物理	吴国忠	咪唑类室温离子液体中的瞬态反应机理及相关研究	光化学反应动力学，分子模拟
25	博士	王鹏	粒子物理与原子核物理	胡钧	基于纳米操纵技术分离与扩增单颗粒病毒的研究	纳米生物学
26	博士	万帆	粒子物理与原子核物理	朱志远	基于远红外太赫兹光谱的过渡金属和钛酸盐材料性质研究	太赫兹光谱研究
27	博士	勇振中	粒子物理与原子核物理	朱志远	基于粒子束技术的一维纳米复合结构及其网络的研究	粒子与碳纳米管相互作用
28	博士	马春旺	粒子物理与原子核物理	沈文庆	中能区远离稳定线奇异核性质的实验研究	中能重离子反应
29	博士	颜廷志	粒子物理与原子核物理	马余刚	^{25}Si 的反应截面及其碎片动量分布测量以及中能轻碎片的集体流性质研究	中能核反应
30	博士	左嘉旭	粒子物理与原子核物理	沈文庆	RHIC-STAR Au+Au 碰撞实验中奇异粒子的产生和可鉴别粒子方位角关联的研究	相对论重离子碰撞物理
31	博士	陈金辉	粒子物理与原子核物理	马余刚	相对论重离子碰撞实验中 phi 介子的产生及奇异夸克性质测量	相对论重离子碰撞
32	博士	弓晓晶	粒子物理与原子核物理	方海平	纳米通道中的水分子传输行为的理论研究	粒子物理与核物理
33	博士	朱伟忠	核技术及应用	徐洪杰	软 X 射线干涉光刻相关技术研究	软 X 射线干涉光刻相关技术研究

2008

No.	学位	学生	专业	导师	论文题目	研究方向
34	博士	尹成科	核技术及应用	戴志敏	上海光源数字化高频低电平系统算法研究	上海光源数字化高频低电平系统算法研究
35	博士	董黎	无机化学	姚思德	M-PEIs 转导 OPN shRNA 抑制肝癌的生长和转移	纳米生物与纳米医学
36	博士	张兆霞	无机化学	王文锋	光敏剂对酶的损伤机理研究	自由基化学和光生物学
37	博士	蔡小青	无机化学	李文新	C_{60} 多羟基衍生物抗氧性质的生物效应研究	多羟基富勒烯衍生物的生物效应
38	博士	徐万帮	无机化学	汪勇先	半导体量子点的制备、修饰及其在离子检测中的应用	纳米材料
39	博士	邓波	无机化学	盛康龙	基于粉体辐射接枝改性的高分子滤膜的制备	高分子材料改性
40	博士	刘玉侠	无机化学	李文新	肿瘤光敏新疗法分子机理研究	光化学和光生物学
41	博士	张艳	无机化学	盛康龙	辐射改性 SBS 及其与 PA6 共混体系性能的研究	高分子材料辐射改性
42	博士	戚明颖	无机化学	吴国忠	咪唑类离子液体辐射效应及其机理的研究	离子液体辐射化学
43	博士	诸颖	无机化学	李文新	碳纳米材料的细胞生物效应研究	纳米生物效应及安全性
44	博士	徐春艳	无机化学	何建华	Ⅱ型限制性内切酶 Sau3AI 的 C 端及其 E64A 突变体的晶体结构与功能研究	蛋白质结构与功能
45	博士	袁启兵	核技术及应用	谷鸣	SSRF 注入引出系统控制技术研究	加速器控制技术
46	博士	刘江峰	核技术及应用	李燕	扫描透射离子显微成像方法研究	基于核技术的分子环境科学研究
47	博士	胡勇	核技术及应用	刘松强	同步辐射光束线中的运动控制系统的研究	大型实验物理装置控制系统
48	博士	王宏飞	核技术及应用	赵振堂	插入件积分场线测量系统的研制	加速器磁铁测量
49	博士	后接	核技术及应用	刘桂民	上海光源储存环闭轨校正与轨道慢反馈研究	加速器技术及应用
50	博士	张同宣	核技术及应用	赵振堂	上海光源零模束流反馈系统研究	加速器高频低电平控制
51	博士	储建华	核技术及应用	赵振堂	C 波段腔式 BPM 与射频前端信号处理系统的研制	束测控制与微波技术
52	博士	金婵	粒子物理与原子核物理	李燕	机动车辆排放颗粒物的特征及相关元素的毒效应	核分析技术及同步辐射技术在环境毒理领域的研究
53	博士	郑明强	无机化学	尹端泓	用于早期诊断 Alzheimer's disease 小分子 PET 显像剂的研究	放射性药物
54	硕士	牛冬校	核技术及应用	沈文庆	减小 DNA 电性质直接测量时接触电阻的探索	生物物理与核物理技术交叉
55	硕士	刘维清	核技术及应用	刘建飞	SSRF 数字化高频低电平接口控制	加速器高频低电平控制技术
56	硕士	师绍猛	☆光学工程	肖体乔	强吸收介质内部低 Z 材料结构的 X 射线显微成像研究	成像光学
57	硕士	罗宏瀚	核技术及应用	薛松	波纹管流固耦合振动的数值模拟研究	流体诱发的管道振动
58	硕士	李烜	核技术及应用	赵明华	直线加速器波导耦合器的仿真与研究	加速器技术及应用
59	硕士	贺周同	粒子物理与原子核物理	巩金龙	金刚石的形核及选择性生长	纳米材料
60	硕士	李原	电磁场与微波技术	李德明	上海光源增强器注入引出研究	加速器物理
61	硕士	任云峰	无机化学	沈玉梅	β-榄香烯-$[M(CO)_3(H_2O)_3]$+ (M=^{188}Re,^{99m}Tc)型配合物的合成及初步生物学评价	放射性药物
62	硕士	闫树华	无机化学	李宾	单个 DNA 分子上的纳米定位沉积	纳米生物学
63	硕士	赵君	无机化学	王敏	茜素红的辐射降解和絮凝脱色研究	辐射技术在环境保护中的应用
64	硕士	刘贵锋	无机化学	沈玉梅	β-榄香烯衍生物的合成及其 ^{99m}Tc 同位素标记	放射性药物
65	硕士	张娟	无机化学	樊春海	金纳米粒子在 DNA 传感器构建中的应用	生物传感器
66	硕士	朱晓伟	无机化学	陆晓峰	热致相分离法制备平片式聚（乙烯-乙烯醇）微孔膜	基于膜分离技术的先进环保与水资源化
67	硕士	高维珏	无机化学	陆晓峰	纳米 TiO_2 对高分子超滤膜的改性研究	基于膜分离技术的先进环保与水资源化
68	硕士	李松焱	粒子物理与原子核物理	方海平	纳米通道中的缺陷对水分子输运的影响	分子动力学研究纳米通道中水分子的行为
69	硕士	许升辉	信息与信息信号处理	沈天健	嵌入式操作系统 uC/OS-Ⅱ在数字化电源控制器上的应用研究	数字化电源控制器的研究

2008

No.	学位	学生	专业	导师	论文题目	研究方向
70	硕士	杨嵩	信息与信息信号处理	冷用斌	基于 EPICS 的跨平台虚拟仪器测试技术研究	分布式数据采集
71	硕士	周晓鸣	电磁场与微波技术	欧阳联华	涡流切割磁铁作用机理的研究	特种磁铁电磁场计算
72	硕士	张甦宁	信息与信息信号处理	李勇平	机读护照的卡上逻辑数据结构实现	生物特征识别技术及应用
73	硕士	鲍强	信息与信息信号处理	李勇平	基于 Java 卡的生物特征电子护照技术研究	生物特征识别技术
74	硕士	段磊	信息与信息信号处理	沈立人	EPICS 通道访问的 Web 服务接口	EPICS 通道访问的 Web 服务接口
75	硕士	朱丹峰	信息与信息信号处理	张宇田	上海 EBIT 离子注入引出系统的调试及改进	加速器控制
76	硕士	仇文君	信息与信息信号处理	沈立人	直线加速器联锁保护系统的 PLC 系统实现	加速器的联锁保护
77	硕士	冀锐敏	核技术及应用	刘桂民	上海光源高频噪声对储存环束流品质的影响	加速器纵向运动
78	硕士	孙晖	☆光学工程	徐洪杰	振动对长程面形仪测量精度的影响研究	光学检测
79	硕士	许珊珊	信息与信息信号处理	叶恺容	束流发射度测量	束流发射度测量
80	硕士	狄兰兰	信息与信息信号处理	谷鸣	亚纳秒触发脉冲延时分配器研制	数字和脉冲电源信号与信息处理
81	硕士	李力	核技术及应用	方国平	工艺冷却水温度控制技术研究	核信息获取、处理及应用
82	硕士	戴兴	信息与信息信号处理	叶恺容	同步光数据采集及处理	数据采集及处理

附录 7

2007–2008 年度研究生录取数据

2007

No.	姓名	专业	培养层次	导师
1	曹喜光	粒子物理与原子核物理	博士研究生	沈文庆
2	范功涛	粒子物理与原子核物理	博士研究生	马余刚
3	傅瑶	粒子物理与原子核物理	博士研究生	沈文庆
4	管娜娜	粒子物理与原子核物理	博士研究生	沈文庆
5	靳富	粒子物理与原子核物理	博士研究生	马余刚
6	李建伟	粒子物理与原子核物理	博士研究生	马余刚
7	李勇	粒子物理与原子核物理	博士研究生	朱志远
8	林栩凌	粒子物理与原子核物理	博士研究生	戴志敏
9	任翠兰	粒子物理与原子核物理	博士研究生	朱志远
10	田健	粒子物理与原子核物理	博士研究生	马余刚
11	周波	粒子物理与原子核物理	博士研究生	方海平
12	李峥	无机化学	博士研究生	汪勇先
13	唐忠锋	无机化学	博士研究生	吴国忠
14	黄立梁	无机化学	博士研究生	沈玉梅
15	李兰婷	无机化学	博士研究生	胡钧
16	刘桂锋	无机化学	博士研究生	王文锋
17	马玉飞	无机化学	博士研究生	尹端沚
18	苏邵	无机化学	博士研究生	樊春海
19	万莹	无机化学	博士研究生	樊春海
20	谢牧云	无机化学	博士研究生	胡钧
21	叶鸣	无机化学	博士研究生	胡钧
22	虞鸣	无机化学	博士研究生	盛康龙
23	张小勇	无机化学	博士研究生	朱智勇
24	张馨允	无机化学	博士研究生	姚思德
25	赵素芳	无机化学	博士研究生	姚思德
26	赵艳凝	无机化学	博士研究生	吴国忠
27	朱长锋	无机化学	博士研究生	樊春海
28	陈荣昌	核技术及应用	博士研究生	肖体乔
29	代秋声	核技术及应用	博士研究生	漆玉金
30	付泽川	核技术及应用	博士研究生	赵振堂
31	龚文波	核技术及应用	博士研究生	李勇平
32	刘鸣	核技术及应用	博士研究生	刘德康
33	陆杰	核技术及应用	博士研究生	周巧根
34	吕清涛	核技术及应用	博士研究生	薛松
35	马明旺	核技术及应用	博士研究生	朱智勇
36	米清茹	核技术及应用	博士研究生	刘松强
37	邱敬科	核技术及应用	博士研究生	余笑寒
38	佟亚军	核技术及应用	博士研究生	肖体乔
39	王超	核技术及应用	博士研究生	李勇平
40	王会军	核技术及应用	博士研究生	许皆平
41	吴坤	核技术及应用	博士研究生	薛松

2007

No.	姓名	专业	培养层次	导师
42	薛艳玲	核技术及应用	博士研究生	徐洪杰
43	杨传俊	核技术及应用	博士研究生	邰仁忠
44	于海波	核技术及应用	博士研究生	刘建飞
45	张祥志	核技术及应用	博士研究生	邰仁忠
46	张雪竹	核技术及应用	博士研究生	漆玉金
47	朱静	核技术及应用	博士研究生	何建华
48	康成	粒子物理与原子核物理	硕士研究生	李晴暖
49	李绍歆	粒子物理与原子核物理	硕士研究生	方德清
50	李永江	粒子物理与原子核物理	硕士研究生	徐望
51	刘丹	粒子物理与原子核物理	硕士研究生	朱智勇
52	马静远	粒子物理与原子核物理	硕士研究生	黄宇营
53	王广华	粒子物理与原子核物理	硕士研究生	刘卫
54	王淑丽	粒子物理与原子核物理	硕士研究生	王东
55	魏勤	粒子物理与原子核物理	硕士研究生	漆玉金
56	武红利	粒子物理与原子核物理	硕士研究生	田文栋
57	薛冰	粒子物理与原子核物理	硕士研究生	朱志远
58	薛亮	粒子物理与原子核物理	硕士研究生	马余刚
59	叶绍强	粒子物理与原子核物理	硕士研究生	蔡翔舟
60	曾建荣	粒子物理与原子核物理	硕士研究生	李燕
61	张琛	粒子物理与原子核物理	硕士研究生	胡钧
62	张萌	粒子物理与原子核物理	硕士研究生	万荣正
63	赵杰	粒子物理与原子核物理	硕士研究生	蔡翔舟
64	周铖龙	粒子物理与原子核物理	硕士研究生	马余刚
65	耿马可	无机化学	硕士研究生	黄庆
66	李海霞	无机化学	硕士研究生	王文锋
67	李剑波	无机化学	硕士研究生	张岚
68	刘伟华	无机化学	硕士研究生	吴国忠
69	裴昊	无机化学	硕士研究生	樊春海
70	孙凯	无机化学	硕士研究生	陆晓峰
71	王成	无机化学	硕士研究生	周伟
72	许晓平	无机化学	硕士研究生	沈玉梅
73	于洋	无机化学	硕士研究生	李景烨
74	张伯武	无机化学	硕士研究生	李景烨
75	周晨	无机化学	硕士研究生	陆晓峰
76	周欢	无机化学	硕士研究生	何建华

2007

No.	姓名	专业	培养层次	导师
77	朱燕	无机化学	硕士研究生	李晓林
78	程琳	光学工程	硕士研究生	王劼
79	郭荣怡	光学工程	硕士研究生	肖体乔
80	雒峰	光学工程	硕士研究生	戴志敏
81	宋春立	光学工程	硕士研究生	邰仁忠
82	王玉丹	光学工程	硕士研究生	肖体乔
83	张宁	光学工程	硕士研究生	冷用斌
84	张晓琳	光学工程	硕士研究生	肖体乔
85	王鑫	电磁场与微波技术	硕士研究生	刘桂民
86	张瑞	电磁场与微波技术	硕士研究生	刘建飞
87	曹新民	信号与信息处理	硕士研究生	赵明华
88	封晨霞	信号与信息处理	硕士研究生	周伟民
89	李志明	信号与信息处理	硕士研究生	邓辉宇
90	刘蒙	信号与信息处理	硕士研究生	漆玉金
91	刘鑫	信号与信息处理	硕士研究生	沈立人
92	毛晴川	信号与信息处理	硕士研究生	夏晓彬
93	孟伟丽	信号与信息处理	硕士研究生	宋世平

2007

No.	姓名	专业	培养层次	导师
94	王靖琰	信号与信息处理	硕士研究生	李勇平
95	谢华忠	信号与信息处理	硕士研究生	张宇田
96	张国辉	信号与信息处理	硕士研究生	李勇平
97	张金金	信号与信息处理	硕士研究生	胡钧
98	张志远	信号与信息处理	硕士研究生	陈建锋
99	周广颖	信号与信息处理	硕士研究生	闫隆
100	朱晓峰	信号与信息处理	硕士研究生	谷鸣
101	蔡军	核技术及应用	硕士研究生	许浒江
102	方文程	核技术及应用	硕士研究生	赵振堂
103	顾月良	核技术及应用	硕士研究生	黎忠
104	赖龙伟	核技术及应用	硕士研究生	冷用斌
105	蓝涛	核技术及应用	硕士研究生	郑丽芳
106	李启明	核技术及应用	硕士研究生	许皆平
107	王迪	核技术及应用	硕士研究生	李德明
108	王晓磊	核技术及应用	硕士研究生	许皆平
109	徐轶超	核技术及应用	硕士研究生	陈永忠
110	杨群	核技术及应用	硕士研究生	徐洪杰
111	易星	核技术及应用	硕士研究生	冷用斌
112	张延乐	核技术及应用	硕士研究生	余笑寒

2008

No.	姓名	专业	培养层次	导师
1	常睿	粒子物理与原子核物理	博士研究生	郃仁忠
2	陈灿	粒子物理与原子核物理	博士研究生	肖体乔
3	樊广伟	粒子物理与原子核物理	博士研究生	徐望
4	贺周同	粒子物理与原子核物理	博士研究生	朱智勇
5	李林	粒子物理与原子核物理	博士研究生	胡钧
6	李薇	粒子物理与原子核物理	博士研究生	马余刚
7	牛冬校	粒子物理与原子核物理	博士研究生	胡钧
8	任杰	粒子物理与原子核物理	博士研究生	李德明
9	任秀平	粒子物理与原子核物理	博士研究生	胡钧
10	沈轶	粒子物理与原子核物理	博士研究生	胡钧
11	孙小艳	粒子物理与原子核物理	博士研究生	马余刚
12	谢巧玲	粒子物理与原子核物理	博士研究生	巩金龙
13	薛超凡	粒子物理与原子核物理	博士研究生	郃仁忠
14	阳丽	粒子物理与原子核物理	博士研究生	方海平
15	杨利峰	粒子物理与原子核物理	博士研究生	徐望
16	张传福	粒子物理与原子核物理	博士研究生	李燕
17	张国强	粒子物理与原子核物理	博士研究生	马余刚
18	周光照	粒子物理与原子核物理	博士研究生	肖体乔
19	周培	粒子物理与原子核物理	博士研究生	马余刚
20	卞晓锴	无机化学	博士研究生	陆晓峰
21	窦强	无机化学	博士研究生	吴国忠
22	段娜	无机化学	博士研究生	胡钧
23	胡文兵	无机化学	博士研究生	樊春海
24	黄卫	无机化学	博士研究生	吴国忠
25	李健	无机化学	博士研究生	何建华
26	施玲丽	无机化学	博士研究生	汪勇先
27	温燕勤	无机化学	博士研究生	樊春海
28	杨璇璇	无机化学	博士研究生	李景烨
29	张鹏	无机化学	博士研究生	王文锋
30	张元庆	无机化学	博士研究生	沈玉梅
31	朱华	无机化学	博士研究生	沈玉梅
32	陈杰	核技术及应用	博士研究生	叶恺容
33	蒋志强	核技术及应用	博士研究生	赵振堂
34	梁平	核技术及应用	博士研究生	李勇平

2008

No.	姓名	专业	培养层次	导师
35.	刘中华	核技术及应用	博士研究生	李勇平
36	罗文	核技术及应用	博士研究生	徐望
37	任玉琦	核技术及应用	博士研究生	肖体乔
38	唐思巍	核技术及应用	博士研究生	刘德康
39	陶世兴	核技术及应用	博士研究生	何建华
40	田丰	核技术及应用	博士研究生	徐洪杰
41	王君	核技术及应用	博士研究生	李德明
42	闫芬	核技术及应用	博士研究生	余笑寒
43	张俊强	核技术及应用	博士研究生	赵明华
44	张伟	核技术及应用	博士研究生	周巧根
45	赵国璧	核技术及应用	博士研究生	冷用斌
46	周娟	核技术及应用	博士研究生	李勇平
47	白凌志	粒子物理与原子核物理	硕士研究生	怀平
48	蔡晓鹭	粒子物理与原子核物理	硕士研究生	徐望
49	陈洁	粒子物理与原子核物理	硕士研究生	方德清
50	陈文豪	粒子物理与原子核物理	硕士研究生	陈敏
51	范雪波	粒子物理与原子核物理	硕士研究生	刘卫
52	韩立欣	粒子物理与原子核物理	硕士研究生	马余刚
53	黄灿	粒子物理与原子核物理	硕士研究生	朱智勇
54	贾彦彦	粒子物理与原子核物理	硕士研究生	李晓林
55	李小芸	粒子物理与原子核物理	硕士研究生	王劼
56	刘敏	粒子物理与原子核物理	硕士研究生	周兴泰
57	刘亚芬	粒子物理与原子核物理	硕士研究生	徐望
58	龙时磊	粒子物理与原子核物理	硕士研究生	李燕
59	梅龙伟	粒子物理与原子核物理	硕士研究生	蔡翔舟
60	戚俊成	粒子物理与原子核物理	硕士研究生	肖体乔
61	申月	粒子物理与原子核物理	硕士研究生	胡钧
62	盛楠	粒子物理与原子核物理	硕士研究生	方海平
63	谭兴兴	粒子物理与原子核物理	硕士研究生	郃仁忠
64	陶城	粒子物理与原子核物理	硕士研究生	田文栋
65	王娟	粒子物理与原子核物理	硕士研究生	李爱国
66	王倩	粒子物理与原子核物理	硕士研究生	徐洪杰

2008				
No.	姓名	专业	培养层次	导师
67	王松	粒子物理与原子核物理	硕士研究生	朱志远
68	王廷栋	粒子物理与原子核物理	硕士研究生	怀平
69	于海生	粒子物理与原子核物理	硕士研究生	黄宇营
70	张彤	粒子物理与原子核物理	硕士研究生	王东
71	张兴民	粒子物理与原子核物理	硕士研究生	周兴泰
72	郑俊义	粒子物理与原子核物理	硕士研究生	余笑寒
73	朱逾卉	粒子物理与原子核物理	硕士研究生	马余刚
74	蔡仁	无机化学	硕士研究生	李景烨
75	陈鹏	无机化学	硕士研究生	侯铮迟
76	崔巍	无机化学	硕士研究生	沈玉梅
77	代彬	无机化学	硕士研究生	李宾
78	高星	无机化学	硕士研究生	黄宇营
79	葛志磊	无机化学	硕士研究生	樊春海
80	耿彦红	无机化学	硕士研究生	刘卫
81	李良	无机化学	硕士研究生	陆晓峰
82	李潇	无机化学	硕士研究生	张岚
83	李晓明	无机化学	硕士研究生	黄庆
84	刘晓鸿	无机化学	硕士研究生	赵红卫
85	刘亚辉	无机化学	硕士研究生	何建华
86	刘艳成	无机化学	硕士研究生	王文锋
87	罗仕海	无机化学	硕士研究生	黎忠
88	毛秀海	无机化学	硕士研究生	李迪
89	戚英娜	无机化学	硕士研究生	吴国忠
90	盛尹祥子	无机化学	硕士研究生	夏晓彬
91	魏敏	无机化学	硕士研究生	李晴暖
92	杨光	无机化学	硕士研究生	沈玉梅
93	苑洪铭	无机化学	硕士研究生	李景烨
94	张惠芳	无机化学	硕士研究生	周兴泰
95	张继超	无机化学	硕士研究生	余笑寒
96	张一	无机化学	硕士研究生	黄庆
97	赵彬	无机化学	硕士研究生	宋世平
98	郑小雪	无机化学	硕士研究生	樊春海
99	周冉冉	无机化学	硕士研究生	郜仁忠
100	刘石磊	光学工程	硕士研究生	王纳秀
101	马春桃	光学工程	硕士研究生	王劼

2008				
No.	姓名	专业	培养层次	导师
102	沈飞	光学工程	硕士研究生	肖体乔
103	孙福权	光学工程	硕士研究生	薛松
104	王宝鹏	光学工程	硕士研究生	王东
105	殷波	电磁场与微波技术	硕士研究生	刘建飞
106	袁刚	电磁场与微波技术	硕士研究生	周兴泰
107	程坤	信号与信息处理	硕士研究生	赵明华
108	丁喻	信号与信息处理	硕士研究生	漆玉金
109	顾俊俊	信号与信息处理	硕士研究生	徐洪杰
110	胡正	信号与信息处理	硕士研究生	黎忠
111	厉娜	信号与信息处理	硕士研究生	赵明华
112	孙发力	信号与信息处理	硕士研究生	夏晓彬
113	孙国民	信号与信息处理	硕士研究生	戴志敏
114	汤宁	信号与信息处理	硕士研究生	赵振堂
115	王雯君	信号与信息处理	硕士研究生	闫隆
116	熊亮	信号与信息处理	硕士研究生	王晓
117	徐玮	信号与信息处理	硕士研究生	万荣正
118	杨桂森	信号与信息处理	硕士研究生	冷用斌
119	张莹	信号与信息处理	硕士研究生	李勇平
120	陈之初	核技术及应用	硕士研究生	冷用斌
121	段雪非	核技术及应用	硕士研究生	刘桂民
122	冯超	核技术及应用	硕士研究生	赵振堂
123	巩文斌	核技术及应用	硕士研究生	朱志远
124	江家友	核技术及应用	硕士研究生	陈志豪
125	李玖栋	核技术及应用	硕士研究生	邓辉宇
126	林作康	核技术及应用	硕士研究生	戴志敏
127	牛晶	核技术及应用	硕士研究生	唐琳
128	宋健	核技术及应用	硕士研究生	漆玉金